# Development and Optimization of Molecularly Imprinted Polymers for the Analysis of Organic Pollutants in Environmental Water Samples

by

© Aliasghar Golbabanezhadazizi

A thesis submitted to the

School of Graduate Studies

in partial fulfillment of the requirements for the degree of

**Doctor of Philosophy**

**Department of Chemistry**

Memorial University of Newfoundland

**January 2020**

St. John's Newfoundland and Labrador

# Abstract

Agricultural, industrial, and municipal water releasing organic contaminants into the environment is of serious ongoing concern. To monitor these waterborne pollutants, sample preparation steps are required prior to analysis. Consequently, massive efforts have been directed toward new approaches that are fast, selective, cost-effective, user-friendly and green. Molecularly imprinted polymers (MIPs) are an elegant solution to add selectivity into sorptive materials.

In this thesis, MIPs were prepared using different polymerization techniques and in various formats such as MIP particles, MIP thin film, and MIP-coated mesh. The prepared sorbents were successfully utilized for extraction of different classes of pollutants such as polycyclic aromatic hydrocarbons (PAHs) and organophosphorus pesticides (OPPs) from water samples. To improve the heterogeneity of MIPs, a controllable polymerization mechanism (reversible addition fragmentation chain transfer (RAFT) polymerization) was implemented for synthesis MIPs on $Fe_3O_4$@$SiO_2$ particles for extraction of PAHs. A tailormade MIP formulation was also created and optimized for selective extraction of OPPs from water. The sorbent formulae are versatile for use in different formats such as thin film and mesh. MIP extraction devices can be readily interfaced with various detection systems such as gas chromatography flame ionization detector (GC-FID), atmospheric pressure chemical ionization gas chromatography-tandem mass spectrometry (APCI-GC-MS/MS) and liquid chromatography -tandem mass spectrometry (LC-MS/MS) using liquid desorption, and thermal desorption. Additionally, these devices can increase the throughput, reliability, and simplicity of environmental analysis. For example, we

developed a new solvent assisted thermal desorption head space (ST-HD) method, which we demonstrate to be excellent for the introduction of analytes enriched by MIP thin films, and it is amenable to direct and semi-automated method improving reproducibility and throughput.

In this thesis, MIP fabrication and performance will be demonstrated and evaluated. The value MIP techniques in providing precious sensitivity, selectivity to the quality of analysis of organic pollutants in water is presented.

## Acknowledgment

I would like to take this opportunity to express my sincere gratitude to the people who have supported and encouraged me to complete my PhD program at Memorial University. Firstly, I would like to appreciate my supervisor, Prof. Christina S. Bottaro, for her guidance, support, knowledge, patience, advice, and wisdom during last four years. She had profound belief in my abilities that allowed me to conduct my favourite research. The fantastic research environment provided by, Prof. Christina S. Bottaro, not only helped me to complete my graduate program but also helped me to shape my professional skills. I was always amazed by her motivation for science which has framed my research perspectives.

I'd also like to extend my gratitude to my supervisory committee members, Prof. Francesca M. Kerton and Dr. Michael J. Katz, for their valuable comments and suggestions.

Many thanks to wonderful people in Bottaro Analytical Group who provided me valuable training and feedback. I have gained precious experiences through collaboration with the past and current students and researchers in this group. I'm extremely grateful to my friend and colleague Evan A. Langille for his constructive comments and relentless support during our collaboration.

I cannot begin to express my thanks to my beloved wife who was also my lab mate, colleague and friend for 10 years. She was always supportive, patient, thoughtful, helpful, and wise. She never let me down. Fereshteh encouraged and helped me to keep moving forward in every hardship. She always inspired me to make my dreams come true and I can't imagine any of these accomplishments with her being in my life. Fereshteh also

extended a great amount of assistance in my project including data collection during my project and writing the manuscripts.

I must thank all my teachers, mentors, profs and supervisors and whoever helped me to reach at this stage in my life.

I’m deeply indebted to my parents who have dedicated their life to me. Special thanks to my two lovely sisters who were always supportive and encouraging. I wish my family a life full of health and happiness.

# Table of Contents

# List of Tables

**Chapter 1:**



**Chapter 2:**

**Chapter 4:**

# List of Figures

**Chapter 1:**

**Chapter2:**

**Chapter 5:**

# List of Symbols, Nomenclature or Abbreviations

| | |
|---|---|
| **2,4-DCP** | 2,4-dichlorophenol |
| **2,4,5-TCP** | 2,4,5-trichlorophenol |
| **2,4,6-TCP** | 2,4,6-trichlorophenol |
| **2-NP** | 2-nithrophenol |
| **2-VP** | 2-vinylpyridine |
| **4-CP** | 4-chlorophenol |
| **4-VP** | 4-vinylpyridine |
| **4-NP** | 4-nitrophenol |
| **4-NAP** | 2-amino-4-nitrophenol |
| **17β-E2** | 17-beta-estradiol |
| **ABDV** | 2,2′-azobis(2,4-dimethylvaleronitrile |
| **ACBN** | 1,1′-Azobis(cyclohexanecarbonitrile) |
| **Ace** | Acenaphthene |
| **Ace-d10** | Acenaphthene-d10 |
| **ACN** | Acetonitrile |
| **Acy** | Acenaphthylene |
| **AEM** | Averaged extracted mass |
| **AIBN** | 2,2′-azobisisobutyronitrile |
| **AM** | Acrylamide |
| **ANOVA** | Analysis of variance |
| **Ant** | Anthracene |

| | |
|---|---|
| **APCI** | Atmospheric pressure chemical ionization |
| **APTS** | 3-aminopropyltriethoxysilane |
| **ATRP** | Atom transfer radical polymerization |
| **BaA** | Benzo(a)anthracene |
| **BaP** | Benzo(a)pyrene |
| **BbF** | Benzo(b)fluoranthene |
| **BBT** | Benzyl benzodithioate |
| **BGP** | Benzo(ghi) perylene |
| **BkF** | Benzo(k)fluoranthene |
| **BPA** | Bisphenol A |
| **BPAF** | 2,2-bis(4-hydroxyphenyl) hexafluoropropane |
| **BPE** | Bisphenol E |
| **BPF** | Bisphenol F |
| **BPM** | Bisphenol M |
| **BPs** | Bisphenols |
| **$C_0$** | Initial concentration |
| **$C_{18}$** | Octadecyl |
| **CCD** | Central composite design |
| **CCLs** | Contaminant Candidate Lists |
| **$C_e$** | Equilibrium concentration |
| **Chry** | Chrysene |
| **Chry-d12** | Chrysene-d12 |
| **CNTs** | Carbon nanotubes |

| | |
|---|---|
| **Conc.** | Concentration |
| **CPE** | Cloud point extraction |
| **CPs** | Chlorophenols |
| **DART** | Direct analysis in real time |
| **DB(ah)A** | Dibenzo(a,h) anthracene |
| **DBP** | Dibutyl phthalate |
| **DCM** | Dichloromethane |
| **DEAEM** | 2-dimethyl aminoethyl methacrylate |
| **DEHP** | Di(2-ethylhexyl) phthalate |
| **DEP** | Diethyl phthalate |
| **DES** | Diethylstilboestrol |
| **DESI** | Desorption electrospray ionization; |
| ***DF*** | Desirability function |
| **DI-SPME** | Direct immersion solid phase microextraction |
| **DLLME** | Dispersive liquid-liquid microextraction |
| **DMP** | Dimethyl phthalate |
| **DMPA** | 2,2-dimethoxy-2-phenylacetophenone |
| **DMSO** | Dimethyl sulfoxide |
| **DS** | Dienestrol |
| **DSPE** | Dispersive solid phase extraction |
| **DVB** | Divinylbenzene |
| **E1** | Estrone |
| **E2** | Estradiol |

| | |
|---|---|
| **E3** | Estriol |
| **EDCs** | Endocrine disrupting chemicals |
| **EF** | Enrichment factor |
| **EGDMA** | Ethylene glycol dimethacrylate |
| **EtOH** | Ethanol |
| **ESI** | Electrospray ionization |
| **EU** | European Union |
| **F-PTW**, | Functionalized potassium tetratitanate whisker |
| **FA** | Formic acid |
| **FFD** | Fractional factorial design |
| **FID** | Flame ionization detector |
| **FL** | Fluorescence |
| **Flu** | Fluorene |
| **Flut** | fluoranthene |
| **FQs** | Fluoroquinolones |
| **FR** | Free radical polymerization |
| **GC** | Gas chromatography |
| **GMA** | Glycidylmethacrylate |
| **GO** | Graphene oxide |
| **HAc** | Acetic acid |
| **HEMA** | 2-hydroxyethyl methacrylate |
| **HF-LPME** | Hollow fiber liquid phase microextraction |
| **HLB** | Hydrophilic-lipophilic balanced |

| | |
|---|---|
| **HS** | Hexestrol |
| **HS-SPME** | Headspace solid phase microextraction |
| **IF** | Imprinting factor |
| **InP** | Indeno(1,2,3-cd) pyrene |
| $\boldsymbol{K}$ | Selectivity coefficient |
| $\boldsymbol{k}$ | Retention factor |
| $\boldsymbol{K'}$ | Relative selectivity coefficient |
| $\boldsymbol{K_d}$ | Distribution coefficient |
| **LC** | Liquid chromatography |
| **LLE** | Liquid–liquid extraction; |
| **LOD** | Limit of detection |
| **LogP** | Logarithm of the partition coefficient |
| **LOQ** | Limit of quantitation |
| **LPME** | Liquid phase microextraction |
| **LR** | Linear range |
| **m/z** | Mass to charge ratio |
| **MAA** | Methacrylic acid; |
| **MCL** | Maximum contamination limit |
| **MeOH** | Methanol |
| **MEPS** | Microextraction by packed sorbent |
| **MIPs** | Molecularly imprinted polymers |
| **MMIPs** | Magnetic molecularly imprinted polymers |

| | |
|---|---|
| **MPS** | 3-methacryloxypropyltrimethoxy-silane |
| **MRM** | Multiple reaction monitoring |
| **MS** | Mass spectrometry |
| **MS/MS** | Tandem mass spectrometry |
| **MW** | molecular weight |
| **MWCNTs** | Multi walled carbon nanotubes; |
| **Naph** | Naphthalene |
| **Naph-d8** | Naphthalene-d8 |
| **NIPAM** | N-isopropylacrylamide |
| **NIPs** | Non-imprinted polymers |
| **NL** | Added concentration is higher than linear range. |
| **NP** | Nonylphenol |
| **NPE** | Nonylphenol ethoxylate; |
| **NQ** | Added concentration is lower than LOQ. |
| **OPPs** | Organophosphorus pesticides |
| **PA** | Polyacrylate |
| **PAHs** | Polycyclic aromatic hydrocarbons |
| **PAN** | Polyacrylonitrile |
| **PCP** | Pentachlorophenol |
| **PDMS** | Polydimethylsiloxane |
| **Per-d12** | Perylene-d12 |
| **PEs** | Phthalate esters |
| **Phe** | Phenanthrene |

| | |
|---|---|
| **Phe-d10** | Phenanthrene-d10 |
| **POPs** | Persistent organic pollutants |
| **PTOP** | 4-tert-octylphenol |
| **Pyr** | Pyrene |
| $Q_e$ | Adsorption capacity |
| $R^2$ | The coefficient of determination for linear regression |
| **RAFT** | Reversible addition fragmentation chain transfer |
| **RDSE** | Rotating-disc sorptive extraction; |
| **rpm** | Rotation per minute |
| **RSD** | Relative standard deviation |
| **RSM** | Response surface methodology |
| **S/N** | Signal-to-noise |
| **SBSE** | Stir bar sorptive extraction |
| **SD** | Standard deviation |
| **SDS** | Sodium dodecyl sulfate |
| **SEM** | Scanning electron microscopy |
| **SLM** | Supported liquid membrane |
| **SMZ** | Sulfamethazine |
| **SMX** | Sulfamethoxazole |
| **SPE** | Solid phase extraction |
| **SPME** | Solid phase microextraction |
| **ST-HD** | Solvothermal headspace desorption |
| **TBBPA** | Tetrabromobisphenol A |

| | |
|---|---|
| **TBBPS** | Tetrabromobisphenol S |
| **TCBPA** | Tetrachlorobisphenol A |
| **TEM** | Transmission electron microscopy |
| **TFME** | Thin film microextraction |
| **TEOS** | Tetraethyl orthosilicate |
| **TMOS** | Tetramethoxysilane |
| **TRIM** | Trimethylolpropane trimethacrylate |
| **UCMRs** | Unregulated Contaminant Monitoring Rules |
| **US-EPA** | The United States-Environmental Protection Agency |
| **UV** | Ultraviolet |
| **v/v,%** | Volume percentage |
| **VTMOS** | Vinyltrimethoxysilane |
| **w/w, %** | Weight percentage |

## Co-authorship statement

The principal author has conducted the research and literature review presented in Chapters 1-4 of this thesis for the degree of Doctor of Philosophy under the supervision of Prof. Christina S. Bottaro.

1- **A. Azizi**, C.S. Bottaro, "A critical review of molecularly imprinted polymers for the analysis of organic pollutants in environmental water samples", *J. Chromatogr. A*, (2019) 460603. This published review is the main part (sections 1.1-1.13) of the literature review presented in Chapter 1. The first author proposed the idea of prepararing this chapter as a review paper and initial topics. After a discussion on topics with the help of the second author (Dr. Christina S. Bottaro), the first author prepared the first draft. Dr. Christina S. Bottaro reviewed the manuscript. Preparation of the manuscript, figures and summary tables for publication, submission, as well as revision of manuscript during peer review process were done by the first author.

2- **A. Azizi**, F. Shahhoseini, C.S. Bottaro, "Magnetic molecularly imprinted polymers prepared by reversible addition fragmentation chain transfer polymerization for dispersive solid phase extraction of polycyclic aromatic hydrocarbons in water", *J. Chromatogr. A*, 1610 (2020) 460534. This published work forms the basis for the work described in Chapter 2. The first author proposed the idea of using MMIPs prepared by RAFT polymerization. After preliminary studies done by the first author, Dr. Christina S. Bottaro proposed using experimental design for optimization. The first author has participated at all stages of the manuscript preparation process: the planning of experiments, preparation of the sorbent, method development and validation, sample preparation, extraction procedures,

instrumental analysis, data processing, experimental design methodology, manuscript writing, and submission, as well as in manuscript replies to reviewers. The contribution of the second author (Fereshteh Shahhoseini) was in the preparation of the sorbent, method development and validation. Additionally, the final version of the manuscript has been reviewed by Dr. Christina S. Bottaro.

3. **A. Azizi**, F. Shahhoseini, A. Modir-Rousta, C.S. Bottaro, "High throughput direct analysis of water using solvothermal headspace desorption with porous thin films", *Anal. Chim. Acta*, 1087 (2019) 51-61. This published work forms the basis for the work described in Chapter 3. The idea of developing a high-throughput technique for analysis of PAHs in water samples was proposed by the first author. The first author contributed to all stages of the manuscript preparation process: the planning of experiments, manufacturing of thin films, method development, sample preparation, extraction procedures, method validation, instrumental analysis, data processing, manuscript writing, and submission, as well as in manuscript replies to reviewers. The contribution of the second author (Fereshteh Shahhoseini) was in the fabrication of extraction devices, execution of extraction experiments during method development and validation. The third author (Ali Modir-Rousta ) proposed the idea of using solvent for desorption of analytes in a headspace sampler. Dr. Christina S. Bottaro and Fereshteh Shahhoseini also contributed in the review of the first draft prepared by the first author.

4. The presented work in Chapter 4 forms the basis for an IP disclosure submitted to Memorial University and one potential IP disclosure which is in preparation. The authors of this work are **Ali Azizi**, Fereshteh Shahhoseini, Evan A. Langille, and Christina S.

Bottaro. The first author finalized the proposal for the development of extraction devices for high-throughput analysis of OPPs using thin film MIPs in consultation with Dr. Christina S. Bottaro. The idea of MIP-coated mesh was the result of a collaborative project by Ali Azizi, Fereshteh Shahhoseini, and Evan A. Langille. The first author contributed to all the stages of manuscript preparation, including the planning of experiments, fabrication, and development of thin films and mesh devices, optimization, method development, sample preparation, extraction procedures, instrumental analysis, data processing, manuscript writing. The contributions of Fereshteh Shahhoseini and Evan A. Langille was in preparation of extraction devices, extraction experiments during method development, validation studies. In addition, the template molecules were prepared by Evan A. Langille. All the authors have reviewed the first draft prepared by the first author.

# Chapter 1: Introduction and critical review of molecularly imprinted polymers for the analysis of organic pollutants in environmental water samples

A. Azizi, C.S. Bottaro. “A critical review of molecularly imprinted polymers for the analysis of organic pollutants in environmental water samples.” J. Chromatogr. A (2019): 460603

## 1.1. Introduction

The ever-increasing release of chemicals from human activities like agriculture and industrial processes has impacted the environment and human health, for example, through exposure to cancer causing or promoting agents [1, 2]. Environmental matrices affected include water, soil, and atmosphere, as well as flora and fauna; all of these are the concern of analytical chemists. Numerous analytical methods, usually including liquid chromatography (LC) and gas chromatography (GC), have been reported for the quantification of pollutants in different samples. Although direct detection methods can improve throughput and reduce errors associated with sample handling, low analyte concentrations, and sample complexity limit their accuracy and suitability. Therefore, simple, rapid, cheap and reliable techniques for clean-up, isolation, and preconcentration of desired compounds from environmental samples are necessary before instrumental analysis [3, 4].

The simplest routine preconcentration method used widely for environmental analysis is liquid-liquid extraction (LLE) [5]. LLE is time-consuming, labor-intensive, and expensive (labor and solvent cost); it also requires large sample volumes and toxic organic solvents. To overcome these disadvantages, extraction techniques such as solid phase extraction (SPE) [6-8], solid phase microextraction (SPME) [9, 10], stir bar sorptive extraction (SBSE) [11, 12], liquid phase microextraction (LPME) [13, 14], and cloud point extraction (CPE) [15, 16] have been developed for isolation and preconcentration of contaminants from environmental samples. Though these methods advance extraction protocols by reducing reagent and sample volumes and time, which have led to adoption in

routine analyses, they suffer from lack of selectivity against interfering compounds and their performance is sensitive to matrix composition [17]. Selective sample preparation methods improve sensitivity and reproducibility by decreasing matrix effects.

One approach to achieving this is by using molecularly imprinted polymers (MIPs), which is the focus of this paper. MIPs, which are frequently described as plastic antibodies and analogous to naturally-occurring antibodies, feature selective recognition properties for target molecules. These synthetic molecular recognition systems are chemically robust and relatively easy to tailor to new analytical targets. MIPs are synthesized (Fig. 1.1) through the copolymerization of a functional monomer and a crosslinker, such as methacrylic acid (MAA) and ethylene glycol dimethacrylate (EGDMA), respectively, in the presence of the template molecule (the target analyte or an analogue with similar chemistry and shape). Polymerization is usually induced with thermal or UV activation of an initiator. After polymerization, the template molecules are removed leaving a polymer containing cavities complementary in shape, size and functional groups to the target molecule. The excellent recognition properties of MIPs compared to non-imprinted polymers (NIPs) are derived from the interactions between the template molecule and a monomer functional group that is present in the pre-polymerization complex. These interactions are easily re-established when the MIPs are exposed to the analyte in the sample matrix. It is this feature that gives MIPs a significant advantage over traditional non-selective sorbents [18]. MIPs which have been utilized in wide range applications including chromatography [19], sensors [20-23], drug delivery [24, 25] and catalysis [26-28], can be implemented as selective extraction phases for sample pretreatment and preconcentration [29-31]. In theory, the selectivity of MIPs should increase the sensitivity and repeatability of water analysis by diminishing the

co-extraction of matrix interferences. This selectivity reduces overlapping chromatographic peaks and matrix effects at detection, particularly ion suppression in mass spectrometry (MS) [32].

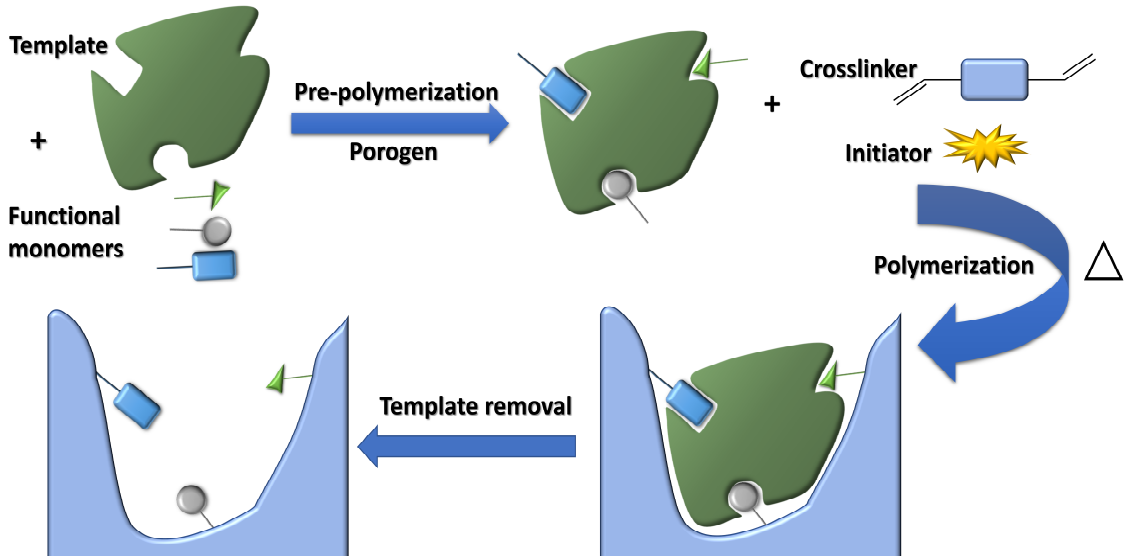


**Fig. 1.1.** Schematic illustration of general preparation procedure for MIPs.

Due to the broad applicability of MIPs, comprehensive reviews on principles of MIPs synthesis, formats, and their applications have been published [33-35]. Chen et al. [36] provided a focused review of the components of MIPs, and novel technologies to prepare MIPs for selective analyte recognition in sample preparation, chromatography, and sensors. SPE, which is a routine and global preconcentration method generally performed using non-selective extraction phases in packed cartridges, was reviewed specifically by Caro et al [37]. Application of MIP-SPE allows for selective adsorption of target analytes during sample loading and removal of matrix components. Following the successful application for SPE packing, MIPs have been developed for use as the extraction phase in

other formats. These techniques are promising for miniaturization, ease of use, direct sampling, and automation. For example, Hu et al. [38] published a review of synthesis of MIPs on magnetic beads, in membranes, and in the forms of SPME and SBSE. Sarafraz-Yazdi and Razavi [39] presented a review of the preparation of MIPs applied in SPME including coated and monolithic fibers, in-tube SPME (coatings and packings), membranes, and sol–gel MIPs. Nanoparticles, which offer a large surface area with the possibility for functionalization, can be used as the supports to fabricate MIP sorbents. Thus MIPs-coated nanoparticles have also been discussed in several reviews [40-42] Ansari's review [42] was particularly useful, with configurations and preparation methods for magnetic molecularly imprinted polymers (MMIPs) discussed in detail. The magnetic properties of MMIPs provide an advantage for dispersive solid phase extraction (DSPE), allowing for fast and efficient collection of sorbent particles [43]. Other nanoparticles such as silica, quantum dots, carbon dots, and gold or silver nanoparticles have been used in core-shell MIPs [44]. Although it has been demonstrated that MIPs introduce selective recognition of analytes in a variety of formats, it is also essential to assess their performance in the context of real sample matrices.

Many authors have reported using MIPs for analysis of environmental, food, and biological samples. Ansari and Karimi [45] detail the synthesis of MIPs in SPE, SPME, and ultrasonic-assisted SPE, sensors, and magnetic separations for a suite of applications for the analysis of drugs in biological and environmental samples. Speltini et al. [46] published an updated review of MIPs applications (2014–2017) in which different formats of MIPs, including offline and online SPE, SPME, SBSE, and DSPE were used for the analysis of contaminants in food and environmental samples. Murray and Örmeci [47] and

Huang et al. [48] provided applications of MIPs in water and wastewater treatment. MIPs can be implemented for selective extraction of organic contaminants from environmental samples [49]. The examples of such applications include polycyclic aromatic hydrocarbons (PAHs) [50], endocrine disrupting chemicals (EDCs) [51], pharmaceuticals [52] and pesticides [53]. There is a wealth of research on such applications, and further details will be presented in this review. Though there are many good reviews of MIP technology in which the authors discuss the applications and novel developments of the materials, MIP technology in water analysis has not been critically assessed.

This review aims to provide a comprehensive evaluation of the selectivity and efficiency of MIPs used in sample preparation step for analysis of organic pollutants in water samples. To achieve this aim, the following topics will be reviewed: synthetic strategies, characterization methodologies, and MIP formula and sample preparation parameter optimization for water analysis, especially environmental waters. The versatility of MIPs has led to the development of several techniques for selective extraction of organic contaminants from aqueous samples, such as MIP-SPE, MIP-DSPE, MIP-SPME, MIP-SBSE, and membrane protected MIPs, which will be discussed and evaluated. The factors that limit the applicability of MIPs for selective extraction and isolation of pollutants from aqueous matrices will be identified. These shortcomings are incompatibility of MIPs with aqueous matrices, poor imprinting effects for water-soluble compounds, heterogeneous and non-specific binding sites, and adsorption of interferences. Novel strategies can be adopted in the synthesis of MIPs to overcome these limitations. Finally, some novel and highlighted applications of MIPs that allow for reducing sample manipulation, and automation of analysis such as direct analysis will be explained.

## 1.2. Synthesis strategies for MIPs

### 1.2.1. Covalent imprinting

MIPs based on the formation of covalent bonds between the template and monomer in pre-polymerization solutions demonstrate the most homogenous structures with well-defined binding sites and cavities because of the fixed stoichiometric ratio of functional monomer to template molecules arising from the specificity of the bond formation [39]. The main drawback of covalent-based MIPs is the need for an appropriate monomer-template complex that could form easily reversible covalent bonds with geometry and chemistry suitable for uptake of targets from aqueous systems [54]. For this reason, covalent strategies are rarely used in water analysis.

### 1.2.2. Non-covalent imprinting

MIPs formed by non-covalent interactions (e.g., hydrogen bonding, ion-pairing, or dipole interactions) between the template and monomer, frequently use an excess of monomer to promote the formation of the monomer-template complex [39]. The selection of the porogenic solvent is particularly important as it should not disrupt the interactions between the monomer and template, e.g., water would interfere with hydrogen bonding [55], and it needs to support the formation of a porous polymer matrix during the phase separation process [56]. The porogen should also be similar in terms of polarity to aqueous matrices to ensure a consistent microenvironment which could facilitate rebinding of the analyte [57]. The selection of the porogen is not trivial, because the features required are

often mutually exclusive. Non-covalent imprinting can introduce many non-specific binding sites because of the excess of functional monomers, which leads to a reduction of the selectivity of extraction.

### 1.2.3. Semi-covalent imprinting

To reduce non-selective binding, a hybrid strategy called semi-covalent imprinting can be implemented [33]. In this approach, template molecules are covalently bound to the functional monomers before polymerization enhancing the selectivity. The analyte rebinds through non-covalent interactions which overcome long equilibrium time as a limitation of covalent approaches [58]. Semi-covalent MIPs feature more homogenous binding sites and rapid mass transfer to both organic and inorganic polymeric networks. Tang et al. [59] synthesized a derivative of the template by reaction between the template (clenbuterol) and methacryloyl chloride as the monomer for polymerization with EGDMA as the crosslinker. Hydrolysis under acidic conditions removed the template and left MIPs with cavities containing active sites for non-covalent interaction (hydrogen bonding). The polymer provided rapid equilibrium for uptake of the analyte within 20 min with high specificity: adsorption capacity, 7.34 for MIPs and 1.99 mg $g^{-1}$ for NIPs.

The covalent complex can be formed through the reaction between phenolic moiety in the template molecule (2,2-bis(4-hydroxyphenyl) hexafluoropropane) and isocyanate group in 3-(triethyloxysily) propyl isocyanate [60]. The obtained complex was incorporated into a sol–gel process in order to prepare a MIP sorbent. Soxhlet extraction was then applied to remove the template from silica-based polymer. Hydrogen bonding between the analyte and –NH2 groups available in the cavities was proposed as the non-

covalent interaction for adsorption of the bisphenol A (BPA) [60]. A similar reaction was also used to form a prepolymer complex in order to imprint estrone (E1) [61]. The formed urethane bond, which is stable at room temperatures and cleavable at high temperature [62], was cleaved by stirring the MIPs in a dimethyl sulfoxide (DMSO) and water solution at 180 °C for 3 h. The prepared MIPs have higher affinity for adsorption of E1 compared to NIPs while no selectivity was observed for adsorption of testosterone propionate as a structural analogue. Therefore, imprinted sites, which are complementary to the analyte and created through a covalent reaction, have ability for selective adsorption of the target molecules through non-covalent interactions.

## 1.3. Determining the performance of MIPs for sample preparation

### 1.3.1. Adsorption studies

To evaluate the performance of MIPs, adsorption properties such as equilibrium adsorption capacity of the synthesized MIP particles should be considered. To obtain the equilibrium adsorption capacity, MIPs are exposed to the analyte in aqueous matrices [63] or in organic solvents such as acetonitrile (ACN) [64] methanol (MeOH) [65], dichloromethane (DCM) [66] or water mixed with an organic solvent [67] for an experimentally determine interval, which is long enough to ensure equilibration. The capacity is calculated using Eq. (1.1) [68]:

$$Q_e = \frac{(C_0 - C_e)V}{W} \qquad (1.1)$$

Where $C_0$ and $C_e$ are the initial and equilibrium concentrations of the analyte in the solution. $V$ and $W$ are the volume of the sample and mass of the polymer used for adsorption.

The selective adsorption properties of MIPs are commonly defined by the imprinting factor (*IF*) obtained as:

$$IF = \frac{Q_{MIP}}{Q_{NIP}} \qquad (1.2)$$

Where, $Q_{MIP}$ and $Q_{NIP}$ are the equilibrium adsorption capacity of the analyte on MIPs and NIPs, respectively [69]. A high *IF* implies that imprinting was successful, with sites that selectively bind analytes in great excess of sites for non-selective uptake approximated by NIPs performance. To evaluate the efficiency and selectivity of fenoprofen-MIPs, 10 mg of MIP and NIP particles were incubated with standard solution of this analyte for 24 h. These experiments yielded $Q_{MIP}$:38.8, $Q_{NIP}$: 20.9 mg $g^{-1}$, and *IF*:1.9, and demonstrated the selectivity of MIPs for fenoprofen [70]. MIPs can be applied for adsorption of other compounds analogous to the analyte or template. There are several terms used to describe this affinity, including distribution coefficients ($K_d$), selectivity coefficients ($K$), and relative selectivity coefficient ($K'$).

$$K_d = \frac{Q_e}{C_e} \qquad (1.3)$$

$$K = \frac{K_{d_{(template\ or\ analyte)}}}{K_{d_{analoge}}} \qquad (1.4)$$

$$K' = \frac{K_{MIP}}{K_{NIP}} \qquad (1.5)$$

Guan et al. [68] reported distribution coefficients for adsorption of 4-nitrophenol (4-NP), as the template molecule used in preparation of the MIPs and other structurally

related compounds. The NIPs depict non-specific sites for adsorption of all compounds and yielded in lower $K_d$ values. Conversely, higher $K_d$ values were obtained using MIPs indicated selective adsorption sites. 2-nithrophenol (2-NP) and 2,4-dichlorophenol (2,4-DCP) as analogues of the template yielded in $K'$ of 13.55 and 11.02, respectively. The higher selectivity of 4-NP-MIPs towards 2-NP compared to that of 2,4-DCP is due to the similar structure and propensity for hydrogen bonding. The importance of functionality in the imprinting effects of MIPs is understandable by comparing the results of $K'$ of these two compounds. However, 2,4-DCP with similar size and shape to the template showed the importance of functionality for adsorption of analogues.

As listed in Tables 1.1 and 1.2, the ability of developed MIPs for selective adsorption of targeted analytes was described by measuring adsorption capacity for the analyte(s). In most of the studies, this property was obtained in organic solvents or a mixture of water and organic solvents. The resultant selective properties in these matrices usually exceed than that of pure aqueous media due to strong non-specific hydrophobic interactions in water as well as disruption of selective interactions such as hydrogen bonding in water [71]. Thus, the adsorption capacity of MIPs in organic solvents cannot represent the real capacity of the material for selective uptake of organic pollutants from water samples. Nevertheless, the higher capacity of MIPs over NIPs shows the specific interactions between the analytes and functional monomers in formed cavities of the MIPs. Lian et al. [72] investigated the behavior of MIPs and NIPs for adsorption of mebendazole from MeOH solution. MIP particles showed a higher capacity compared to NIP particles. The prepared MIPs demonstrated great potentials for the preconcentration of mebendazole

in seawater samples. Moreover, the higher extraction efficiency of analytes enriched by MIP-SPE compared to NIP-SPE exhibits the imprinting effect of MIPs. MIPs prepared for selective extraction of non-steroidal anti-inflammatory drugs from wastewater and river water samples indicated 2 times higher extraction efficiency than the corresponding NIPs [73].

### 1.3.2. Chromatographic evaluation

Another measure to describe the selectivity of imprinted polymers is chromatographic evaluation. The retention factor of analytes using chromatographic columns packed with both MIPs and NIPs as sorbents is determined as below:

$$k = \frac{t_R - t_0}{t_0} \qquad (1.6)$$

$$IF = \frac{k_{MIP}}{k_{NIP}} \qquad (1.7)$$

The selectivity is explained by *IF* obtained by dividing the retention factor of MIPs ($k_{MIP}$) over that of NIPs ($k_{NIP}$) [74]. The specific interactions used to fabricate MIPs such as hydrogen bonding formed through complexation of monomer and template are greater than the non-specific interactions like hydrophobic interaction observed in both MIPs and NIPs. Therefore, weakly retained analytes by the NIP stationary phase were easily washed by the mobile phase.

**Table 1.1.** Bulk polymerization procedures for MIP-SPE of environmental water samples.

| Analytes (Matrix) | Template/Monomer/Crosslinker/(Ratio)/Porogen (Volume)/Initiator Template removal | SPE conditions | Adsorption and selectivity evaluation | Ref. |
|---|---|---|---|---|
| Clenbuterol (potable water) | Clenbuterol/Methacryloyl chloride/EGDMA/(1:2)/ MeOH:Ethyl acetate(3 mL+2 mL)/AIBN MeOH/ HAc (90:10, v/v) | Cartridge: 100 mg Conditioning: MeOH (5 mL), $H_2O$ (5 mL) Sample: 50 mL Washing:- Elution: MeOH: HAc (80:20, v/v) 15 mL | Binding experiment: 30 mg MIPs in5 mL MeOH solution; shaken at 300 rpm for 60 min<br>• $Q_{MIP}$:7.34 mg $g^{-1}$ at 120 mg $L^{-1}$<br>• $Q_{NIP}$:1.99 mg $g^{-1}$ at 120 mg $L^{-1}$<br>Comparing selectivity for analogues | [59] |
| Non-steroidal anti-inflammatory drugs (river water, wastewater) | Diclofenac/MAA/EGDMA (0.3:1.2:7.2 mmol) Toluene (1.2 mL)/AIBN Sonication with MeOH/ HAc (90:10, v/v) 15 min | Cartridge: 100 mg (32-63 µm) in MeOH slurry Conditioning: MeOH (5 mL) Water (5 mL) Sample: 10 mL Washing: DCM: ACN (94:6), 3 mL Elution: DCM: MeOH (85:15), 3 mL | 10 mg MIPs in 1 mL ACN solution<br>• $Q_{MIP}$:127.2 µmol $g^{-1}$<br>• $Q_{NIP}$: 21 µmol $g^{-1}$<br>Selective retention of analyte using MIP-SPE in presence of analogues | [64] |
| Non-steroidal anti-inflammatory drugs (wastewater and river water) | Templates/2-VP/EGDMA/ (1:8:80)/Toluene/ACN (50 mL/25 mL)/ACBN ACN: HAc (90:10, v/v) | Cartridge: 50 mg (25-50 µm) Conditioning: ACN (2 mL), $H_2O$ (2mL, pH: 2.5) Sample: 50 mL Washing: $H_2O$: MeOH (90:10, 2 mL) Elution: ACN: HAc | • Higher recovery for MIPs compared with NIPs<br>Cleaner chromatogram compared with Oasis MAX | [73] |
| FQs (river water) | Enrofloxacin/Urea-methacrylamide/EGDMA/(0.5:0.5:1:20)/ACN (5.6 mL)/ABDV - MeOH (100 mL) - MeOH/ $H_2O$ (0.1MHCl) (90:10, v/v) - MeOH | Cartridge: 150 mg (25-50 µm) Conditioning: 10 mL of buffer Sample: 10 mL Washing: 5mL of ACN/$H_2O$ Elution: 1mL of 2% TFA in MeOH | 10 mg MIPs in 2 mL ACN/water (1:9, v/v) solution Better efficiency for rebinding and chromatographic separation of analytes | [75] |
| Non-steroidal anti-inflammatory drugs (wastewater) | Ketoprofen/2-VP/EGDMA/toluene/ACN (10 mL, 9:1, v/v)/ACBN ACN: HAc (90:10, v/v) | Cartridge: 14 mg (25-90 µm) Conditioning: 6 mL MeOH, 6 mL $H_2O$ Sample: 50 mL Washing: triethylamine in $H_2O$ (1 mL, 95:5, v/v) Elution: MeOH (1 mL) | Comparison with structural competitors. | [76] |

*(continued on next page)*

**Table 1.1.** (*Continued*)

| Analytes (Matrix) | Template/Monomer/Crosslinker/(Ratio)/Porogen (Volume)/Initiator Template removal | SPE conditions | Adsorption and selectivity evaluation | Ref. |
|---|---|---|---|---|
| Non-steroidal anti-inflammatory drugs (wastewater) | Fenoprofen/2-VP/EGDMA/toluene/ACN (10 mL, 9:1, v/v)/ACBN Soxhlet extraction with MeOH: (90:10, v/v), MeOH | Cartridge: 50 mg (25–50 µm) Conditioning: 5 mL MeOH, 5 mL $H_2O$ Sample: 50 mL Washing: triethylamine in $H_2O$ (1 mL, 95:5, v/v) Elution: ACN (3 mL) | 10 mg in 11 mL for 24 h. • $Q_{MIP}$:38.8 mg $g^{-1}$ • $Q_{NIP}$: 20.9 mg $g^{-1}$ Exhaustive extraction of target analytes compared to <33% for structural analogues Cleaner chromatograms compared to Oasis HLB sorbent | [70] |
| Benzimidazol pesticides (seawater) | Mebendazole/MAA/EGDMA (1:4:20)/ACN (7.5 mL)/AIBN Soxhlet extraction with MeOH: HAc (50:50, v/v) | Cartridge: 20 mg (75-106 µm) Conditioning: MeOH: HAc (2 mL,9:1, v/v), MeOH (2 mL) Sample: 10 mL Washing: $H_2O$ 1 mL Elution: MeOH: HAc (1 mL, 1:1 v/v) | 10 mg MIPs in 5 mL MeOH solution • $Q_{MIP}$> $Q_{NIP}$ $Q_{MIP}$:10.46 mg $g^{-1}$ | [72] |
| Neonicotinoid pesticides (tap water) | Imidacloprid/MAA/EGDMA (1:4:10)/ACN (3.5 mL)/AIBN Soxhlet extraction | Cartridge: 100 mg Conditioning: MeOH (5 mL), $H_2O$ (5 mL) Sample: 10 mL Washing: ACN: $H_2O$ 1:4 (1 mL) Elution: MeOH (4 mL) | Comparing the MIP-SPE efficiency with NIP-SPE | [77] |
| Triazine pesticides (surface water) | Atrazine/MAA/EGDMA (1:4:3.96)/Toluene (7 mL)/AIBN Soxhlet extraction with MeOH | Cartridge: 150 mg (38-106 µm) Conditioning: 12 mL MeOH: HAc / $H_2O$ 20 mL Sample: 500 mL Washing: DCM 3 mL Elution: MeOH 12 mL | • $Q_{MIP}$: 0.00251, $Q_{MIP}$; 0.00064 mg $g^{-1}$ Higher extraction efficiency than commercial $C_{18}$ and activated carbons | [78] |
| Guanosine pesticide (seawater) | Guanosine/MAA/EGDMA (1:4:20)/DMSO (15 mL)/AIBN Soxhlet extraction with MeOH: HAc (90:10, v/v) | Cartridge: 50 mg (200-450 µm) Conditioning: 5 mL MeOH and 5 mL $H_2O$ Sample: 5 mL Washing: 1 mL 0.1 mol/L glacial acetic acid Elution: MeOH: $H_2O$ (1 mL, 95: 5 v/v) | Sample loading with 20 mg $L^{-1}$aqueous solution • $Q_{MIP}$: 0.008560; $Q_{NIP}$: 0.006293 mg $g^{-1}$ at 200 µg $L^{-1}$ | [79] |

*(continued on next page)*

**Table 1.1.** (*continued*)

| Analytes (Matrix) | Template/Monomer/Crosslinker/(Ratio)/Porogen (Volume)/Initiator Template removal | SPE conditions | Adsorption and selectivity evaluation | Ref. |
|---|---|---|---|---|
| Triazine pesticides (drinking water) | Ametryn/MAA/EGDMA/(1:4.49:22.28)/ACN (6.41 mL)/AIBN Soxhlet extraction with MeOH: (90:10, v/v), MeOH | Cartridge: 120 mg (50-105 µm) Conditioning: MeOH, $H_2O$ (5 mL) Sample: 10 mL Washing: ACN:8 mL Elution: MeOH (5 mL) | Comparing the efficiency for MIP-SPE with NIP-SPE | [80] |
| Phenols (reservoir, river, tap water, and wastewater) | Phenols/MAA/DVB (1:4:20)/ACN/toluene (4 mL, 3:1, v/v)/AIBN Soxhlet extraction with ACN: HAc (90:10, v/v) | Cartridge: 60 mg Conditioning: ACN/HAc (3 mL, 9:1, v/v), 6 mL ACN and 3 mL $H_2O$ Sample: 15 mL Washing: 3 mL $H_2O$ Elution: ACN: HAc (0.4 mL, 99: 1 v/v) | 2 mg MIPs in 4 mL aqueous solution /shaken for 24 h<br>• $Q_{MIP} > Q_{NIP}$<br>*IF*>2 for phenols | [81] |
| Phenols (tap water, river water sewage water) | 2,4,6-TCP//MAA/EGDMA (1:4:20)/ACN(6 mL)/AIBN Soxhlet extraction with ACN: HAc (90:10, v/v) | Cartridge: 300 mg (32–40 µm) Conditioning: MeOH (10 mL) $H_2O$ (10 mL) Sample: 10 mL Washing: MeOH (2mL) Elution: ACN/ HAc (9:1), 2 mL | 5 mg MIPs in 5 mL solution oscillated for 20 h<br>• $Q_{MIP}$: 197.27 mg $g^{-1}$; $Q_{NIP}$: 111.48 mg $g^{-1}$<br>Chromatographic *IF*: Phenol: 1.17/4-CP: 1.19/2,4,6-TCP: 1.68/PCP: 1.22 | [82] |
| EDCs (tap and river water) | 2,2',4,4'-tetrehydroxy benzophenone/4-VP/EGDMA (1:4:20)/ACN (5.6 mL)/AIBN Soxhlet extraction with MeOH/ HAc (90:10, v/v) | Cartridge: 200 mg (30–60 µm) Conditioning: MeOH (3 mL) 3 mL $H_2O$ Sample: 200 mL Washing: ACN/ $H_2O$ (1:1, v/v) 2 mL Elution: MeOH/TFA (98:2, v/v) 6 mL | 40 mg MIPs in 2 mL ACN shaken for 24 h at150 rpm Higher adsorption capacity of MIPs compared to NIPs | [74] |
| EDCs (lake, river and tap water) | E1/AM/MPTMS (1:3:9)/6.1 mL of DMSO, 1.0 mL toluene/AIBN Soxhlet extraction with MeOH/ HAc (90:10, v/v), 48 h | Cartridge: 100 mg Conditioning: MeOH (5 mL) $H_2O$ (5 mL) Sample: 10 mL Washing: - Elution: 1.2 mL of MeOH/$H_2O$/ HAc (95:5:5, v/v/v) | 20 mg MIPs in10 mL ethanol solution<br>• $Q_{MIP}$: E1: 2.42; E3: 0.62; DES: 0.71<br>• $Q_{NIP}$: E1: 0.64; E3: 0.50; DES: 0.52<br>• *K´*: E3: 3.34 and DES: 2.98<br>Comparing chromatogram with $C_{18}$-SPE | [83] |

*(continued on next page)*

**Table 1.1.** (*continued*)

| Analytes (Matrix) | Template/Monomer /Crosslinker/(Ratio) /Porogen (Volume)/Initiator Template removal | SPE conditions | Adsorption and selectivity evaluation | Ref. |
|---|---|---|---|---|
| BPs (river water) | BPE/4-VP/EGDMA (1:4:20)/MeOH (12 mL)/AIBN MeOH/ HAc (80:20, v/v) | Cartridge: 80 mg (25-38 µm)<br>Conditioning: 4 mL $H_2O$<br>Sample: 250 mL<br>Washing: 3.0 mL of MeOH/$H_2O$ (10:90, v/v), solution (65:35, v/v)<br>2.0 mL of MeOH:0.05%triethylamine MeOH: $H_2O$<br>Elution: 4.0 mL of 5% HAc in MeOH | 40 mg in 2 mL MeOH solution<br>• $Q_{MIP}$: 30, $Q_{NIP}$: 10 µmol $g^{-1}$ at 2 mmol $L^{-1}$<br>Chromatographic *IF* and cross-selectivity | [84] |
| Triazine pesticides (influent, tap and river water) | Atrazine/MAA/EGDMA (1:4:28) Chloroform (2.2 mL)/AIBN Soxhlet extraction with MeOH: HAc (99:1, v/v) | Cartridge: 10 mg (<40 µm)<br>Conditioning: MeOH (0.5 mL), $H_2O$ (0.5 mL)<br>Sample: 10 mL<br>Washing $H_2O$ (10 mL), DCM (1 mL):<br>Elution: MeOH/HAc (99:1, 0.4 mL) | • Compare with commercial cartridge<br>Cleaner chromatogram and reduce co-extracted matrix molecules | [85] |
| EDCs (potable water) | Fluorinated BPA/4-VP/TRIM (1:6:6)/ACN (1.5 mL)/AIBN Soxhlet extraction with MeOH | Cartridge: 250 mg (15–38 µm)<br>Conditioning: $H_2O$ (5×1 mL)<br>Sample: 1 mL<br>Washing: $H_2O$: MeOH (2:8, 2×1 mL), $H_2O$: MeOH (1:1, 2×1 mL)<br>Elution: MeOH (2×1 mL)<br>MeOH (2×1 mL) | • Chromatographic evaluation (*IF*) for templates and analogues<br>Comparing with OASIS HLB cartridge | [86] |
| Climbazole (river and tap water samples) | Miconazole/MAA/EGDMA (1:4:20) ACN (11.2 mL)/AIBN Soxhlet extraction with MeOH: HAc (90:10, v/v) for 24 h | Cartridge: 200 mg (30–60 µm)<br>Conditioning: 3 mL ACN<br>Sample: 500 mL<br>Washing: $H_2O$ (3 mL) and ACN (2 mL)<br>Elution: 4 mL MeOH – TFA (98: 2, v/v) | 20 mg in 2 mL ACN solution incubated at 145 rpm for 24 h<br>• $Q_{MIP}$>$Q_{NIP}$<br>• Chromatographic evaluation; IF (Miconazole: 10.9, Climbazole: 7.0<br>Selective MIP-SPE recovery of analytes compared to BPA with similar LogP | [87] |

**4-CP**, 4-chlorophenol; **ABDV**: 2,2′-azobis(2,4-dimethylvaleronitrile; **ACBN**, 1,1′-azobis(cyclohexanecarbonitrile); **AIBN**, 2,2′-azobisisobutyronitrile; **E3**, Estriol; **PCP:** Penta chlorophenol.

The difference between the retention factor of analyte in MIP and NIP columns indicates the specific binding sites responsible for selective retention of analytes in MIP columns. In a study conducted to prepare MIPs for phthalate esters (PEs), the chromatographic *IF* exhibits the importance of size and shape of the analytes, di(2-ethylhexyl) phthalate (DEHP): 12.86; dimethyl phthalate (DMP): 1.413, diethyl phthalate (DEP): 1.609, and dibutyl phthalate (DBP): 2.635. By using a DEHP-imprinted polymer with a long and branched alkyl chain, this analyte was selectively adsorbed compared to other PEs with straight alkyl chains. Low distribution coefficients and *IF* values for the analogues illustrate that similar functionality could cause a slight selectivity but not superior suitability of MIPs over NIPs [66].

There is also a correlation between the retention of analytes using MIP-columns (*K* and *IF* values) and capacity factors for adsorption of analytes. Feng et al. [82] synthesized MIPs using 2,4,6-trichlorophenol (2,4,6-TCP) as a template. The adsorption isotherms illustrated 197.27 mg $g^{-1}$ and 111.48 mg $g^{-1}$ as $Q_{max}$ for MIPs and NIPs, respectively. Moreover, the retention factors of the template obtained by packed columns are $K_{MIP}$: 1.90 and $K_{NIP}$: 1.13. This agreement between the values obtained using adsorption isotherms and chromatographic retention factors demonstrates the imprinting effects of using the template to prepare selective sorbents for phenols.

**Table 1.2.** Other polymerization techniques for MIP-SPE for preparation of environmental water samples.

| Analytes (Matrix) | Sorbent | SPE Conditions: | Adsorption and selectivity evaluation | Ref. |
|---|---|---|---|---|
| azo dye acid orange II (wastewater) | Substrate: $Fe_3O_4$<br>Surface modifier: Silica<br>Analyte/3-(triethoxysilyl)propyl Isocyanate/TEOS/ tetrahydrofuran<br>• Surface polymerization<br>Film thickness: 400-800 nm | 100 mg<br>Conditioning: -<br>Sample: 50 mL<br>Washing: -<br>Elution: Online SPE | 15 mg in 10 mL water shaken at 200 rpm<br>• Equilibration: More than 90.86% in 5 min; 97.2% 20 min<br>• Adsorption capacity: $Q_{MIP}$:50.91 and $Q_{NIP}$: 9.932 mg $g^{-1}$ at 140 mg $L^{-1}$<br>Comparing MIPs and NIPs for analogues | [88] |
| Triazine pesticides (distilled water) | Substrate: $TiO_2$<br>Surface modifier: APTS<br>Propazine/MAA/ EGDMA/Toluene/AIBN<br>• Surface polymerization<br>Film thickness: 25-37 nm | 200 mg<br>Conditioning: MeOH (5 mL), $H_2O$ (5 mL)<br>Sample: 20 mL<br>Washing: 2 mL MeOH / $H_2O$ (1:4, v/v)<br>Elution: 2 mL MeOH | 5 mg MIPs in 5 mL solution shaken at 100 rpm<br>• Equilibration: 90% (8 hours); 100% (15 hours)<br>• Adsorption capacity: $Q_{MIP}$: 6.8076 and $Q_{NIP}$: 0.4243 mg $g^{-1}$<br>*IF*: 16.04 | [89] |
| Organophosphorus pesticides (tap water) | polymer<br>• Malathion/MAA/EGDMA/ACN:$CHCl_3$ (1:1)/AIBN<br>Precipitation polymerization | 200 mg<br>Conditioning: MeOH (4 mL), $H_2O$ (4 mL)<br>Sample: 20 mL<br>Washing: MeOH/$H_2O$ (8 mL) (4:6, v/v)<br>Elution: MeOH/HAc (8 mL) (90:10, v/v) | 30 mg of MIPs in 10 mL MeOH/$H_2O$ (60:40, v/v)<br>• Equilibration: 30 min<br>• Adsorption capacity: $Q_{MIP}$: 14.4 $Q_{NIP}$: 7.8 mg $g^{-1}$<br>Comparing the adsorption capacity of MIPs and NIPs for analytes in individual and mixed solution | [90] |
| Sulfonylurea herbicides (contaminated water) | • Chlorsulfuron/MAA/MeOH: toluene/EGDMA/AIBN<br>• Precipitation polymerization<br>Particle size: 50-75 μm | 250 mg<br>Conditioning: MeOH (5 mL), $H_2O$ (5 mL)<br>Sample: 25 mL<br>Washing: -<br>Elution: MeOH /HAc (5 mL) (90:10, v/v) | 50 mg MIPs in 5 ml MeOH solution<br>• $Q_{MIP}/Q_{NIP}$=5.5<br>Comparing bounded amount of MIPs and NIPs for template and analogues | [91] |
| Organochlorine pesticides (river and rural water) | Substrate: Silica gel<br>BPA/1-(triethoxysilyl) propyl-3-aminopropyl imidazole bromide/tetrahydrofuran: MeOH/-<br>Monomer: ionic liquid<br>Sol gel<br>Ionic liquid-based MIPs | 150 mg,<br>Conditioning: MeOH (3 mL)<br>Sample: 100 mL<br>Washing: -<br>Elution: DCM (12 mL) | 20 mg MIPs in 10 mL of MeOH: $H_2O$ (50:50, v/v) solution shaken for 2 h at 190 rpm<br>• Equilibration: > 75% in 5 and equilibrium in 60 min<br>• Adsorption capacity: $Q_{MIP}$: 30.01 and $Q_{NIP}$: 14.23 mg $g^{-1}$ for BPA<br>Higher extraction recovery of analyte with MIPs compared to NIPs and $C_{18}$ | [92] |

*(continued on next page)*

**Table 1.2.** (*Continued*)

| Analytes (Matrix) | Sorbent | SPE Conditions: | Adsorption and selectivity evaluation | Ref. |
|---|---|---|---|---|
| Phenols (tap, river and lake waters) | Substrate: F-PTW<br>Surface modifier: MPS<br>2-NP/N.A./EGDMA /ACN/AIBN<br>Surface polymerization<br>Film thickness: MIPs: 28.37 and NIPs: 26.73 | 100 mg/100 mL<br>Conditioning: ACN (5 mL), $H_2O$ (5 mL)<br>Sample: 100 mL<br>Washing: ACN (3 mL)<br>Elution: ACN: MeOH (3 mL) (95:5, v/v). | 10 mg MIPs in 20 mL solution<br>- Adsorption capacity: 2-NP: $Q_{MIP}$:23.62 and $Q_{NIP}$: 12.48 mg $g^{-1}$; 3-NP: $Q_{MIP}$: 15.32 and $Q_{NIP}$: 25.44 mg $g^{-1}$; 4-NP: $Q_{MIP}$: 15.99 and $Q_{NIP}$: 24.53 mg $g^{-1}$; 2,4,6-TCP: $Q_{MIP}$:20.68 and $Q_{NIP}$: 2.32 mg $g^{-1}$<br>*IF*: 2-NP: 2.746, 3-NP 3.219, 4-NP 2.561, and 2,4,6-TCP: 1.214 | [93] |
| Phenols (lake and river waters) | Substrate: Silica gel<br>Surface modifier: APTS<br>Diphenolic Acid, BPA/TMOS/MeOH<br>Surface polymerization (Sol-gel) | 500 mg<br>Conditioning: MeOH (5 mL)<br>Sample: 50 mL<br>Washing: -<br>Elution: MeOH: HAc: $H_2O$ (2 mL) (90:5:5, v/v) | 20 mg MIPs in MeOH solution shaken for 1 h<br>• Equilibration: MIPs: 15 min and NIPs: 30 min<br>• Adsorption capacity: $Q_{MIP\text{-}DPA}$: 45, $Q_{MIP\text{-}BPA}$: 38 and $Q_{NIP}$:22 mg $g^{-1}$<br>Comparing the recovery for analytes between MIPs and NIPs | [94] |
| Phenols (reservoir and river water) | Multi-analytes /MAA/DVB/ACN /toluene(3:1, v/v)/AIBN<br>Precipitation polymerization | 60 mg<br>Conditioning: ACN: HAc (3 mL) (9:1, v/v), ACN (6 mL) $H_2O$ (3 mL)<br>Sample: 25 mL<br>Washing: $H_2O$ (3 mL)<br>Elution ACN (400 µL) containing 1% HAc(v/v) | 2 mg in 4 mL aqueous solution shaken for 24 h<br>• $Q_{MIP}$>$Q_{NIP}$ for all phenols<br>*IF*> 2 | [81] |
| Phenols and phenoxy acid herbicides (surface and ground water) | BPA/4-VP/EGDMA/Toluene/AIBN<br>precipitation polymerization | 100 mg<br>Conditioning: DCM (5 mL), ACN/HAc (5 mL) (9:1, v/v) and 10 mL of $H_2O$<br>Sample: 250 mL<br>Washing: DCM (5 mL)<br>Elution: ACN/HAc (5 mL) (9:1, v/v) | Better performance compared with $C_{18}$ and HLB cartridges | [95] |
| 4-Methylimidazole (lake, ground, river and water) | Substrate: DVB<br>Polymer: 4-methylimidazole/ MAA/ethylene dimethacrylate/Chloroform/AIBN<br>Surface polymerization | 50 mg<br>Conditioning: –<br>Sample: 8 mL<br>Washing: –<br>Elution: MeOH/$H_2O$/HAc acid (1 mL) (80/20/0.04) | 20 mg MIPs in 2 ml ACN solution<br>• Equilibration: 40 min<br>• Adsorption capacity: $Q_{MIP}$: 416, $Q_{NIP}$: 227 µmol $g^{-1}$<br>• Chromatographic validation<br>Similar adsorption capacity of MIPs and NIPs for analogues | [96] |

*(continued on next page)*

**Table 1.2.** (*Continued*)

| Analytes (Matrix) | Sorbent | SPE Conditions: | Adsorption and selectivity evaluation | Ref. |
|---|---|---|---|---|
| BPA (tap, lake, and drinking waters) | Substrate: Silica<br>Polymer: BPAF-Si/TEOS<br>Covalent polymerization | 600 mg<br>Conditioning: MeOH, $H_2O$<br>Sample: 1 mL<br>Washing: 1 mL $H_2O$<br>Elution: 2 mL MeOH | • 40 mg MIPs in 1 mL of BPA aqueous solution containing 5% MeOH<br>Equilibration: 1 min | [97] |
| PEs (bottled water) | DBP /MAA/EGDMA/ACN/ AIBN<br>Precipitation polymerization | 200 mg<br>Conditioning: MeOH (15 mL), $H_2O$ (15 mL)<br>Sample: 25 mL<br>Washing: 1 mL, ACN: MeOH (1:1),<br>Elution: MeOH (4 mL) | • MIP-SPE Capacity: 0.980 22 mg $g^{-1}$<br>Higher sorption capacity of MIPs compared with NIPs, $C_{18}$, MWCNTs | [98] |
| DEHP (wastewater) | methacrylamide /N,N_-methylene-bis-acrylamide/DMF and $H_2O$ (2:8), 20 mL mineral oil<br>Suspension polymerization | 5 mg<br>Conditioning: $H_2O$ (5 mL)<br>Sample: 5 mL<br>Washing: -<br>Elution: Chloroform (1 mL)<br>Reuse 6 cycles | 5 mg MIPs in 5 mL $CH_2Cl_2$solution in<br>• Equilibration: 15 min<br>• Adsorption capacity: $Q_{MIP}$: 49.829 and $Q_{NIP}$:19.661 mg $g^{-1}$<br>• *IF*: DEHP:12.86; DMP: 1.413, DEP: 1.609, DBP:2.635<br>• Comparison with commercial cartridges<br>Fewer interfering peaks compared to HLB | [66] |
| Diclofenac (tap, river and wastewater) | Diclofenac/2-VP/EGDMA/ (0.67:2.56:13.88)/Toluene (60mL)/AIBN/<br>Precipitation polymerization | 35mg<br>Conditioning: MeOH (5 mL), $H_2O$ (5 mL)<br>Sample 1000mL<br>Washing, ACN/$H_2O$ (2 mL) (40:60, v/v)<br>Elution MeOH: HAc (9:1, v/v) | 10 mg in 10 mL solution Shaken for 2 h<br>• Equilibration:15 min for MIPs; 15 % of MIP for NIP particles at the same time<br>• Adsorption capacity: $Q_{MIP}$: 324.8 and $Q_{NIP}$:45.2 mg $g^{-1}$<br>Matrix effect: comparison with $C_{18}$ cartridge and NIPs | [99] |
| Acidic pharmaceuticals (lake and wastewater) | Multi-analytes/2-VP/EGDMA/CAN: toluene (50:50, v/v) /AIBN<br>precipitation polymerization | 15 mg<br>Conditioning: MeOH (3 mL), $H_2O$ (3 mL)<br>Sample: 5 mL<br>Washing: DCM/CAN (2 mL) (94:6, v/v).<br>Elution: MeOH/HAc (2 mL) (9:1, v/v) | • Adsorption capacity: Ketoprofen: 0.0487, naproxen: 0.0607, Clofibric acid: 0.052, diclofenac :0.0613 and Ibuprofen: 0.0607 mg $g^{-1}$<br>Comparing efficiency for MIPs and NIPs and compare with $C_{18}$ | [100] |

*(continued on next page)*

**Table 1.2.** (*Continued*)

| Analytes (Matrix) | Sorbent | SPE Conditions: | Adsorption and selectivity evaluation | Ref. |
|---|---|---|---|---|
| FQs (wastewater) | Ciprofloxacin/MAA/EGDMA (0.11:0.88:2.2) MeOH (12 mL) AIBN precipitation polymerization (60 °C) | 100 mg<br>Conditioning: MeOH: HAc (10 mL) (50:50, v/v), MeOH (10 mL) and 10 mL of $H_2O$<br>Sample: 1.6 mL<br>Washing: MeOH (5 mL), H2O (1 mL)<br>Elution: MeOH: HAc (50:50, v/v) | • Higher extraction recovery of MIP-SPE compared with NIP-SPE<br>Good affinity for FQs compared with NP, DMP, caffeine, DEHP, E2, and Octocrylene | [101] |
| FQs (Tap, mineral and river waters) | Substrate: Silica beads Enoxacin/MAA and TFMAA/EGDMA/ACN/ADBV Precipitation - polymerization | 30 mg<br>Conditioning: 10 mL of 2% (v/v) MeOH/TFA and 10 mL of 0.1 M HAc<br>Sample: 10 mL<br>Washing: 2 mL 20:80 (v/v) ACN: $H_2O$ and 0.005% TFA<br>Elution: 1 mL of 2% TFA in MeOH | - | [102] |
| Nitrosamines (tap, bottled, and river waters) | Multi-analytes/MAA/EGDMA/ACN:$H_2O$ (3:2, v/v)/AIBN precipitation polymerization (60 °C) | 90 mg<br>Conditioning: DCM (3×3 mL), MeOH (3×3 mL), $H_2O$ (3×3 mL)<br>Sample: 1000 mL<br>Washing: $H_2O$ (3×3 mL)<br>Elution: MeOH (4 × 3 mL) | • 10 mg MIPs in 10 mL aqueous solution shaken for 24 h<br>• Equilibrium between 50 and120 min<br>$Q_{MAX}$; MIPs: 714–865 and NIPs: 71–191 μg $g^{-1}$ | [103] |

**BPAF**, 2,2-bis(4-hydroxyphenyl); **F-PTW**, Functionalized potassium tetratitanate whisker; **TMOS**, Tetramethoxysilane.

### 1.3.3. Cross-selectivity of MIPs

MIPs can be deployed for extraction of a class of analytes. The cross-selectivity of MIPs towards analogous of the template can represent the specificity of MIPs for the analysis. These selective sorbents used for simultaneous enrichment of a group of environmental pollutants, can be developed using either single [95] or multi-templated [100] approach. Bisphenol E (BPE)-MIPs were applied as the stationary phase for retention of phenolic compounds [84]. The MIPs provided high *IF* for bisphenols (BPs) including

BPA: 2.6 for bisphenol F (BPF): 2.7, bisphenol M (BPM): 2.4, tetrachlorobisphenol A (TCBPA): 2.1 and tetrabromobisphenol A (TBBPA): 1.8, even though other phenolic compounds such as 2-NP and 2,4,5-trichlorophenol (2,4,5-TCP) are not selectively retained by MIP-columns.

### 1.3.4. Other methodologies to determine selective recognition

The selectivity of MIPs for sample preparation is demonstrated by the effect of imprinting on clean-up of the extraction product, the higher extraction efficiency of MIPs in contrast with commercial or NIP sorbents, and better accuracy and precision of MIPs for sample preparation. The chromatograms obtained by MIPs and NIPs for the analysis of triazines were compared. As indicated in Fig. 1.2, MIPs resulted in a more preconcentrated extraction product. Signal to noise ratios, sensitivity, and selectivity of the method are also enhanced due to specific recognition of triazines using the MIP sorbent [104].

Cleaner chromatograms obtained by MIP cartridges compared to commercial cartridges revealed the selectivity of the MIP material towards analytes and reduced extraction of matrix components. Zarejousheghani et al. [85] compared a commercial styrene-divinylbenzene column to a MIP column to analyze an analyte-free matrix (wastewater). Total ion chromatogram for the commercial SPE revealed a complicated mixture,in comparison; MIP-SPE showed a reduced background signal by decreasing the co-extraction of matrix components [85]. The selectivity of MIPs can be demonstrated by comparing the chromatograms obtained by MIP and NIP cartridges after loading a sample containing analyte and structurally related compounds.

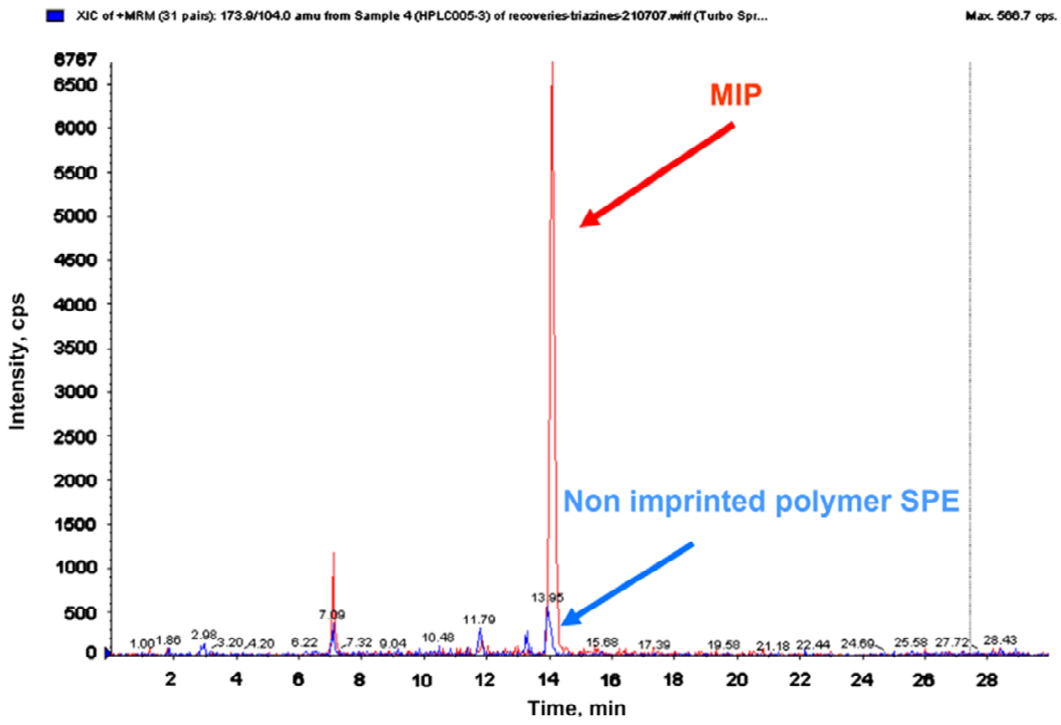


**Fig. 1.2.** Obtained chromatograms of water sample spiked with triazine after extraction using MIP-SPE and NIP-SPE. Reprinted from [104] with permission from Elsevier.

In one of these studies, non-steroidal anti-inflammatory drugs were extracted using a MIP-SPE prepared by diclofenac as the template molecule [64]. The washing solvent is DCM/ACN mixture (94:6, v/v) and elution solvent is DCM/MeOH mixture (85:15, v/v). The template and analogues were removed from the NIP cartridge in the washing step, while the washing solvent can only remove analogues from MIP cartridge. Therefore, the template molecule was selectively retained on the MIPs during the washing step and yielded 98% recovery after elution step. This selective rebinding demonstrates successful imprinting of diclofenac in both functionality and shape of the MIP microstructure. Duan et al. [100] synthesized MIPs for the selective enrichment of acidic pharmaceuticals from environmental water samples. Commercial $C_{18}$ SPE cartridges have similar adsorption

properties compared with MIP-SPE in clean water toward these acidic analytes, but its performance in real waters such as lake and wastewater was diminished. This reduction is due to non-polar interactions between carbon–hydrogen bonds of the analytes and carbon-hydrogen bonds of the $C_{18}$ sorbent. These interactions, which are non-specific, yielded an early breakthrough of the analytes using $C_{18}$ cartridges in the presence of matrix interferences. Another feature of MIPs is to enhance the precision and accuracy of the analytical method through selective adsorption of analytes [95]. As can be observed in Fig. 1.3**,** co-extraction of the matrix components can cause overlapping chromatographic peaks or reduce the signal intensity using conventional SPE cartridge phases. For example, diuron which was extracted using $C_{18}$ and hydrophilic-lipophilic balanced (HLB) cartridges, can overlap with BPA as the target analyte. However, analytes adsorbed by non-selective interactions can be rinsed from MIPs during the washing step and analytes adsorbed by selective interactions with imprinted cavities were desorbed during elution step which increases the reliability and sensitivity of the analysis [95].

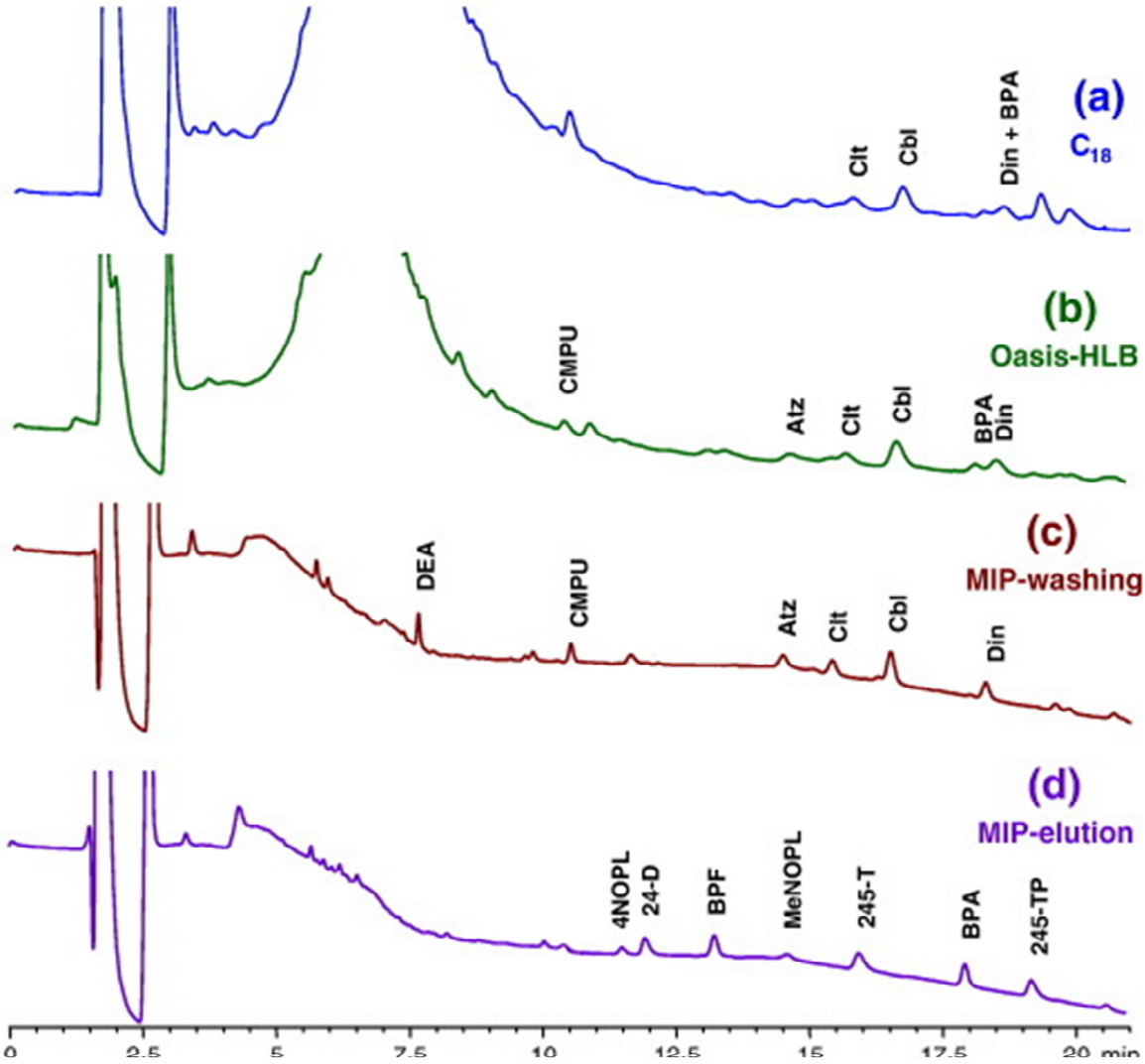


**Fig. 1.3.** Chromatograms obtained of river water samples after preconcentration using: A) $C_{18}$-SPE; B) Oasis HLB-SPE; C) MIP-SPE, washing step; D) MIP-SPE, elution step. Reprinted from [95] with permission from Elsevier.

## 1.4. Optimization of MIP formulae

There are several factors in preparation of MIPs which can be optimized to improve the selectivity, including the type of template, monomer(s), and crosslinker(s) as well as their relative ratios. The type of porogenic solvent and its volume is also important. For this

purpose, MIPs with different formulae can be prepared and used for binding experiments to determine the optimum composition of the MIP formula leading to the highest selectivity [105].

The selection of template is a crucial step especially for the analysis of a group of compounds with MIPs prepared using a pseudo template. The template should pose structural similarities to the analytes and functionalities to form maximum binding affinities. A competitive study between BPA and diphenolic acid with similar structures indicated that diphenolic acid with the functional group could form stronger H-bonding as compared to BPA as a template. The efficiency of SPE for TBBPA, diethylstilbestrol (DES), nonylphenol (NP), and 2,4,5-TCP by using diphenolic acid-MIPs were higher than that of BPA-MIP [94]. Chromatographic characteristics of MIP packed columns can be implemented to select a suitable template. Individual templates were used for the preparation of MIP columns for benzophenones [106]. 2,2,4,4-tetrahydroxybenzophenone imprinted polymer between other individual benzophenones provided the highest imprinting and capacity factors among all analogues. The superior selectivity confirms the formation of recognition sites through the hydroxyl groups using this molecule. Sun et al. [53] proposed a screening step for selecting the template. They injected potential molecules into a non-imprinted column of MAA-EGDMA-ACN to investigate the affinity of potential templates which can be further assessed using chromatographic evaluation and binding experiments.

Sun et al. [64] reported NMR studies to analyze the recognition mechanisms and selection of a suitable template. They utilized $^{1}$H NMR to investigate interactions of both diclofenac and 2-vinylpyridine (2-VP) at different amounts. Proton shift of carboxyl groups

in the template from 11.204 to 10.846 ppm by increasing the concentration of monomer indicates ionic interaction responsible for molecular recognition. The cost and time required for SPE or chromatographic optimization can be reduced using simulation. Simulation methods can be used for selecting structural analogue [107] or functional monomer [108]. This methodology provides the minimum energy level of the template–monomer complex and assists finding the most suitable composition.

Optimization of the template–monomer ratio also preserves the best efficiency and selectivity. A high ratio of template to monomer (1:2) diminishes the recognition of the polymer due to an excess amount of the template and lower number of specific binding sites. On the other hand, lower ratios of template (1:8) yield in decreased number of the template–monomer complex in pre-polymerization solution and specific cavities for selective adsorption. The standard ratio of analyte to functional monomer in most of the studies is 1:4 [77]. The ratio of monomer: crosslinker needs to be optimized according to the efficiency, selectivity and required rigidity of the MIPs which can be varied according to the format and application. In the clenbuterol-MIPs developed by Tang et al. [59] the optimum ratio of monomer–crosslinker was 1:2 providing the highest adsorption capacity and imprinting effect. The higher amount of crosslinker generated a rigid structure with steric hinderance impeded template removal and formation of specific cavities for selective adsorption.

The solvent plays a critical role in non-covalent MIPs. It can be optimized via chromatographic evaluation. Three porogenic solvents including ACN, chloroform and toluene were used to imprint phenols. The retention factors and *IFs* of analytes obtained by MIP and NIP columns showed that ACN has a better ability to provide selective retention

of chlorophenols (CPs) [55]. Zhang et al. [109] adopted a polarizable continuum model to investigate the effect of solvent on the selectivity of atrazine-MIPs. According to their calculation, toluene with smaller dipole moment is a more favorable solvent than ACN due to less interruption of MAA and atrazine complex allowing for higher imprinting effect. Because of the similarities between toluene and atrazine, this solvent resulted in a porogen imprinting effect and ~10 times higher adsorption capacity than ACN. However, the specificity of the toluene-MIPs for atrazine compared to other pesticides is lower than ACN-MIPs due to the large pore size obtained using toluene. Therefore, selection of the porogenic system relies on different properties of MIPs such as binding capacity, imprinting effects, the number and size of pores, and specificity.

Experimental design can be utilized for preparation of MIPs. Hao et al. [51] used a response surface methodology with central composite design to prepare a MIP coating at the surface of functionalized nanoparticles. The influencing factors included glutaraldehyde as the active groups at the surface of nanoparticles, monomer selection, preparation temperature and time. The response which was the difference between the adsorption capacity of MIPs and NIPs was obtained for the designed experiments. The obtained results were evaluated using analysis of variance (ANOVA) to investigate the significant factors. A quadratic polynomial model containing regression coefficients and their significance was obtained. The optimum level of each parameter can be achieved by designing the response surface based on experimental levels of variables. The maximum response of the surfaces was explained by the corresponding level of experimental variables that lead to higher response.

## 1.5. MIP-SPE

SPE is a routine sample preparation method for water analysis and is used to perform clean-up, preconcentration, class fraction and extraction of analytes. In this technique, materials such as $C_{18}$, HLB, and ion-exchange stationary phases have been applied to extract compounds with a wide range of physicochemical properties (i.e., solubility, pKa, LogP, and functional groups) [110]. To enhance selectivity in SPE and analytical reproducibility and sensitivity, MIPs can be deployed as sorbent [52]. MIP-SPE as the most common application of MIPs in sample pre-treatment is executed by packing synthesized sorbent into cartridges using dry [59] or slurry packing [73, 77, 86]. Selective extraction of analytes is achieved by regular steps of SPE including conditioning, sample loading, washing and elution [33]. As illustrated by Fig. 1.4a, after conditioning of the MIP cartridge using an appropriate solvent to increase the surface area and activate binding sites, the sample solution is loaded. MIP cavities retained the analytes by adsorption through selective interactions during the washing step while interferences are removed due to weak non-selective adsorption. A desorption solvent capable of disturbing the interactions between imprinted binding sites and analytes was applied for elution. The eluent can be directly analyzed using a quantification method or dried and reconstituted with a suitable solvent for the detection system used. MIP-SPE has been widely used as preconcentration method for selective analysis of pollutants in various water samples such as wastewater [111], seawater [112], river water [113] and drinking water [103].

The similarities in structure and functionalities of the template and analytes are responsible for selective recognition of MIP-SPE for structurally related compounds. For

example, the efficiency of SPE using fluoroquinolone-imprinted MIPs was 60% for flumequine compared to 100% for fluoroquinolones (FQs). This difference is related to the piperazinyl ring of FQs, which is caused by imprinted cavities [101]. The sensitivity of the analytical method obtained by MIP-SPE can be enhanced by 2–4 times than that obtained by non-selective SPE protocols such as an HLB phase. However, careful washing steps should be implemented for conventional SPE to remove the co-retained compounds, MIP-SPE provides a more sensitive method without optimized washing steps [52]. MIP-SPE was used for extraction of different environmental pollutants. As mentioned in Section 1.3.1, the adsorption capacity of MIPs can be obtained by incubation of the sorbent with an analyte solution. Another measure is obtaining the adsorption capacity of MIPs and NIPs packed in cartridges. In a study to develop MIP-SPE for atrazine herbicides, the adsorption capacities of MIPs and NIPs were obtained 2.51 and 0.64 μg $g^{-1}$, respectively [78].

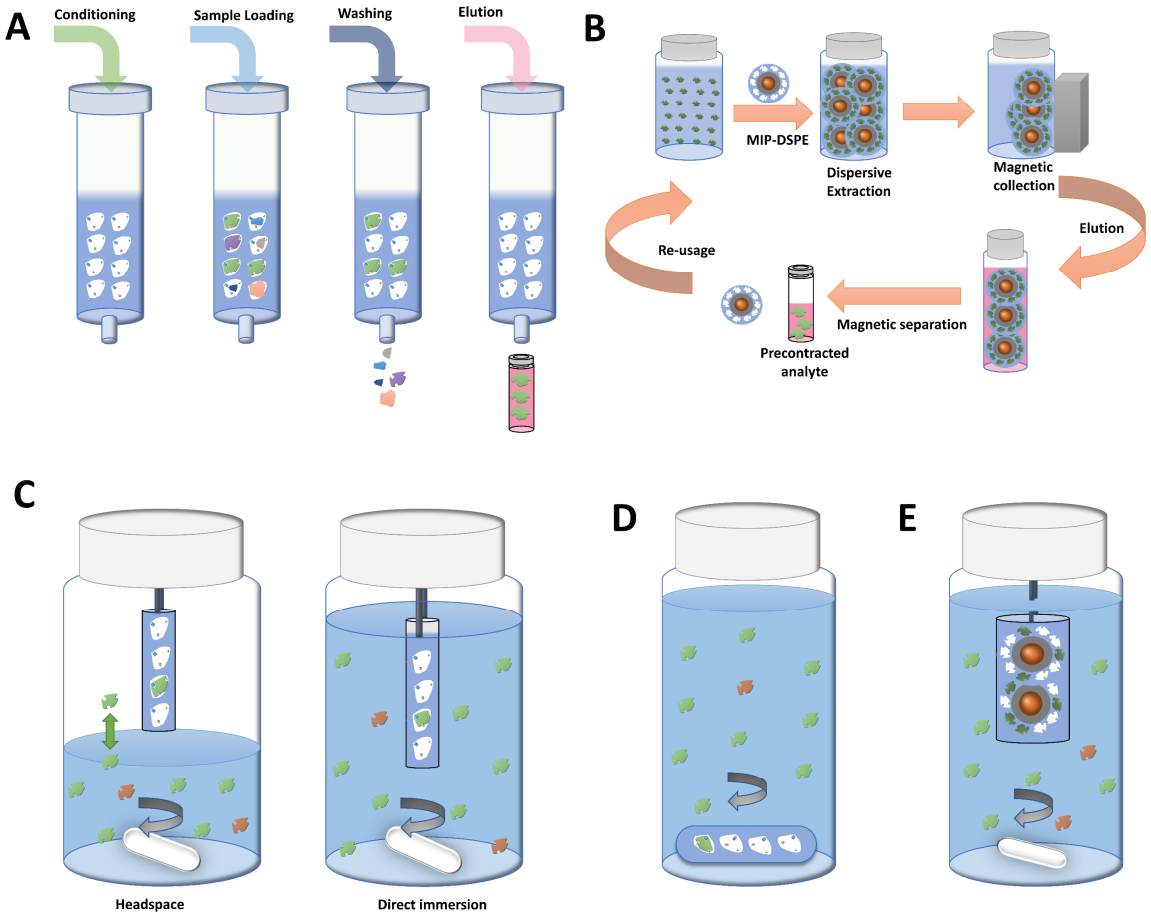


**Fig. 1.4.** Schematic representation of the application of MIPs as sorbents in different extraction techniques: A) MIP-SPE; B) MIP-DSPE; C) MIP-SPME; D) MIP-SBSE; E) SLM-MIPs

Commercial MIP-SPE cartridges were also used for measurement of pharmaceuticals such as non-steroidal anti-inflammatory drugs [114], β-blockers [115, 116] and antidepressants [52] in wastewater and neutral waters. MIP-SPE cartridges were used for preconcentration of an estrogen (DES) in seawater. The complicated matrix due to the salinity disturbs the binding affinity of the polymer toward the analytes. This interference can be minimized using MIP-SPE [67]. Online MIP-SPE enables simultaneous

extraction and detection of the analytes with reduced analysis time and increased repeatability due to the elimination of multiple transfers and clean up steps [88]. A miniaturized format of SPE, namely pipette-tip SPE, can be performed by packing low amount of MIP particles (2 mg) in a pipette-tip [117]. A high extraction efficiency (97%) was obtained for methyl red from 10 mL water samples using such amount of sorbent. The elution step can be performed by several aspirating/dispensing cycles and allows for high throughput. Additionally, the small bed is advantageous to reduce the solvent consumption and required time for evaporation.

### 1.5.1. Synthesis of MIPs for SPE

#### *1.5.1.1. Bulk polymerization*

In MIP-SPE, the polymeric material is usually synthesized by bulk polymerization through thermal or photoinitiation. After grinding and sieving the resultant polymer, the MIP particles collected and subjected for template removal. The SPE cartridges packed with MIP particles are used for selective extraction of target analytes. These selective sorbents synthesized through bulk polymerization offer several advantages such as stability, robustness, resistance to a wide range of pH, temperature, and organic solvents. Moreover, it is notable that the preparation of MIPs is easy and cheap in comparison to natural antibodies. This polymerization technique is the most common method to prepare MIPs for analysis of environmental contaminants such as pharmaceuticals [59], pesticides [72], EDCs [74], and BPs [84] from water samples. A comprehensive list of the developed methods and the obtained results are summarized in Table 1.1. The adsorption capacity of MIPs is more than that of commercial $C_{18}$ and activated carbon [78]. However,

bulk polymerization is a time-consuming method for the preparation of selective materials for SPE cartridges and provides inaccessible sites for specific interactions. Additionally, the synthesized MIPs lead to a low yield of produced sorbent due to the waste of fine particles. The selective sites of synthesized particles are destroyed during grinding, and this can reduce adsorption capacity and selectivity [99]. Therefore, other polymerization methods should be considered to prepare MIPs.

*1.5.1.2. Surface polymerization*

The surface imprinting technology is a powerful tool to deposit a thin layer of polymeric material on different substrates such as carbon nanotubes (CNTs), $Fe_3O_4$, $TiO_2$, $SiO_2$. This layer of MIPs containing imprinted cavities at the surface of the particles provides more accessible adsorption sites, rapid mass transfer, and fast binding kinetics and high selectivity [94].

$TiO_2$ with low toxicity and photo and chemo stability is cheap and easy to prepare. The prepared nanoparticles (21 nm) were modified with immobilization of 3-aminopropyltriethoxysilane (APTS) (silanization) and acryloylation with acryloyl chloride. The synthesized particles (25 nm) were introduced during the polymerization reaction of MAA to form a thin and uniform MIP shell (25–37 nm). These thin film-coated nanoparticles yielded rapid equilibration (90% equilibrium within 8 h incubation). The higher capacity of MIPs over NIPs (16.02 times in water) indicates the formation of specific cavities in the presence of the template leading to excellent recognition properties for triazine herbicides in water samples [89]. For $Fe_3O_4$-MIPs, the magnetic particles were firstly coated with silica (Stöber process) and then functionalized with 3-

methacryloyloxypropyltrimethoxysilane (MPS). For this purpose, MPS was sonicated with toluene and then added to a solution of $Fe_3O_4$@ $SiO_2$ in toluene for 10 min. A solution of MPS in toluene was dropped into $Fe_3O_4$@ $SiO_2$ solution within 30 min. The resultant solution was stirred for 24 h under $N_2$ protection at 110 °C. Similar adsorption kinetics of MIPs and NIPs reveals that adsorption sites are at the surface of the core-shell adsorbent material. Higher extraction capacity of MIPs over NIPs proved the selective sites of MIPs for adsorption of sulfonamides [118]. A thin layer of MIP can also be formed at the surface of silica. The resulting MIPs have a fast mass transfer of analytes and saturation of sorption capacity could occur within 1 min [97].

Instead of template–monomer interactions, the interaction between the template and functional groups at the surface of the substrate can be used to form cavities containing imprinted sites. In this surface polymerization technique, MPS is grafted onto the surface of potassium tetratitanate whisker. These grafted functional groups form complexes through inter-molecular interactions with template molecules which then yields imprinted crosslinked sorbent with reactive sites. The template removal was completed using Soxhlet extraction in MeOH and resulted in the formation of complementary cavities towards 2-NP. Close relative separation factors obtained for 3-NP and 4-NP with a similar structure to the template. Thus, MIPs have good affinity towards these analytes due to the presence of phenyl groups with nitryl groups. However, the high relative separation factor (3.969) for 2,4,6-TCP showed that cavities with similar shape could not adsorb selectively through H-binding formed by the imprinting process [93].

*1.5.1.3. Precipitation polymerization*

Another way to solve the associated difficulties with bulk polymerization is precipitation polymerization. In precipitation polymerization, a similar procedure to the bulk polymerization is adopted, but large volumes of porogen are used. Larger volumes of porogen result in MIP particles with spherical morphology and larger surface area [98]. Lu et al. [81] used a precipitation method for the synthesis of a multi-templated MIPs and NIPs for recognition of phenolic compounds. In comparison with bulk polymerization, precipitation polymerization increased the sorption capacity of the material due to the larger surface area from ~481 to ~759 $m^2$ $g^{-1}$ and yielded a more homogeneous morphology. The MIPs provided higher affinity towards the templates compared to NIPs. However, structural analogues were similarly adsorbed by both the MIPs and NIPs due to non-specific adsorption. In a similar study, a diclofenac-imprinted polymer prepared by precipitation polymerization enhanced the adsorption capacity by ten times compared to MIPs prepared by bulk polymerization and sample breakthrough volume from 200 to 1000 mL [64, 99]. The higher adsorption capacity is the result of a larger surface area of the porous structure and a more significant number of binding sites for recognition of analytes. Additionally, the rapid equilibrium time of these MIPs resembles the accessibility of synthesized MIPs through the precipitation method for sample preparation [81]. The selection of porogen in precipitation polymerization is crucial and needs careful optimization since the effect of the solvent on the size of the pores and the surface area of the polymer [90].

*1.5.1.4. Pickering emulsion polymerization*

Precipitation polymerization employs a large volume of porogen and is limited by the need for highly specific reaction conditions. The Pickering emulsion approach has been used to prepare regular MIP particles with accessible imprinting sites and overcomes some of the challenges of precipitation methods. The Pickering emulsion uses solid particles to stabilize the formation of droplets in a mixture of two immiscible liquids, eliminating or reducing the reliance on surfactant emulsifiers [63, 119], leading to cheap and environmentally friendly procedures [120]. Sun et al. [63] used silica nanoparticles as the stabilizer. Therefore, surface tension between two immiscible phases is reduced and polymerization occurred in the stabilized droplets. After polymerization, the mixture containing the MIPs is treated with hydrofluoric acid to remove the silica particles. The resulting imprinted polymers can be used for selective extraction of pollutants directly from water and wastewater or from a nonpolar phase after solvent extraction to isolate hydrophobic compounds.

To avoid strongly caustic properties of hydrofluoric acid, several other stabilizers were proposed to prepare Pickering emulsion such as attapulgite [119], graphene oxide (GO) [121], and halloysite nanotubes [122]. Holloysite nanotubes ($Al_2Si_2O_5(OH)_4 \cdot nH_2O$) have also been used as stabilizers to prepare water compatible MIPs. The surfaces of these MIPs are hydrated and there is a possibility of multiple-site binding due to negatively ($SiO_2$) and positively charged ($Al_2O_3$) sites which provide better imprinting in water samples. Adsorption studies of analytes demonstrated that equilibration of polymers synthesized through Pickering emulsion was faster than for particles made using conventional polymerization processes. The MIPs exhibited a large capacity for adsorption

of 2,4-dichlorophenoxyacetic acid in water in comparison to NIPs. $Q_{MIP}$ and $Q_{NIP}$ were 60 and 32 mg $g^{-1}$, respectively. Furthermore, the adsorption of phenoxyacetic acid with similar functionality but different structure to the template molecule was determined using prepared sorbents, $Q_{MIP}$: 25 mg $g^{-1}$ and $Q_{NIP}$:20 mg $g^{-1}$ [120]. These studies demonstrated the suitability of Pickering polymerization to prepare MIPs for selective extraction of target molecules.

### 1.5.2. MIP-SPE parameters

Several factors are influencing the efficiency of MIP-SPE (Fig. 1.4a) and selectivity of this technique that should be optimized such as pH and salinity for rebinding solution, wash solvent and elution solvent [80].

#### *1.5.2.1. pH of rebinding*

The pH of the sample can influence the efficiency of rebinding analytes to the recognition sites of MIPs, especially for acidic or basic analytes. Adjustment of sample pH for phenolic compounds as weak acids showed that neutral pH is the optimum value for water samples. In neutral conditions, phenols exist in their molecular forms and bind strongly with MIPs synthesized based on hydrogen bonding [81]. A similar trend was observed for rebinding atrazine through selective interactions of H-binding. Atrazine is adsorbed weakly by H-bonding sites within cavities due to the formation of protonated carboxylic groups of this analyte [85]. For extraction of acidic pharmaceuticals, the extraction efficiency was remained unchanged in the range of 3 and 8; however, increasing the selectivity of MIPs over NIPs at pH>4 suggested that this range is suitable for extraction

of these analytes through selective interactions with MIPs [100]. Additionally, the extraction efficiency of PEs has shown no changes at different pH (3, 5, 7 and 9) due to selective binding sites of MIPs. Thus, MIP-SPE cartridges can be used for the analysis of real samples without sample manipulation, such as pH adjustment [98].

*1.5.2.2. Effect of salinity*

In order to employ MIP-SPE for environmental analysis, especially seawater samples, the efficiency of the MIP sorbents in saline environments needs to be assessed. Salt addition is used in LLE-based extraction techniques to reduce the solubility of analytes in the aqueous samples. This parameter improves analytes' mass transfer towards the extraction phase. However, this effect could be varying depending on the nature of the analytes and nature of the polymer, particularly the interaction used in MIPs to adsorb analytes. Guan et al. [93] investigated the efficiency of MIP-SPE for the extraction of phenols from water. Their results showed an increase from ~70 to ~90% for nitrophenols and from 30% to 50% for 2,4,6-TCP. This enhancement is due to lowered solubilities of these analytes in water. The solubility of analytes and their working range in the water is also crucial to assess the efficiency of MIP-SPE in saline environments. The extraction of non-steroidal anti-inflammatory drugs was remained unchanged by increasing the salt content [73]. Due to the exhaustive nature of SPE, salt addition is not always used to improve the extraction efficacity; however; it is essential to investigate MIP-SPE in real samples. Characteristics of these complex matrices include salinity, pH and dissolved organic matter that can influence extraction efficiency. For example, the extraction

efficiency of malachite green using MIP-SPE reduced from 88.56% in standard aqueous solution to 30.63–59.62 in seawater samples [123].

*1.5.2.3. Wash solvent*

One of the most common interactions in the literature, which is used to form the template–monomer complex in the pre-polymerization mixture, is hydrogen bonding. This interaction is strong in aprotic and slightly polar solvents used for the pre-polymerization mixture. However, the uptake efficiency and selectivity of analyses due to hydrogen bonding are reduced in highly polar solvents such as water. Hydrophobicity is superior in aqueous matrices which leads to adsorption of analytes through non-specific binding sites [124]. The selectivity of MIP sorbents and precision of the method are reduced by co-extraction of the matrix components. Implementation of a suitable washing step can reduce the interfering compounds retained by the MIPs making MIP-SPE suitable for environmental analysis [78]. This solvent should be strong enough to overcome non-specific interactions between the polymeric network and the analyte and ineffective on specific interactions between imprinted sites and the analytes. In other words, this is solvent should poorly elute the analytes and readily wash off interferences. ACN is a polar solvent with weak hydrogen-bonding properties is unable to break the specific hydrogen-bonding interaction, however; most of the interferences adsorbed to the MIPs through hydrophobic interaction leading to non-selectivity are washed out [86].

Different washing solvents can be used for this step depending on the nature of the analyte and the polymer such as DCM for CPs [71], $H_2O$ for mebendazole [72], ACN: $H_2O$ (1:1) for benzophenones [74], $H_2O$ followed by DCM for atrazine [85]. A mixture of DCM

and ACN for acidic pharmaceuticals [100] from a polymer onto which the analytes are adsorbed selectively through H-binding interaction. A higher proportion of ACN or other polar solvents such as MeOH could ruin the selective interactions. A suitable washing solvent is very helpful especially in complex matrices such as wastewater samples. Although a diclofenac imprinted polymer could retain some co-existing pharmaceuticals such as carbamazepine as well as the analyte, application of ACN/water (40:60, v/v) as a washing solvent removed co-extracted interferences. This interfering molecule was not bound to imprinted cavities as strongly as diclofenac due to improper size and functionality [99]. Application of MIPs for the analysis of a group of analytes with a range of polarity and solubility such as the analysis of EDCs necessitates the implementation of several rinsing steps [86]. The washing solvent obtained at different steps can be analyzed either individually or cumulatively to ensure complete removal of interferences [65]. The volume of the washing solvent should be enough to disturb non-specific polymer–analyte interactions and remove interferences from the sorbent [78].

*1.5.2.4. Elution solvent*

The retained analytes were eluted with a solvent capable complete desorption. Selection of solvent depends on the nature of analytes and interaction used for selective retention on MIP-SPE such MeOH [76, 78] or a mixture of MeOH with water for polar pesticides [79]. Due to the presence of hydrogen bonding which is responsible for retention mechanism by MIP-SPE, usage of a solution containing acetic acid (HAc) with MeOH [59] or ACN [73] to ensure desorption of analytes is necessary. The presence of HAc improves the efficiency of elution of analytes such as phenols [82] from MIP-SPE. The possible

explanation is a competition of HAc with functional groups in the binding sites which facilitates the release of analyte from MIP-SPE bed. Sun et al. [74] utilized a solution of TFA (2%,) as a protic solvent in MeOH to disturb H-bonding between MIPs and benzophenones.

In MIP-SPE, loading organic solvents during different steps causes swelling of packed polymeric sorbent. This swelling reduces available selective sites and increases channels, void effects, back pressure and volume of organic solvents required for elution of analytes as well as the analysis time. Reducing the amount of MIP sorbent can decrease this effect but results in low sorption capacity of the cartridge. To deal with swelling of MIP particles, they are embedded with silica gel with a low affinity towards atrazine. This mixed bed SPE (using 10 mg of sorbent) yielded a higher extraction efficiency and lower limit of detection compared with conventual MIPs or other commercially available sorbents due to the homogenous dispersion of MIPs in the silica gel and availability of the imprinted sites. In addition to the sensitivity using mixed bed SPE-MIPs, the reproducibility between different columns was increased from ±53 % to ±16.1% [85].

*1.5.2.5. Other factors influencing MIP-SPE efficiency*

Conditioning the MIP-SPE column before sample loading activates adsorption sites and maximizes the selective interactions on MIPs structure [37]. As shown in Tables 1.1 and 1.2, conditioning can be performed using organic solvents (i.e., MeOH and ACN) and water. The pH of water in the conditioning step can be optimized to increase the selectivity of adsorption. The effect of flow rate on the efficiency of MIP-SPE should be optimized. An increased flow rate can cause low efficiency due to insufficient time for interactions

between the analyte and selective polymeric phase, on the other hand, a low flow rate could reduce the efficiency by additional interactions [82, 98]. Optimization of the mass of the polymer packed in the cartridge is a variable that could affect the selectivity of the sorbent. The amount of the polymer should be enough for specific sample volume and concentration. However, decreasing the amount of packed MIPs in the column could reduce non-specific interactions resulting in the selective adsorption of analytes by smaller volumes of MIPs [82]. Another crucial factor for MIP-SPE is the breakthrough volume by which adsorption capacity of packing, MIPs, can be calculated [52].

## 1.6. MIP-DSPE

MIP-SPE cartridges have been widely used for selective extraction of analytes from environmental water samples. However, the packing of MIPs in SPE cartridges has potential drawbacks, such as clogged columns when using complex matrices and swelling of the MIPs in organic solvents, both of which can increase the back pressure and consumption of organic solvents [88]. DSPE overcomes these issues by allowing for dispersion of MIP particles into the sample. There has been lots of applications of MIP particles used for extraction process followed by collection of MIP particles using filtration [125] or centrifugation [126]. However, incorporation of a magnetic nanoparticle core aids in the recovery of the solid phase (Fig. 1.4b). The application of nanomaterials in sample preparation is appealing because of the intrinsic features of nanoparticles. These particles have small size yielding high surface areas and suitable for miniaturized sample preparation techniques [127]. Additionally, these materials can be easily functionalized to introduce

selective sites for uptake of analytes such as R-$NH_2$ for H-bonding [88]. Therefore, development of synthetic strategies based on surface polymerization of MIPs onto the solid substrate allows for the combination of nanotechnology with MIP technology. The core-shell MIPs are dispersed in the solution via ultrasonic dispersion [88], magnetic stirring [128], or mechanical shaking [129, 130] to extract analytes. After that the particles are magnetically collected, and enriched analytes are desorbed using a proper solvent. The dispersion technique reduces the sample preparation time and enhances the extraction efficiency due to the rapid mass transfer of analytes. This acceleration is attributed to the large surface area of MIP particles and accessible imprinted sites on the coated thin layer.

Iron nanoparticles ($Fe_3O_4$) [108] and CNTs [131] have been used as substrates for MIP-DSPE. $Fe_3O_4$ with relatively low toxicity, low cost, and easy preparation are extensively applied in combination with MIPs due to the effectiveness of magnetic collection rather than filtration or centrifugation [44]. $Fe_3O_4$ is usually synthesized through co-precipitation of $Fe^{+2}$ and $Fe^{+3}$ in presence of sodium hydroxide [128] or ammonium hydroxide [67]. A conventional method to prepare them as substrate for MMIPs is to functionalize with oleic acid [128, 132-134]. $Fe_3O_4$@MIPs have been used for selective extraction of sulfonamides [128], FQs [132], BPA [133], and CPs [134] from environmental water samples. To avoid aggregation of $Fe_3O_4$, these nanoparticles can be coated with $SiO_2$ through the Stöber process. In this process, tetraethyl orthosilicate (TEOS) is hydrolyzed under basic conditions [67] (Fig. 1.5). The $SiO_2$ coating is an ideal substrate to form MIPs owing to excellent properties such as chemical and thermal stability and easy modification of the silica surface for further polymerization steps [44].The resultant core-shell $Fe_3O_4$@$SiO_2$ are functionalized with vinyl groups using silane coupling

agents such as MPS [135], vinyltrimethoxysilane (VTMOS) [136] , and APTS [137]. Sinalization allows for grafting MIPs during the polymerization reaction. This general procedure has been employed in a wide range of applications such as extraction of phenols [137], pesticides [130], pharmaceuticals [134] and EDCs [67] from water samples (Table 1.3). As can be seen in the Table 1.3, MMIPs show excellent efficiency in the extraction of organic pollutants from water samples. Additionally, most of the selectivity studies which were performed in an aqueous media revealed selectivity of the MIPs compared to NIPs due to the accessibility of the MIP binding sites at the surface of the core-shell particles. Optimization of the MIP coating is a crucial part of MIP-DSPE which is possible using molecular simulation. Yang et al. [137] simulated interaction between phenol as a template and different monomers including MAA, acrylamide (AM), and 4-vinylpyridine (4-VP). The composition containing MAA and phenol giving the most stable binding energy provided satisfactory selectivity (*IF*~3) can be used for other phenols ($K'_{4\text{-NP}}$>20).

Like silica coating, fly ash was proposed by Pan et al. [138] to avoid aggregation of $Fe_3O_4$ nanoparticles. The fly ash contains negative charges due to the presence of $Al_2(SO_4)_3$ and $SiO_2$ groups. These groups can electrostatically bind to iron cations in coprecipitation reaction with iron particles and used as a substrate for selective polymeric sorbents. These MMIPs, which were examined using rebinding studies in aqueous matrices [67, 130, 133, 139, 140] have been demonstrated as selective sorbent and used for to perform DSPE for enrichment of pollutants in environmental waters. Conversely, the rebinding studies can be performed in organic solvents [51, 141] or a mixture of water with organic solvents [118,

138]. These rebinding media which can not reflect the interactions in aqueous media, are not able to provide an accurate measure of selectivity of MMIPs.

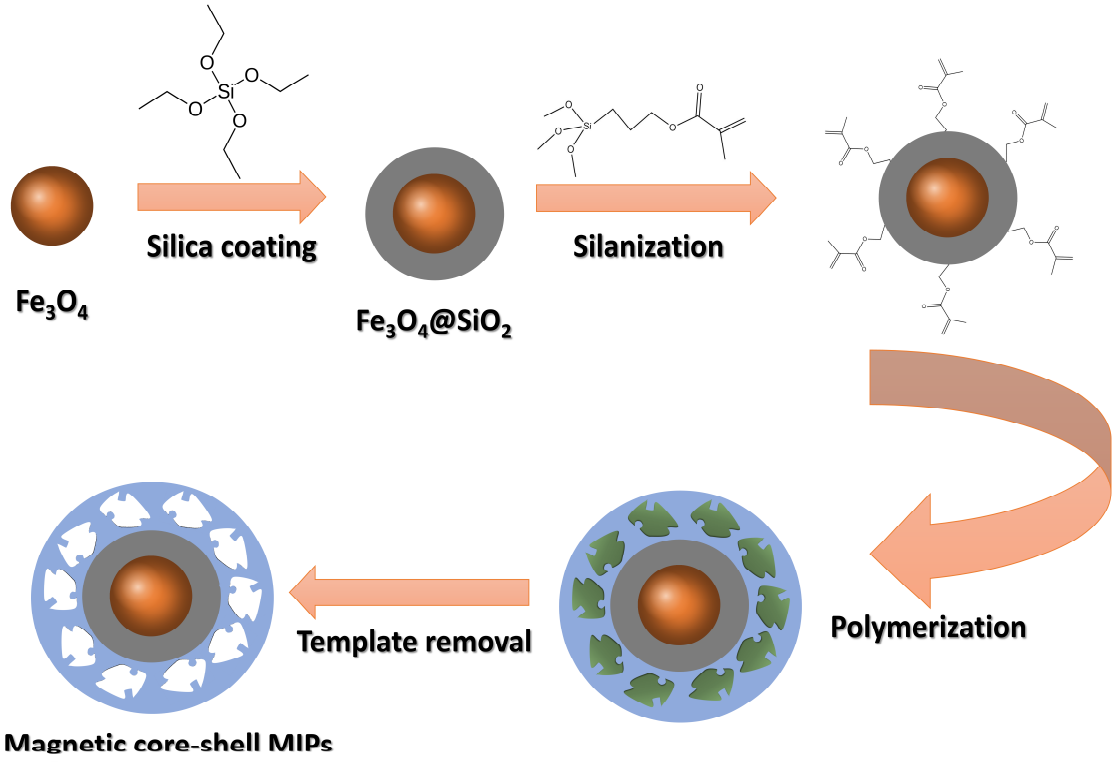


**Fig. 1.5.** Schematic representation of the preparation of MMIPs.

Various carbon-based materials have been employed as a substrate to grow selective binding sites to uptake analytes from aqueous matrices. CNTs are common materials in SPE packings due to its large surface area, mechanical strength, and chemical stability. Rao et al. [142] developed a substrate by a combination of CNTs and $Fe_3O_4$ to synthesize core-shell MIPs. Their results showed that CNTs@$Fe_3O_4$@MIPs could be effectively employed for selective extraction of EDCs. Because of the presence of binding sites on a thin layer of MIPs (30–35 nm) on the surface of the sorbent, the equilibrium state is achieved rapidly (20 min). Mesoporous carbon on $Fe_3O_4$ is prepared by carbonization of $Fe_3O_4$@$SiO_2$ and removal of $SiO_2$ using NaOH etching [143]. These particles used as a substrate for surface

polymerization of MIPs provided pore size 9.9 nm, and large BET surface area 430.25 $m^2$ $g^{-1}$. $Fe_3O_4$@void@C-MIPs allow for large adsorption capacity 92–123.9 mg $g^{-1}$ for selectivity (*IF:* 2.3–3.8) for extraction of PEs. The higher adsorption capacity of $Fe_3O_4$@void@C-MIPs as compared to $Fe_3O_4$@$SiO_2$@C-MIPs showed that the cavities between the two layers provided sufficient recognition sites for higher adsorption of target molecules [143].

Multifunctional supports can be deployed to imprint target molecules and increase selective binding sites. Chitosan with amino and hydroxyl groups was coprecipitated with $Fe_3O_4$ to achieve support to form MMIPs. As a result, sulfamethazine (SMZ) and sulfamethoxazole (SMX) were selectively adsorbed from water samples with an *IF* 3.2 and 3.48, respectively [144]. The GO/chitosan incorporated magnetic support was also proposed by Barati et al. [145]. GO as a carbon-based material with large surface area and oxygen-containing functionalities (epoxy, hydroxyl and carboxylic groups) in combination with chitosan-$Fe_3O_4$ can form porous MMIPs. The $Fe_3O_4$@chitosan@GO@MIPs possessed adsorption capacity of 66.2 mg $g^{-1}$ and *IF* 4 for fluoxetine in water samples. Mesoporous silica can surely be an excellent choice to increase the porosity of substrate and thus the total adsorption capacity of MMIPs. Wei et al. [134] synthesized dual template MIPs on the surface of magnetic mesoporous silica for extraction of antibiotics from water samples. The resultant polymer with a spherical shape, rough surface, and a diameter ranging from 120-300 nm, showed adsorption capacity 146.5 and 190.1 mg $g^{-1}$ for chloramphenicol and florfenicol, respectively.

**Table 1.3.** Application of MMIPs for selective extraction of analytes from water samples.

| Analytes (Matrix) | Substrate–Functionalization agent | Template/ Monomer/ Crosslinker/ Porogen | Template removal | Rebinding solution | Adsorption and selectivity evaluation | Ref. |
|---|---|---|---|---|---|---|
| FQs (lake water, river water, sewage water) | $Fe_3O_4$-Oleic acid | Ciprofloxacin/ MAA/EGDMA (1:8:20)/Ethanol | MeOH/ HAc (1:1, v/v) | $H_2O$ | $Q_{MIP}$: 0.13 mmol $g^{-1}$<br>$Q_{NIP}$: 0.05 mmol $g^{-1}$<br>• Comparing absorbed amount of MIPs and NIPs for the template and structural analogues FQs antibiotics | [132] |
| *p*-Aminosalicylic acid (wastewater) | $Fe_3O_4$-VTEOS | *p*-Aminosalicylic acid/MAA/EGDMA/(1:6:30)/ACN | MeOH/ HAc (8:2, v/v) at 60 °C | $H_2O$ | $Q_{MIP}$: 70.92 mg $g^{-1}$<br>• *IF*: 3<br>• Lower capacity for Salicylic acid, Nitrazepam, Diclofenac, and Ibuprofen | [140] |
| Amphenicol antibiotics (tap water) | $Fe_3O_4$@$SiO_2$-VTMOS | Chloramphenicol and Florfenicol/MAA/EGDMA (1:1:4:16) $H_2O$/Chloroform | MeOH/ HAc (9:1) | $H_2O$ | • Chloramphenicol: $Q_{MIP}$:146.5, $Q_{NIP}$: 55 mg $g^{-1}$; Florfenicol: $Q_{MIP}$: 190.1. $Q_{NIP}$: 44 mg $g^{-1}$<br>• *IF*: Chloramphenicol and Florfenicol ~3, Thiamphenicol ~1 | [134] |
| Antidepressant drugs (tap water, well water and spring water) | $Fe_3O_4$@Chitosan@GO-acrylic acid | Fluoxetine/MAA/EGDMA (1:8:20)/ACN | MeOH/ HAc (9:1, v/v) | $H_2O$ | • $Q_{MIP}$: 66.2 mg $g^{-1}$<br>• *IF*:4 | [145] |
| Sulfonamide antibiotics (river and lake water) | $Fe_3O_4$–Oleic acid | Sulfamethoxydiazine/MAA/EGDMA (1:4:20)/DMSO | MeOH/ HAc (8:2) | $H_2O$ | • $Q_{MIP}$: 121.5; $Q_{NIP}$: 23.9 µmol $g^{-1}$<br>• *IF*: Sulfadiazine: 3.2 sulfamethoxydiazine:3.3, Sulfamonomethoxine: 3.3 and Sulfaquinoxaline: 1.9 | [128] |
| Dicofol and Chlorpyrifos (MeOH) | $Fe_3O_4$ | Dicofol and Chlorpyrifos-methyl/poly (Styrene-co-MAA)/Chloroform | MeOH | $H_2O$ | • Dicofol: $Q_{MIP}$: 41.82, $Q_{NIP}$:7 mg $g^{-1}$; Chlorpyrifos-methyl: $Q_{MIP}$: 36.22, $Q_{NIP}$: 7 mg $g^{-1}$<br>• Selectivity towards analogues such as Procymidone, Chlorpyrifos, and Fenvalerate was measured | [139] |

*(continued on next page)*

**Table 1.3.** (*Continued*)

| Analytes (Matrix) | Substrate-Functionalization agent | Template/ Monomer/ Crosslinker/ Porogen | Template removal | Rebinding solution | Adsorption and selectivity evaluation | Ref. |
|---|---|---|---|---|---|---|
| Sulfonylurea herbicides (rice water) | $Fe_3O_4$@ $SiO_2$-MPS | Bensulfuron-methyl/MAA/ TRIM (1:4:10) /DMF | MeOH/ HAc (9:1, v/v) | MeOH/ $H_2O$ (3:7) | $Q_{MIP}$: 37.32; $Q_{NIP}$: 18.45 mg $g^{-1}$<br>*IF*: 2.02<br>*K′*: Bensulfuron-methyl: 9.981; Triasulfuron: 7.187; Prosulfuron 3.333; Pyrazosulfuron-ethyl: 3.637; and Propazine: 1 | [118] |
| Organophosphorus pesticides (well and tap water) | $Fe_3O_4$@ $SiO_2$ | Diazinon/MAA/EGDMA (1:10:100)/ Chloroform | MeOH/ HAc (1:1, v/v) | $H_2O$ | Higher adsorption capacity of MIPs compared with NIPs<br>Selectivity studies for template and two analogues | [130] |
| Sulfonamide antibiotics (drinking water, river water and lake water) | $Fe_3O_4$/Chitosan–MPS | SMX, SMZ/2-VP/TRIM (1:1:4:24)/ACN/toluene (3:1, v/v) | MeOH: TFA (9:1, v/v) MeOH | $H_2O$ | SMZ: $Q_{MIP}$: 4.13 mg $g^{-1}$<br>SMX: $Q_{MIP}$ :4.32 mg $g^{-1}$<br>*IF*: SMZ: 3.20; SMX: 3.48<br>*K′*: 1.14-3.16 for structural analogues | [144] |
| Phenols (water) | $Fe_3O_4$@ $SiO_2$–MPS | 4-NP/MAA/DVB (0.125:0.625: 0.35)/ACN (10 mL) | MeOH/ HAc (9:1, v/v) | $H_2O$ | $Q_{MIP}$: 43.4, $Q_{NIP}$: 14.5 mg $g^{-1}$<br>No IF for analogues including 1,3-Dihydroxybenzene and BPA | [135] |
| Phenols (water) | $Fe_3O_4$@$SiO_2$–APTS | Phenol/MAA/ EGDMA (1:3:5) Toluene | MeOH/ HAc (8:2, v/v) | $H_2O$ | $Q_{MIP}$: 0.15, $Q_{NIP}$: 0.05 mmol $g^{-1}$<br>*K′*(4-NP): 20.754 | [139] |
| Phenols (distilled water) | Fly-ash@$Fe_3O_4$-MPS | Nonyl phenol/MAA/ EGDMA/DMSO, $H_2O$ | Soxhlet extraction; MeOH/ HAc (97:3, v/v) | EtOH/ $H_2O$ (1:1) | $Q_{MIP}$: 434.8, $Q_{NIP}$: 357.1 mg $g^{-1}$<br>Higher adsorption capacity of MIPs compared to NIPs for template and other phenolic compounds | [138] |
| Phenols (drinking water) | Hallosite/NTs/$Fe_3O_4$–MPS | 2,4,5-TCP/MAA/EGDMA/NIPAM (1:4:20:10)/DMSO, $H_2O$ | Soxhlet extraction; MeOH/HAc (95:5, v/v) | $H_2O$ | $Q_{MIP}$: 197.8, $Q_{NIP}$: 122.6 mg $g^{-1}$<br>No selectivity for structural analogues | [146] |
| CPs (seawater) | $Fe_3O_4$–Oleic acid | PCP/ St-DVB-GMA)/EtOH | MeOH/ HAc (1:1, v/v) | $H_2O$ | $Q_{MIP}$: 0.1181-0.1185 mg $g^{-1}$ | [134] |
| CPs (river water and tap water) | Attapulgite@$Fe_3O_4$–Oleic acid | 2,4-DCP/MAA/EGDMA (1:6:20)/DMSO | Soxhlet extraction MeOH/HAc (95:5, v/v) | $H_2O$ | $Q_{MIP}$: 145.79 mg $g^{-1}$<br>*K′*: 4-CP: 3.478; 2,4-DCP: 2.318; 2,4,6-TCP: 4.379; and BPA: 4.838 | [147] |

*(continued on next page)*

**Table 1.3.** (*Continued*)

| Analytes (Matrix) | Substrate-Functionalization agent | Template/ Monomer/ Crosslinker/ Porogen | Template removal | Rebinding solution | Adsorption and selectivity evaluation | Ref. |
|---|---|---|---|---|---|---|
| Nitrophenols (deionized water) | Wallostine@$Fe_3O_4$ | 4-NAP/MAA (1:4) St/EGDMA/ACN: $H_2O$ | Soxhlet extraction; MeOH | $H_2O$ | • $Q_{MIP}$:36.62, $Q_{NIP}$: 21.36 mg $g^{-1}$<br>• *K′*: 2-NP: 4.114, 4-NP: 7.920 | [147] |
| BPA (lake water) | $Fe_3O_4$–Oleic acid | BPA/MAA/EGDMA/ Mini-emulsion polymerization | EtOH/ HAc (19:1, v/v) | $H_2O$ | • $Q_{MIP}$: 122.2, $Q_{NIP}$: 54.9 mg $g^{-1}$<br>• *IF*: 3.5<br>• Separation factor (*β)*: BPA/E2=23.6; BPA/E3=8.8; and (*β):*BPA/DES=3.7 | [133] |
| PEs (–) | $Fe_3O_4$ @$SiO_2$–MPS | DEHP/MAA/ EGDMA(1:4:20)/ACN | MeOH/HAc (9:1) | EtOH | • $Q_{MIP}$: 4.74 mg $g^{-1}$, and $Q_{NIP}$: 2.35 mg $g^{-1}$<br>• IF for DEHP: 3.012, diallyl phthalate 1.547, and DBP: 1.788 | [148] |
| EDCs (seawater) | $Fe_3O_4$@ $SiO_2$–MPS | DS/MAA/EGDMA/ACN | Soxhlet extraction MeOH/ HAc (9:1, v/v) | $H_2O$ | $Q_{MIP}$: 4.68, $Q_{NIP}$: 1.72 mg $g^{-1}$<br>• *IF* for DS: 2.09, DES: 1.4, and β-E2: 1.14 | [67] |
| EDCs (tap water, rainwater and river water) | MWNTs@$Fe_3O_4$ | PTOP/4-VP (1:4) TEOS/ACN | MeOH/ HAc (9:1, v/v) | MeOH | • $Q_{MIP}$: 31.05, $Q_{NIP}$: 9.64 mg $g^{-1}$<br>*K′*: NPE: 1.96, BPA: 1.75, and TBBPA: 1.8 | [142] |
| EDCs (lake, river, and wastewater) | $Fe_3O_4$ @glutaraldehyde-aldehyde | 17β-E2/ gelatin/ACN | EtOH/ HAc (96:4) | EtOH | • $Q_{MIP}$: 10.02, $Q_{NIP}$: 1.89 mg $g^{-1}$<br>Selectivity coefficient: E3: 1.92, DES: 7.07 | [51] |
| Flame retardants (wastewater and tap water) | $Fe_3O_4$-APTS | TBBPS/TEOS (sol-gel) | Soxhlet extraction; MeOH/HAc (95:5, v/v) | MeOH /$H_2O$ (3:7) | • $Q_{MIP}$: 0.6898, $Q_{NIP}$: 0.3061 mg $g^{-1}$<br>*IF*: BPA: 1.639 | [149] |
| 2,4,6-trinitrotoluene (TNT) (tap water, water well, and seawater) | $Fe_3O_4$@ $SiO_2$–MPS | 2,4,6-trinitrotoluene /MAA/EGDMA (1:4:20)/ACN | MeOH/ HAc (9:1, v/v) | $H_2O$ | • $Q_{MIP}$: 40.39, $Q_{NIP}$: 18.45 mg $g^{-1}$<br>*K′* for 4-NP: 1.65, Nitrobenzene: 1.63, 2,4-Dinitrotoluene: 1.24 | [150] |

**4-NAP**, 2-amino-4-nitrophenol; **GMA**, Glycidylmethacrylate; **NPE**, Nonylphenol ethoxylate; **PTOP**, 4-tert-octylphenol; **TBBPS**, Tetrabromobisphenol S.

Wallosite particles as inexpensive materials containing silica groups can be used to enhance the mechanical properties of MMIPs [147]. These particles are firstly

functionalized with amino and carboxylic groups and attached to $Fe_3O_4$ via the polyol-medium solvothermal method. The prepared support is coated with MIPs through microwave heating-initiated polymerization with good performance of the extraction of nitrophenols from the water sample. Pan et al. [146] introduced another naturally occurring nanostructure, hallosite nanotubes, containing a two-layered aluminosilicate similar to CNTs. This nanostructure is purified under acidic conditions and then attached to $Fe_3O_4$ via electrostatic attractions. The synthesized substrate for MIPs showed not only thermal stability but also high adsorption capacity (197.8 mg $g^{-1}$) due to its nanostructure network. Attapulgite can also be incorporated with $Fe_3O_4$ to avoid fragility of polymeric sorbent. Coprecipitation of attapulgite with $Fe_3O_4$ provided support to synthesize 2,4-DCP imprinted MMIPs for CPs priority pollutants. The MMIPs which showed high adsorption capacity for the template (145.79 mg $g^{-1}$) and sufficient $K'$ for other CPs (2.31–4.37) could be reused five times with no reduction in efficiency [147]. Ionic liquids, which have been used in different applications, can be covalently incorporated into the MIPs structure. The functional groups of ionic liquids increase the interaction of analytes with the sorbent through π-π, electrostatic, dipole–dipole interactions and hydrogen bonding and enhance the capacity of ionic liquid-based MIPs for organochlorine pesticides [151].

Emulsion polymerization used for imprinting water-soluble molecules in oil/water system can be conducted using functionalized magnetic NPs as stabilizers. Hang et al. [122] used vinyl functionalized magnetic hallosite nanotubes as a substrate to prepare MMIPs for pyrethroid pesticides. The template molecule can be grafted on to outer polymeric layer of core-shell nanoparticles [134]. For grafting, a self-assembled complex between pentachlorophenol (PCP) and tetraethylenepentamine is added to $Fe_3O_4$@polymer which

resulted in grafting the template molecules through ring-opening reactions. After successful grafting, the template molecule is removed. The prepared MIPs showed high extraction efficiency for CPs (88.7–98.7%) in a large sample volume (500 mL) by using only 20 mg of the synthesized sorbent [134]. MMIPs are also commercially available and have been used for extraction of PAHs [152]. The extraction water sample contains 10% ACN to increase the extraction efficiency of analytes. After 10 min shaking, the analytes were enriched (42-100% efficiency) to MMIPs followed by three successive desorption steps using ACN (5 mL). The approach provided a green method for 16 PAHs with high sensitivity, detection limits ranged from 1.3 to 969 ng $L^{-1}$ [152].

## 1.7. MIP-SPME

SPE, a validated alternative to LLE, is commonly used by the US-EPA, and valued for using less organic solvents than LLE. The application of this method has been restricted by the main drawback, analyte breakthrough when large volumes of samples are analyzed. The other drawback is the loss of analyte during the filtration process when such a process is required for real samples, especially hydrophobic ones [153]. Arthur and Pawliszyn [154] introduced SPME as a miniaturized extraction technique, which relies on the equilibrium of the analytes between the extraction phase and the sample matrix instead of exhaustive removal of compounds. Given the significant benefits of SPME, such as rapidness, simplicity, greenness, high enrichment and convenience of integrating into portable instruments, it has been widely applied for environmental analysis [155]. Despite developments of SPME for sample pretreatment, there are only a few commercially

available SPME devices, most of which show low selectivity towards target analytes leading to enrichment a vast range of molecules that can limit sensitivity and cause matrix effects. Partitioning of analytes between the sample solution and the extraction phase is the driving force in SPME and can be improved by designing a suitable MIP coating [156]. MIPs-coated fibers as a first solid phase for SPME was proposed by Koster et al. [157] in 2001 for analysis of biological samples. Hu et al. [158] silanized silica fibers as the substrate then immersed them in a pre-polymerization solution to achieve a film with a desirable thickness (75 μm). Using silanized metal support to prepare MIP-SPME leads to a chemically bound coating and robust SPME device with a reduced risk of breakage typically associated with commercial SPME fibers [159]. The metal wire was firstly anodized leaving a porous layer of $Al_2O_3$ to enhance the surface area and adsorption capacity of the sorbent. The hydroxyl functional groups were formed through the immersion of anodized wire in sodium hydroxide before the silanization process. After the pre-polymer solution was sprayed at the surface of the wire, it was cured under UV irradiation. The spraying distance, polymerization time and the number of polymerization or spraying cycles were optimized to obtain the desired thickness. The obtained MIPs-coated wire with thermal and chemical stability showed selective recognition towards triazine compared to untargeted analytes.

MIPs have been extensively employed for extraction of organic contaminants from water samples using direct immersion solid phase microextraction (DI-SPME) (Fig. 1.4c) [39], however the evaluative criteria for selectivity of MIP coating is controversial. Terzopoulou et al. developed MIP-SPME fibers for extraction of antiviral drugs in surface waters and wastewater samples [160]. The imprinted sorbent showed 37.4% extraction

recovery while non-imprinted polymer resulted in 3.3%, an *IF* of 11.3. In addition to the adsorption efficiency of MIP-SPME, the selectivity of the proposed device for uptake of abacavir was compared with the uptake of two antiviral drugs, acyclovir, and adefovir-dipivoxil. MIP-bars can be used as selective SPME device by polymerization inside a capillary and pulling out the prepared bars after polymerization [161]. The MIP bars yielded 1.7 times higher extraction efficiency for BPA in aqueous medium than NIP bars and recovered 65–89% at equilibrium conditions in 120 min. The substrate-less MIP-fibers can also be formed inside a fused silica capillary as a mold [162]. The silica wall was etched using an hydrofluoric acid solution after polymerization. The prepared MIP-fiber which is stable up to 320 °C can be used for direct introduction of the extracted analytes on to a GC column using thermal desorption. MIP-fibers exhibited an excellent selectivity towards trimethyl phosphate, $Q_{max}$ for MIP and NIP fibers are 1600 and 160 μg $g^{-1}$, respectively.

To overcome the fragility of SPME fibers, an organic–inorganic MIP was prepared using the sol–gel process to fabricate a more robust SPME coating [163]. The sol–gel process is a convenient method under mild conditions at low temperatures. For the preparation of sorbent, the template solution was firstly prepared by mixing TEOS and ethanol (EtOH) at 50 ºC, followed by adding diclofenac and HCl. The prepared solution was subjected to the pre-polymerization solution consisting of monomer, crosslinker, and initiator. Multi-walled carbon nanotubes (MWCNTs) were added to increase the kinetic mass transfer of the analyte between an aqueous phase and sorbent. After homogenization by an ultrasonic bath to obtain a gel-like solution, the sorbent was reinforced in a hollow fiber and applied for extraction of diclofenac from different samples. Sol–gel technology without conventional reagents and procedures for MIPs was also used to fabricate selective

SPME fibers [164]. In this procedure, a polysiloxane nanofiber was formed on a silanized stainless steel wire and used with thermal desorption due to the high thermal stability. The process was initiated with the hydrolysis of the methoxy groups of the methyltriethoxysilane using HCl followed by condensation at room temperature under stirring for 20 h. After removal of the template using thermal treatment, selective sites were formed for adsorption of analytes through H-bonding between silanol groups and analytes. The proposed nanofibers which are thermally and chemically stable showed excellent selectivity towards structurally similar compounds with amino functional groups. Furthermore, this coating provided higher extraction efficiency compared to conventional SPME fiber such as PDMS and PA which is caused by larger surface area of polysiloxane nanofibers.

Zarejousheghani et al. [165] proposed an in–tube–MIP-SPME method based on in-situ synthesis of MIPs. In this approach, an open tubular capillary was placed inside another capillary filled with a pre-polymerization solution. A metal rod inserted in the middle of the capillaries was used to control the thickness of polymer and was removed after polymerization. The proposed in tube-MIP-SPME device used for analysis alkylated and chlorinated phenols in wastewater also showed potential for automation. Monolith MIPs were also used for pipette tip-SPME by polymerization of prepolymer solution in a micropipette tip [166]. The micropipette tip, which is more durable than a capillary, was connected to a syringe and used for simultaneous cleanup and preconcentration of the analyte. The resulting eluate can be directly collected using glass-lined pipe and analyzed. To increase the extraction capacity of SPME devices, Wang et al. [167] developed a MIP-SPME device by coating inner and outer sides of a capillary. The prepared extraction

devices with a 6 µm coating thickness provided higher extraction efficiency than polydimethylsiloxane (PDMS, 100 µm), polyacrylate (PA, 85 µm), and polydimethylsiloxane /divinylbenzene (PDMS/DVB, 65 µm).

The efficiency of MIP-SPME has some shortfalls for extraction of organic pollutants especially polar compounds in aqueous matrices. A combination of dispersive liquid–liquid extraction (DLLME) and SPME can be adopted to extract polar analytes. 1,2-benzenediol as a polar compound was derivatized to form a less polar compound, following with extraction using an organic solvent. The SPME fiber prepared by coating a stainless still wire with $SiO_2$ and MIPs was used for selective extraction of the concentrated product. This synergic strategy has led to a selective and highly sensitive enrichment technique for polar compounds in water samples [168]. Headspace-solid phase microextraction (HS-SPME) which is another mode of SPME can also be performed using selective MIPs. This method has several advantages such as better efficiency and lower interferences for the extraction of volatile compounds [169].

## 1.8. MIP-SBSE

SPME is a common microextraction technique for the solvent-less measurement of pollutants in environmental samples based on simplicity and portability of this device [9]; however, there are several disadvantages associated with SPME technique such as low extraction efficiency due to the low amount of sorbent coated on SPME fibers, fragility and lack of robustness and reproducibility of SPME fibers [170, 171]. SBSE demonstrated in Fig. 1.4d, is another solvent-less microextraction technique and introduced by Baltussen et

al. [172]. PDMS is the common commercially available coating for SBSE and has restricted its use to the extraction of non-polar compounds due to the hydrophobic nature of the polymer [173]. Additionally, the lack of the selectivity is the second disadvantages of SBSE coatings which result in co-extraction of interferences. Thus, utilization of MIPs as a coating for SBSE could extend the range of applicability of SBSE in complex aqueous samples. The MIP-SBSE has been used for extraction of pollutants from environmental water samples which are summarized in Table 1.4.

The first application of MIP-SBSE was determination of organophosphorus pesticides in environmental samples [174]. The MIP-SBSE device was prepared on a PDMS coated stir bar as a substrate by formation of a 180 µm film using formic acid and a nylon-6 polymer solution containing monocrotophos as the template. However, the developed coating was used for extraction of analytes from dichloromethane DCM solutions. In-situ polymerization was also used for the preparation of MIP-SBSE with increased stability of the coated stir bar. In this method, a glass bar is first treated with a silanization reagent (MPS), followed by immersion of the glass bars in the pre-polymerization solution. The MIP-SBSE devices were used for determination of dienestrol (DS) and hexestrol (HS) in wastewater [175], Bensulfuron-methyl in tap water [176], and sulfonylurea herbicides in river water [177]. Multi templated MIP-SBSE devices were also reported for the determination of estrogens in river and lake water samples [178]. Addition of estradiol (E2) and BPA as the template has resulted in the creation of cavities for recognition of two groups of EDCs with different structures.

**Table 1.4.** MIP-SBSE methods used for extraction of environmental pollutants.

| Analyte (Matrix) | Template/Monomer/ Crosslinker | solvent | T/UV | Selectivity | Extraction Capacity | Ref. |
|---|---|---|---|---|---|---|
| Organophosphorus pesticides (DCM solution) | Monocrotophos/Nylon-6 | formic acid | room temp | Comparison of chromatograms of MIPs and NIPs | - | [174] |
| Sulfonylurea herbicides (tap water) | Bensulfuron-Methyl/MAA/EGDMA | ACN | 60 ºC | *IF*= 2.60 | - | [176] |
| Sulfonylurea herbicides (river water) | Metsulfuron-methyl/MAA/EGDMA | ACN | 60 ºC | *IF* for Metsulfuron-methyl: 4.6 | 270.6 ng for MIP coating and 97.5 for NIP coating | [177] |
| EDCs (wastewater) | DES/4-VP/EGDMA | ACN | 70 ºC | Peak area: MIPs/NIPs: DS: 1.64 and HS 1.71 | MIPs>1200 µg $L^{-1}$ NIPs: 1000 µg $L^{-1}$ | [175] |
| EDCs (river and lake water) | BPA, E2/MAA/EGDMA | MeOH: ACN (1:1, v/v) | 60 ºC | *IF*:BPA=1.5 E2= 1.2 | $Q_{max}$: BPA: MIPs: 6530, NIPs 4508 ng E2: MIPs: 6536, NIPs:5520 ng | [178] |
| BPA (tap water) | 4,4′-dihydroxybiphenyl/4-VP/EGDMA | toluene | 65~70 ºC | Extracted BPA in presence of interferences MIPs >7 times NIPs >24 times of PDMS bar | - | [179] |
| BPA (river and lake water) | 4,4'-dihydroxydiphenylmethane/AM/EGDMA | MeOH | 60 ºC | Relative selectivity: 3.2 | $Q_{max}$ MIPs: 9300 nmol $g^{-1}$ NIPs: 1600 nmol $g^{-1}$ | [180] |
| CPs (seawater) | 2-CP/4-VP/EGDMA | ACN | 60 ºC | Higher extraction efficiency for MIPs than NIPs | - | [181] |
| Glyphosate (river water) | Glyphosate/ DEAEM and N-allylthiourea/(EGDMA) | MeOH: $H_2O$ (90:10, v/v) | UV | - | - | [182] |

Sol–gel technology, which has been used for the preparation of MIP particles [94], also was used for the preparation of SBSE coatings [179]. In this method, MIP particles were synthesized by polymerization of 4-VP and EGDMA in the presence of 4,4′-dihydroxybiphenyl as a dummy template at the surface of silica particles. The obtained dummy template–MIPs were entangled into the sol–gel structure and coated on the treated

glass bar. MIPs-coated stir bars have a homogeneous surface which showed a high affinity for BPA. The extracted amount of BPA, in the presence of an increasing concentration of four analogues as interferences, was seven times more than that of NIP-SBSE, and 24 times that of a PDMS bar.

One of the problems associated with SBSE is physical damage of the sorptive phase due to contact with glassware at high stirring rates. Therefore, development of extraction devices to prevent deterioration of the extraction phase offers much more flexibility regarding applying high stirring rates to have fast mass transfer kinetics such as rotating-disc sorptive extraction (RDSE) [183]. A Teflon disk equipped with a magnetic stir bar with a diameter of 1.5 cm and the internal cavity of 0.44 $cm^3$ was filled with MIP particles. Afterward, the rotating disc was covered with a fiberglass filter and sealed with a Teflon ring. The RDSE device was utilized for extraction of anti-inflammatory drugs in water samples [184]. Monolithic MIPs-coated rotating disk [185] was also proposed by coating the teflon support. An etching step was performed to introduce functional groups and reduce hydrophobicity. After vinylization, an in-situ polymerization under inert conditions resulted in creation of MIPs-coated disks capable of exhaustive extraction (100% extraction recovery) from a large sample volume (200 mL). Liu et al. [180] developed a barbell-shaped stir bar by using medical silicone tubes as wheels to avoid the friction of the polymer coated on a capillary glass tube. The MIP coating consists of in-situ polymerization of AM as functional monomer and EGDMA as a crosslinker. In the polymerization process, a dummy template (BPF) with a similar structure to BPA was used to recognize the analyte from water samples without template bleeding. The silicone wheels which are easy to reinstall provided the application of developed MIP-SBSE for 100 extraction cycles in

comparison to the 40–50 cycle lifespan of traditional SBSE devices. The proposed BPF-dummy template MIP-SBSE was evaluated in term of selectivity, and reproducibility and stability. The *IF* was more than 3.2 and was obtained for BPA, with a relative standard deviation (RSD) of 3.5% for five replicated extractions of 50 μg $L^{-1}$ BPA solutions. BPF-dummy template MIP-SBSE lowered the lower limit of detection (LOD) of the method, 0.003 μg $L^{-1}$, in comparison to the in the literature with LOD 2.4 μg $L^{-1}$ obtained for MIP-SPME fibers [186].

Another drawback of MIP-based microextraction techniques applied for analysis of environmental samples is the lack of water compatible sorbents especially for polar compounds. Gomez-Caballero et al. [182] developed a water compatible stir bar for selective extraction of glyphosate , a polar herbicide, from river water samples. The glyphosate-imprinted MIP coating was prepared by polymerization of 2-dimethyl aminoethyl methacrylate (DEAEM) and EGDMA in a MeOH:$H_2O$ (90:10 v/v). The MeOH:$H_2O$ mixture was used to eliminate non-specific hydrophobic interactions and increase extraction selectivity of rebinding in aqueous samples. After optimization of MIPs composition and MIP-SBSE procedure, extraction of glyphosate in presence of 100 μg $L^{-1}$ four analogues proved the selectivity of proposed method.

## 1.9. Membrane-related MIPs

LPME is an alternative to traditional extraction methods and is performed using a very small amount (μL) of extraction solvent instead of large amounts of solvents associated with most LLE methods. In hollow fiber-liquid phase microextraction (HF-

LPME) the analytes are extracted based on distribution between the aqueous solution and the extraction solvent (donor and acceptor phase, respectively), which are separated by a polypropylene hollow fiber. HF-LPME provides several benefits such as simultaneous clean-up and preconcentration, high efficiencies and high enrichment factors, and environmentally friendliness [187]. Nevertheless, the lack of selective extraction of target compounds has limited their application. The application of MIPs as an acceptor phase for the recognition of analytes improves the selectivity by increasing the distribution coefficient. Moreover, this combination could overcome the selective recognition of analytes with high polarity in aqueous matrices. In this approach, a MIPs-coated silica fiber was inserted in a porous polypropylene hollow fiber membrane impregnated with a water-immiscible solvent. In this example, toluene was employed to form a supported liquid membrane (SLM) [188]. The extraction process proceeds by diffusion of analytes and the compatible interferences from aqueous sample into the small volume acceptor phase and through the SLM. The enrichment was completed by the selective absorption of target molecules on recognition sites of MIPs-coated fiber. Incorporation of HF-LPME and MIP-SPME resulted in several advantages including good barrier characteristics of the membranes, enhanced sensitivity by employing a double extraction process; the obtained LODs (0.006–0.02 μg $L^{-1}$) were lower than those of MIP-SPME (0.18–0.30 μg $L^{-1}$) and HF-LPME (0.08–0.20 μg $L^{-1}$), increased selectivity due to a non-polar acceptor being in contact with MIP cavities and avoiding water disturbance by using SLM.

As mentioned earlier, the fragility of SPME fibers is one of the main disadvantages of this technique. According to Diaz-Alvarez et al. [189], MIP beads can be implemented in HF-LPME by packing sulfadimethoxine-imprinted beads into a lumen of porous

propylene hollow fiber (Fig. 1.4e). After immobilization of toluene in the pores of the fiber, the fiber was used for extraction of sulfonamides from water samples to the organic solvent of toluene where MIP beads could uptake analytes with more selectivity. The next steps include washing to remove interferences, drying to remove organic solvent and elution for desorption of bounded analytes to MIPs for further analysis. This method was also utilized for selective enrichment and cleanup of triazines in tap and reservoir water samples [190]. A comparison of HF-LPME performed by using MIPs, NIPs and organic solvent alone for extraction of 17β-estradiol (17β-E2) in wastewater samples depicts the selectivity of the proposed method [191].

Tan et al. [192] suggested a method where MIP coatings were applied onto the surface of MWCNTs due to the outstanding sorption capacity of CNTs. MWCNTs were firstly functionalized carboxylic acid (–COOH) groups followed by introduction of vinyl groups (–CH═$CH_2$) at the surface of MWCNTs–COOH. The next step is formation of a MIP layer (15–20 nm thickness) at surface of MWCNTs–CH═$CH_2$ for fast adsorption and desorption. The MIP–MWCNTs were packed into a polypropylene membrane envelope and clamped to a paper clip. This self-stirred microextraction device increased mass transfer and reduced adsorption of analytes on the hydrophobic stir bar. The membrane protected-MWCNTs-MIPs, which was applied to the extraction of triazines spiked in river water and wastewater, showed high selectivity and enrichment capability towards analytes (40 mL of sample solution in comparison to 100 μL of final solution for analysis).

The MIPs-coated hollow fiber can be used for extraction of analytes from water samples [193]. In this procedure, a group of end-sealed hollow fibers were placed inside a Pasteur pipette containing pre-polymerization solution. The polymerization started with

thermal initiation for a certain amount of time. After the gel-phase formation, which is a cloudy state, the fibers were withdrawn from the solution. The polymerization was completed by incubating each fiber at 60 ºC. The required time for gel formation was optimized for 32.5 min. Shorter exposure time yielded irreproducible results while longer thermal polymerization could result in highly crosslinked polymer formed pipette and makes it difficult to separate fibers. As shown in Fig. 1.6a, a uniform MIP layer formed at the surface of the hollow fiber and can be used as an extraction device for quantitation of triazine herbicides [193] and fluoroquinolone antibiotics [194] in water samples. MIP-fibers demonstrated a larger adsorption capacity extraction compared to NIP-fibers (Fig. 1.6b) due to the presence of selective sites responsible for extraction of analytes.

The MIP-MWCNTs with excellent adsorption properties as well as selectivity and stability were utilized for electro-membrane extraction. In this procedure, the formation of H-bonding between the analyte and cavities of the MIPs increase the selectivity of the diffusion of the target compounds from aqueous sample towards the acceptor phase [195]. Incorporation of MIP particles in a polymeric substrate is another methodology to perform extraction of analytes from water samples. Rozaini et al. [196] dispersed MIP particles in an agarose polymer to obtain a mixed matrix membrane for preconcentration of sulfonamide antibiotics in water samples. This format allows for a straightforward preconcentration method with simultaneous advantages of both MIPs and membranes.

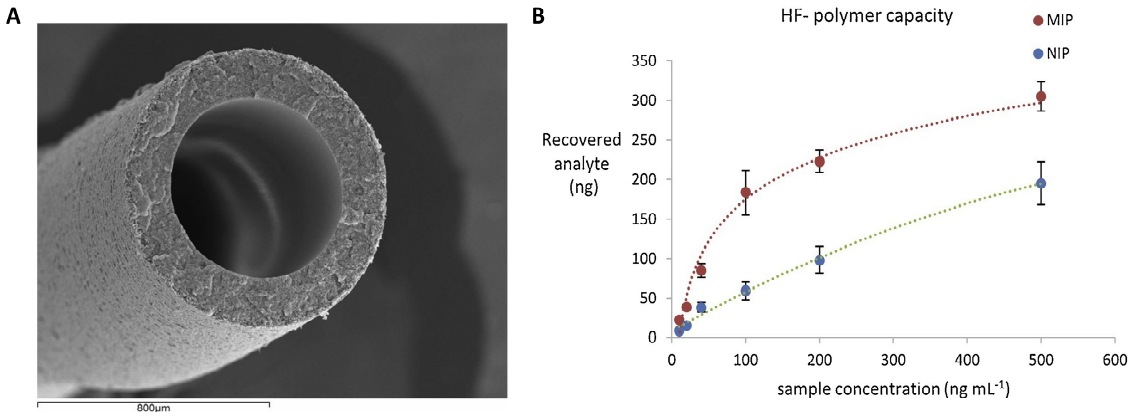


**Fig. 1.6.** A) Cross-section detail of MIPs-coated hollow fiber. Reprinted from [193] with permission from Elsevier. B) The extracted amount of ciprofloxacin recovered by MIPs and NIPs-coated hollow fibers at different concentration of upload solution. Reprinted from [194] with permission from Elsevier.

## 1.10. Optimization of MIP-based microextraction techniques

There are many factors in MIP-based microextraction techniques that need to be optimized for maximum sensitivity of the analysis. The key parameters influencing sample preparation are sample agitation, extraction time, extraction temperature, pH, ionic strength, and volume of sample solution as well as desorption conditions.

After the preparation of MIPs (i.e., MIP-fiber or MIP-stir bar), a solvent treatment removes template molecules and results in selective binding sites [168]. Besides, a thermal conditioning step after template removal reduces bleeding from the polymeric network and decreases background noise [162]. MIPs can be used for extraction of organic contaminants from water samples directly [157, 167, 168, 178, 180, 196] or with pre-conditioning steps [128, 165, 166, 193, 194] prior to each extraction/desorption cycle These sorbents with porous structure contains cavities with imprinting binding sites which can adsorb analytes

selectively. Following template removal and drying steps, shrinking MIPs could change the position of binding sites. Zarejousheghani et al. [165] used ACN and water to condition in-tube MIP-SPME. They suggested that ACN, which was the porogenic solvent in the fabrication process, results in the positioning of cavities complementary to the analytes. Extraction of analytes using SLM-MIPs is based on partitioning between three phases including an aqueous sample, an organic phase inside the hollow fiber membrane, and MIPs [188]. In this extraction technique, conditioning MIPs with the organic solvent is crucial. Diaz-Alvarez et al. [189] immersed a MIPs-packed capillary in 4.5 mL toluene under stirring for 5 min. This solvent enhances the transport of analytes from the sample towards MIPs and acts as an acceptor phase. Moreover, it minimizes non-selective adsorption of analytes due to the absence of water which introduces adsorption of matrix components. Solvents such as toluene [188, 189, 192], a mixture of toluene and ACN (95:5, v/v) [190], and hexane/ethyl acetate (3:2, v/v) [191] can be applied as the acceptor phase and the conditioning solvent for SLM-MIPs.

Most of the microextraction techniques, such as SBSE, DSPE, follow SPME theory [197]. In this theory, analytes partition between the sample and adsorption sites on MIPs. Extracted mass of analytes is increased by exposure time until an equilibrium condition is achieved [198]. Agitating the sample solution increases the mass transfer of analytes from the bulk of the solution to the surface of the sorbent and reduces the thickness of the boundary layer and equilibrium time. Higher agitation also leads to greater sensitivity at non-equilibrium conditions [199]. In this regard, the sampling rate must be investigated during the development of MIP-based microextraction techniques such as MIP-SPME [162], MIP-SBSE [181], and SLM-MIPs [189]. However, very high agitation rates might

reduce the reliability of the extraction process by introducing air bubbles to the surface of MIPs [164], or instability of the MIP device [192]. Optimization of extraction time is also necessary to ensure maximum efficiency. MIPs can shorten equilibration time due to their highly porous structure and the possibility to fabricate a thin polymeric layer in comparison to semi-permeable phases used in commercial SPME devices [158]. The utilization of MIP-DSPE can significantly reduce the time for equilibration of analytes between the sample solution and MMIPs. Yang et al. [143] achieved quantitative adsorption of PEs in water in 10 min using 15 mg MMIPs shaken in a 10 mL sample solution.

The volume of the sample solution, which has been scaled down in microextraction techniques, must be studied. Increasing the volume of solution enhances the preconcentration factor by increasing the extracted mass of analytes and lowers the extraction efficiency of analytes reducing the distribution coefficient in larger sample volumes [166, 199]. The effect of sample volume on MIP-DSPE is more significant than the other techniques due to the effective dispersion of MIP particles in the sample. Consequently, simultaneous optimization of MIPs mass and sample volume, which depend on each other, can be conducted using experimental design [200]. Careful optimization of temperature is required during microextraction procedures. Higher temperatures increase the diffusion coefficient in direct and headspace exposure modes and reduce equilibrium time. However, distribution coefficients and the extracted amount of analytes will be reduced at levanted temperatures [199]. As described by Mohammadi et al. [201], extraction efficiency using chlorpyrifos-imprinted fibers showed an improvement by increasing the temperature from 25 °C to 45 °C followed by a decline in the range of 45–65 °C. As mentioned in Section 1.5.2.1, the pH of extraction is a useful parameter for

adsorption using MIPs. The effect of pH is more pronounced for non-exhaustive extraction techniques that use small amounts of an extraction phase. The pH of sample solution can determine the functionality of imprinted sites as well as targeted analytes. This effect was illustrated by changing pH in the range of 2–8 for the extraction of bensulfuron methyl with MIP-SBSE. The optimum pH value was obtained at 4 and showed the maximum hydrogen bonding for selective adsorption [176]. Salt addition is usually employed in MIP-HS-SPME to reduce the solubility of analytes in the sample and increase their headspace concentration. However, salt content during direct exposure of MIPs can increase or decrease the efficiency of adsorption. Cai et al. [162] investigated the salt effect on the efficiency of MIPs for the extraction of trimethyl phosphate. The results represented optimum values at 25% and 10% NaCl (w/v) for HS-SPME and DI-SPME, respectively. The effect of salt addition in SLM can be considerably variable depending on the type of analyte, particularly for large volume studies when the partition coefficient of analytes can be improved. Extraction recovery of triazines as polar analytes was obtained in the range of 78% and 104% using SLM-MIP from 150 mL sample solution [190].

After adsorption from water samples, quantitative desorption must be conducted before instrumental analysis. This step is performed either by thermal or solvent desorption. For solvent desorption, the selection of solvent depends on the nature of analytes and compatibility with MIPs and detection systems. Different types of solvents were used for desorption of analytes from MIPs such as cyclohexane for PAHs [202], MeOH for diclofenac [163] MeOH/HAc (95:5, v/v) for sulfonamides [128], ACN for pyrethroid pesticides [203], $Na_2HPO_4$ (10 mM) for glyphosate [182], etc. Furthermore, the volume of solvent and desorption time must be considered to avoid carry-over effects. Extensive post-

cleaning steps are required to avoid carry-over (30 min washing using 50 mL MeOH) [204]. Regarding MIPs stability, thermal desorption can be used to introduce analytes into GC systems [205, 206]. Elevated temperature in thermal desorption can deform cavities, reduce signal, deteriorate the extraction device, and contaminate the injection port of GC [159, 201]. Thus, the temperature and time required for desorption must be carefully investigated.

## 1.11. Challenges of MIPs for environmental analysis

### 1.11.1. Extraction of water-soluble compounds

Selective rebinding of water-soluble compounds from environmental water samples is problematic. This issue raised from the weak interactions during template–monomer complexation due to the disturbance of the hydrogen bonding by polar solvents. To solve this problem, different strategies can be adopted. One solution is polymerization of hydrophilic monomers in a water/MeOH porogenic system to increase the interaction with the water-soluble templates. Polymerization of 1-(α-methyl acrylate)-3-methylimidazolium bromide (monomer) with trimethylolpropane trimethacrylate (TRIM) (crosslinker) in the presence of tartrazine (template) in a MeOH: water (8:2, v/v) yielded MIPs with good specificity towards the water-soluble dyes compared to MIPs prepared by MAA and 4-VP. The higher efficiency of this water compatible MIPs is the result of formed complex in prepolymer mixture due to electrostatic and π-π stacking interactions with the template molecules [207].

Another solution is to dissolve the template in water and transfer it into a nonpolar solvent system in which non-covalent interactions, which is usually used for the synthesis of MIPs, are established. These stronger interactions are not disturbed which lead to selective recognition of analytes. Zarejousheghani et al. [208] applied (vinylbenzyl)trimethylammonium chloride as an ion-pairing reagent to transfer a negatively charged acesulfame as a sweetener from water into the chloroform in which polymerization reaction occurs. This transfer agent was incorporated in the polymerization reaction, and the yielded MIPs contained ammonium groups showed good selectivity towards acesulfame and homologues with negatively charged sulfonyl groups. The MIPs also reduced the matrix effects for extraction of acesulfame from influent and effluent water samples compared to styrene-divinylbenzene polymer as a general commercial SPE cartridge. Sodium dodecyl sulfate (SDS) was also used to form ion-pair complex with pyridoxine [209].

### 1.11.2. Water compatibility of MIPs

MIPs are usually synthesized in organic solvents such as toluene causing low efficiency of these polymeric sorbents in aqueous samples. Incompatibility of hydrophobic MIPs with aqueous samples raised this issue. The interaction between the binding sites of MIPs and analytes can be enhanced during polymerization using water [210] or a mixture of water with miscible organic solvents [182] as the porogenic solvent. Another strategy is to use a hydrophilic coating. Gelatin is a hydrophilic coating with a broad range of functionalities such as $–NH_2$, –COOH, and –OH groups, and hydrophobic chains and can be used to obtain hydrophilic MIPs. The prepolymer complex formed through non-covalent

interactions and incorporated in polymerization through amino groups of the gelatin with aldehyde-modified magnetic nanoparticles. The rebinding studies of the synthesized water compatible MIPs yielded in $Q_{max}$: 10.02 mg $g^{-1}$ for MIPs and $Q_{max}$: 1.89 mg $g^{-1}$ for NIPs. The results demonstrated successful imprinting of template using gelatin as a monomer [51]. This polymer was successfully applied for the exhaustive extraction of 17β-E2 (88.3% to 99.1% recovery) from water samples [51]. Cyclodextrin and its derivatives have hydrophilic functional groups on the surface. They were applied to enhance water compatibility while their lipophilic inner cavities increase adsorption through inclusion complexes [211] or selective interactions (hydrogen bonding) with the target analytes [203]. These macromolecules were implemented in the MIPs structure using grafting onto the surface of silica support [211] or incorporation in polymerization step [212].

Addition of co-monomers to the polymerization components is another strategy to increase the hydrophilicity of MIPs [213]. For example, 2-acrylamido-2-methylpropanesulfonic acid, a water-soluble monomer, was incorporated as comonomer with styrene [214]. Other hydrophilic monomers are 2-hydroxyethyl methacrylate (HEMA) and N-isopropylacrylamide (NIPAM) that can be added to the polymerization components to form a copolymer [215], or grafted onto a hydrophobic surface as hydrophilic brushes [216]. J. Dai et al. [216] showed that grafting HEMA brushes over core-shell composite reduced the water contact angle from 122.2° to 70.6°, enhancing hydrophilicity (Fig. 1.7). Using hydrophilic crosslinkers such as polyethylene glycol can reduce non-specific hydrophobic interactions and enhance MIPs selectivity in comparison with conventional crosslinkers such as EGDMA or DVB for adsorption of estrogens from environmental water samples [217].

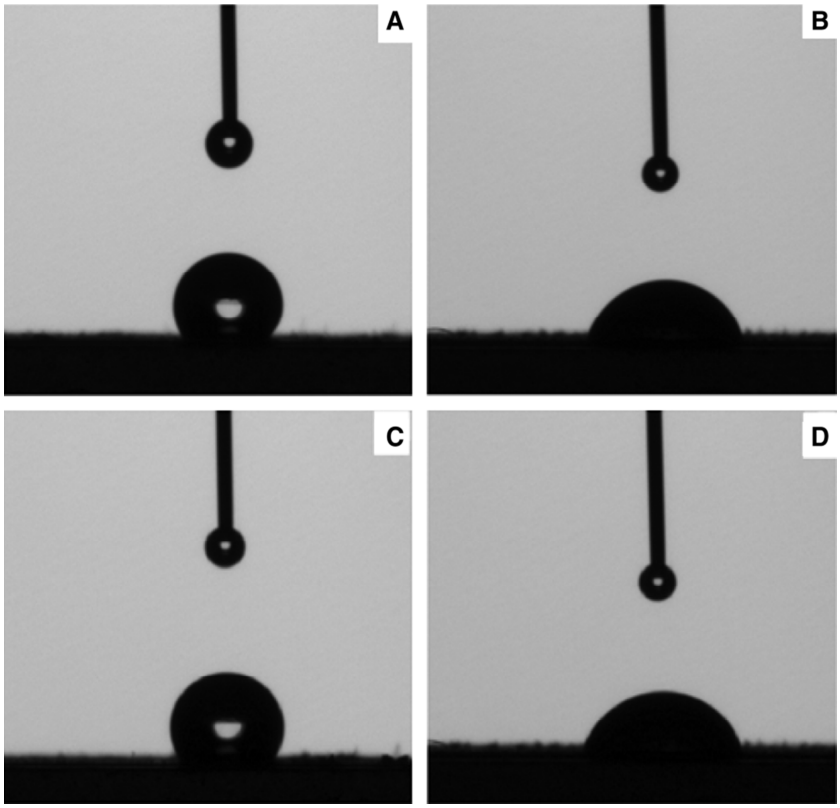


**Fig. 1.7.** Water contact angle profiles MIPs (A, B) and NIPs (C, D) without (A,C) and with HEMA hydrophilic brushes (B, D). Reprinted from [216] with permission from John Wiley and Sons.

The recognition of analytes in aqueous matrices is difficult due to weak interactions such as hydrogen bonding used for the formation of template–monomer complexes. Sellergren et al. [218] proposed a monomer with the ability to form stoichiometric interactions with the template. This method was used for imprinting enrofloxacin for FQs through ionic interactions between a carboxylic group of the template and urea-based monomer (1-(4-vinylphenyl)-3-(3,5-bis(trifluoromethyl)phenyl) urea) [75]. To synthesize the polymeric network, methacrylamide was used as a co-monomer, EGDMA a crosslinker and ACN as porogenic solvent. The formation of ionic interactions was confirmed by chromatographic retention of the template using a MIPs-packed column. The template was

in a protonated form during washing with ACN. Increasing the water content of the mobile phase caused the formation of deprotonated enrofloxacin that could interact with the binding sites of the MIP stationary phase. Chromatographic evaluation and rebinding experiments depicted that imprinted sites can stoichiometrically interact with the FQs (*IF* of 4 for enrofloxacin), especially for structural analogues with low $PK_a$ such as flumequine and oxolinic acid which are in carboxylic form at neutral pH.

### 1.11.3. Homogeneity of MIPs

Synthesis of MIPs using free radical polymerization (FRP) does not allow for good control of the number and size of macromolecules and polymer architecture because of fast chain propagation and irreversible termination reactions [219]. The MIPs synthesized by FRP contain inaccessible and heterogeneous binding sites leading to slow mass transfer and low selectivity [220]. To solve these issues, controlled radical polymerization such as reversible addition fragmentation chain transfer (RAFT) polymerization [215, 221-223], atom transfer radical polymerization (ATRP) [224] and ring-opening metathesis polymerization [225] have been proposed and applied for extraction of analytes.

In ATRP, an alkyl halide initiates the reaction with metal complex and yields radicals. An equilibrium is established between dormant species and radicals. The low concentration of radicals results in insignificant termination reactions and well control over the length and structure of polymer [226]. In a study conducted by Zhang et al. [227], 2, 2-bipyridyl and cuprous chloride were used as ligand and catalyst, respectively. The imprinted polymeric microspheres of MAA was obtained by 1-chloro-1-ethyl benzene as the initiator and utilized for selective extraction of pyrethroids.

Immobilization of initiator onto the surface of substrates such as yeast enables to create well-controlled core-shell MIPs for selective rebinding of cefalexin. The imprinting of target molecules was confirmed by higher adsorption capacity with MIPs (34.07 mg $g^{-1}$) while NIPs yielded 15.48 mg $g^{-1}$ [228]. By using yeast as a green, inexpensive and accessible material which has amino groups, the substrate is ready for grafting initiator and surface polymerization [224]. The main limitations of ATRP polymerization are removal of metal complex from the final products and special methods to minimize the oxygen content in reaction chamber [229].

In RAFT polymerization, the control of polymer structure relies on a RAFT agent which is usually a dithioester creating living radical initiators during polymerization [220]. Like FRP, the propagating radicals are generated by using an initiator, then they react with C=S bond in RAFT agent and form intermediate RAFT radicals. These intermediates form the reactants, a polymeric RAFT compound, or another radical. The reversible chain transfer and living polymeric chains could lead to proper propagation of all chains with a narrow dispersion of molecular weights (chain equilibrium in Fig. 1.8) [226].

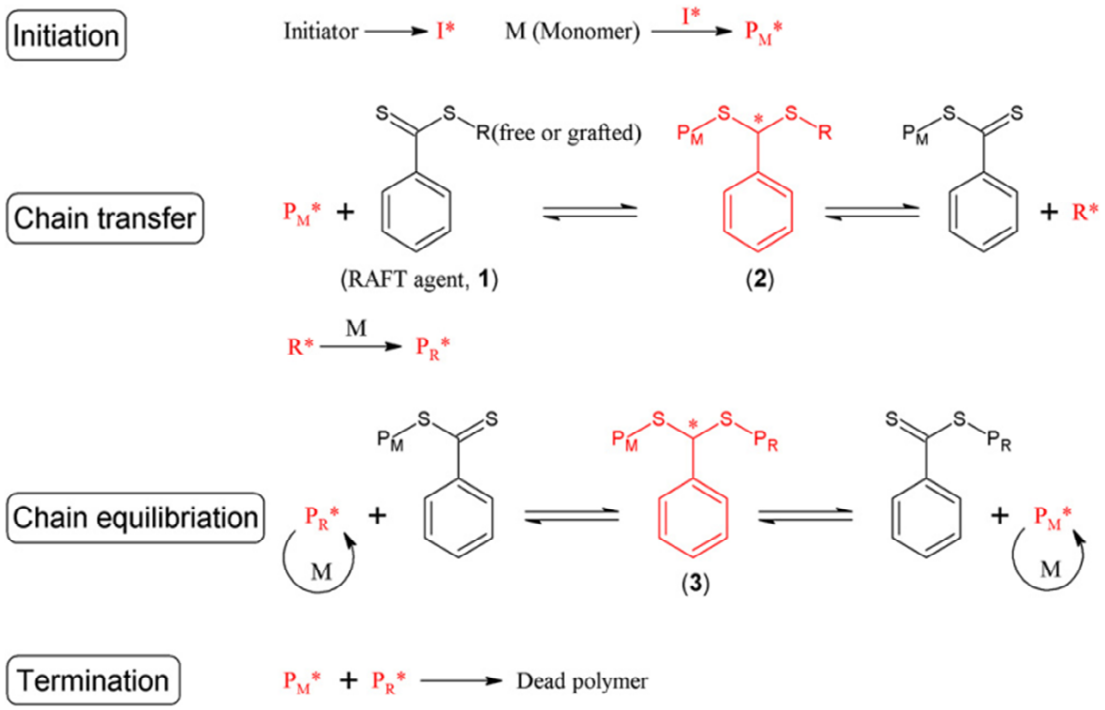


**Fig. 1.8.** Schematic representation of RAFT polymerization mechanism. Reprinted from [220] with permission from Elsevier.

In the first type RAFT-based MIPs for sample preparation of pollutants, the RAFT agent was immobilized on to the surface of silica particles. This process involves a substitute reaction of Ph–$CS_2$–MgBr with functionalized silica (chlorinated) nanoparticles. The homogenous binding sites were created by grafting the copolymer of 4-VP and EGDMA onto the surface of RAFT-functionalized NPs [230]. Chang et al. [231] used core-shell MIPs prepared by RAFT polymerization for the uptake of 2,4-DCP from water samples. Faster equilibration of $SiO_2$-RAFT@MIPs (40 min) compared to $SiO_2$@MIPs (>120 min) showed the more accessible binding sites and higher saturation capacity ($SiO_2$-RAFT@MIPs: 4.25 and $SiO_2$@MIPs: 3.07 mg $g^{-1}$). This improvement in adsorption capacity was achieved using RAFT initiation polymerization.

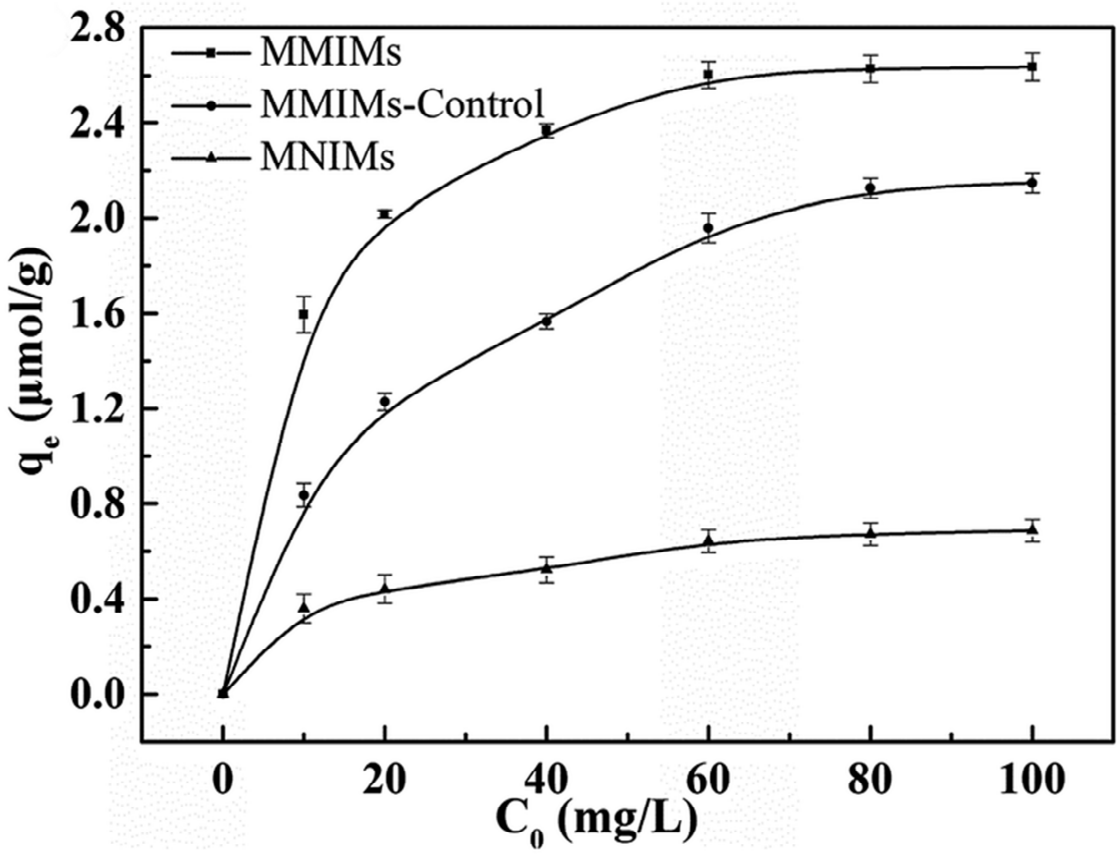


**Fig. 1.9.** Static adsorption isotherms of 17β-E2 onto RAFT-MIPs, Control-MIPs and RAFT-NIPs. Reprinted from [232] with permission from The Royal Society of Chemistry.

RAFT initiated polymerization was also used to create a thin nano-film (22 nm) on magnetic core shell particles. An excellent selectivity was obtained using $Fe_3O_4$@$SiO_2$-RAFT@MIPs in contrast with $Fe_3O_4$@$SiO_2$-RAFT@NIP, 21.30 and 5.018 mg $g^{-1}$; saturation capacity, respectively. The agreement between rebinding study and Langmuir isotherm indicated that the number of heterogeneous sites was reduced using RAFT polymerization [233]. In another example, Li et al. [232] reported BET analysis of 17β-E2-MIPs prepared by RAFT polymerization. Larger specific surface area and cumulative pore volume and smaller pore diameter represented a uniform and regular spherical structure of

polymer obtained RAFT-initiated polymer. As it is illustrated in Fig. 1.9, the RAFT-MIPs showed higher adsorption capacity than the control MIPs synthesized without RAFT agents. RAFT-MIPs serve more substantial imprinting effect and improved selectivity of the measurement. Utilization of RAFT agent such as benzyl benzodithioate as one of the polymerization components is another strategy which has been applied to graft homogenous MIPs for selective recognition of BPA [234] and PAHs [200] from environmental waters

## 1.12. Prospects for direct and online measurements using MIPs in environmental analysis

MIPs have shown great potential for the analysis of organic contaminants during the last decade. These sorptive materials are not only selective but also deployable for online and direct analysis. Using an online extraction procedure allows for simultaneous preconcentration and determination of analytes [235]. Watabe et al. [236] used online MIP-SPE coupled with LC for the determination of 17β-E2 in river water. By loading the water sample onto a MIP column, which was the pretreatment column, the analytes were preconcentrated. The analytes were then eluted from the MIP column and separated in the analytical column. Online MIP-SPE eliminates all manual and time-consuming steps for conditioning, sample loading, washing, and elution. Besides, higher sensitivity can be achieved by loading a large sample volume (i.e. 50 mL) instead of a portion (a few μL) of a preconcentrated sample. As a result, high-throughput and automated methods can be developed for the analysis of pollutants in water using online MIP-SPE-LC [237].

Microextraction by packed sorbent (MEPS) is a miniature SPE by which all sample pretreatment steps can be completed in a single extraction device. The extraction device consists of a syringe with a packed sorbent (1–4 mg) for loading water samples (μL to mL). Low-volume eluents resulting from MEPS allow for direct injection into LC systems. Thus fully automated protocols with minimal sample manipulation can be achieved [238]. MEPS in combination with MIPs have been reported for extraction and determination of FQs in wastewater samples [101]. MIP-MEPS was also reported as an online sample clean-up followed by GC analysis. The elution product was directly injected on to GC-MS with the large volume injection [239]. In addition to automation and reducing the cost of analysis, MIP-MEPS is an environmentally friendly technique using small volumes of samples and reagents.

Ambient ionization techniques such as desorption electrospray ionization (DESI) and direct analysis in real time (DART) have made revolutionary progress in trace analysis by the elimination of chromatographic steps and facilitating directed sample introduction into an MS with sample dissolution or other sample preparation methods. These techniques directly ionize the targeted compounds under ambient condition with minimal consumption of toxic organic solvents [240]. However, direct introduction of real sample can contaminate instruments, and matrix components can lead to significant signal suppression. Miniaturized sample preparation techniques using MIPs as the sorbent with these direct measurement methods is an elegant solution [241, 242]. MIP thin film, which is a new format on MIP-SPME and developed in our group for several classes of organic pollutants [241, 243, 244], can be employed for sample preparation followed by direct introduction methods. In one of these studies, a MIP thin film has been used for the selective extraction

of 2,4-dichlorophenoxyacetic acid as a pollutant from environmental water samples directly analyzed by DESI-MS [241]. The results of MIP-DESI showed feasibility for high-throughput analysis of targeted analytes and the possibility of on-site sampling, minimizing the errors associated with sample handling and reducing the cost of analysis.

Solvent desorption required before chromatographic measurement requires toxic organic solvents and additional steps for evaporation and reconstitution of analytes. Recently, a novel desorption technique was developed in our group [245, 246] , after extraction of analytes, the MIP thin film containing enriched analytes was transferred into headspace vial. The targeted analytes were directly introduced into GC via thermal desorption which minimizes errors for solvent desorption and cost of analysis. This automated desorption technique is a green analytical method that can be used for industrial labs performing environmental monitoring with a large number of samples.

## 1.13. Conclusions on MIPs for environmental analysis

Arising from the rapidly growing interest in selective sorbents for sample preparation, the development of MIPs used for different sample preparation techniques, especially MIP-SPE will remain one of the main themes in the sample preparation field. MIPs for online SPE and μ-SPE is an attractive application which can improve water analysis using automated extraction and quantitation. The high efficiency associated with the combination of nanoparticles with MIPs especially MMIPs, encourages researchers to develop core-shell MIPs for faster analysis. The advantages of MIP-SPME and other SPME-based extraction techniques (i.e., simultaneous clean-up and enrichment,

portability, field sampling, compatibility for coupling with detection systems) will expand the application of MIPs as sampling, extraction and analysis interfaces in water analysis. Additionally, recent progress in modern polymerization procedures for synthesis of homogenous and water compatible polymers will result in a huge improvement in selectivity and recognition properties of sorbents designed for the uptake of environmental pollutants. Finally, MIPs are easy to modify and manipulate in such a way that they can be used to accelerate and miniaturize sample preparation steps through innovations like MMIPs or thin film-MIPs yielding inexpensive, sensitive, selective, and environmentally-friendly methods with higher reproducibility for tracing environmental pollutants.

## 1.14. Thesis objectives

MIPs are tailor-made sorbents which are used in the analysis of water before instrumental analysis. The excellent performance of MIPs has been demonstrated by the introduction of selective materials with reduced matrix effect and high adsorption capacities in for sample preparation field. To assess the potentials and boost the prospects of these materials for environmental analysis, the objectives of this thesis include:

- **A review of MIP sorbents for sample preparation in water analysis:** A critical evaluation of MIPs in the analysis of environmental waters is provided in Chapter 1. MIPs are discussed based on the preparation of materials, applications in different formats, and recent developments. The selectivity and efficiency of MIPs are evaluated based on the rebinding medium. The limitations of MIPs for water analysis were also

discussed. Direct and online measurement techniques using MIPs that can promote the quality of water analysis are described.

- **Development of homogenous MIPs:** MIPs have been used extensively for extraction using dispersion-based techniques. However, MIPs are heterogeneous materials resulting in slower adsorption/desorption process than for solvents, relatively low selectivity and repeatability. To overcome these problems, a controlled polymerization technique named reversible addition fragmentation chain transfer (RAFT) polymerization was used to prepare MIPs in Chapter 2.
- **Application of MIP sorbents in different extraction techniques:** Ease of preparation is one of the most appealing features of MIPs. Therefore, MIPs were fabricated using various preparation protocols, including: a surface polymerization to prepare MMIPs for DSPE in Chapter 2, and a drop-casting method to prepare extraction devices for thin film microextraction (TFME) in Chapters 3 and 4.
- **Development of MIP-coated mesh:** Mesh devices have recently received much attention due to the potentials for being coupled with MS detection systems. In Chapter 4, we report single-use MIP-coated mesh for the first time. These mesh devices, which are optimized and validated for extraction of OPPs from water samples, can be coupled to a handheld mass spectrometer.
- **Optimization strategies for MIP-based extraction:** Optimization of extraction parameters are essential in order to guarantee a practical and reliable sample preparation step. In this context, different optimization strategies are presented (i.e., experimental design in Chapter 2 and one-at-a-time methodology in Chapters 3 and 4).

- **Development of a direct analysis technique using solvothermal headspace desorption (ST-HD):** MIPs have been widely used to introduce the preconcentrated samples using solvent desorption. To reduce such sample manipulation in the lab as well as the environmental impacts of analytical techniques, we introduce a new technique in Chapter 3. In this work, the key parameters are optimized, and a mechanism is introduced that explains the enhancement of analyte desorption compared to conventional thermal desorption techniques.
- **Development of a protocol for fabrication of thin film MIPs:** Although there has been an impressive growth in MIP research and technology, MIP sorbents in thin film format can suffer from poor selectivity due to substantial presence of non-selective adsorption sites. In Chapter 4, a new MIP with exceptional selectivity and performance for the extraction of OPPs is presented.
- **Validation thin film MIPs and MIP-coated mesh:** Although MIP based microextraction devices particularly thin films, have been used for many applications, a comprehensive evaluation of these devices from an analytical point of view for the quantitation of organic pollutants has not been fully investigated. Therefore, MIP materials are validated for the extraction of these pollutants from water samples in Chapters 2, 3 and 4.
- **Analysis of complicated environmental samples using MIPs:** One of the main limitations of sorbents is the poor performance in real samples due to complex matrices. In Chapters 2 and 3, we utilized MIP sorbents for the extraction of PAHs in a complex

matrix, specifically produced water samples, i.e. wastewater from offshore sites oil and gas operations.

## 1.15. References


[1] M.N. Chong, B. Jin, C.W.K. Chow, C. Saint, Recent developments in photocatalytic water treatment technology: a review, Water Res., 44 (2010) 2997-3027.

[2] M.C.R. Alavanja, J.A. Hoppin, F. Kamel, Health effects of chronic pesticide exposure: cancer and neurotoxicity, Annu. Rev. Public Health, 25 (2004) 155-197.

[3] A. Chisvert, J.L. Benedé, A. Salvador, Current trends on the determination of organic UV filters in environmental water samples based on microextraction techniques–A review, Anal. Chim. Acta, 1034 (2018) 22-38.

[4] E. Carasek, L. Morés, J. Merib, Basic principles, recent trends and future directions of microextraction techniques for the analysis of aqueous environmental samples, Trends Environ. Anal, 19 (2018) e00060.

[5] O.P. Heemken, H. Reincke, B. Stachel, N. Theobald, The occurrence of xenoestrogens in the Elbe river and the North Sea, Chemosphere, 45 (2001) 245-259.

[6] O. Ballesteros, A. Zafra, A. Navalón, J.L. Vílchez, Sensitive gas chromatographic–mass spectrometric method for the determination of phthalate esters, alkylphenols, bisphenol A and their chlorinated derivatives in wastewater samples, J. Chromatogr. A, 1121 (2006) 154-162.

[7] Y.-Y. Zhou, X.-P. Yan, K.-N. Kim, S.-W. Wang, M.-G. Liu, Exploration of coordination polymer as sorbent for flow injection solid-phase extraction on-line coupled with high-performance liquid chromatography for determination of polycyclic aromatic hydrocarbons in environmental materials, J. Chromatogr. A, 1116 (2006) 172-178.

[8] R.M. Marcé, F. Borrull, Solid-phase extraction of polycyclic aromatic compounds, J. Chromatogr. A, 885 (2000) 273-290.

[9] É.A. Souza-Silva, R. Jiang, A. Rodríguez-Lafuente, E. Gionfriddo, J. Pawliszyn, A critical review of the state of the art of solid-phase microextraction of complex matrices I. Environmental analysis, TrAC, Trends Anal. Chem., 71 (2015) 224-235.

[10] D.W. Potter, J. Pawliszyn, Rapid determination of polyaromatic hydrocarbons and polychlorinated biphenyls in water using solid-phase microextraction and GC/MS, Environ. Sci. Technol., 28 (1994) 298-305.

[11] F. David, P. Sandra, Stir bar sorptive extraction for trace analysis, J. Chromatogr. A, 1152 (2007) 54-69.

[12] E. Pérez-Carrera, V.M.L. León, A.G. Parra, E. González-Mazo, Simultaneous determination of pesticides, polycyclic aromatic hydrocarbons and polychlorinated biphenyls in seawater and interstitial marine water samples, using stir bar sorptive extraction–thermal desorption–gas chromatography–mass spectrometry, J. Chromatogr. A, 1170 (2007) 82-90.

[13] L. Zhao, H.K. Lee, Application of static liquid-phase microextraction to the analysis of organochlorine pesticides in water, J. Chromatogr. A, 919 (2001) 381-388.

[14] Y. Wang, Y.C. Kwok, Y. He, H.K. Lee, Application of dynamic liquid-phase microextraction to the analysis of chlorobenzenes in water by using a conventional microsyringe, Anal. Chem., 70 (1998) 4610-4614.

[15] W. Ling, G.-b. Jiang, Y.-q. Cai, H.E. Bin, Y.-w. Wang, D.-z. Shen, Cloud point extraction coupled with HPLC-UV for the determination of phthalate esters in environmental water samples, J. Environ. Sci., 19 (2007) 874-878.

[16] D. Bai, J. Li, S.B. Chen, B.H. Chen, A novel cloud-point extraction process for preconcentrating selected polycyclic aromatic hydrocarbons in aqueous solution, Environ. Sci. Technol., 35 (2001) 3936-3940.

[17] P. Lucci, O. Núñez, M.T. Galceran, Solid-phase extraction using molecularly imprinted polymer for selective extraction of natural and synthetic estrogens from aqueous samples, J. Chromatogr. A, 1218 (2011) 4828-4833.

[18] L. Chen, S. Xu, J. Li, Recent advances in molecular imprinting technology: current status, challenges and highlighted applications, Chem. Soc. Rev., 40 (2011) 2922-2942.

[19] V.T. Remcho, Z.J. Tan, Peer Reviewed: MIPs as Chromatographic Stationary Phases for Molecular Recognition, Anal. Chem., 71 (1999) 248A-255A.

[20] H.Y. Xiang, W.G. Li, Electrochemical sensor for trans-resveratrol determination based on indium tin oxide electrode modified with molecularly imprinted self-assembled films, Electroanalysis, 21 (2009) 1207-1210.

[21] A. Valero-Navarro, A. Salinas-Castillo, J.F. Fernández-Sánchez, A. Segura-Carretero, R. Mallavia, A. Fernández-Gutiérrez, The development of a MIP-optosensor for the detection of monoamine naphthalenes in drinking water, Biosens. Bioelectron., 24 (2009) 2305-2311.

[22] A. Mujahid, P.A. Lieberzeit, F.L. Dickert, Chemical sensors based on molecularly imprinted sol-gel materials, Materials, 3 (2010) 2196-2217.

[23] D. Lakshmi, A. Bossi, M.J. Whitcombe, I. Chianella, S.A. Fowler, S. Subrahmanyam, E.V. Piletska, S.A. Piletsky, Electrochemical sensor for catechol and dopamine based on a catalytic molecularly imprinted polymer-conducting polymer hybrid recognition element, Anal. Chem., 81 (2009) 3576-3584.

[24] C. Alvarez-Lorenzo, A. Concheiro, Molecularly imprinted polymers for drug delivery, J. Chromatogr. B, 804 (2004) 231-245.

[25] B. Sellergren, C.J. Allender, Molecularly imprinted polymers: A bridge to advanced drug delivery, Adv. Drug Del. Rev., 57 (2005) 1733-1741.

[26] G. Wulff, Enzyme-like catalysis by molecularly imprinted polymers, Chem. Rev., 102 (2002) 1-28.

[27] A. Strikovsky, J. Hradil, G. Wulff, Catalytically active, molecularly imprinted polymers in bead form, React. Funct. Polym., 54 (2003) 49-61.

[28] O. Ramström, K. Mosbach, Synthesis and catalysis by molecularly imprinted materials, Curr. Opin. Chem. Biol., 3 (1999) 759-764.

[29] X. Song, J. Li, J. Wang, L. Chen, Quercetin molecularly imprinted polymers: Preparation, recognition characteristics and properties as sorbent for solid-phase extraction, Talanta, 80 (2009) 694-702.

[30] B. Rezaei, S. Mallakpour, N. Majidi, Solid-phase molecularly imprinted pre-concentration and spectrophotometric determination of isoxicam in pharmaceuticals and human serum, Talanta, 78 (2009) 418-423.

[31] T. Jiang, L. Zhao, B. Chu, Q. Feng, W. Yan, J.M. Lin, Molecularly imprinted solid-phase extraction for the selective determination of 17β-estradiol in fishery samples with high performance liquid chromatography, Talanta, 78 (2009) 442-447.

[32] P.E. Grimmett, J.W. Munch, Development of EPA Method 525.3 for the analysis of semivolatiles in drinking water, Anal. Methods, 5 (2013) 151-163.

[33] C. He, Y. Long, J. Pan, K. Li, F. Liu, Application of molecularly imprinted polymers to solid-phase extraction of analytes from real samples, J. Biochem. Bioph. Methods, 70 (2007) 133-150.

[34] G. Vasapollo, R.D. Sole, L. Mergola, M.R. Lazzoi, A. Scardino, S. Scorrano, G. Mele, Molecularly imprinted polymers: present and future prospective, Int. J. Mol. Sci., 12 (2011) 5908-5945.

[35] F.G. Tamayo, E. Turiel, A. Martín-Esteban, Molecularly imprinted polymers for solid-phase extraction and solid-phase microextraction: recent developments and future trends, J. Chromatogr. A, 1152 (2007) 32-40.

[36] L. Chen, X. Wang, W. Lu, X. Wu, J. Li, Molecular imprinting: perspectives and applications, Chem. Soc. Rev., 45 (2016) 2137-2211.

[37] E. Caro, R.M. Marcé, F. Borrull, P.A.G. Cormack, D.C. Sherrington, Application of molecularly imprinted polymers to solid-phase extraction of compounds from environmental and biological samples, TrAC, Trends Anal. Chem., 25 (2006) 143-154.

[38] Y. Hu, J. Pan, K. Zhang, H. Lian, G. Li, Novel applications of molecularly-imprinted polymers in sample preparation, TrAC, Trends Anal. Chem., 43 (2013) 37-52.

[39] A. Sarafraz-Yazdi, N. Razavi, Application of molecularly-imprinted polymers in solid-phase microextraction techniques, TrAC, Trends Anal. Chem., 73 (2015) 81-90.

[40] L. Xie, R. Jiang, F. Zhu, H. Liu, G. Ouyang, Application of functionalized magnetic nanoparticles in sample preparation, Anal. Bioanal. Chem., 406 (2014) 377-399.

[41] V.V. Tolmacheva, V.V. Apyari, E.V. Kochuk, S.G. Dmitrienko, Magnetic adsorbents based on iron oxide nanoparticles for the extraction and preconcentration of organic compounds, J. Anal. Chem., 71 (2016) 321-338.

[42] S. Ansari, Application of magnetic molecularly imprinted polymer as a versatile and highly selective tool in food and environmental analysis: Recent developments and trends, TrAC, Trends Anal. Chem., 90 (2017) 89-106.

[43] L. Chen, B. Li, Application of magnetic molecularly imprinted polymers in analytical chemistry, Anal. Methods, 4 (2012) 2613-2621.

[44] M. Niu, C. Pham-Huy, H. He, Core-shell nanoparticles coated with molecularly imprinted polymers: a review, Microchim. Acta, 183 (2016) 2677-2695.

[45] S. Ansari, M. Karimi, Novel developments and trends of analytical methods for drug analysis in biological and environmental samples by molecularly imprinted polymers, TrAC, Trends Anal. Chem., 89 (2017) 146-162.

[46] A. Speltini, A. Scalabrini, F. Maraschi, M. Sturini, A. Profumo, Newest applications of molecularly imprinted polymers for extraction of contaminants from environmental and food matrices: A review, Anal. Chim. Acta, 974 (2017) 1-26.

[47] A. Murray, B. Örmeci, Application of molecularly imprinted and non-imprinted polymers for removal of emerging contaminants in water and wastewater treatment: a review, Environ. Sci. Pollut. R., 19 (2012) 3820-3830.

[48] D.-L. Huang, R.-Z. Wang, Y.-G. Liu, G.-M. Zeng, C. Lai, P. Xu, B.-A. Lu, J.-J. Xu, C. Wang, C. Huang, Application of molecularly imprinted polymers in wastewater treatment: a review, Environ. Sci. Pollut. R., 22 (2015) 963-977.

[49] A. Martín-Esteban, Recent molecularly imprinted polymer-based sample preparation techniques in environmental analysis, Trends Environ. Anal, 9 (2016) 8-14.

[50] X. Song, J. Li, S. Xu, R. Ying, J. Ma, C. Liao, D. Liu, J. Yu, L. Chen, Determination of 16 polycyclic aromatic hydrocarbons in seawater using molecularly imprinted solid-phase extraction coupled with gas chromatography-mass spectrometry, Talanta, 99 (2012) 75-82.

[51] Y. Hao, R. Gao, L. Shi, D. Liu, Y. Tang, Z. Guo, Water-compatible magnetic imprinted nanoparticles served as solid-phase extraction sorbents for selective determination of trace 17beta-estradiol in environmental water samples by liquid chromatography, J. Chromatogr. A, 1396 (2015) 7-16.

[52] K. Demeestere, M. Petrovic, M. Gros, J. Dewulf, H. Van Langenhove, D. Barcelo, Trace analysis of antidepressants in environmental waters by molecularly imprinted polymer-based solid-phase extraction followed by ultra-performance liquid chromatography coupled to triple quadrupole mass spectrometry, Anal. Bioanal. Chem., 396 (2010) 825-837.

[53] X. Sun, M. Wang, L. Yang, H. Wen, L. Wang, T. Li, C. Tang, J. Yang, Preparation and evaluation of dummy-template molecularly imprinted polymer as a potential sorbent for solid phase extraction of imidazole fungicides from river water, J. Chromatogr. A, 1586 (2019) 1-8.

[54] E. Turiel, A. Martín-Esteban, Molecularly imprinted polymers for sample preparation: a review, Anal. Chim. Acta, 668 (2010) 87-99.

[55] P. Qi, J. Wang, J. Jin, F. Su, J. Chen, 2,4-Dimethylphenol imprinted polymers as a solid-phase extraction sorbent for class-selective extraction of phenolic compounds from environmental water, Talanta, 81 (2010) 1630-1635.

[56] P. Van de Witte, P.J. Dijkstra, J.W.A. Van den Berg, J. Feijen, Phase separation processes in polymer solutions in relation to membrane formation, J. Membr. Sci., 117 (1996) 1-31.

[57] D.A. Spivak, Optimization, evaluation, and characterization of molecularly imprinted polymers, Adv. Drug Del. Rev., 57 (2005) 1779-1794.

[58] Y. Wang, M. Tian, K. Yu, L. Li, Z. Zhang, L. Li, A versatile strategy to fabricate magnetic dummy molecularly imprinted mesoporous silica particles for specific magnetic separation of bisphenol A, New J. Chem., 43 (2019) 3400-3408.

[59] Y. Tang, J. Lan, X. Gao, X. Liu, D. Zhang, L. Wei, Z. Gao, J. Li, Determination of clenbuterol in pork and potable water samples by molecularly imprinted polymer through the use of covalent imprinting method, Food Chem., 190 (2016) 952-959.

[60] D. Yu, X. Hu, S. Wei, Q. Wang, C. He, S. Liu, Dummy molecularly imprinted mesoporous silica prepared by hybrid imprinting method for solid-phase extraction of bisphenol A, J. Chromatogr. A, 1396 (2015) 17-24.

[61] X. Wang, L. Wang, X. He, Y. Zhang, L. Chen, A molecularly imprinted polymer-coated nanocomposite of magnetic nanoparticles for estrone recognition, Talanta, 78 (2009) 327-332.

[62] C.D. Ki, C. Oh, S.-G. Oh, J.Y. Chang, The Use of a Thermally Reversible Bond for Molecular Imprinting of Silica Spheres, J. Am. Chem. Soc., 124 (2002) 14838-14839.

[63] H. Sun, Y. Li, J. Yang, X. Sun, C. Huang, X. Zhang, J. Chen, Preparation of dummy-imprinted polymers by Pickering emulsion polymerization for the selective determination of seven bisphenols from sediment samples, J. Sep. Sci., 39 (2016) 2188-2195.

[64] Z. Sun, W. Schussler, M. Sengl, R. Niessner, D. Knopp, Selective trace analysis of diclofenac in surface and wastewater samples using solid-phase extraction with a new molecularly imprinted polymer, Anal. Chim. Acta, 620 (2008) 73-81.

[65] J. Yin, Z. Meng, M. Du, C. Liu, M. Song, H. Wang, Pseudo-template molecularly imprinted polymer for selective screening of trace beta-lactam antibiotics in river and tap water, J. Chromatogr. A, 1217 (2010) 5420-5426.

[66] H. Shaikh, N. Memon, H. Khan, M.I. Bhanger, S.M. Nizamani, Preparation and characterization of molecularly imprinted polymer for di(2-ethylhexyl) phthalate:

application to sample clean-up prior to gas chromatographic determination, J. Chromatogr. A, 1247 (2012) 125-133.

[67] X.-P. He, Z.-R. Lian, L.-J. Tan, J.-T. Wang, Preparation and characterization of magnetic molecularly imprinted polymers for selective trace extraction of dienestrol in seawater, J. Chromatogr. A, 1469 (2016) 8-16.

[68] W. Guan, J. Pan, X. Wang, W. Hu, L. Xu, X. Zou, C. Li, Selective recognition of 4-nitrophenol from aqueous solution by molecularly imprinted polymers with functionalized tetratitanate whisker composites as support, J. Sep. Sci., 34 (2011) 1244-1252.

[69] W. Zhang, X. She, L. Wang, H. Fan, Q. Zhou, X. Huang, J. Tang, Preparation, characterization and application of a molecularly imprinted polymer for selective recognition of sulpiride, Materials, 10 (2017) 475.

[70] Z.E. Mbhele, S. Ncube, L.M. Madikizela, Synthesis of a molecularly imprinted polymer and its application in selective extraction of fenoprofen from wastewater, Environ. Sci. Pollut. R., 25 (2018) 36724-36735.

[71] E. Herrero-Hernandez, R. Carabias-Martinez, E. Rodriguez-Gonzalo, Behavior of phenols and phenoxyacids on a bisphenol-A imprinted polymer. Application for selective solid-phase extraction from water and urine samples, Int. J. Mol. Sci., 12 (2011) 3322-3339.

[72] Z. Lian, Z. Liang, J. Wang, Selective extraction and concentration of mebendazole in seawater samples using molecularly imprinted polymer as sorbent, Mar. Pollut. Bull., 91 (2015) 96-101.

[73] L.M. Madikizela, L. Chimuka, Determination of ibuprofen, naproxen and diclofenac in aqueous samples using a multi-template molecularly imprinted polymer as selective adsorbent for solid-phase extraction, J. Pharm. Biomed. Anal., 128 (2016) 210-215.

[74] H. Sun, Y. Li, C. Huang, J. Peng, J. Yang, X. Sun, S. Zang, J. Chen, X. Zhang, Solid-phase extraction based on a molecularly imprinted polymer for the selective determination of four benzophenones in tap and river water, J. Sep. Sci., 38 (2015) 3412-3420.

[75] E. Benito-Pena, J.L. Urraca, B. Sellergren, M.C. Moreno-Bondi, Solid-phase extraction of fluoroquinolones from aqueous samples using a water-compatible stochiometrically imprinted polymer, J. Chromatogr. A, 1208 (2008) 62-70.

[76] S.S. Zunngu, L.M. Madikizela, L. Chimuka, P.S. Mdluli, Synthesis and application of a molecularly imprinted polymer in the solid-phase extraction of ketoprofen from wastewater, C. R. Chim., 20 (2017) 585-591.

[77] J. Tang, M. Zhang, G. Cheng, Y. Lu, Development and Application of Molecularly Imprinted Polymer as Solid Phase Extraction of Imidacloprid in Environmental Samples, J. Liq. Chromatogr. Rel. Technol., 32 (2008) 59-71.

[78] P. Kueseng, M.L. Noir, B. Mattiasson, P. Thavarungkul, P. Kanatharana, Molecularly imprinted polymer for analysis of trace atrazine herbicide in water, J. Environ. Sci. Health. B, 44 (2009) 772-780.

[79] X.Q. Mei, X.P. He, J.T. Wang, Molecularly imprinted polymer as efficient sorbent of solid-phase extraction for determination of gonyautoxin 1,4 in seawater followed by high-performance liquid chromatography-fluorescence detection, Anal. Bioanal. Chem., 408 (2016) 5737-5743.

[80] A.R. Koohpaei, S.J. Shahtaheri, M.R. Ganjali, A.R. Forushani, F. Golbabaei, Optimization of solid-phase extraction using developed modern sorbent for trace determination of ametryn in environmental matrices, J. Hazard. Mater., 170 (2009) 1247-1255.

[81] W. Lu, X. Wang, X. Wu, D. Liu, J. Li, L. Chen, X. Zhang, Multi-template imprinted polymers for simultaneous selective solid-phase extraction of six phenolic compounds in water samples followed by determination using capillary electrophoresis, J. Chromatogr. A, 1483 (2017) 30-39.

[82] Q.Z. Feng, L.X. Zhao, W. Yan, J.M. Lin, Z.X. Zheng, Molecularly imprinted solid-phase extraction combined with high performance liquid chromatography for analysis of phenolic compounds from environmental water samples, J. Hazard. Mater., 167 (2009) 282-288.

[83] S. Wang, Z. Xu, G. Fang, Y. Zhang, J. He, Separation and determination of estrone in environmental and drinking water using molecularly imprinted solid phase extraction coupled with HPLC, J. Sep. Sci., 31 (2008) 1181-1188.

[84] J. Yin, Z. Meng, Y. Zhu, M. Song, H. Wang, Dummy molecularly imprinted polymer for selective screening of trace bisphenols in river water, Anal. Methods, 3 (2011) 173-180.

[85] M. Zarejousheghani, P. Fiedler, M. Moder, H. Borsdorf, Selective mixed-bed solid phase extraction of atrazine herbicide from environmental water samples using molecularly imprinted polymer, Talanta, 129 (2014) 132-138.

[86] F. Canale, C. Cordero, C. Baggiani, P. Baravalle, C. Giovannoli, C. Bicchi, Development of a molecularly imprinted polymer for selective extraction of bisphenol A in water samples, J. Sep. Sci., 33 (2010) 1644-1651.

[87] X. Sun, M. Wang, J. Peng, L. Yang, X. Wang, F. Wang, X. Zhang, Q. Wu, R. Chen, J. Chen, Dummy molecularly imprinted solid phase extraction of climbazole from environmental water samples, Talanta, 196 (2019) 47-53.

[88] J. Zhan, G. Fang, Z. Yan, M. Pan, C. Liu, S. Wang, Preparation of a semicovalent, molecularly surface imprinted polymer for the rapid determination of trace acid orange II in food and environmental samples, Anal. Bioanal. Chem., 405 (2013) 6353-6363.

[89] H.R. Geng, S.S. Miao, S.F. Jin, H. Yang, A newly developed molecularly imprinted polymer on the surface of TiO2 for selective extraction of triazine herbicides residues in maize, water, and soil, Anal. Bioanal. Chem., 407 (2015) 8803-8812.

[90] H.G. Zuo, J.X. Zhu, C.R. Zhan, L. Shi, M. Xing, P. Guo, Y. Ding, H. Yang, Preparation of malathion MIP-SPE and its application in environmental analysis, Environ. Monit. Assess., 187 (2015) 394.

[91] X.W. Fu, Y.J. Wu, J.R. Qu, H. Yang, Preparation and utilization of molecularly imprinted polymer for chlorsulfuron extraction from water, soil, and wheat plant, Environ. Monit. Assess., 184 (2012) 4161-4170.

[92] X. Gao, M. Pan, G. Fang, W. Jing, S. He, S. Wang, An ionic liquid modified dummy molecularly imprinted polymer as a solid-phase extraction material for the simultaneous determination of nine organochlorine pesticides in environmental and food samples, Anal. Methods, 5 (2013) 6128.

[93] W. Guan, C. Han, X. Wang, X. Zou, J. Pan, P. Huo, C. Li, Molecularly imprinted polymer surfaces as solid-phase extraction sorbents for the extraction of 2-nitrophenol and isomers from environmental water, J. Sep. Sci., 35 (2012) 490-497.

[94] Y.M. Yin, Y.P. Chen, X.F. Wang, Y. Liu, H.L. Liu, M.X. Xie, Dummy molecularly imprinted polymers on silica particles for selective solid-phase extraction of tetrabromobisphenol A from water samples, J. Chromatogr. A, 1220 (2012) 7-13.

[95] E. Herrero-Hernandez, E. Rodriguez-Gonzalo, M.S. Andrades, S. Sanchez-Gonzalez, R. Carabias-Martinez, Occurrence of phenols and phenoxyacid herbicides in environmental waters using an imprinted polymer as a selective sorbent, Sci. Total Environ., 454-455 (2013) 299-306.

[96] G. Zhu, J. Fan, X. Gao, J. Wang, A surface molecularly imprinted polymer for selective extraction and liquid chromatographic determination of 4-methylimidazole in environmental samples, Adsorpt. Sci. Technol., 31 (2013) 791-806.

[97] X. Hu, X. Wu, F. Yang, Q. Wang, C. He, S. Liu, Novel surface dummy molecularly imprinted silica as sorbent for solid-phase extraction of bisphenol A from water samples, Talanta, 148 (2016) 29-36.

[98] M.C. Barciela-Alonso, N. Otero-Lavandeira, P. Bermejo-Barrera, Solid phase extraction using molecular imprinted polymers for phthalate determination in water and wine samples by HPLC-ESI-MS, Microchem. J., 132 (2017) 233-237.

[99] C.M. Dai, X.F. Zhou, Y.L. Zhang, S.G. Liu, J. Zhang, Synthesis by precipitation polymerization of molecularly imprinted polymer for the selective extraction of diclofenac from water samples, J. Hazard. Mater., 198 (2011) 175-181.

[100] Y.P. Duan, C.M. Dai, Y.L. Zhang, C. Ling, Selective trace enrichment of acidic pharmaceuticals in real water and sediment samples based on solid-phase extraction using multi-templates molecularly imprinted polymers, Anal. Chim. Acta, 758 (2013) 93-100.

[101] A. Prieto, S. Schrader, C. Bauer, M. Moder, Synthesis of a molecularly imprinted polymer and its application for microextraction by packed sorbent for the determination of fluoroquinolone related compounds in water, Anal. Chim. Acta, 685 (2011) 146-152.

[102] M.D. Luaces, J.L. Urraca, M.C. Pérez-Conde, N.C.M. Alfonso, A.C. Valdés-González, A.M. Gutiérrez, M.C. Moreno-Bondi, Chemiluminescence analysis of enrofloxacin in surface water using the tris(1,10-phenantroline)–ruthenium(II)/peroxydisulphate system and extraction with molecularly imprinted polymers, Microchem. J., 110 (2013) 458-464.

[103] Z. Li, J. Wang, X. Chen, S. Hu, T. Gong, Q. Xian, A novel molecularly imprinted polymer-solid phase extraction method coupled with high performance liquid chromatography tandem mass spectrometry for the determination of nitrosamines in water and beverage samples, Food Chem., 292 (2019) 267-274.

[104] M. Jesús García-Galán, M. Silvia Díaz-Cruz, D. Barceló, Determination of triazines and their metabolites in environmental samples using molecularly imprinted polymer extraction, pressurized liquid extraction and LC–tandem mass spectrometry, Journal of Hydrology, 383 (2010) 30-38.

[105] M. Valtchev, B.S. Palm, M. Schiller, U. Steinfeld, Development of sulfamethoxazole-imprinted polymers for the selective extraction from waters, J. Hazard. Mater., 170 (2009) 722-728.

[106] H. Sun, Y. Li, C. Huang, J. Peng, J. Yang, X. Sun, S. Zang, J. Chen, X. Zhang, Solid-phase extraction based on a molecularly imprinted polymer for the selective determination of four benzophenones in tap and river water, J. Sep. Sci., 38 (2015) 3412-3420.

[107] M. Marć, A. Panuszko, J. Namieśnik, P.P. Wieczorek, Preparation and characterization of dummy-template molecularly imprinted polymers as potential sorbents for the recognition of selected polybrominated diphenyl ethers, Anal. Chim. Acta, 1030 (2018) 77-95.

[108] J. Xie, J. Xie, J. Deng, X. Fang, H. Zhao, D. Qian, H. Wang, Computational design and fabrication of core–shell magnetic molecularly imprinted polymer for dispersive micro-solid-phase extraction coupled with high-performance liquid chromatography for the determination of rhodamine 6G, J. Sep. Sci., 39 (2016) 2422-2430.

[109] M. Zhang, L. Gu, G. Kong, Y. Zheng, Y. Han, Z. Li, J. Shi, J. Peng, Comparative analysis of atrazine molecularly imprinted polymers using acetonitrile and toluene as solvents, J. Appl. Polym. Sci., 136 (2019) 47190.

[110] A. Andrade-Eiroa, M. Canle, V. Leroy-Cancellieri, V. Cerdà, Solid-phase extraction of organic compounds: a critical review (Part I), TrAC, Trends Anal. Chem., 80 (2016) 641-654.

[111] X. Sun, J. Peng, M. Wang, J. Wang, C. Tang, L. Yang, H. Lei, F. Li, X. Wang, J. Chen, Determination of nine bisphenols in sewage and sludge using dummy molecularly imprinted solid-phase extraction coupled with liquid chromatography tandem mass spectrometry, J. Chromatogr. A, 1552 (2018) 10-16.

[112] Z. Lian, J. Wang, Selective detection of chloramphenicol based on molecularly imprinted solid-phase extraction in seawater from Jiaozhou Bay, China, Mar. Pollut. Bull., 133 (2018) 750-755.

[113] P. Kadhirvel, A. Combès, L. Bordron, V. Pichon, Development and application of water-compatible molecularly imprinted polymers for the selective extraction of carbamazepine from environmental waters, Anal. Bioanal. Chem., 411 (2019) 525–1536.

[114] T. Martinez-Sena, S. Armenta, M. Guardia, F.A. Esteve-Turrillas, Determination of non-steroidal anti-inflammatory drugs in water and urine using selective molecular

imprinted polymer extraction and liquid chromatography, J. Pharm. Biomed. Anal., 131 (2016) 48-53.

[115] S. Morante-Zarcero, I. Sierra, Simultaneous Enantiomeric Determination of Propranolol, Metoprolol, Pindolol, and Atenolol in Natural Waters by HPLC on New Polysaccharide-Based Stationary Phase using a Highly Selective Molecularly Imprinted Polymer Extraction, Chirality, 24 (2012) 860-866.

[116] M. Gros, T.-M. Pizzolato, M. Petrović, M.J.L. de Alda, D. Barceló, Trace level determination of β-blockers in waste waters by highly selective molecularly imprinted polymers extraction followed by liquid chromatography–quadrupole-linear ion trap mass spectrometry, J. Chromatogr. A, 1189 (2008) 374-384.

[117] S.H. Hashemi, M. Kaykhaii, A.J. Keikha, Z. Sajjadi, Application of Box-Behnken design in response surface methodology for the molecularly imprinted polymer pipette-tip solid phase extraction of methyl red from seawater samples and its determination by spectrophotometery, Mar. Pollut. Bull., 137 (2018) 306-314.

[118] S.S. Miao, M.S. Wu, H.G. Zuo, C. Jiang, S.F. Jin, Y.C. Lu, H. Yang, Core–Shell Magnetic Molecularly Imprinted Polymers as Sorbent for Sulfonylurea Herbicide Residues, J. Agric. Food. Chem., 63 (2015) 3634-3645.

[119] J. Pan, L. Li, H. Hang, R. Wu, X. Dai, W. Shi, Y. Yan, Fabrication and evaluation of magnetic/hollow double-shelled imprinted sorbents formed by Pickering emulsion polymerization, Langmuir, 29 (2013) 8170-8178.

[120] C. Zhou, H. Li, H. Zhou, H. Wang, P. Yang, S. Zhong, Water-compatible halloysite-imprinted polymer by Pickering emulsion polymerization for the selective recognition of herbicides, J. Sep. Sci., 38 (2015) 1365-1371.

[121] Y. Li, Y. Sun, J. Chen, X. Zhu, H. Li, S. Huang, Y. Hu, Q. Chen, S. Zhong, Graphene oxide as a sacrificial material for fabricating molecularly imprinted polymers via Pickering emulsion polymerization, RSC Adv., 6 (2016) 74654-74661.

[122] H. Hang, C. Li, J. Pan, L. Li, J. Dai, X. Dai, P. Yu, Y. Feng, Selective separation of lambdacyhalothrin by porous/magnetic molecularly imprinted polymers prepared by Pickering emulsion polymerization, J. Sep. Sci., 36 (2013) 3285-3294.

[123] Z. Lian, J. Wang, Molecularly imprinted polymer for selective extraction of malachite green from seawater and seafood coupled with high-performance liquid chromatographic determination, Mar. Pollut. Bull., 64 (2012) 2656-2662.

[124] H. Zhang, Water-compatible molecularly imprinted polymers: Promising synthetic substitutes for biological receptors, Polymer, 55 (2014) 699-714.

[125] E. Abdollahi, M. Abdouss, A. Mohammadi, Synthesis of a nano molecularly imprinted polymeric sorbent for solid phase extraction and determination of phenytoin in plasma, urine, and wastewater by HPLC, RSC Adv., 6 (2016) 39095-39105.

[126] W. Lu, J. Liu, J. Li, X. Wang, M. Lv, R. Cui, L. Chen, Dual-template molecularly imprinted polymers for dispersive solid-phase extraction of fluoroquinolones in water

samples coupled with high performance liquid chromatography, Analyst, 144 (2019) 1292-1302.

[127] J. Płotka-Wasylka, N. Szczepańska, M. de la Guardia, J. Namieśnik, Modern trends in solid phase extraction: new sorbent media, TrAC, Trends Anal. Chem., 77 (2016) 23-43.

[128] H. Chen, Y. Zhang, B. Gao, Y. Xu, Q. Zhao, J. Hou, J. Yan, G. Li, H. Wang, L. Ding, Fast determination of sulfonamides and their acetylated metabolites from environmental water based on magnetic molecularly imprinted polymers, Environ. Sci. Pollut. R., 20 (2013) 8567-8578.

[129] L. Guo, X. Ma, X. Xie, R. Huang, M. Zhang, J. Li, G. Zeng, Y. Fan, Preparation of dual-dummy-template molecularly imprinted polymers coated magnetic graphene oxide for separation and enrichment of phthalate esters in water, Chem. Eng. J., 361 (2019) 245-255.

[130] A. Bazmandegan-Shamili, S. Dadfarnia, A.M.H. Shabani, M. Saeidi, M.R. Moghadam, High-performance liquid chromatographic determination of diazinon after its magnetic dispersive solid-phase microextraction using magnetic molecularly imprinted polymer, Food Anal. Methods, 9 (2016) 2621-2630.

[131] R. Gao, X. Kong, F. Su, X. He, L. Chen, Y. Zhang, Synthesis and evaluation of molecularly imprinted core–shell carbon nanotubes for the determination of triclosan in environmental water samples, J. Chromatogr. A, 1217 (2010) 8095-8102.

[132] L. Chen, X. Zhang, Y. Xu, X. Du, X. Sun, L. Sun, H. Wang, Q. Zhao, A. Yu, H. Zhang, Determination of fluoroquinolone antibiotics in environmental water samples based on magnetic molecularly imprinted polymer extraction followed by liquid chromatography–tandem mass spectrometry, Anal. Chim. Acta, 662 (2010) 31-38.

[133] Z.H.U. Li-Li, C.A.O. Yu-Hua, C.A.O. Guang-Qun, Preparation and application of core-shell magnetic imprinted nanoparticles for bisphenol A, Chinese J. Anal. Chem., 41 (2013) 1724-1728.

[134] H. Shen, B. Liu, Q. Xiang, C. Wang, S.Q. Mao, Highly selective amino-functionalized magnetic molecularly imprinted polymers: absorbents for dispersive solid phase extraction and trace level analysis of chlorophenols in seawater, RSC Adv., 6 (2016) 81330-81340.

[135] L. Chang, S. Chen, X. Li, Synthesis and properties of core-shell magnetic molecular imprinted polymers, Appl. Surf. Sci., 258 (2012) 6660-6664.

[136] S. Wei, J. Li, Y. Liu, J. Ma, Development of magnetic molecularly imprinted polymers with double templates for the rapid and selective determination of amphenicol antibiotics in water, blood, and egg samples, J. Chromatogr. A, 1473 (2016) 19-27.

[137] W. Yang, L. Liu, X. Ni, W. Zhou, W. Huang, H. Liu, W. Xu, Computer-aided design and synthesis of magnetic molecularly imprinted polymers with high selectivity for the removal of phenol from water, J. Sep. Sci., 39 (2016) 503-517.

[138] J. Pan, L. Li, H. Hang, H. Ou, L. Zhang, Y. Yan, W. Shi, Study on the nonylphenol removal from aqueous solution using magnetic molecularly imprinted polymers based on fly-ash-cenospheres, Chem. Eng. J., 223 (2013) 824-832.

[139] T. Yang, S. Feng, Y. Lu, C. Yin, J. Wang, Dual-template magnetic molecularly imprinted particles with multi-hollow structure for the detection of dicofol and chlorpyrifos-methyl, J. Sep. Sci., 39 (2016) 2388-2395.

[140] H. Bagheri, K. Molaei, A.A. Asgharinezhad, H. Ebrahimzadeh, M. Shamsipur, Magnetic molecularly imprinted composite for the selective solid-phase extraction of p-aminosalicylic acid followed by high-performance liquid chromatography with ultraviolet detection, J. Sep. Sci., 39 (2016) 4166-4174.

[141] X. Xie, X. Pan, S. Han, S. Wang, Development and characterization of magnetic molecularly imprinted polymers for the selective enrichment of endocrine disrupting chemicals in water and milk samples, Anal. Bioanal. Chem., 407 (2015) 1735-1744.

[142] W. Rao, R. Cai, Y. Yin, F. Long, Z. Zhang, Magnetic dummy molecularly imprinted polymers based on multi-walled carbon nanotubes for rapid selective solid-phase extraction of 4-nonylphenol in aqueous samples, Talanta, 128 (2014) 170-176.

[143] R. Yang, Y. Liu, X. Yan, S. Liu, H. Zheng, An effective method for the synthesis of yolk–shell magnetic mesoporous carbon-surface molecularly imprinted microspheres, J. Mater. Chem. A, 4 (2016) 9807-9815.

[144] S. Qin, L. Su, P. Wang, Y. Gao, Rapid and selective extraction of multiple sulfonamides from aqueous samples based on Fe 3 O 4–chitosan molecularly imprinted polymers, Anal. Methods, 7 (2015) 8704-8713.

[145] A. Barati, E. Kazemi, S. Dadfarnia, A.M.H. Shabani, Synthesis/characterization of molecular imprinted polymer based on magnetic chitosan/graphene oxide for selective separation/preconcentration of fluoxetine from environmental and biological samples, J. Ind. Eng. Chem., 46 (2017) 212-221.

[146] J. Pan, B. Wang, J. Dai, X. Dai, H. Hang, H. Ou, Y. Yan, Selective recognition of 2, 4, 5-trichlorophenol by temperature responsive and magnetic molecularly imprinted polymers based on halloysite nanotubes, J. Mater. Chem., 22 (2012) 3360-3369.

[147] X. Wang, H. Mao, W. Huang, W. Guan, X. Zou, J. Pan, Y. Yan, Preparation of magnetic imprinted polymer particles via microwave heating initiated polymerization for selective enrichment of 2-amino-4-nitrophenol from aqueous solution, Chem. Eng. J., 178 (2011) 85-92.

[148] X. Yuan, T. Liu, L. Gao, L. Xing, Y. Zhu, S. Li, A convenient separation method for di (2-ethylhexyl) phthalate by novel superparamagnetic molecularly imprinted polymers, RSC Adv., 8 (2018) 36191-36199.

[149] X. Wang, P. Huang, X. Ma, H. Wang, X. Lu, X. Du, Preparation and evaluation of magnetic core-shell mesoporous molecularly imprinted polymers for selective adsorption of tetrabromobisphenol S, Talanta, 166 (2017) 300-305.

[150] A.R. Zarei, R.S. Zafarghandi, Selective determination of 2, 4, 6-trinitrotoluene in water samples based on magnetic imprinted nanoparticles via grafting polymerization, J. Braz. Chem. Soc., 26 (2015) 741-747.

[151] F. Qiao, M. Gao, H. Yan, Molecularly imprinted ionic liquid magnetic microspheres for the rapid isolation of organochlorine pesticides in environmental water, J. Sep. Sci., 39 (2016) 1310-1315.

[152] M. Villar-Navarro, M.J. Martín-Valero, R.M. Fernández-Torres, M. Callejón-Mochón, M.Á. Bello-López, Easy, fast and environmental friendly method for the simultaneous extraction of the 16 EPA PAHs using magnetic molecular imprinted polymers (mag-MIPs), J. Chromatogr. B, 1044 (2017) 63-69.

[153] H. Piri-Moghadam, F. Ahmadi, J. Pawliszyn, A critical review of solid phase microextraction for analysis of water samples, TrAC, Trends Anal. Chem., 85 (2016) 133-143.

[154] C.L. Arthur, J. Pawliszyn, Solid phase microextraction with thermal desorption using fused silica optical fibers, Anal. Chem., 62 (1990) 2145-2148.

[155] N. Reyes-Garcés, E. Gionfriddo, G.A. Gómez-Ríos, M.N. Alam, E. Boyacı, B. Bojko, V. Singh, J. Grandy, J. Pawliszyn, Advances in solid phase microextraction and perspective on future directions, Anal. Chem., 90 (2017) 302-360.

[156] A. Kumar, A.K. Malik, D.K. Tewary, B. Singh, A review on development of solid phase microextraction fibers by sol–gel methods and their applications, Anal. Chim. Acta, 610 (2008) 1-14.

[157] E.H.M. Koster, C. Crescenzi, W. den Hoedt, K. Ensing, G.J. de Jong, Fibers coated with molecularly imprinted polymers for solid-phase microextraction, Anal. Chem., 73 (2001) 3140-3145.

[158] X. Hu, J. Pan, Y. Hu, Y. Huo, G. Li, Preparation and evaluation of solid-phase microextraction fiber based on molecularly imprinted polymers for trace analysis of tetracyclines in complicated samples, J. Chromatogr. A, 1188 (2008) 97-107.

[159] D. Djozan, B. Ebrahimi, M. Mahkam, M.A. Farajzadeh, Evaluation of a new method for chemical coating of aluminum wire with molecularly imprinted polymer layer. Application for the fabrication of triazines selective solid-phase microextraction fiber, Anal. Chim. Acta, 674 (2010) 40-48.

[160] Z. Terzopoulou, M. Papageorgiou, G.Z. Kyzas, D.N. Bikiaris, D.A. Lambropoulou, Preparation of molecularly imprinted solid-phase microextraction fiber for the selective removal and extraction of the antiviral drug abacavir in environmental and biological matrices, Anal. Chim. Acta, 913 (2016) 63-75.

[161] Y. Liu, D. Wang, F. Du, W. Zheng, Z. Liu, Z. Xu, X. Hu, H. Liu, Dummy-template molecularly imprinted micro-solid-phase extraction coupled with high-performance liquid chromatography for bisphenol A determination in environmental water samples, Microchem. J., 145 (2019) 337-344.

[162] C. Cai, P. Zhang, J. Deng, H. Zhou, J. Cheng, Ultrasensitive determination of highly polar trimethyl phosphate in environmental water by molecularly imprinted polymeric fiber headspace solid-phase microextraction, J. Sep. Sci., 41 (2018) 1104-1111.

[163] A.A. Pebdani, A.M. Shabani, S. Dadfarnia, S. Khodadoust, Solid phase microextraction of diclofenac using molecularly imprinted polymer sorbent in hollow fiber combined with fiber optic-linear array spectrophotometry, Spectrochim. Acta. A Mol. Biomol. Spectrosc., 147 (2015) 26-30.

[164] M. Saraji, N. Mehrafza, A simple approach for the preparation of simazine molecularly imprinted nanofibers via self-polycondensation for selective solid-phase microextraction, Anal. Chim. Acta, 936 (2016) 108-115.

[165] M. Zarejousheghani, M. Moder, H. Borsdorf, A new strategy for synthesis of an in-tube molecularly imprinted polymer-solid phase microextraction device: selective off-line extraction of 4-nitrophenol as an example of priority pollutants from environmental water samples, Anal. Chim. Acta, 798 (2013) 48-55.

[166] T. Du, J. Cheng, M. Wu, X. Wang, H. Zhou, M. Cheng, An in situ immobilized pipette tip solid phase microextraction method based on molecularly imprinted polymer monolith for the selective determination of difenoconazole in tap water and grape juice, J. Chromatogr. B Analyt. Technol. Biomed. Life Sci., 951-952 (2014) 104-109.

[167] X. Wang, P. Huang, X. Ma, X. Du, X. Lu, Enhanced in-out-tube solid-phase microextraction by molecularly imprinted polymers-coated capillary followed by HPLC for Endocrine Disrupting Chemicals analysis, Talanta, 194 (2019) 7-13.

[168] M. Zhang, J. Huang, Layer-by-layer coated molecular-imprinted solid-phase microextraction fibers for the determination of polar compounds in water samples, RSC Adv., 6 (2016) 94098-94104.

[169] H. Hashemi-Moghaddam, M. Hosseni, M. Mohammadhosseini, Preparation of molecularly imprinted polymers on the surface of optical fiber for HS-solid-phase microextraction of phenol, Sep. Sci. Technol., (2017) 1-9.

[170] A. Prieto, O. Basauri, R. Rodil, A. Usobiaga, L.A. Fernandez, N. Etxebarria, O. Zuloaga, Stir-bar sorptive extraction: A view on method optimisation, novel applications, limitations and potential solutions, J. Chromatogr. A, 1217 (2010) 2642-2666.

[171] J.L. Benede, A. Chisvert, D.L. Giokas, A. Salvador, Development of stir bar sorptive-dispersive microextraction mediated by magnetic nanoparticles and its analytical application to the determination of hydrophobic organic compounds in aqueous media, J. Chromatogr. A, 1362 (2014) 25-33.

[172] E. Baltussen, P. Sandra, F. David, C. Cramers, Stir bar sorptive extraction (SBSE), a novel extraction technique for aqueous samples: theory and principles, J. Microcolumn Sep., 11 (1999) 737-747.

[173] M. Kawaguchi, R. Ito, K. Saito, H. Nakazawa, Novel stir bar sorptive extraction methods for environmental and biomedical analysis, J. Pharm. Biomed. Anal., 40 (2006) 500-508.

[174] X. Zhu, J. Cai, J. Yang, Q. Su, Y. Gao, Films coated with molecular imprinted polymers for the selective stir bar sorption extraction of monocrotophos, J. Chromatogr. A, 1131 (2006) 37-44.

[175] S. Nong, P. Lin, X. Huang, D. Yuan, Preparation of a stir bar sorptive extraction coating based on molecularly imprinted polymer and its application in the extraction of dienestrol and hexestrol in complicated samples, Chinese Journal of Chromatography, 30 (2012) 1133-1142.

[176] C. Chen, L. Yang, J. Zhou, Trace bensulfuron-methyl analysis in tap water, soil, and soybean samples by a combination of molecularly imprinted stir bar sorption extraction and HPLC-UV, J. Appl. Polym. Sci., 122 (2011) 1198-1205.

[177] X.U. Zhi-gang, D.U. Zhuo, L. Hai-xian, H.U. Yu-ling, L.I. Gong-ke, Metsulfuron-methyl molecularly imprinted stir bar sorptive extraction coupled with high performance liquid chromatography for trace sulfonylurea herbicides analysis in complex samples, Chem. Res. Chin. Univ., 28 (2012) 594-599.

[178] Z. Xu, Z. Yang, Z. Liu, Development of dual-templates molecularly imprinted stir bar sorptive extraction and its application for the analysis of environmental estrogens in water and plastic samples, J. Chromatogr. A, 1358 (2014) 52-59.

[179] N. Sheng, F. Wei, W. Zhan, Z. Cai, S. Du, X. Zhou, F. Li, Q. Hu, Dummy molecularly imprinted polymers as the coating of stir bar for sorptive extraction of bisphenol A in tap water, J. Sep. Sci., 35 (2012) 707-712.

[180] R. Liu, F. Feng, G. Chen, Z. Liu, Z. Xu, Barbell-shaped stir bar sorptive extraction using dummy template molecularly imprinted polymer coatings for analysis of bisphenol A in water, Anal. Bioanal. Chem., 408 (2016) 5329-5335.

[181] S.H. Hashemi, F. Najari, Response Surface Methodology of Pre-Concentration of Chorophenols from Seawater Samples by Molecularly Imprinted Stir Bar Sorptive Extraction Combined with HPLC: Box–Behnken Design, J. Chromatogr. Sci., 57 (2018) 279-289.

[182] A. Gomez-Caballero, G. Diaz-Diaz, O. Bengoetxea, A. Quintela, N. Unceta, M.A. Goicolea, R.J. Barrio, Water compatible stir-bar devices imprinted with underivatised glyphosate for selective sample clean-up, J. Chromatogr. A, 1451 (2016) 23-32.

[183] P. Richter, C. Leiva, C. Choque, A. Giordano, B. Sepulveda, Rotating-disk sorptive extraction of nonylphenol from water samples, J. Chromatogr. A, 1216 (2009) 8598-8602.

[184] V. Manzo, K. Ulisse, I. Rodriguez, E. Pereira, P. Richter, A molecularly imprinted polymer as the sorptive phase immobilized in a rotating disk extraction device for the determination of diclofenac and mefenamic acid in wastewater, Anal. Chim. Acta, 889 (2015) 130-137.

[185] A. Sorribes-Soriano, R. Arráez-González, F.A. Esteve-Turrillas, S. Armenta, J.M. Herrero-Martínez, Development of a molecularly imprinted monolithic polymer disk for agitation-extraction of ecgonine methyl ester from environmental water, Talanta, 199 (2019) 388-395.

[186] F. Tan, H. Zhao, X. Li, X. Quan, J. Chen, X. Xiang, X. Zhang, Preparation and evaluation of molecularly imprinted solid-phase microextraction fibers for selective extraction of bisphenol A in complex samples, J. Chromatogr. A, 1216 (2009) 5647-5654.

[187] J. Lee, H.K. Lee, K.E. Rasmussen, S. Pedersen-Bjergaard, Environmental and bioanalytical applications of hollow fiber membrane liquid-phase microextraction: a review, Anal. Chim. Acta, 624 (2008) 253-268.

[188] Y. Hu, Y. Wang, Y. Hu, G. Li, Liquid-liquid-solid microextraction based on membrane-protected molecularly imprinted polymer fiber for trace analysis of triazines in complex aqueous samples, J. Chromatogr. A, 1216 (2009) 8304-8311.

[189] M. Diaz-Alvarez, F. Barahona, E. Turiel, A. Martin-Esteban, Supported liquid membrane-protected molecularly imprinted beads for micro-solid phase extraction of sulfonamides in environmental waters, J. Chromatogr. A, 1357 (2014) 158-164.

[190] E. Turiel, M. Diaz-Alvarez, A. Martin-Esteban, Supported liquid membrane-protected molecularly imprinted beads for the solid phase micro-extraction of triazines from environmental waters, J. Chromatogr. A, 1432 (2016) 1-6.

[191] O. Nemulenzi, B. Mhaka, E. Cukrowska, O. Ramstrom, H. Tutu, L. Chimuka, Potential of combining of liquid membranes and molecularly imprinted polymers in extraction of 17beta-estradiol from aqueous samples, J. Sep. Sci., 32 (2009) 1941-1948.

[192] F. Tan, M. Deng, X. Liu, H. Zhao, X. Li, X. Quan, J. Chen, Evaluation of a novel microextraction technique for aqueous samples: porous membrane envelope filled with multiwalled carbon nanotubes coated with molecularly imprinted polymer, J. Sep. Sci., 34 (2011) 707-715.

[193] F. Barahona, M. Diaz-Alvarez, E. Turiel, A. Martin-Esteban, Molecularly imprinted polymer-coated hollow fiber membrane for the microextraction of triazines directly from environmental waters, J. Chromatogr. A, 1442 (2016) 12-18.

[194] F. Barahona, B. Albero, J.L. Tadeo, A. Martín-Esteban, Molecularly imprinted polymer-hollow fiber microextraction of hydrophilic fluoroquinolone antibiotics in environmental waters and urine samples, J. Chromatogr. A, 1587 (2019) 42-49.

[195] Z. Tahmasebi, S.S. Davarani, A.A. Asgharinezhad, An efficient approach to selective electromembrane extraction of naproxen by means of molecularly imprinted polymer-coated multi-walled carbon nanotubes-reinforced hollow fibers, J. Chromatogr. A, 1470 (2016) 19-26.

[196] M.N.H. Rozaini, N.-f. Semail, B. Saad, S. Kamaruzaman, W.N. Abdullah, N.A. Rahim, M. Miskam, S.H. Loh, N. Yahaya, Molecularly imprinted silica gel incorporated with agarose polymer matrix as mixed matrix membrane for separation and preconcentration of sulfonamide antibiotics in water samples, Talanta, (2019).

[197] H. Piri-Moghadam, M.N. Alam, J. Pawliszyn, Review of geometries and coating materials in solid phase microextraction: opportunities, limitations, and future perspectives, Anal. Chim. Acta, 984 (2017) 42-65.

[198] G. Ouyang, J. Pawliszyn, A critical review in calibration methods for solid-phase microextraction, Anal. Chim. Acta, 627 (2008) 184-197.

[199] S. Risticevic, H. Lord, T. Gorecki, C.L. Arthur, J. Pawliszyn, Protocol for solid-phase microextraction method development, Nat. Protoc., 5 (2010) 122.

[200] A. Azizi, F. Shahhoseini, C.S. Bottaro, Magnetic molecularly imprinted polymers prepared by reversible addition fragmentation chain transfer polymerization for dispersive solid phase extraction of polycyclic aromatic hydrocarbons in water, J. Chromatogr. A, (2019) 460534.

[201] V. Mohammadi, M. Saraji, M.T. Jafari, Direct molecular imprinting technique to synthesize coated electrospun nanofibers for selective solid-phase microextraction of chlorpyrifos, Microchim. Acta, 186 (2019) 524.

[202] M. Khajeh, M. Sharifirad, M. Bohlooli, M. Ghaffari-Moghaddam, Magnetic molecularly imprinted polymers–silver nanoparticle based micro-solid phase extraction for the determination of polycyclic aromatic hydrocarbons in water samples, RSC Adv., 6 (2016) 54702-54708.

[203] Y. Liu, Y. Liu, Z. Liu, F. Du, G. Qin, G. Li, X. Hu, Z. Xu, Z. Cai, Supramolecularly imprinted polymeric solid phase microextraction coatings for synergetic recognition nitrophenols and bisphenol A, J. Hazard. Mater., 368 (2019) 358-364.

[204] Y. Liu, Y. Liu, Z. Liu, X. Hu, Z. Xu, β-Cyclodextrin molecularly imprinted solid-phase microextraction coatings for selective recognition of polychlorophenols in water samples, Anal. Bioanal. Chem., 410 (2018) 509-519.

[205] D. Djozan, M. Mahkam, B. Ebrahimi, Preparation and binding study of solid-phase microextraction fiber on the basis of ametryn-imprinted polymer: Application to the selective extraction of persistent triazine herbicides in tap water, rice, maize and onion, J. Chromatogr. A, 1216 (2009) 2211-2219.

[206] D. Djozan, B. Ebrahimi, Preparation of new solid phase micro extraction fiber on the basis of atrazine-molecular imprinted polymer: Application for GC and GC/MS screening of triazine herbicides in water, rice and onion, Anal. Chim. Acta, 616 (2008) 152-159.

[207] X. Luo, Y. Zhan, X. Tu, Y. Huang, S. Luo, L. Yan, Novel molecularly imprinted polymer using 1-(α-methyl acrylate)-3-methylimidazolium bromide as functional monomer for simultaneous extraction and determination of water-soluble acid dyes in wastewater and soft drink by solid phase extraction and high performance liquid chromatography, J. Chromatogr. A, 1218 (2011) 1115-1121.

[208] M. Zarejousheghani, S. Schrader, M. Moder, P. Lorenz, H. Borsdorf, Ion-exchange molecularly imprinted polymer for the extraction of negatively charged acesulfame from wastewater samples, J. Chromatogr. A, 1411 (2015) 23-33.

[209] T. Alizadeh, Development of a molecularly imprinted polymer for pyridoxine using an ion-pair as template, Anal. Chim. Acta, 623 (2008) 101-108.

[210] W. Luo, L. Zhu, C. Yu, H. Tang, H. Yu, X. Li, X. Zhang, Synthesis of surface molecularly imprinted silica micro-particles in aqueous solution and the usage for selective off-line solid-phase extraction of 2, 4-dinitrophenol from water matrixes, Anal. Chim. Acta, 618 (2008) 147-156.

[211] S.S. Miao, H.Z. Wang, Y.C. Lu, H.R. Geng, H. Yang, Preparation of Dufulin imprinted polymer on surface of silica gel and its application as solid-phase extraction sorbent, Environ. Sci-Proc. Imp., 16 (2014) 932-941.

[212] Z. Zhang, X. Chen, W. Rao, H. Chen, R. Cai, Synthesis and properties of magnetic molecularly imprinted polymers based on multiwalled carbon nanotubes for magnetic extraction of bisphenol A from water, J. Chromatogr. B, 965 (2014) 190-196.

[213] F. Duan, C. Chen, L. Chen, Y. Sun, Y. Wang, Y. Yang, X. Liu, Y. Qin, Preparation and Evaluation of Water-Compatible Surface Molecularly Imprinted Polymers for Selective Adsorption of Bisphenol A from Aqueous Solution, Ind. Eng. Chem. Res., 53 (2014) 14291-14300.

[214] F. Duan, C. Chen, X. Zhao, Y. Yang, X. Liu, Y. Qin, Water-compatible surface molecularly imprinted polymers with synergy of bi-functional monomers for enhanced selective adsorption of bisphenol A from aqueous solution, Environ. Sci. Nano, 3 (2016) 213-222.

[215] J. Sun, J. Dai, W. Ma, L. Gao, A. Xie, J. He, Z. Zhou, C. Li, Y. Yan, Surface hydrophilic imprinted particles via a green precipitation polymerization for selective removal of tetracycline from aqueous solution, J. Iran. Chem. Soc., 13 (2016) 489-497.

[216] J. Dai, Z. Zhou, Y. Zou, X. Wei, X. Dai, C. Li, Y. Yan, Surface imprinted core-shell nanorod with ultrathin water-compatible polymer brushes for specific recognition and adsorption of sulfamethazine in water medium, J. Appl. Polym. Sci., 131 (2014).

[217] M. Yagishita, T. Kubo, T. Nakano, F. Shiraishi, T. Tanigawa, T. Naito, T. Sano, S.F. Nakayama, D. Nakajima, K. Otsuka, Efficient extraction of estrogen receptor–active compounds from environmental surface water via a receptor-mimic adsorbent, a hydrophilic PEG-based molecularly imprinted polymer, Chemosphere, 217 (2019) 204-212.

[218] J.L. Urraca, M.C. Moreno-Bondi, A.J. Hall, B. Sellergren, Direct extraction of penicillin G and derivatives from aqueous samples using a stoichiometrically imprinted polymer, Anal. Chem., 79 (2007) 695-701.

[219] Y. Fuchs, O. Soppera, K. Haupt, Photopolymerization and photostructuring of molecularly imprinted polymers for sensor applications—A review, Anal. Chim. Acta, 717 (2012) 7-20.

[220] X. Hu, Y. Fan, Y. Zhang, G. Dai, Q. Cai, Y. Cao, C. Guo, Molecularly imprinted polymer coated solid-phase microextraction fiber prepared by surface reversible addition–fragmentation chain transfer polymerization for monitoring of Sudan dyes in chilli tomato sauce and chilli pepper samples, Anal. Chim. Acta, 731 (2012) 40-48.

[221] X. Xie, X. Liu, X. Pan, L. Chen, S. Wang, Surface-imprinted magnetic particles for highly selective sulfonamides recognition prepared by reversible addition fragmentation chain transfer polymerization, Anal. Bioanal. Chem., 408 (2016) 963-970.

[222] M. Yang, Y. Zhang, S. Lin, X. Yang, Z. Fan, L. Yang, X. Dong, Preparation of a bifunctional pyrazosulfuron-ethyl imprinted polymer with hydrophilic external layers by reversible addition–fragmentation chain transfer polymerization and its application in the sulfonylurea residue analysis, Talanta, 114 (2013) 143-151.

[223] F. Chen, J. Zhang, M. Wang, J. Kong, Magnetic molecularly imprinted polymers synthesized by surface-initiated reversible addition-fragmentation chain transfer polymerization for the enrichment and determination of synthetic estrogens in aqueous solution, J. Sep. Sci., 38 (2015) 2670-2676.

[224] X. Li, J. Pan, J. Dai, X. Dai, L. Xu, X. Wei, H. Hang, C. Li, Y. Liu, Surface molecular imprinting onto magnetic yeast composites via atom transfer radical polymerization for selective recognition of cefalexin, Chem. Eng. J., 198 (2012) 503-511.

[225] X. Wang, L. Chen, X. Xu, Y. Li, Synthesis of molecularly imprinted polymers via ring-opening metathesis polymerization for solid-phase extraction of bisphenol A, Anal. Bioanal. Chem., 401 (2011) 1423.

[226] H. Zhang, Controlled/“living” radical precipitation polymerization: a versatile polymerization technique for advanced functional polymers, Eur. Polym. J., 49 (2013) 579-600.

[227] M. Zhang, J. He, Y. Shen, W. He, Y. Li, D. Zhao, S. Zhang, Application of pseudo-template molecularly imprinted polymers by atom transfer radical polymerization to the solid-phase extraction of pyrethroids, Talanta, 178 (2018) 1011-1016.

[228] X. Li, J. Pan, J. Dai, X. Dai, H. Ou, L. Xu, C. Li, R. Zhang, Removal of cefalexin using yeast surface-imprinted polymer prepared by atom transfer radical polymerization, J. Sep. Sci., 35 (2012) 2787-2795.

[229] H.-S. Wang, M. Song, T.-J. Hang, Functional interfaces constructed by controlled/living radical polymerization for analytical chemistry, ACS applied materials & interfaces, 8 (2016) 2881-2898.

[230] C.-H. Lu, W.-H. Zhou, B. Han, H.-H. Yang, X. Chen, X.-R. Wang, Surface-imprinted core− shell nanoparticles for sorbent assays, Anal. Chem., 79 (2007) 5457-5461.

[231] L. Chang, Y. Li, J. Chu, J. Qi, X. Li, Preparation of core-shell molecularly imprinted polymer via the combination of reversible addition-fragmentation chain transfer polymerization and click reaction, Anal. Chim. Acta, 680 (2010) 65-71.

[232] J. Li, R. Dong, X. Wang, H. Xiong, S. Xu, D. Shen, X. Song, L. Chen, One-pot synthesis of magnetic molecularly imprinted microspheres by RAFT precipitation polymerization for the fast and selective removal of 17β-estradiol, RSC Adv., 5 (2015) 10611-10618.

[233] Y. Li, X. Li, J. Chu, C. Dong, J. Qi, Y. Yuan, Synthesis of core-shell magnetic molecular imprinted polymer by the surface RAFT polymerization for the fast and selective removal of endocrine disrupting chemicals from aqueous solutions, Environ. Pollut., 158 (2010) 2317-2323.

[234] X. Wu, X. Wang, W. Lu, X. Wang, J. Li, H. You, H. Xiong, L. Chen, Water-compatible temperature and magnetic dual-responsive molecularly imprinted polymers for recognition and extraction of bisphenol A, J. Chromatogr. A, 1435 (2016) 30-38.

[235] E. Rodríguez, F. Navarro-Villoslada, E. Benito-Peña, M.D. Marazuela, M.C. Moreno-Bondi, Multiresidue Determination of Ultratrace Levels of Fluoroquinolone Antimicrobials in Drinking and Aquaculture Water Samples by Automated Online Molecularly Imprinted Solid Phase Extraction and Liquid Chromatography, Anal. Chem., 83 (2011) 2046-2055.

[236] Y. Watabe, T. Kubo, T. Nishikawa, T. Fujita, K. Kaya, K. Hosoya, Fully automated liquid chromatography–mass spectrometry determination of 17β-estradiol in river water, J. Chromatogr. A, 1120 (2006) 252-259.

[237] T. Kubo, K. Kuroda, Y. Tominaga, T. Naito, K. Sueyoshi, K. Hosoya, K. Otsuka, Effective determination of a pharmaceutical, sulpiride, in river water by online SPE-LC–MS using a molecularly imprinted polymer as a preconcentration medium, J. Pharm. Biomed. Anal., 89 (2014) 111-117.

[238] J. Pereira, J. Gonçalves, V. Alves, J.S. Câmara, Microextraction using packed sorbent as an effective and high-throughput sample extraction technique: Recent applications and future trends, Sample Prep., 1 (2013) 38-53.

[239] A. Prieto, A. Vallejo, O. Zuloaga, A. Paschke, B. Sellergen, E. Schillinger, S. Schrader, M. Möder, Selective determination of estrogenic compounds in water by microextraction by packed sorbents and a molecularly imprinted polymer coupled with large volume injection-in-port-derivatization gas chromatography–mass spectrometry, Anal. Chim. Acta, 703 (2011) 41-51.

[240] M.-Z. Huang, S.-C. Cheng, Y.-T. Cho, J. Shiea, Ambient ionization mass spectrometry: a tutorial, Anal. Chim. Acta, 702 (2011) 1-15.

[241] G. Van Biesen, J.M. Wiseman, J. Li, C.S. Bottaro, Desorption electrospray ionization-mass spectrometry for the detection of analytes extracted by thin-film molecularly imprinted polymers, Analyst, 135 (2010) 2237-2240.

[242] H.Y. Hijazi, C.S. Bottaro, Analysis of thiophenes in seawater: Molecularly imprinted polymer thin-film extraction with desorption electrospray ionization mass spectrometry, Int. J. Mass spectrom., 443 (2019) 9-15.

[243] O.A. Gryshchenko, S.C. Bottaro, Development of Molecularly Imprinted Polymer in Porous Film Format for Binding of Phenol and Alkylphenols from Water, Int. J. Mol. Sci., 15 (2014).

[244] F. Shahhoseini, A. Azizi, S.N. Egli, C.S. Bottaro, Single-use porous thin film extraction with gas chromatography atmospheric pressure chemical ionization tandem mass spectrometry for high-throughput analysis of 16 PAHs, Talanta, 207 (2020) 120320.

[245] H.Y. Hijazi, C.S. Bottaro, Selective determination of semi-volatile thiophene compounds in water by molecularly imprinted polymer thin films with direct headspace gas chromatography sulfur chemiluminescence detection, Analyst, 143 (2018) 1117-1123.

[246] A. Azizi, F. Shahhoseini, A. Modir-Rousta, C.S. Bottaro, High throughput direct analysis of water using solvothermal headspace desorption with porous thin films, Anal. Chim. Acta, 1087 (2019) 51-61.

# Chapter 2: Magnetic molecularly imprinted polymers prepared by reversible addition fragmentation chain transfer polymerization for dispersive solid phase extraction of polycyclic aromatic hydrocarbons in water

A. Azizi, F. Shahhoseini, C.S. Bottaro. “Magnetic molecularly imprinted polymers prepared by reversible addition fragmentation chain transfer polymerization for dispersive solid phase extraction of polycyclic aromatic hydrocarbons in water.” J. Chromatogr. A 1610 (2020) 460534.

## 2.1. Introduction

Polycyclic aromatic hydrocarbons (PAHs) can be considered as persistent organic pollutants (POPs) in the environment and accumulate in biological systems due to their hydrophobic nature [1]. These pollutants, which are well known as carcinogenic, mutagenic and teratogenic compounds, threaten human health, and the ecosystem [2, 3]. PAHs were also determined to be effective on the global carbon cycle by inhibiting the growth of diatoms [4]. PAHs have mainly originated through the exposure of organic compounds to high temperatures with low or no oxygen, called pyrogenic PAHs. The other major source is petrogenic PAH formation during the mutation of crude oil [3]. Petrogenic PAHs can be introduced into water resources during production and transportation. For example, produced water which is the main discharge of oil and gas industries contains large quantities of these pollutants [5, 6]. These hydrophobic contaminants with relatively low solubility (Table 2.1) can be deposited onto sediments and eliminated through microbiological degradation [7]. However, resuspension of sediments particularly in coastal areas, which is caused either by natural forces such as waves, currents, storms or human-related activities such as dredging, trawling, and shipping traffic, decreases the degradation rate [7]. Therefore PAHs have been recognized as priority pollutants by regulatory agencies such as United States-Environmental Protection Agency (US-EPA) [8] and European Union [9].

The most common methods to trace and quantify PAHs in the environment rely on chromatographic methods such as gas chromatography (GC) [10] and liquid chromatography (LC) [11]. A sample preparation step is required before analysis to

preconcentrate the target analytes and remove matrix components, particularly when tracking very low concentrations (pg $mL^{-1}$ as limits for PAHs) in environmental waters. Liquid–liquid extraction (LLE) is the conventional extraction technique for isolation of PAHs from water samples [12]. However, LLE needs a large volume of organic solvents and is time-consuming. Additionally, the formation of emulsions reduces efficiency of the extraction and precision of analysis [13]. There are several newer extraction techniques such as solid phase extraction (SPE) [14], solid phase microextraction (SPME) [15], stir bar sorptive extraction (SBSE) [16], and dispersive liquid-liquid microextraction (DLLME) [17] for preconcentration and determination of PAHs. These techniques improve conventional extraction protocols by reducing consumed reagents, sample volume requirements and preparation time. Nevertheless they are non-selective methods reducing the reliability of the quantitation by co-extraction of interfering compounds associated with environmental samples [18]. The interfering compounds in real samples are problematic because they can reduce the quality of the analysis by complications such as overlapping chromatographic peaks and matrix-induced effects. These can influence fundamental processes like detector response and column behavior, which lead to inaccuracies in quantitation [19].

Molecularly imprinted polymers (MIPs), similar to synthetic antibodies, are alternative sorptive phases in sample preparation and introduce selectivity into pretreatment methods for environmental [20], food [21], and biological [22] samples. MIPs are synthesized through copolymerization of a functional monomer and a crosslinking agent in the presence of a template molecule interacting with the functional monomer. After polymerization, the template molecule is removed creating recognition sites

complementary to the target molecule in shape, size, and functional groups [23]. MIPs have been widely utilized as the extraction phase in the various formats such as MIP-SPE [24], MIP-SPME [25], and MIP-SBSE [26]. Nanoparticles have been gaining attention in analytical chemistry because of their large specific surface area and the possibility of functionalization with innovative sorptive phases like MIPs [27]. The MIP-coated nanoparticles are used for dispersive solid phase extraction (DSPE) by distribution of the extraction phase in the sample instead of sequestered as packing in a column or on a disk [28]. The dispersion of small particles in the sample leads to numerous extraction microenvironments, which translates into better access to selective recognition sites [29]. The main advantages of dispersive-based SPE techniques using MIPs are fast selective adsorption and rapid desorption of analytes due to favorable mass transfer phenomena, leading to high efficiency along with reduced solvent consumption [30].

Despite considerable benefits of MIPs for the enrichment of analytes, these sorbents are heterogeneous polymeric materials [31]. Therefore, these polymeric sorbents include inaccessible and heterogeneous adsorption sites causing slow mass transfer and low selectivity [32]. This heterogeneity is caused by fast chain propagation and irreversible termination reactions in the free radical polymerization mechanism(s) used to prepare MIPs [33]. To improve the homogeneity of the sorbent, controlled radical polymerization strategies such as reversible addition fragmentation chain transfer (RAFT) polymerization are used to prepare MIP coating [34, 35]. In this polymerization, the chain transfer step is reversible and relies on RAFT radicals or living polymeric chains that allow for constrained propagation of all chains with a narrow dispersion of molecular weights [36]. Therefore, a homogenous polymeric network is obtained which enhances the selective recognition of

targeted analytes [37]. RAFT polymerization also provides more accessible sites for adsorption and thus faster mass transfer of analytes [38]. RAFT-MIPs have been reported for extraction of organic pollutants from environmental samples such as 2,4-dichlorophenoxyacetic acid [35], bisphenol A [39, 40], 2,4-dichlorophenol [38], and diethylstilbestrol [41] from water samples and 17β-estradiol [42] and sulfonylurea herbicides from soil samples [43].

MIPs have been previously reported for the enrichment of PAHs [44-49], and yet, selective recognition of PAHs by MIPs continues to be limited by lack of functionality on aromatic rings and therefore, a reliance on hydrophobic interactions with the polymeric coating for adsorption [48]. An additional mode of non-covalent interactions used for aromatic compounds is hydrogen bonding [50]. Thus, phenol is used as a pseudo-template; the aromaticity supports hydrogen bonding and π–π interactions and the hydroxyl group hydrogen bonding. Both modes can be exploited in establishing monomer–template interactions and the creation of recognition sites for PAHs in the polymer.

The magnetic molecularly imprinted polymers (MMIPs) are prepared on silica core–shell magnetic nanoparticles ($Fe_3O_4$@$SiO_2$) as a substrate. Magnetic collection of the MMIPs facilitates sample preparation by reducing time required for sorbent collection after extraction, washing and elution by eliminating filtration or centrifugation steps [51]. The MIP coating is prepared in a thin layer with a uniform distribution of the binding sites via RAFT polymerization. RAFT-MMIPs, which have not been reported for enrichment of PAHs, is utilized for DSPE of these analytes from water samples. The ultra-thin coating along with fast dispersion of MMIPs in the sample is achieved using an ultrasonic bath, minimizing equilibration time for extraction and desorption of PAHs.

Optimization of MMIP-DSPE procedure, which is crucial to obtain a desirable efficiency, provides information on sorbent characteristics for adsorption and affinity of the selected PAHs towards MMIPs. Therefore, a multivariate method is employed for the optimization of variables influencing the extraction of PAHs. A screening step with a fractional factorial design (FFD) is used to determine the essential factors. A response surface methodology (RSM) based on central composite design (CCD) and desirability function (*DF*) is then applied to optimize the important factors. Finally, the performance of the optimized MMIP-DSPE method is evaluated through sensitivity, selectivity, accuracy, and precision tests for trace analysis of PAHs in environmental samples.

## 2.2. Experimental

### 2.2.1. Reagents and materials

Naphthalene (Naph, 99%), acenaphthylene (Acy, 99%), acenaphthene (Ace, 99%), fluorene (Flu, 98%), phenanthrene (Phe, ≥99.5 %), anthracene (Ant, ≥99.0%), fluoranthene (Flut, 98.7 %), pyrene (Pyr, ≥99.0%), chrysene (Chry), benzo(a)anthracene (BaA, 99%), benzo(b)fluoranthene (BbF, 98%), benzo(k)fluoranthene (BkF, ≥99 %), benzo(a)pyrene (BaP, ≥96%), indeno(1,2,3-cd) pyrene (InP), dibenzo(a,h) anthracene (DB(ah)A), and benzo(ghi) perylene (BGP, 98%) as well as deuterated PAHs: naphthalene-d8 (Naph-d8, 99 atom % D), acenaphthene-d10 (Ace-d10, 99 atom % D), phenanthrene-d10 (Phe-d10, 98% CP), chrysene-d12 (Chry-d12), perylene-d12 (Per-d12, 98 atom %D), tetramethyl orthosilicate (TMOS, 98%), 3-methacryloxypropyltrimethoxysilane (MPS, 98%), methacrylic acid (MAA, 99%), isopropyl acrylamide (NIPAM, 97%), benzyl

benzodithioate (BBT, 96%) phenol (≥99.5%), ethyleneglycol dimethacrylate (EGDMA, 98%), and 1,1′-azobis(cyclohexanecarbonitrile) (ACBN, 98%) were purchased from Sigma-Aldrich (Oakville, ON, Canada). Iron(III) chloride hexahydrate ($FeCl_3 \cdot 6H_2O$) and iron(II) chloride tetrahydrate ($FeCl_2 \cdot 4H_2O$), Optima grade methanol, acetonitrile, hexane, and toluene were purchased from Fisher Scientific (Whitby, ON, Canada). Absolute ethanol was purchased from Greenfield Global Inc. (Brampton, ON, Canada). Sodium chloride (NaCl, 99%) and glacial acetic acid (>99.7%) were purchased from ACP chemicals (Montreal, QC, Canada).

Ultrapure water (18.2 $M\Omega.cm^{-1}$) was produced by an SYBRON/Barnstead water purification system (Boston, MA, USA). Individual stock solutions of PAHs were prepared in acetonitrile: acetone (1:1, v/v) at 1000 mg $L^{-1}$. Acetone has been used in this binary solvent system to dissolve all the analytes along with acetonitrile to avoid solvent loss and changing the concentration of stock solutions. Working standards, which were added to the water samples before performing the extraction, were prepared from the stock solutions by diluting in pure acetonitrile. To obtain the instrument calibration curves for the analytes for the calculation of extracted mass, multi-standards of PAHs were prepared in toluene. All the solutions were stored at 4 °C in a refrigerator prior to use.

**Table 2.1.** Target analytes with physical and chemical properties [52, 53].

| Compound | Structure | MW (g $mol^{-1}$) | Solubility in water (mg $L^{-1}$) | LogP |
|---|---|---|---|---|
| Naph | 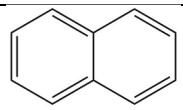 | 128.17 | 31 | 3.30 |
| Acy | 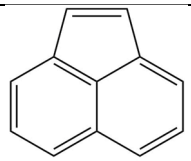 | 152.20 | 16.1 | 3.94 |
| Ace | 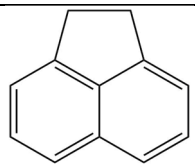 | 154.21 | 3.8 | 3.92 |
| Flu | 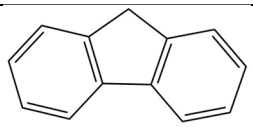 | 166.22 | 1.9 | 4.18 |
| Phe | 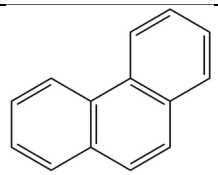 | 178.23 | 1.1 | 4.46 |
| Ant | 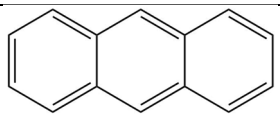 | 178.23 | 0.045 | 4.45 |
| Flut | 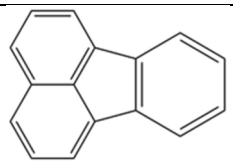 | 202.26 | 0.26 | 5.16 |
| Pyr | 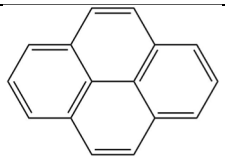 | 202.26 | 0.132 | 4.88 |

*(continued on next page)*

**Table 2.1.** (*continued*)

| Compound | Structure | MW (g $mol^{-1}$) | Solubility in water (mg $L^{-1}$) | LogP |
|---|---|---|---|---|
| BaA | 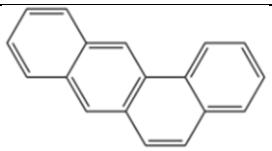 | 228.29 | 0.011 | 5.76 |
| Chry | 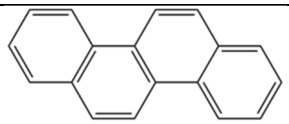 | 228.29 | 0.0015 | 5.81 |
| BbF | 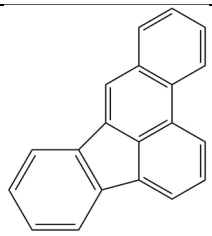 | 252.32 | 0.0015 | 5.78 |
| BkF | 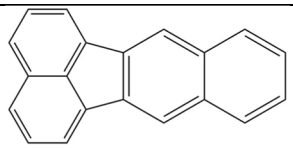 | 252.32 | 0.0008 | 6.11 |
| BaP | 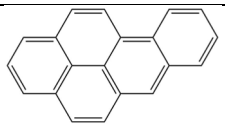 | 252.32 | 0.0038 | 6.13 |
| InP | 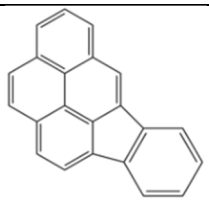 | 276.34 | 0.062 | 6.58 |
| DB(ah)A | 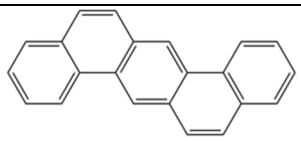 | 278.35 | 0.0005 | 6.75 |
| BGP | 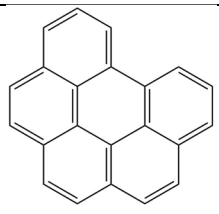 | 276.34 | 0.00026 | 7.1 |

### 2.2.2. Instrumentation and operating conditions

An Agilent 7890B GC instrument (Agilent Technologies, CA, U.S.A.) coupled to Waters Xevo TQ-S equipped with an atmospheric pressure chemical ionization source (APCI) was utilized for all analyses. A 7693A Automatic Liquid Sampler (Agilent Technologies, CA, USA) was used to inject 1-µL of sample in pulsed splitless mode (25 psi, 1 min) with a liner temperature of 280 °C. Separations were performed using a DB-5MS column (30 m×0.250 mm, 0.25 µm film thickness) purchased from Agilent Technologies. Helium (5 UHP) (Praxair, Canada) was employed as the carrier gas at a constant flow rate of 1.2 mL $min^{-1}$. The oven temperature program was as follows: initial temperature of 80 °C held for 2 min; increased to 220 °C at 25 C $min^{-1}$, then to 240 °C at 10 °C $min^{-1}$, to 280 °C at 3 °C $min^{-1}$, and finally to 300 °C at 10 °C $min^{-1}$ and held for 2.5 min. The temperature of the transfer line from GC to the ion source was 300 °C with $N_2$ as make-up gas (NM32LA, Peak Scientific, Scotland, UK) flowing at 280 mL $min^{-1}$. The temperature of the ion source was 150 °C with $N_2$ as the auxiliary gas and cone gas flow rates operated at 200 and 190 L per hour, respectively. The corona pin was operated in constant current mode at 2 µA. MRM transitions, cone voltages and collision energies used for all compounds are included in Table 2.2.

The crystalline structure of the nanoparticles was studied by using Ultima-IV x-ray diffractometer (Rigaku, Japan) equipped with a Cu source (wavelength: 1.54 nm) and a scintillation detector. The operation conditions are 40 kV, 44 mA, a scan rate of 1 θ $min^{-1}$ and step size of 0.002 2θ. FT-IR spectroscopy was conducted using a Bruker ALPHA instrument equipped with an ATR sample adapter. Scans were collected using a range of 4000–400 $cm^{-1}$ and a resolution of 1.5 $cm^{-1}$. Morphological studies were conducted by

taking micrographs using a Quanta 650 FEG (field emission gun) SEM (FEI, OR, USA). The instrument was operated at a constant 5.0 kV and the detector was an ETD. Transmission electron microscopy (TEM) images were taken using a Tecnai G2 Spirit Transmission Electron Microscope (FEI, OR, USA).

**Table 2.2.** Summary of tandem mass spectrometry parameters using APCI-GC-MS/MS.

| Compound | RT (min) | Precursor ion (m/z) | Product ion (m/z) | Cone voltage (V) | Collision energy (eV) |
|---|---|---|---|---|---|
| Naph-d8 | 5.82 | 136 | 108 | 55 | 20 |
| Naph | 5.84 | 128 | 102 | 55 | 20 |
| Acy | 7.41 | 152 | 151 | 65 | 28 |
| Ace-d10 | 7.54 | 164 | 162 | 40 | 20 |
| Ace | 7.57 | 154 | 153 | 40 | 20 |
| Flu | 8.09 | 166 | 165 | 35 | 20 |
| Phe-d10 | 9.17 | 188 | 186 | 65 | 25 |
| Phe | 9.20 | 178 | 177 | 65 | 25 |
| Ant | 9.27 | 178 | 177 | 65 | 25 |
| Flut | 11.03 | 202 | 201 | 70 | 35 |
| Pyr | 11.49 | 202 | 201 | 70 | 35 |
| BaA | 14.87 | 228 | 228 | 30 | 15 |
| Chry-d12 | 14.90 | 240 | 240 | 30 | 15 |
| Chry | 15.00 | 228 | 228 | 30 | 15 |
| BbF | 19.24 | 252 | 252 | 30 | 15 |
| BkF | 19.38 | 252 | 252 | 30 | 15 |
| BaP | 20.67 | 252 | 252 | 30 | 15 |
| Per-d12 | 20.94 | 264 | 264 | 30 | 15 |
| InP | 25.39 | 276 | 276 | 40 | 15 |
| DB(ah)A | 25.55 | 278 | 278 | 40 | 15 |
| BGP | 26.27 | 276 | 276 | 40 | 15 |

### 2.2.3. Synthesis procedure

*2.2.3.1. Synthesis of magnetic nanoparticles*

Magnetic iron nanoparticles were prepared using the co-precipitation technique [54]. Firstly 0.4 M of HCl and 0.7 M of $NH_4OH$ solutions were prepared and deoxygenated by passing nitrogen through the solution for 15 min. Then 8.5 g of $FeCl_3 \cdot 6H_20$ and 3.0 g of $FeCl_2 \cdot 4H_2O$ which were previously ground using a mortar and pestle, were dissolved in 38 mL of the 0.4 M HCl solution. The synthesis procedure was performed in an ultrasonic bath by rapid addition of the acidic mixed iron salt solution into 375 mL of the 0.7 M ammonium hydroxide solution. After sonication for 30 min, the $Fe_3O_4$ particles were stored in this reaction solution before use to avoid aggregation.

*2.2.3.2. Preparation of $Fe_3O4@SiO_2$*

A silica coating prepared through the Stöber process is used to reduce the amount of agglomeration of the magnetic nanoparticles [39]. For this purpose, a 54 mL aliquot of the solution containing 500 mg $Fe_3O_4$ was washed with ultrapure water three times. Then the wet particles were dispersed in a solution containing 500 mL of ethanol and 100 mL of ultrapure water. After 10 min magnetic stirring at 1200 rpm, ammonium hydroxide was used to adjust the pH to 10.5 before addition of TMOS (5 mL). The coating process was completed by mixing the solution for 12 h stirred at 1200 rpm which lead to the formation of $Fe_3O_4@SiO_2$. After synthesis, the particles were collected using a 4" × 2" × 2" neodymium block magnet from Apex Magnets (Petersburg, WV, USA). The collected particles were washed with ethanol (3 × 150 mL) and nanopore water (3 × 150 mL ) and subsequently dried in a vacuum oven at 50 °C overnight.

*2.2.3.3. Preparation of vinyl functionalized-$Fe_3O4@SiO_2$*

Dried $Fe_3O_4@SiO_2$ (1 g) was dispersed in a mixed solution of ethanol (75 mL) and ultrapure water (25 mL). The acidity of the solution was adjusted to a pH of 4.0 using acetic acid. After addition of 25 mL MPS solution in ethanol (1.2 wt%) under $N_2$, the solution was stirred for 24 h [39]. The resultant core–shell nanoparticles coated with the silane coupling agent were washed with ethanol (3×150 mL) and ultrapure water (3×150 mL), dried and used as the substrate to prepare the MMIP.

*2.2.3.4. Preparation of RAFT-MMIP*

In order to prepare RAFT-MMIP, a published procedure [39] with some modifications has been used. The pre-polymerization solution for synthesis of MMIP was prepared by dissolving MAA (2 mmol) and NIPAM (2 mmol) as functional monomers and phenol (0.5 mmol) in 200 mL of acetonitrile. The solution was kept at 4 °C in the dark for 12 h to form the template-monomer complex. The functionalized nanoparticles were then dispersed in the prepolymer solution and degassed for 15 min to remove oxygen which interferes with the radical polymerization. After reaching the temperature of 60 °C using an oil bath under $N_2$, EGDMA (5.83 mmol), BBT (200 μL) and ACBN (99.2 mg) were added. The polymerization was conducted for 24 h at 75–78 °C. The synthesized MMIP particles were washed with methanol/acetic acid (9:1, v/v) to remove the template from the polymer structure. Finally, the MMIP particles were washed with methanol and dried using a vacuum oven at 50 °C. Non-imprinted polymer, named MNIP, was synthesized as a control sorbent with an identical procedure except for excluding the template when forming

the prepolymer-solution. To evaluate the effect of RAFT polymerization on sorbent performance, MMIP and MNIP particles were also prepared without using BBT and considered as C-MMIP and C-MNIP, respectively.

### 2.2.4. Magnetic molecularly imprinted polymer-dispersive solid phase extraction (MMIP-DSPE)

The extraction of PAHs from water samples using MMIP-DSPE procedure is presented in Fig. 2.1. A mixture of 16 PAHs was spiked into the ultrapure water to obtain final concentration of 2000 pg $mL^{-1}$ for 8 low molecular weight PAHs (Naph, Acy, Ace, Flu, Phe, Ant, Flut and Pyr) and 250 pg $mL^{-1}$ for 8 high molecular weight PAHs (BaA, Chry, BbF, BkF, BaP, InP, DB(ah)A and BGP). The organic solvent content of the sample solution was maintained below 1% to avoid any effect of solvent during extraction. Addition of a standard solution into the water samples versus preparing solutions in a volumetric flask before extraction eliminates the loss of hydrophobic analytes which tend to stick to the walls of the glassware. 10 mg of MMIP particles were dispersed in a water sample using an ultrasonic bath for 2 min which is then followed by magnetic collection of the sorbent for 5 min using the magnet. After decanting the supernatant, the sorbent was washed with 1 mL of ultrapure water to remove salts and undesirable polar contaminants adsorbed by interaction through non-selective binding sites. The sorbent was then dried under a gentle nitrogen stream to minimize the final water content. For desorption of PAHs, 500 µL of hexane was added into the vial and sonicated for 2 min. The supernatant, which can easily be removed from the sorbent by applying a magnet, was transferred into GC vials. Finally, the solvent was gently evaporated under a stream of nitrogen before being

reconstituted in 100 µL of toluene with a higher boiling point than hexane in order to perform GC runs with a higher initial temperature. The preconcentrated PAHs were transferred into insert vials and subsequently analyzed by APCI-GC–MS/MS.

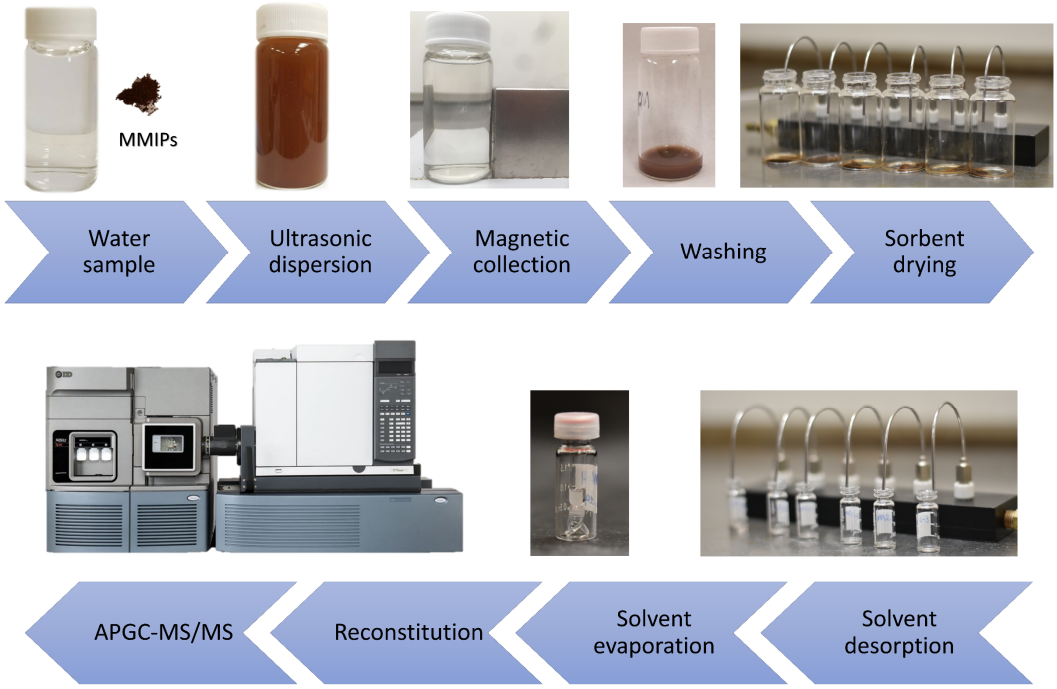


**Fig. 2.1.** Experimetal set-up for extraction and determination using proposed MMIP–DSPE–APCI-GC–MS/MS procedure.

### 2.2.5. Experimental design

The potentially important parameters on the MMIP-DSPE were selected after preliminary studies. These factors include the mass of MMIPs, sample volume, salt content, collection time, desorption volume, and desorption time. A STATISTICA 10.0 (Stat Soft Inc., Tulsa, USA) was used to generate the design of experiment (DOE) and process the

data. The factors were screened using the Plackett–Burman design consisting of a fractional factorial ($2^{6-2}$) design with a set of 16 experiments.

The effect of each variable was investigated through its effect of the response of analytes. Since optimization of 16 individual PAHs with varying solubility is difficult, the analytes were divided into 3 groups dependent on relative polarity including group 1 (Naph, Acy, Ace, Flu, Phe, Ant, Flut and Pyr), group 2 (BaA and Chry) and group 3 (BbF, BkF, BaP, InP, DB(ah)A and BGP). CCD, introduced by Box and Wilson, was utilized for optimization of the most significant factors which resulted in quadratic polynomial models [55]. In a CCD, the total number of experiments (N) is obtained by incorporation of $2^f$ factorial points ($N_f$) (f: number of factors), 2f star points ($N_\alpha$), and one or more central points ($N_0$) (Eq. 2.1)

$$N = N_f + N_\alpha + N_0 \qquad (2.1)$$

The level of star points ensuring the rotatability of the obtained CCD model are located at ±α from the center values and calculated at ±1.681 using Eq. 2.2 [56]:

$$\alpha = \sqrt[4]{N_f} \qquad (2.2)$$

Moreover, the total number of replicates at the central level of each variable guaranteeing the orthogonality of the model was calculated to equal to 9 using Eq. 2.3 as below [57]:

$$\alpha = \sqrt{\frac{\sqrt{(N_f \times (N_0 + N_f + N_\alpha)} - N_f}{2}} \qquad (2.3)$$

Averaged extracted mass (AEM) of analytes in each the 3 groups were used for simultaneous optimization of extraction of 16 PAHs and provided a quadratic model for each group:

$$Y = b_0 + \sum_{i=1}^{n} b_i X_i + \sum_{i=1}^{n} \sum_{i=1}^{n} b_{ij} X_i X_j + \sum_{i=1}^{n} b_{ii} X_i^2 \qquad (2.4)$$

where Y is a dependent variable (AEM for groups 1–3 in the present work), $X_i$ is an independent variable, $b_0$ is the constant coefficient, $b_i$ is the coefficient of the linear effect, $b_{ij}$ is the coefficient of the interaction effect, and $b_{ii}$ is the coefficient of the squad effect. The quadratic polynomial models (as Eq. 2.4) were obtained to predict the response of each dependant variables for extraction analytes.

*DF* is used to find the best level of each variable and optimize the response [58]. This function is obtained by transforming each response into an individual *DF* ($df_i$). By using optimization criteria and fitted models in CCD, this function (as Eq. 2.5) varied between 0 (for undesirable response) and 1 (desirable response) as follows [59]:

$$df_i = \begin{cases} 0 & if\ \ Y_i < L_i \\ \left(\frac{Y_i - L_i}{U_i - L_i}\right)^s & if L_i \le Y_i \le U_i \\ 1 & if\ \ Y_i > U_i \end{cases} \qquad (2.5)$$

In *DF* equation, $U_i$ and $L_i$ are the upper and lower values desired for the dependant variable $Y_i$ and $s$ is the weight to achieve a desirable response. The $df$ for different responses are then combined to obtain the global desirability as a joint response using Eq. 2.6. [60]

$$D = \left(df_1^{r_1} \times df_2^{r_2} \times \dots\dots \times df_n^{r_n}\right)^{\frac{1}{\Sigma ri}} = \left(\prod_{i=1}^{n} df_i^{ri}\right)^{\frac{1}{\Sigma ri}} \qquad (2.6)$$

In this equation, $r_i$ is the importance of each response compared to the others [59]. The desirability profile achieved for each response can be employed to predict the levels of factors providing the most desirable response.

### 2.2.6. Environmental water samples

For validation studies, a river water sample was collected from the Waterford river in St. John's, NL, Canada. The sample was stored at 4 °C before extraction. The river sample was analyzed and verified as "non-detect" to further evaluate the suitability of a matrix-matched calibration curve. Produced water which is the main discharged waste during oil extraction has a complex matrix with high content of organic and inorganic compounds [5, 6]. To determine PAHs in produced water, a sample was received from an offshore site in sealed bottles and kept at 4 °C until use was used for this study. The water samples were filtered through 0.2 mm filters before the extraction process as it is described in Section 2.4.

## 2.3. Results and discussion

### 2.3.1. Characterization studies

FT-IR spectra of the synthesized particles including $Fe_3O_4$, $Fe_3O_4$@$SiO_2$, $Fe_3O_4$@$SiO_2$-MPS, C-MMIP, MMIP, and MNIP were obtained to confirm the successful preparation of the sorbent. As presented in Fig. 2.2, the absorption characteristic band at 560 $cm^{-1}$ represents the stretching of Fe–O in the synthesized spinal $Fe_3O_4$ nanoparticles [61]. The peaks at 802 and 1040 $cm^{-1}$ on $Fe_3O_4$@$SiO_2$ spectra which correspond to the symmetric stretching of Si–O–Si and asymmetric stretching of Si–O, respectively, can confirm the formation of a silica layer on the surface of the magnetic nanoparticles [62]. Additionally, the presence of the absorption peaks of C=O bonds at 1725 $cm^{-1}$, $CH_2$ at 2958 $cm^{-1}$ and $CH_3$ at 2992 $cm^{-1}$ on C-MMIP, MMIP and MNIP spectra indicate the

grafting of polymeric coatings over the core–shell nanoparticles [63]. The stretching vibration of C=S bond at 1150 in MMIP and MNIP compared to C-MMIP revealed that the polymeric coatings in MMIP and MNIP sorbent have been formed through RAFT polymerization mechanism [41].

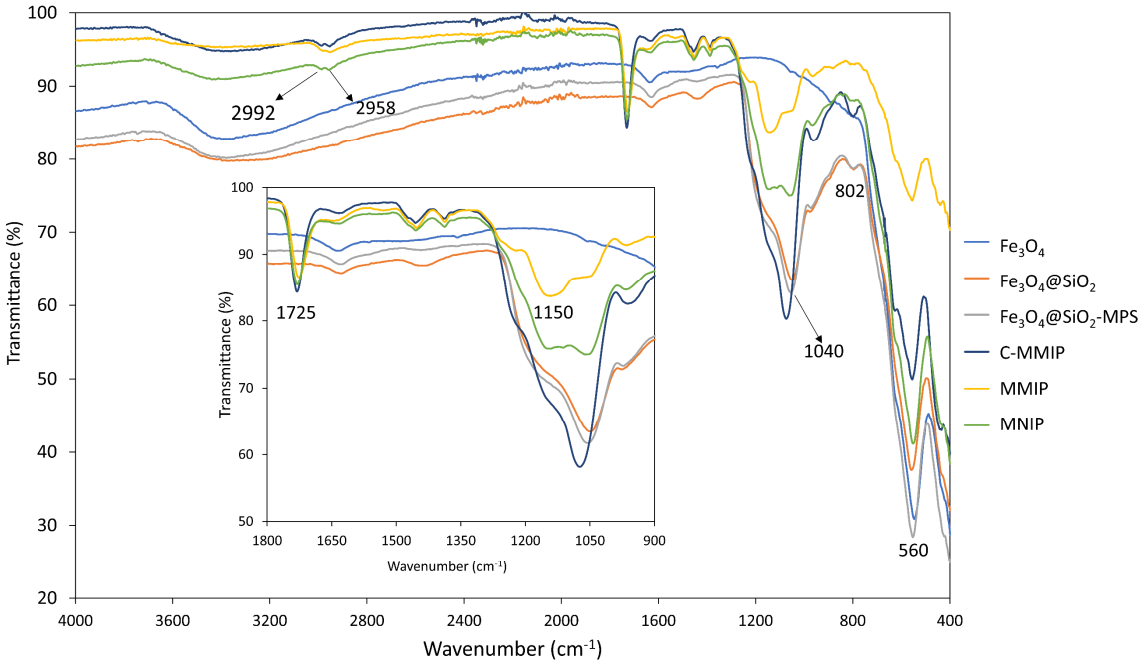


**Fig. 2.2.** FT-IR spectra of $Fe_3O_4$, $Fe_3O_4$@$SiO_2$, $Fe_3O_4$@$SiO_2$-MPS, C-MMIP, MMIP, and MNIP.

The XRD spectra of synthesized nanoparticles were acquired and shown in Fig. 2.3. The result of $Fe_3O_4$ specifies six peaks in the range of 2θ which characterize the pure $Fe_3O_4$ with inverse spinal structure confirming the successful synthesis of the magnetic substrate for the sorbent. A similar pattern was observed for the coated nanoparticles exhibited that the coating with silica shell, surface modification and grafting thin polymeric phase have no effects on the crystalline structure of the magnetic nanoparticles [64].

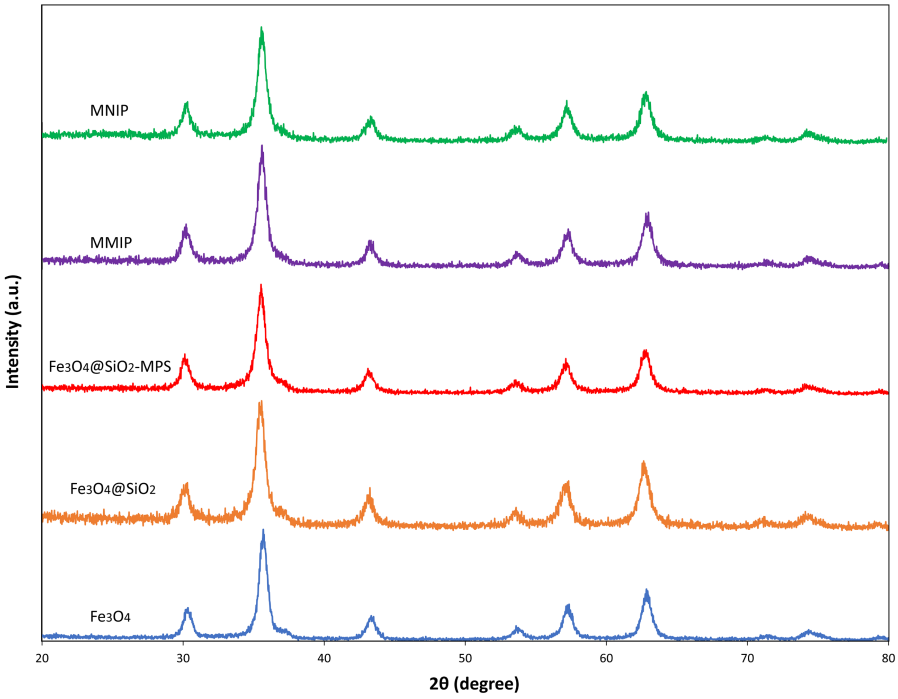


**Fig. 2.3.** XRD spectra of nanoparticles at each stage of production including $Fe_3O_4$, $Fe_3O_4$@$SiO_2$, $Fe_3O_4$@$SiO_2$-MPS, MMIP, and MNIP.

The morphological studies were performed by obtaining scanning electron micrographs which are shown in Fig. 2.4. As can be observed, the $Fe_3O_4$ substrate agglomerated due to their magnetic properties. The silica coating reduced this aggregation of the substrate by forming a shell over the magnetic core. The scanning electron micrograph of the synthesized MMIP (Fig. 2.4c) reveals that these particles have an averaged size of 100 nm with less aggregation and a uniform formation of polymeric coating. Therefore, these particles with large surface area which can be effectively dispersed in aqueous using an ultrasonic bath provide a rapid equilibrium between the sample and the sorbent and a large adsorption capacity for uptake of analytes.

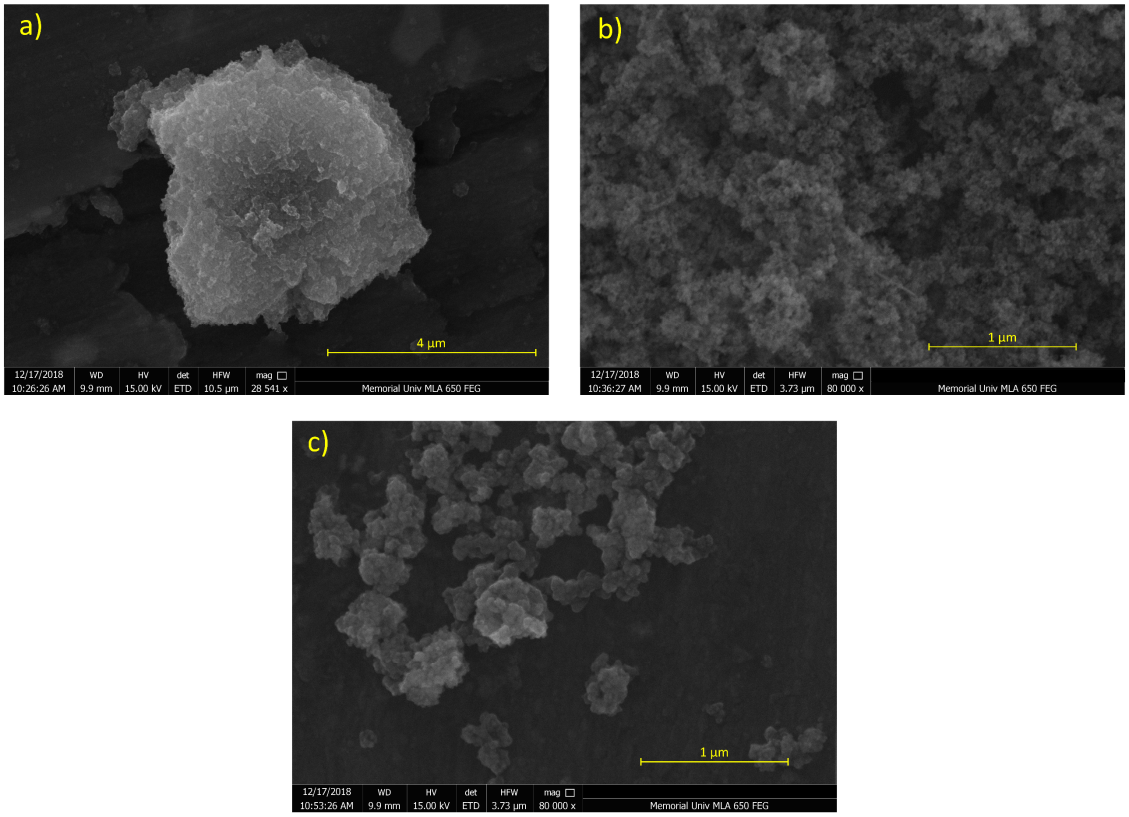


**Fig. 2.4.** Scanning electron micrographs of a) $Fe_3O_4$, b) $Fe_3O_4$@$SiO_2$, and c) MMIP.

Fig. 2.5 demonstrates the TEM images of $Fe_3O_4$, $Fe_3O_4$@$SiO_2$, C-MMIP and MMIP. The formation of MIP coating can be observed in C-MMIP prepared by a conventional surface polymerization and MMIP prepared by RAFT polymerization. However, the MIP layer formed in presence of RAFT agent is thinner and more uniform which provides rapid mass transfer during adsorption/desorption steps as well as homogenous and selective binding sites.

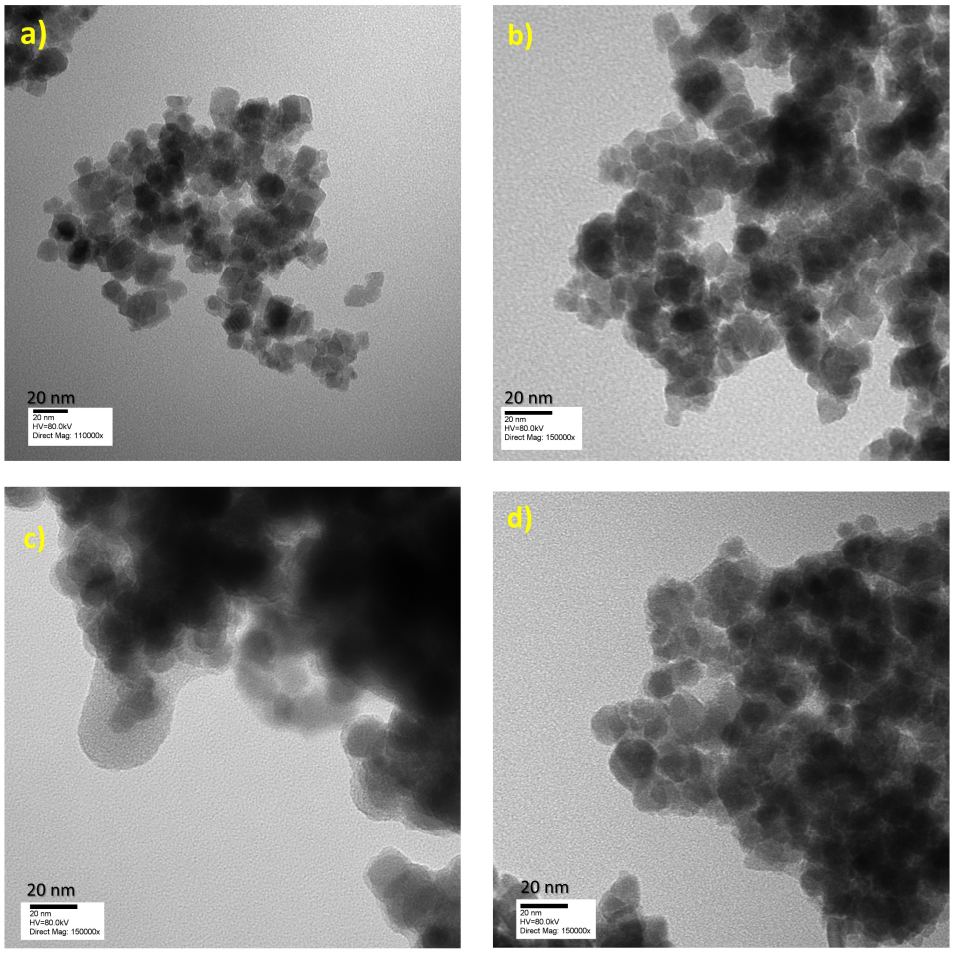


**Fig. 2.5.** TEM images of a) $Fe_3O_4$, b) $Fe_3O_4$@$SiO_2$, c) C-MMIP, and d) MMIP.

### 2.3.2. Selection of the desorption solvent

The desorption solvent plays a vital role in the sensitivity and repeatability of a preconcentration technique by ensuring a complete desorption of the analytes from the sorbent. Additionally, the desorption solvent used in MMIP-DSPE must be easily separated from the particles allowing for rapid sample preparation. Therefore, solvents with the capability of desorbing PAHs from the MMIPs including methanol, acetonitrile, hexane, and toluene were selected and tested. Using methanol and acetonitrile for desorption of

analytes resulted in the formation of a suspension of the MMIPs in the solution requiring a longer collection time after desorption as well as careful filtration of the solution to avoid introducing particulate residue into the chromatographic system. To avoid filtration and potential errors associated with this extra step, the samples desorbed by methanol and acetonitrile were not analyzed. Hexane and toluene which can be easily separated from the MMIPs without the need for filtration of the samples. Both solvents recovered the analytes with the same efficiencies. However, hexane demonstrated a higher reproducibility and higher volatility and therefore is better suited for desorption and solvent evaporation.

### 2.3.3. Screening the significant parameters

A two-level FFD comprising 16 ($2^{6-2}$) experiments was conducted to investigate the importance of 6 variables. These variables, their codes and the level of screening are presented in Table 2.3. The sequence of experiments was randomized to minimize the uncontrollable variables during experimental design [65].

**Table 2.3.** Factors, codes, low and high levels in the screening experiments.

| Factors | Levels | |
|---|---|---|
| | Low (−1) | High (+1) |
| ($X_1$) Mass of polymer (mg) | 5 | 10 |
| ($X_2$) Sample volume (mL) | 10 | 20 |
| ($X_3$) Salt addition (NaCl concentration; w/v) (%) | 0 | 10 |
| ($X_4$) Collection time (min) | 2 | 5 |
| ($X_5$) Desorption volume (µL) | 500 | 1000 |
| ($X_6$) Desorption time (min) | 2 | 10 |

The importance of the parameters considered in the screening step can be illustrated using Pareto charts. In these charts, the standardized effects of three groups of PAHs were plotted regarding the analysis of variance (ANOVA) tests of the AEM of PAHs in each group (Fig. 2.6). The length of each bar in the chart is proportional to the estimated effect of that parameter. The parameters which exceed the reference line (95% of the confidence interval) are significant. Sample volume has a significant effect on the extracted mass of all 16 PAHs due to increased loaded mass of PAHs in the sample solution as well as dispersion of sorbent in the sample. Moreover, the addition of salt, 10 % compared to 0 %, has a positive influence on the extraction of PAHs. Increasing the mass of the polymer from 5 to 10 mg has positive effects on the efficiency 2 groups due to the enhancement of the partition coefficients of these analytes with higher solubility in the sample matrix. Nevertheless, this parameter is not significant for group 3 because of their hydrophobic nature which favors their extraction toward MMIP phase, consequently, MMIP mass, sample volume, and salt addition are the important parameters and were further assessed during CCD optimization. Other parameters have no significant effect on the extraction of PAHs in their determined range, therefore, the following experiments were performed by fixing these parameters according to the sign of their estimated effect on the Pareto charts (i.e., 5 min collection time, 500 µL desorption solvent, and 2 min desorption time).

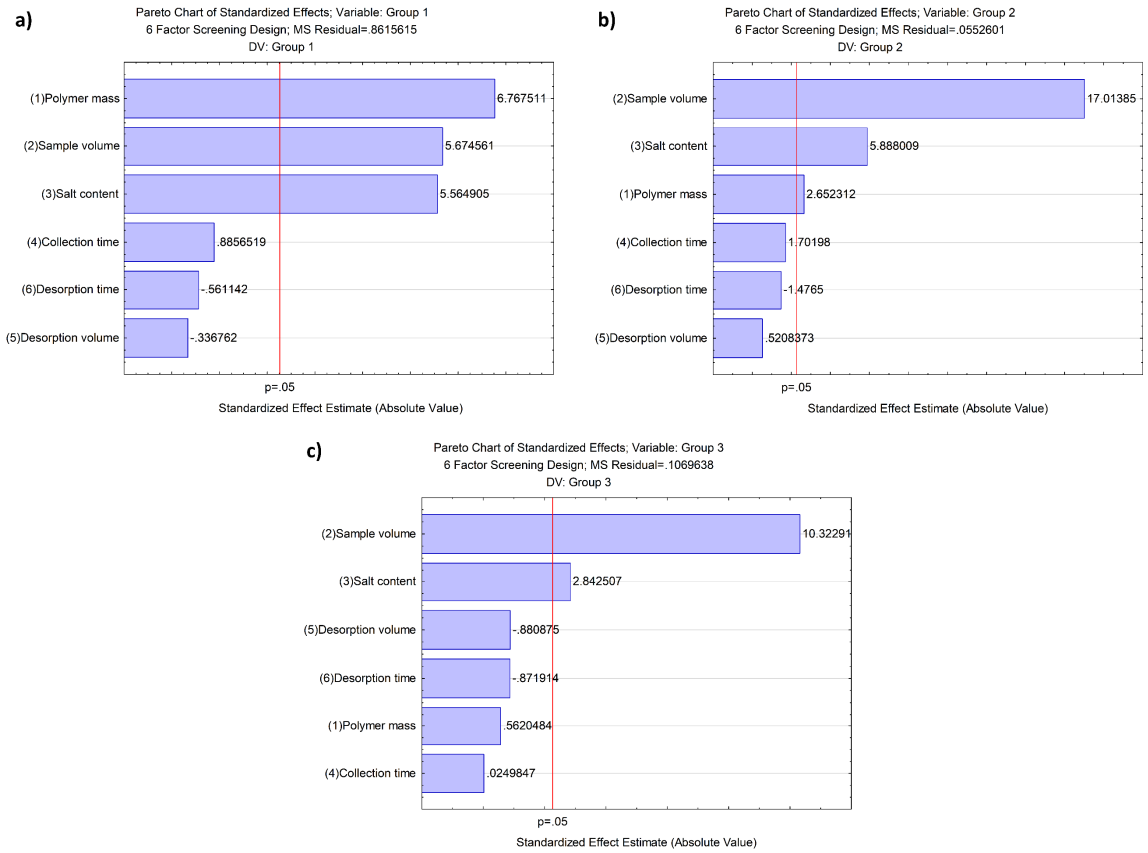


**Fig. 2.6.** Pareto charts of the standardized effects in the screening step a) group 1 , b) group 2, and c) group 3; sample solution containing 2000 pg $mL^{-1}$ of Naph, Acy, Ace, Flu, Phe, Ant, Flut and Pyr and 250 pg $mL^{-1}$of BaA, Chry, BbF, BkF, BaP, InP, DB(ah)A and BGP; extraction: 2 min ultrasonic dispersion; desorption solvent: hexane; internal standards: Naph-d8, Ace-d10 and Phe-d10: 50000 pg $mL^{-1}$ Chry-d12, Per-d12: 1000 pg $mL^{-1}$.

### 2.3.4. Central composite design

The second optimization step was conducted using a CCD with 23 randomized experiments including 9 replicates at the center point. Table 2.4 presents the variables selected from the screening step with their codes, and levels, the designed matrix and the response of each experiment.

**Table 2.4.** Main factors, symbols, levels and design matrix for the CCD.

| Factor | Code | Levels | | | | |
|---|---|---|---|---|---|---|
| | | -1.681 | -1 | 0 | 1 | 1.681 |
| Mass of polymer (mg) | $X_1$ | 3.2955 | 5 | 7.5 | 10 | 11.704 |
| Sample volume (mL) | $X_2$ | 6.59105 | 10 | 15 | 20 | 23.40895 |
| Salt addition (%) | $X_3$ | 6.59105 | 10 | 15 | 20 | 23.40895 |
| # | $X_1$ | $X_2$ | $X_3$ | Group 1 | Group 2 | Group 3 |
| 1 | -1 | -1 | -1 | 7.32424 | 1.95183 | 2.62867 |
| 2 | -1 | -1 | 1 | 9.56362 | 2.48721 | 2.35118 |
| 3 | -1 | 1 | -1 | 11.14484 | 4.71166 | 4.33170 |
| 4 | -1 | 1 | 1 | 12.94872 | 3.57052 | 3.46292 |
| 5 | 1 | -1 | -1 | 10.79566 | 2.45913 | 2.63126 |
| 6 | 1 | -1 | 1 | 11.15466 | 1.90746 | 1.59689 |
| 7 | 1 | 1 | -1 | 16.80002 | 4.98668 | 4.41181 |
| 8 | 1 | 1 | 1 | 20.84067 | 4.14860 | 4.19295 |
| 9 | -1.68179 | 0 | 0 | 8.88362 | 3.54922 | 3.62951 |
| 10 | 1.68179 | 0 | 0 | 17.39330 | 3.26966 | 3.34166 |
| 11 | 0 | -1.68179 | 0 | 8.09670 | 1.67746 | 1.75685 |
| 12 | 0 | 1.68179 | 0 | 15.07387 | 3.77358 | 3.47664 |
| 13 | 0 | 0 | -1.68179 | 12.25251 | 3.79508 | 3.49163 |
| 14 | 0 | 0 | 1.68179 | 17.14403 | 3.52931 | 3.19179 |
| 15 | 0 | 0 | 0 | 14.85570 | 3.09526 | 3.50179 |
| 16 | 0 | 0 | 0 | 14.93115 | 3.19268 | 3.57118 |
| 17 | 0 | 0 | 0 | 15.78191 | 2.86925 | 4.01891 |
| 18 | 0 | 0 | 0 | 15.96825 | 3.73205 | 3.45315 |
| 19 | 0 | 0 | 0 | 14.04876 | 2.99748 | 3.78471 |
| 20 | 0 | 0 | 0 | 15.89377 | 3.88862 | 3.53291 |
| 21 | 0 | 0 | 0 | 14.94815 | 3.08338 | 3.32124 |
| 22 | 0 | 0 | 0 | 15.00729 | 3.21392 | 3.60631 |
| 23 | 0 | 0 | 0 | 15.99560 | 2.92933 | 4.04533 |

Quadratic polynomial models comprising the main effects, quadratic effects, interaction effects were achieved for 3 groups of PAHs by plotting the responses versus experimental variables (Eqs. 2.7-2.9).

AEM Group 1= 15.279541995342+2.4105942586511*$X_1$- 0.84486216978798*$X_1$^2 + 2.5357422860659*$X_2$-1.3939954056786*$X_2$^2+1.2205925223985*$X_3$-0.29338459444058*$X_3$^2 + 1.0605830839484*$X_1X_2$+ 0.044549591418375*$X_1X_3$ +0.40576960905098*$X_2$*$X_3$ (2.7)

AEM Group2= 3.2222357776469 + 0.022735412587118*$X_1$+ 0.068092459936878*$X_1$^2+0.88871644467729*$X_2$-0.17371044160568*$X_2$^2-0.1788461068959 8*$X_3$ +0.15745612544376*$X_3$^2+0.11569460360344*$X_1X_2$-0.097998720184401*$X_1X_3$-0.24536626039647*$X_2X_3$ (2.8)

AEM Group3= 3.6465985320358-0.031168095167348*$X_1$-0.040296964295063*$X_1$^2+0.73836282400194*$X_2$-0.34747730658789*$X_2$^2-0.21262317094149*$X_3$-0.091163204479559*$X_3$^2+0.1952302437265*$X_1X_2$-0.013372292834466*$X_1X_3$+0.028026739421684*$X_2X_3$ (2.9)

The results of CCD step were further evaluated through ANOVA for each group (Tables 2.5–2.7). In these tables, statistical parameters values including the sum of square (SS), the degree of freedom (df), mean of the square (MS), *F* and *p*-values were included. The square of the coefficient of determination ($R^2$) which is a measure of the global fit of the model needs to be at least 0.80 for a good fit of a model [66]. The $R^2$ values were obtained 0.96372 for group 1, 0.85789 for group 2, and 0.87861 for group 3 implying that these models can describe the changes in the response of each group. [65]. The *p*-values <0.05were statistically important at 95 % confidence level in these tables. Since *"lack of fit (LOF) p*-value*"* of three calculated models is greater than 0.05, *LOF* is considered insignificant relative to the pure error of the models.

**Table 2.5.** Analysis of variance (ANOVA) for CCD (Group 1)

| Factor | SS | df | MS | F | P | |
|---|---|---|---|---|---|---|
| (1) Polymer mass(L) | 79.3594 | 1 | 79.35939 | 175.5889 | 0.000001 | Significant |
| Polymer mass(Q) | 11.3416 | 1 | 11.34165 | 25.0943 | 0.001041 | Significant |
| (2) Sample volume(L) | 87.8133 | 1 | 87.81330 | 194.2939 | 0.000001 | Significant |
| Sample volume(Q) | 30.8764 | 1 | 30.87644 | 68.3166 | 0.000034 | Significant |
| (3) Salt content(L) | 20.3466 | 1 | 20.34658 | 45.0184 | 0.000151 | Significant |
| Salt content(Q) | 1.3677 | 1 | 1.36766 | 3.0261 | 0.120125 | Not significant |
| 1L by 2L | 8.9987 | 1 | 8.99869 | 19.9103 | 0.002105 | Significant |
| 1L by 3L | 0.0159 | 1 | 0.01588 | 0.0351 | 0.855990 | Not significant |
| 2L by 3L | 1.3172 | 1 | 1.31719 | 2.9144 | 0.126178 | Not significant |
| Lack of Fit | 5.4582 | 5 | 1.09164 | 2.4153 | 0.128338 | Not significant |
| Pure Error | 3.6157 | 8 | 0.45196 | | | |
| Total SS | 250.1145 | 22 | | | | |

**Table 2.6.** Analysis of variance (ANOVA) for CCD (Group 2)

| Factor | SS | df | MS | F | P | |
|---|---|---|---|---|---|---|
| (1) Polymer mass(L) | 0.00706 | 1 | 0.00706 | 0.05640 | 0.818242 | Not significant |
| Polymer mass(Q) | 0.07367 | 1 | 0.07367 | 0.58865 | 0.464980 | Not significant |
| (2) Sample volume(L) | 10.78640 | 1 | 10.78640 | 86.18505 | 0.000015 | Significant |
| Sample volume(Q) | 0.47946 | 1 | 0.47946 | 3.83100 | 0.086017 | Not significant |
| (3) Salt content(L) | 0.43683 | 1 | 0.43683 | 3.49031 | 0.098674 | Not significant |
| Salt content(Q) | 0.39393 | 1 | 0.39393 | 3.14760 | 0.113963 | Not significant |
| 1L by 2L | 0.10708 | 1 | 0.10708 | 0.85560 | 0.382027 | Not significant |
| 1L by 3L | 0.07683 | 1 | 0.07683 | 0.61388 | 0.455897 | Not significant |
| 2L by 3L | 0.48164 | 1 | 0.48164 | 3.84835 | 0.085430 | Not significant |
| Lack of Fit | 1.12717 | 5 | 0.22543 | 1.80126 | 0.218848 | Not significant |
| Pure Error | 1.00123 | 8 | 0.12515 | | | |
| Total SS | 14.97761 | 22 | | | | |

**Table 2.7.** Analysis of variance (ANOVA) for CCD (Group 3)

| Factor | SS | df | MS | F | P | |
|---|---|---|---|---|---|---|
| (1)Polymer mass(L) | 0.01327 | 1 | 0.013267 | 0.2118 | 0.657619 | Not significant |
| Polymer mass(Q) | 0.02580 | 1 | 0.025802 | 0.4119 | 0.538962 | Not significant |
| (2)Sample volume(L) | 7.44543 | 1 | 7.445429 | 118.8562 | 0.000004 | Significant |
| Sample volume(Q) | 1.91848 | 1 | 1.918481 | 30.6259 | 0.000551 | Significant |
| (3)Salt content(L) | 0.61741 | 1 | 0.617407 | 9.8561 | 0.013817 | Significant |
| Salt content(Q) | 0.13205 | 1 | 0.132052 | 2.1080 | 0.184590 | Not significant |
| 1L by 2L | 0.30492 | 1 | 0.304919 | 4.8676 | 0.058420 | Not significant |
| 1L by 3L | 0.00143 | 1 | 0.001431 | 0.0228 | 0.883624 | Not significant |
| 2L by 3L | 0.00628 | 1 | 0.006284 | 0.1003 | 0.759559 | Not significant |
| Lack of Fit | 0.94327 | 5 | 0.188654 | 3.0116 | 0.080470 | Not significant |
| Pure Error | 0.50114 | 8 | 0.062642 | | | |
| Total SS | 11.89891 | 22 | | | | |

The response of each group has been correlated to the experimental levels of factors by drawing three-dimensional plots in which AEM was plotted versus two experimental parameters while the other factor was considered constant (Fig. 2.7). The response plots for group 1 containing analytes with lower extraction efficiency are shown in Fig. 2.7a. The relationship between polymer mass and sample volume (Fig. 2.7a–i) shows that increasing the mass of the sorbent yielded a higher extracted mass of group 1 with *p* value of 0.000001 for linear effect (Table 2.5). The enhancement is attributed to the higher mass of sorbent causing an increased partitioning of analytes between the sample solution and the sorbent. This plot (AEM versus polymer mass-sample volume) reached a maximum at a low sample volume and decreased by further addition of polymer implying the insufficient dispersion of sorbent in the sample solution. The effect of polymer mass on the extraction of two other groups (see Figs. 2.7b–i, and 2.7c–i) is not significant which can also be concluded through ANOVA tests (Tables 2.6 and 2.7) with *p* values of 0.818242 and 0.657619 for group 2 and 3, respectively. The sample volume intensified the extracted mass of analytes in three groups by increasing the loaded PAHs in the original sample solution in addition to the dispersion effect. The *p* values for the linear effect of sample volume on extracted mass of three groups are 0.000001 for group 1, 0.000015 for group 2 and 0.000004 for group 3 . This trend (AEM versus sample volume) hits a peak followed by a decline at larger sample volumes due to the infinite dispersion of MMIP particles which can not be collected sufficiently from the sample. A glance at polymer mass vs. sample volume plots (Fig. 2.7a, b, c–i) declares the adverse effect of large sample volumes which is more pronounced in small amounts of extraction phase. Another variable which is widely used to improve the extraction of analytes in LLE and DLLME is the addition of salt. This effect called “salting-

out" is caused by expelling hydrophobic analytes from the sample solution to the extraction phase.

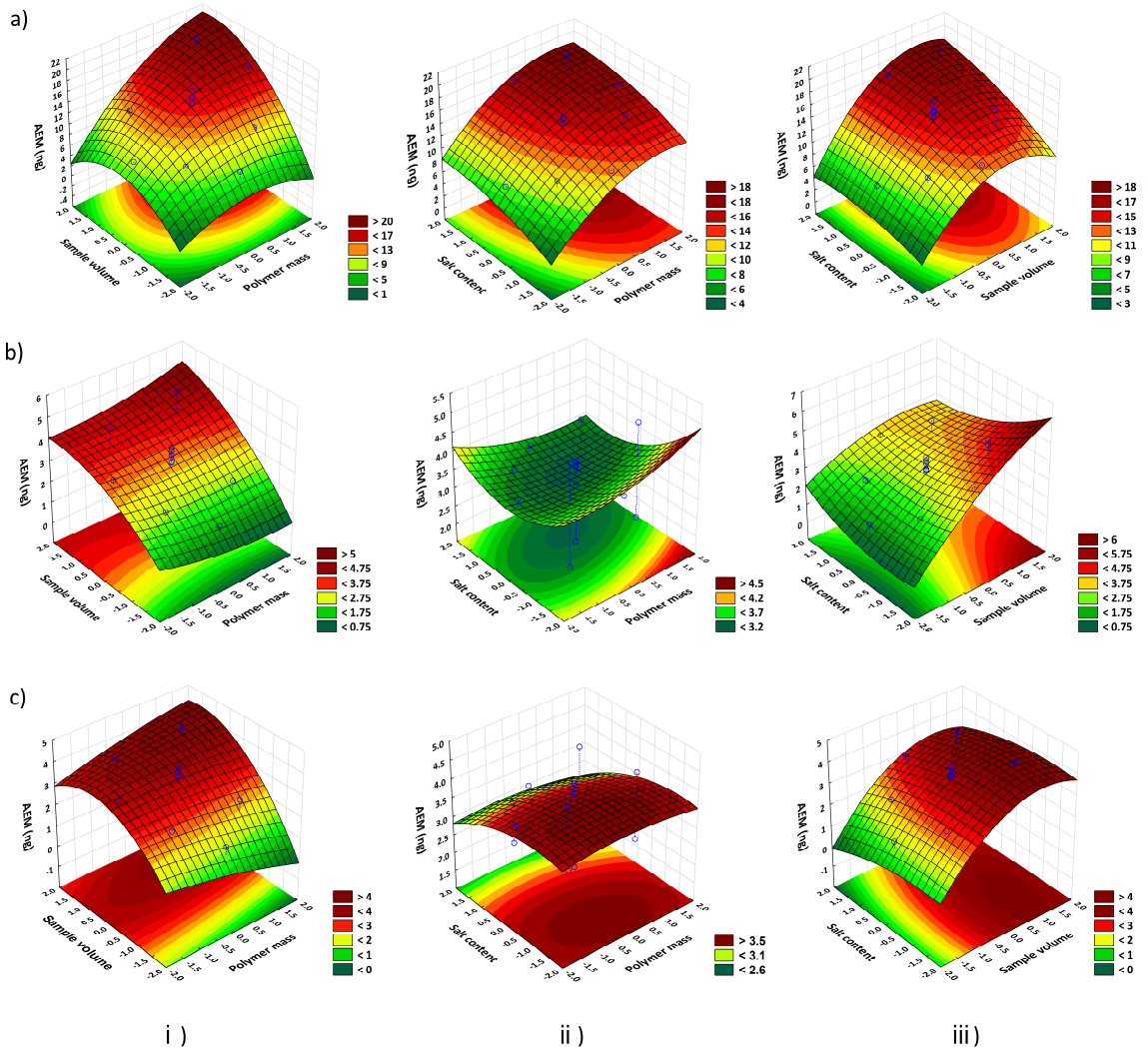


**Fig. 2.7.** The response surface plots of AEM for 3 groups of PAHs: a) group 1, b) group 2 , and c) group 3 versus: polymer mass-sample volume (i), polymer mass-salt content (ii), and sample volume-salt content (iii); sample solution containing 2000 pg $mL^{-1}$ of Naph, Acy, Ace, Flu, Phe, Ant, Flut and Pyr and 250 pg $mL^{-1}$of BaA, Chry, BbF, BkF, BaP, InP, DB(ah)A and BGP; extraction: 2 min ultrasonic dispersion; magnetic collection 5 min, Desorption: 500 µL hexane, 2 min ultrasonic dispersion; internal standards: Naph-d8, Ace-d10 and Phe-d10: 50000 pg $mL^{-1}$ Chry-d12, Per-d12: 1000 pg $mL^{-1}$.

The salt effect is a significant parameter for the extraction of group 1 ($p$: 0.000151) and 3 ($p$: 0.184590) while the extraction of group 2 was not affected profoundly ($p$: 0. 098674). In group 1, AEM was enlarged by salt addition as shown in plots Fig. 2.7a-ii and -iii, however, salt content caused a slight decrease for extraction of 6 heavy PAHs (Fig. 2.7c-ii and -iii) because of the low solubility of these analytes in water which is further reduced by salt content and may cause the analytes to adsorb onto the walls of the sample vial.

### 2.3.5. Desirability function

Simultaneous optimization of MMIP-DSPE is of utmost importance in quantitation of PAHs using this method because of various solubility and hydrophobicity of these analytes. Therefore, *DF* was employed to maximize the response of the analytes in the 3 groups. According to the result of CCD step, the minimum and maximum AEM values obtained for each group were considered as the least desirable ($df$=0) and the most desirable ($df$=1) responses, respectively. The corresponding desirability score for each group was illustrated in the left-hand panel of Fig. 2.8a, in addition to *DF* profile of dependents and a composite desirability (right-hand side of Fig. 2.8a). The *DF* optimization allows for the observation of how the changes in the level of the variables can simultaneously influence the response and overall desirability of the experiment. The desirability of 1.0 was set as a goal in the calculations of the optimum conditions.

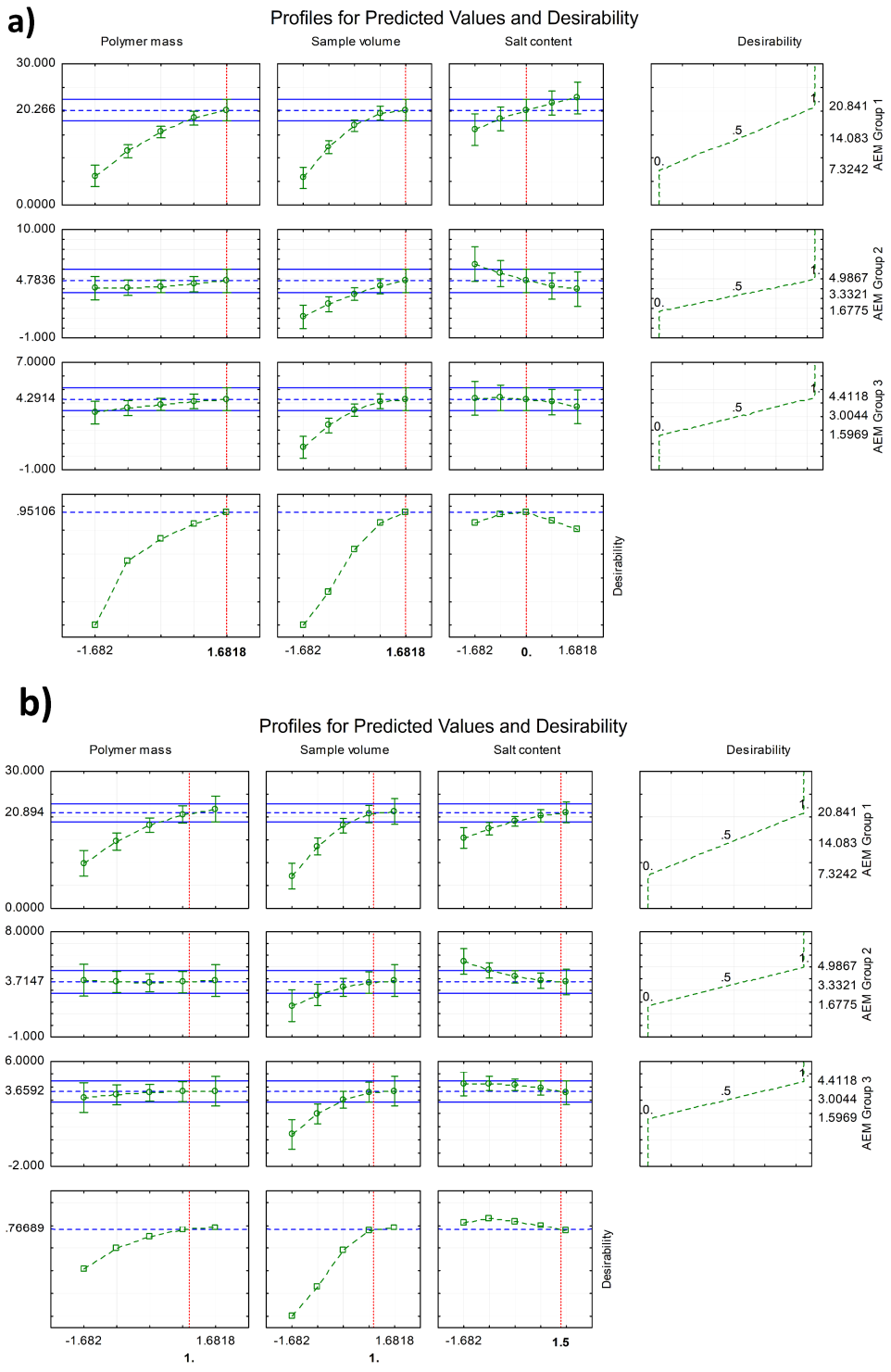


**Fig. 2.8.** Profiles for predicated values and desirability function a) using optimum *DF* for extraction of PAHs using MMIP-DSPE; b) using user-specified parameters for extraction of PAHs using MMIP-DSPE.

The optimal levels of variables were obtained at +1.6818 for both polymer mass and sample volume and 0 for salt content with a high overall desirability (0.95106). These variables responded AEM of 20.266 ng (group 1), 4.7836 ng (group 2) 4.29142 ng (group 3). However, due to operational limitations and the diverse response of PAHs to the changes in the level of variables, a compromised optimization strategy by using user-specified optimization in the *DF* was employed (Fig. 2.8b). In this optimization strategy, the importance of the variables on the response of three individual groups was considered according to the ANOVA results obtained in the CCD (Tables 2.5–2.7). In STATISTICA 10.0, the *DF* can be plotted with various levels of each parameter to observe the predicted values for three responses. Therefore, polymer mass and sample volume were both set at the +1 level since larger sample volumes, and polymer mass increase the cost and analysis time. To optimize the amount of salt in the extraction process, a careful examination of three groups of analytes was conducted. As discussed in CCD, this variable has a positive effect on the extracted mass of group 1, no significant effect on group 2 and a slight negative effect on group 3. As a compromise, the salt content was set at +1.5 to observe the salting out effect and achieve a more sensitive method for extraction of 8 light PAHs with higher solubility in water. Therefore, the user-specified *DF* optimization contributes a sensitive determination of group 1, while the proposed levels of variables provide enough sensitivity for the other 2 groups due to their exhaustive extraction.

### 2.3.6. Selectivity evaluation for extraction of PAHs

Regarding the hydrophobic nature of the MMIPs and the hydrophobicity of the PAHs, selectivity studies were conducted using a large sample volume (40 mL) and a small amount of the sorbents (i.e. $Fe_3O_4$ and $Fe_3O_4$@$SiO_2$, C-MNIP, C-MMIP, MNIP and MMIP; 5 mg). The small ratio of MMIP mass as compared to sample volume provides the opportunity for MMIP to adsorb analytes through selective recognition sites in addition to non-selective sites. Additionally, the experiments were performed with no salt to avoid the salting-out effect. The obtained data in Fig. 2.9 revealed adsorption of PAHs from the sample solution using $Fe_3O_4$ and $Fe_3O_4$@$SiO_2$ nanoparticles which is due to intrinsic properties of these particles with a large surface area especially for analytes with higher LogP values. The extracted mass of PAHs using MNIPs indicates adsorption of the analytes using non-selective recognition sites on the polymeric layer which coats the core–shell particles. Creation of selective recognition sites through imprinted cavities was determined to be superior for the extraction of PAHs using MMIPs. As can be seen in the Fig. 2.9, the adsorption of PAHs using MMIPs was higher than that of MNIPs particularly for lighter PAHs with lower LogP values and higher solubility in the water. Although PAHs have no specific functionalities and mainly adsorb by hydrophobic interactions, preparation of MMIPs using RAFT polymerization and a pseudo template generate cavities suitable for the adsorption of the PAHs using π–π interactions and H-bonding in addition to non-specific interactions. Therefore, this polymerization strategy caused shaped and functionalized imprinted polymeric coating for the selective adsorption of PAHs. Furthermore, the polymeric coatings either MMIPs or MNIPs enhance the reproducibility of the enrichment due to less aggregation of nanoparticles. The C-MMIP showed similar

adsorption behavior to MMIP with lower repeatability this is mainly to due heterogenous distribution of the binding sites in C-MMIP. Interestingly, C-MNIP have higher adsorption than MNIP due a higher population of non-specific binding sites created through a free radical polymerization. Therefore, it can be concluded that RAFT polymerization can enhance the selectivity through homogenously distributed binding sites.

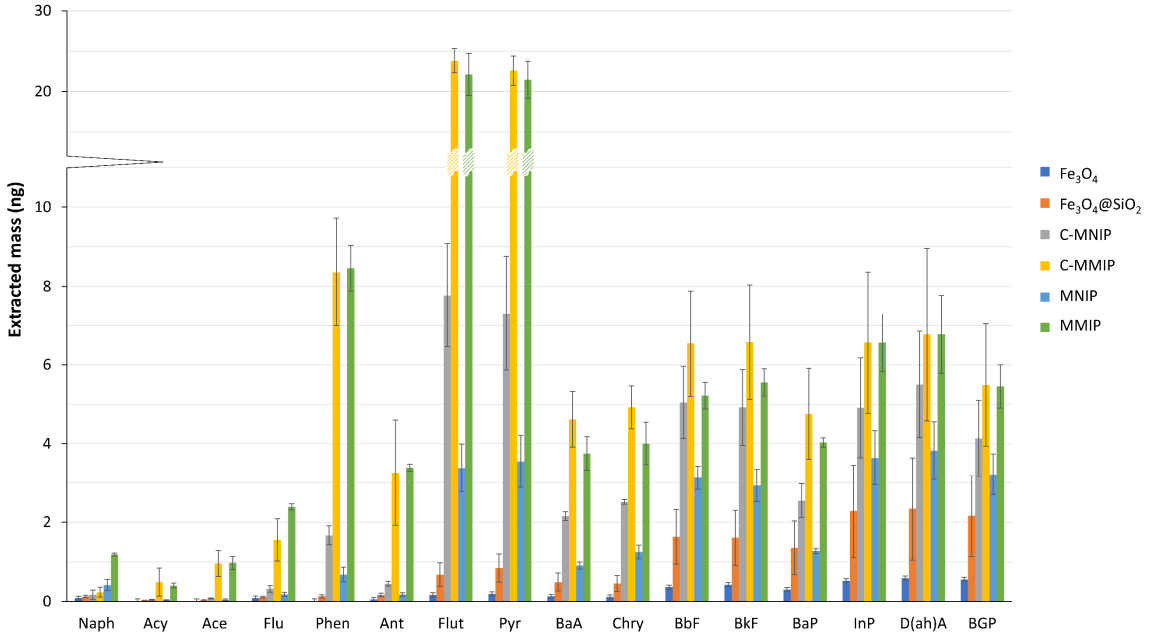


**Fig. 2.9.** Comparison of performance of $Fe_3O_4$, $Fe_3O_4$@$SiO_2$, C-MNIP, C-MMIP, MNIP and MMIP for extraction of PAHs from water samples. sample: 40 mL sample solution containing 1600 pg $mL^{-1}$ of Naph, Acy, Ace, Flu, Phe, Ant, Flut and Pyr and 200 pg $mL^{-1}$of BaA, Chry, BbF, BkF, BaP, InP, DB(ah)A and BGP; extraction: 2 min ultrasonic dispersion; magnetic collection 5 min, Desorption: 500 µL hexane; internal standards: Naph-d8, Ace-d10 and Phe-d10: 50000 pg $mL^{-1}$ Chry-d12, Per-d12: 1000 pg $mL^{-1}$; Extraction recovery (%) using MMIP: Naph: 1.8, Acy: 0.6, Ace: 1.5, Flu: 3.7, Phen: 13.2, Ant: 5.3, Flut: 34.6, Pyr: 33.5, BaA: 46.9, Chry: 50.1, BbF: 65.2, BkF: 69.4, BaP: 50.4, InP: 82.1, DB(ah)A: 84.7, BGP: 68.2.

### 2.3.7. Analytical performance of the MMIP–DSPE–APCI-GC–MS/MS for determination of PAHs

The proposed DSPE method using RAFT-MMIPs as a selective sorbent was evaluated for the analytical figures of merits including linear range (LR), correlation coefficient ($R^2$), limit of detection (LOD), and limit of quantitation (LOQ). These tests were completed using optimized conditions and summarized in Table 2.8. LOD and LOQ defined as signal-to-noise (S/N) ratio of 3 and 10, respectively, for each analyte, were obtained by analyzing blank ultrapure water samples containing internal standards. The acceptance criteria for calibration curves consisted of a determination coefficient ($R^2$) higher than 0.99 and an intercept higher than the LOD. Weighted calibration curves using 1/x as the weighting factor were used to achieve better fitting and more accuracy of quantification, particularly for lower concentrations. Calibration points were prepared by adding standard PAHs solutions into ultrapure water to obtain 1–50000 pg $mL^{-1}$ exhibiting a good correlation to signal with $R^2$ values greater than 0.99. Preparation of a broad range of concentrations is required due to the varying solubility of different PAHs in the aqueous environment. In the present work, the dynamic ranges were obtained in ppt to sub-ppb levels for high M.W. PAHs with lower solubility in water and ppb to ppm levels for low M.W. PAHs with increasing solubility. LOD and LOQ for target analytes were in the range of 1–100 pg $mL^{-1}$ and 2–200 pg $mL^{-1}$, respectively. This range of sensitivity achieved is due to the selectivity and efficiency of the proposed MMIPs allowing for the development of a single method of extraction and analysis for 16 PAHs in the aqueous matrix. Apart from the extraction of analytes using RAFT-MMIPs, performing the desorption with small volumes of solvent and solvent evaporation to increase the enrichment factor (EF) have

resulted in a sensitive method. The obtained LOQ values are lower than the maximum contamination limit (MCL) by US-EPA [67] and can meet the criteria regulated by European Union for human consumption [68] and environmental quality standard [69]. For example, the regulated concentration of BaP in the water intended for human consumption is 10 pg $mL^{-1}$, whereas sum of concentrations of BbF, BkF, BGP and InP must not exceed 100 pg $mL^{-1}$ [68]. The obtained LODs using MMIP-DSPE for these analytes were 1-2 pg $mL^{-1}$.

Accuracy and precision of the method were evaluated by extracting PAHs at five levels of concentration in the linear range including 7.5, 35, 140, 350. 7000 pg $mL^{-1}$ (Table 2.9) in one day. The precision of the method was determined as the relative standard deviation (RSD%) for a triplicate MMIP-DSPE-APCI-GC-MS/MS experiment per concentration. The accuracy was obtained in the range 72.3–135 % for extraction and analysis PAHs with satisfactory precision, i.e., 1.2–28%. The obtained calibration curves in ultrapure water were utilized as matrix-matched calibration for a river sample as the real environmental sample. Table 2.10 presents the results for river water at different levels of PAHs to obtain 15, 80, 250, 2500 and 25000 pg $mL^{-1}$. The acquired accuracy and precision show the potential of the MMIP-DSPE for quantitation of PAHs in real samples without the standard addition method. For further evaluation of the MMIP-DSPE for water analysis, the accuracy of two samples (ultrapure and river water) were shown in histograms in the range of 70–80%, 80–120%, 120–130%, and >130%. As illustrated by Fig. 2.10, this method produced accurate results with more than 77% of the results in the acceptable range of 80–120%.

**Table 2.8.** Figures of merit for determination 16 PAHs in the water samples under optimized MMIP-DSPE conditions (n = 3).

| PAHs | Internal standard [a] | LOD (pg $mL^{-1}$) | LOQ (pg $mL^{-1}$) | LR (pg $mL^{-1}$) | Equation | $R^2$ |
|---|---|---|---|---|---|---|
| Naph | Naph-d8 | 100 | 200 | 200-50000 | $y = 1.85 \times 10^{-3} (\pm 1.60 \times 10^{-5})x + 2.75 \times 10^{-1} (\pm 3.34 \times 10^{-1})$ | 0.9997 |
| Acy | Ace-d10 | 10 | 20 | 20-50000 | $y = 1.10 \times 10^{-4} (\pm 8.28 \times 10^{-7})x + 4.83 \times 10^{-3} (\pm 6.40 \times 10^{-3})$ | 0.9997 |
| Ace | Ace-d10 | 10 | 20 | 20-50000 | $y = 1.05 \times 10^{-3} (\pm 2.43 \times 10^{-5})x + 3.28 \times 10^{-2} (\pm 2.26 \times 10^{-2})$ | 0.9979 |
| Flu | Phen-d10 | 40 | 100 | 100-50000 | $y = 2.74 \times 10^{-3} (\pm 4.76 \times 10^{-5})x + 9.55 \times 10^{-1} (\pm 9.10 \times 10^{-1})$ | 0.9982 |
| Phen | Phen-d10 | 10 | 20 | 20-20000 | $y = 1.31 \times 10^{-3} (\pm 2.65 \times 10^{-5})x + 1.15 \times 10^{-1} (\pm 1.91 \times 10^{-1})$ | 0.9967 |
| Ant | Phen-d10 | 20 | 40 | 40-20000 | $y = 6.60 \times 10^{-4} (\pm 6.78 \times 10^{-6})x - 9.84 \times 10^{-3} (\pm 1.18 \times 10^{-2})$ | 0.9995 |
| Flut | Phen-d10 | 20 | 20 | 20-20000 | $y = 2.26 \times 10^{-3} (\pm 2.90 \times 10^{-5})x - 1.38 \times 10^{-2} (\pm 2.50 \times 10^{-2})$ | 0.9992 |
| Pyr | Phen-d10 | 20 | 40 | 40-10000 | $y = 2.29 \times 10^{-3} (\pm 6.00 \times 10^{-6})x - 3.69 \times 10^{-2} (\pm 2.33 \times 10^{-2})$ | 1.0000 |
| BaA | Chry-d12 | 1 | 2 | 2-1000 | $y = 1.23 \times 10^{-2} (\pm 6.70 \times 10^{-5})x - 1.98 \times 10^{-2} (\pm 2.46 \times 10^{-2})$ | 0.9998 |
| Chry | Chry-d12 | 1 | 2 | 2-1000 | $y = 1.26 \times 10^{-2} (\pm 3.26 \times 10^{-5})x + 2.79 \times 10^{-2} (\pm 1.20 \times 10^{-2})$ | 1.0000 |
| BbF | Per-d12 | 1 | 2 | 2-1000 | $y = 2.52 \times 10^{-2} (\pm 2.00 \times 10^{-4})x - 1.46 \times 10^{-1} (\pm 7.33 \times 10^{-2})$ | 0.9996 |
| Bkf | Per-d12 | 1 | 2 | 2-400 | $y = 1.97 \times 10^{-2} (\pm 1.66 \times 10^{-4})x - 5.12 \times 10^{-3} (\pm 2.70 \times 10^{-2})$ | 0.9996 |
| BaP | Per-d12 | 2 | 4 | 4-1000 | $y = 1.56 \times 10^{-2} (\pm 1.50 \times 10^{-4})x - 7.94 \times 10^{-2} (\pm 5.83 \times 10^{-2})$ | 0.9994 |
| InP | Per-d12 | 2 | 4 | 4-4000 | $y = 8.29 \times 10^{-3} (\pm 8.61 \times 10^{-5})x - 3.02 \times 10^{-1} (\pm 1.25 \times 10^{-1})$ | 0.9991 |
| DB(ah)A | Per-d12 | 1 | 2 | 2-250 | $y = 4.03 \times 10^{-3} (\pm 1.64 \times 10^{-4})x + 2.00 \times 10^{-2} (\pm 1.42 \times 10^{-2})$ | 0.9917 |
| BGP | Per-d12 | 1 | 2 | 2-250 | $y = 6.40 \times 10^{-3} (\pm 2.49 \times 10^{-4})x - 1.54 \times 10^{-2} (\pm 2.15 \times 10^{-2})$ | 0.9925 |

[a] Concentration of internal standards in the water samples: Naph-d8, Ace-d10 and Phe-d10: 1000 pg $mL^{-1}$; Chry-d12, Per-d12: 100 pg $mL^{-1}$.

**Table 2.9.** Method validation summary for simultaneous determination 16 PAHs in the water samples using optimized MMIP-DSPE conditions (n=3).

| PAHs | Recovery (%) | EF | Inter-batch RSD (%) | Accuracy (%)[a] | | | | | Precision RSD (%) | | | | |
|---|---|---|---|---|---|---|---|---|---|---|---|---|---|
| | | | | 7.5 | 35 | 140 | 350 | 7000 | 7.5 | 35 | 140 | 350 | 7000 |
| Naph | 4.5 | 8.9 | 4.9 | NQ[b] | NQ | NQ | 81.0 | 74.6 | – | – | – | 1.5 | 5.5 |
| Acy | 25.2 | 50.4 | 6.4 | NQ | 113 | 95.3 | 82.8 | 86.0 | – | 9.7 | 4.4 | 17 | 17 |
| Ace | 24.8 | 49.6 | 2.2 | NQ | 87.1 | 94.9 | 80.2 | 72.3 | – | 6.5 | 8.6 | 10 | 13 |
| Flu | 58.1 | 116.3 | 4.1 | NQ | NQ | 80.7 | 87.4 | 86.8 | – | – | 28 | 14 | 4.6 |
| Phen | 84.5 | 169.0 | 2.4 | NQ | 115 | 126 | 126 | 111 | – | 12 | 4.4 | 7.2 | 2.2 |
| Ant | 77.4 | 154.8 | 1.9 | NQ | NQ | 105 | 101 | 89.8 | – | – | 3.6 | 9.4 | 1.2 |
| Flut | 97.0 | 193.9 | 5.1 | NQ | 109 | 135 | 112 | 96.4 | – | 22 | 2.2 | 17 | 6.0 |
| Pyr | 84.8 | 169.7 | 3.1 | NQ | NQ | 122 | 98.1 | 84.1 | – | – | 3.0 | 15 | 4.0 |
| BaA | 90.5 | 180.9 | 7.9 | 100 | 101 | 102 | 99.1 | NL[C] | 4.7 | 4.5 | 1.2 | 3.7 | – |
| Chry | 89.4 | 178.9 | 6.9 | 106 | 108 | 111 | 111 | NL | 5.3 | 3.6 | 2.9 | 13 | – |
| BbF | 94.8 | 189.6 | 3.6 | 91.4 | 105 | 108 | 99.8 | NL | 1.9 | 9.3 | 6.1 | 11 | – |
| Bkf | 92.1 | 184.3 | 5.2 | 97.0 | 127 | 121 | 127 | NL | 5.3 | 11 | 5.6 | 18 | – |
| BaP | 84.8 | 169.6 | 7.7 | 88.8 | 92.1 | 104 | 115 | NL | 4.2 | 11 | 5.3 | 13 | – |
| InP | 92.4 | 184.9 | 7.0 | 96.8 | 95.3 | 95.8 | 106 | NL | 14 | 13 | 3.3 | 11 | – |
| DB(ah)A | 95.6 | 191.2 | 4.4 | 90.3 | 104 | 130 | NL | NL | 12 | 4.6 | 22 | – | – |
| BGP | 83.7 | 167.4 | 6.1 | 90.4 | 102 | 105 | NL | NL | 3.8 | 17 | 11 | – | – |

[a] Concentration of internal standards in the water samples:Naph-d8, Ace-d10 and Phe-d10: 1000 pg $mL^{-1}$ Chry-d12, Per-d12: 100 pg $mL^{-1}$; all the concentrations are in pg $mL^{-1}$.

[b] NQ: Added concentration is lower than LOQ.

[c] NL: Added concentration is higher than linear range.

**Table 2.10.** Matrix-matched results for determination 16 PAHs in river water samples under optimized MMIP-DSPE conditions (n=3).

| Added Conc[a] | 15 | | | 80 | | | 250 | | | 2500 | | | 25000 | | |
|---|---|---|---|---|---|---|---|---|---|---|---|---|---|---|---|
| PAHs | Found conc ±SD | Accuracy (%) | RSD (%) | Found conc ±SD | Accuracy (%) | RSD (%) | Found conc ±SD | Accuracy (%) | RSD (%) | Found conc ±SD | Accuracy (%) | RSD (%) | Found conc ±SD | Accuracy (%) | RSD (%) |
| Naph | NQ[b] | - | - | NQ | - | - | 247.2±49.2 | 98.9 | 20 | 2477.9±341.7 | 99.1 | 14 | 20035.3±2314.8 | 80.1 | 12 |
| Acy | NQ | - | - | 109.7±16.8 | 137 | 15 | 332.2±17.6 | 133 | 5.3 | 3209.0±234.7 | 128 | 7.3 | 28742.0±1788.5 | 115 | 6.2 |
| Ace | NQ | - | - | 73.8±15.9 | 92.2 | 22 | 227.3±16.5 | 90.9 | 7.3 | 2090.6±156.0 | 83.6 | 7.5 | 21219.3±1394.1 | 84.9 | 6.6 |
| Flu | NQ | - | - | NQ | - | - | 305.7±20.1 | 122 | 6.6 | 2566.1±73.1 | 103 | 2.8 | 27905.6±1551.1 | 112 | 5.6 |
| Phen | NQ | - | - | 100.6±8.8 | 126 | 8.7 | 313.6±18.6 | 125 | 5.9 | 3215.8±40.4 | 129 | 1.3 | 30958.1±1161.0 | 124 | 3.8 |
| Ant | NQ | - | - | 107.9±16.1 | 135 | 15 | 300.6±14.5 | 120 | 4.8 | 2912.0±89.5 | 116 | 3.1 | 30669.3±3665.6 | 123 | 12 |
| Flut | NQ | - | - | 98.8±6.1 | 124 | 6.1 | 290.2±21.9 | 116 | 7.6 | 2598.1±422.2 | 104 | 16 | NL[c] | - | - |
| Pyr | NQ | - | - | 89.0±1.9 | 111 | 2.1 | 245.9±18.4 | 98.3 | 7.5 | 2163.0±389.3 | 86.5 | 18 | NL | - | - |
| BaA | 15.5±0.9 | 103 | 6.0 | 88.7±12.6 | 111 | 14 | 252.1±14.6 | 101 | 5.8 | NL | - | - | NL | - | - |
| Chry | 15.5±0.6 | 103 | 3.6 | 87.9±10.9 | 110 | 12 | 237.6±18.3 | 95.0 | 7.7 | NL | - | - | NL | - | - |
| BbF | 13.9±0.8 | 92.7 | 6.0 | 78.0±4.2 | 97.5 | 5.4 | 219.4±18.4 | 87.8 | 8.4 | NL | - | - | NL | - | - |
| Bkf | 15.9±0.6 | 106 | 3.7 | 93.2±14.7 | 117 | 16 | 247.1±14.3 | 98.8 | 5.8 | NL | - | - | NL | - | - |
| BaP | 15.6±0.7 | 104 | 4.6 | 91.8±18.6 | 115 | 20 | 245.3±20.4 | 98.1 | 8.3 | NL | - | - | NL | - | - |
| InP | 13.7±1.0 | 91.3 | 7.3 | 64.4±4.0 | 80.5 | 6.2 | 184.9±20.0 | 74.0 | 11 | 2029.6±39.1 | 81.2 | 1.9 | NL | - | - |
| DB(ah)A | 17.0±1.2 | 113 | 7.0 | 107.0±6.2 | 134 | 5.8 | 304.2±21.2 | 122 | 7.0 | NL | - | - | NL | - | - |
| BGP | 14.4±1.8 | 96.0 | 13 | 80.2±3.7 | 100 | 4.6 | 237.3±15.7 | 94.9 | 6.6 | NL | - | - | NL | - | - |

[a] Concentration of internal standards in the water samples: Naph-d8, Ace-d10 and Phe-d10: 1000 pg $mL^{-1}$ Chry-d12, Per-d12: 100 pg $mL^{-1}$; all the concentrations are in pg $mL^{-1}$

[b] NQ: Added concentration is lower than LOQ.

[c] NL: Added concentration is higher than linear range.

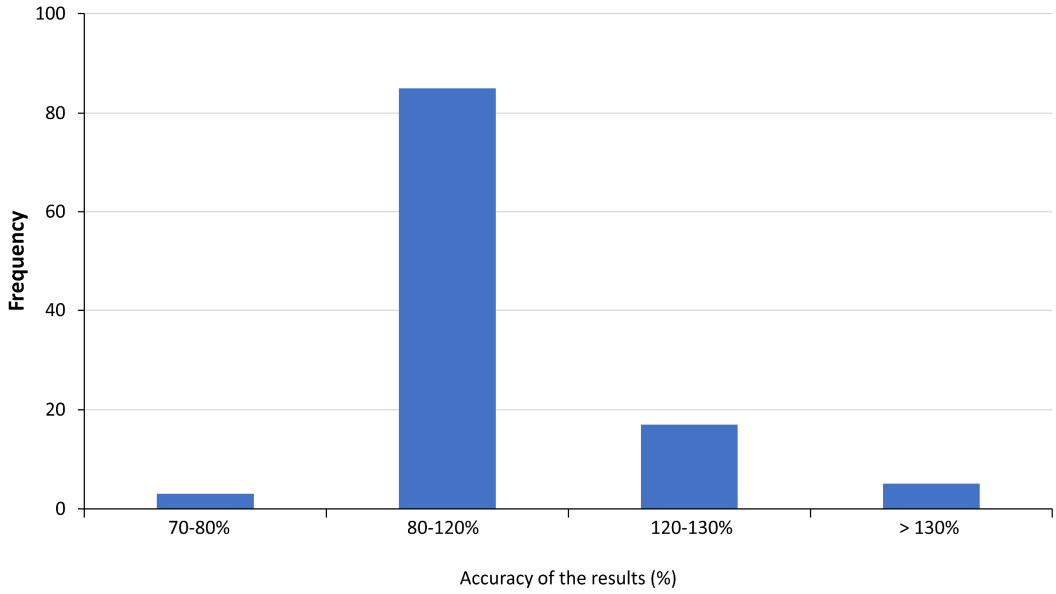


**Fig. 2.10.** Accuracy of the MMIP-DSPE method for analysis PAHs in water samples.

A comparison of the procedure summery and performance of our proposed MMIP-DSPE with previously reported methods using MIP materials is shown in Table 2.11. This method showed desirable LODs for the quantitative analysis of PAHs with small amount of the sorbent and high extraction recovery values, particularly for heavier PAHs, which are of concern at trace levels. Our method is able to perform selective extraction without adding organic modifiers required for efficient adsorption of these analytes [44]. This is mainly due to well dispersion of prepared MMIP particles with uniform and thin coating in water samples. In conventional polymerization, long intervals are required for equilibrium adsorption due to inaccessibility of binding sites [48]. The accessibility of binding sites can be significantly enhanced using RAFT polymerization and thin and homogenous polymeric layer which also helps the creation of selective binding sites. Homogenous RAFT-MMIP also allows for an efficient desorption using a single-step elution with a small volume of solvent instead of multi-steps elution with larger quantities of solvents [47, 48].

**Table 2.11**. Comparison of MMIP-DSPE with other methods for the determination of PAHs.

| Method | Sample pretreatment | Performance | Sample analysis | Ref. |
|---|---|---|---|---|
| **MMIP-DSPE-HPLC-FL** | Sorbent: MMIP particles (20 mg)<br>Sample volume: 35 mL<br>Rebinding media: water-acetonitrile (90:10, v:v)<br>Extraction time: 10 min<br>Desorption: 3×5 mL of acetone | Selectivity:-<br>LOD: 1.3–969 pg $mL^{-1}$<br>Recovery: 46–100% | 16 PAHs in tap water, mineral water, lake water and river water | [44] |
| **MMIP-DSPE-GC-MS** | Sorbent: MMIP particles (5 mg for light PAHs, and 20 mg for heavy PAHs)<br>Sample volume: 20 mL<br>Rebinding media: water+80 µL acetone<br>Extraction time: 15 min<br>Desorption: 2 × 5 mL acetone | Selectivity: Similar extraction efficiency for MIP and NIP, better repeatability of MIP compared to NIP<br>LOD: 30–750 pg $mL^{-1}$<br>Recovery: 75.6–100.6% | 16 PAHs in sea water | [45] |
| **MIP-DSPE-FL** | Sorbent: MIP microspheres (10 mg)<br>Sample volume: 10 mL<br>Rebinding media: water acetonitrile (99:1, v/v)<br>Extraction time: 3 h<br>Desorption: - | Selectivity: adsorption capacity for BaP: MIP: 75.9 µg $g^{-1}$; NIP: 14.8 µg $g^{-1}$<br>LOD: –<br>Recovery: 98% | BaP in sediment | [46] |
| **MIP-DSPE-GC-MS** | Sorbent: bulk-polymerized MIP particles (10 mg)<br>Sample volume: 2 mL<br>Rebinding media: cyclohexane<br>Extraction time: 3 h<br>Desorption solvent: hexane(3 × 1 mL) | Selectivity: Adsorption capacity MIP: 5 mg $g^{-1}$<br>LOD:-<br>Recovery: 100% | - | [47] |
| **MIP-SPE-GC-MS** | Sorbent: Sol-gel MIP particles (150 mg)<br>Sample volume: 30 mL<br>Rebinding media: water<br>Extraction time: -<br>Desorption solvent: DCM/acetic acid (9:1, v/v) (5 ×2 mL) | Selectivity: imprinting factor of 1.50 – 3.12<br>LOD:5.2–12.6–pg $mL^{-1}$<br>Recovery: 93.2% | 16 PAHs in sea water | [48] |
| **Thin film-MIP-GC-MS** | Sorbent: Bulk-polymerized thin films<br>Sample volume: 80 mL<br>Rebinding media: water<br>Extraction time: 2 h<br>Desorption solvent: Ethyl ether (10.0 mL) | Selectivity: relative slope of calibration curves ( $\frac{m_{MIP}}{M_{NIP}}$ ) ~2<br>LOD: 1.5–18 pg $mL^{-1}$<br>Recovery: 28–47% | 4 PAHs in wastewater and sea water | [49] |
| **MMIP-DSPE-APCI-GC-MS/MS** | Sorbent: RAFT-MMIP particles (10 mg)<br>Sample volume: 20 mL<br>Rebinding media: Water<br>Extraction time: 2 min<br>Desorption solvent: hexane (0.5 mL) | Selectivity: Higher efficiency of MIP compared to NIP (MIP/NIP extraction efficiency 1.7–19.4)<br>LOD: 1–100 pg $mL^{-1}$<br>Recovery: 4.5–97% | 16 PAHs in river water and produced water | This work |

### 2.3.8. Determination of PAHs in complex aqueous matrices

To evaluate the applicability of the proposed method, a produced water sample as a complex matrix was analysed using MMIP-DSPE methodology. The sample was treated as described in the experimental section for extraction and quantitation. The sample was spiked with the standards of PAHs in order to perform the standard addition method (Fig. 2.11). As it is shown in Table 2.12, Naph demonstrated the highest concentration in the produced water sample, 360 ng $mL^{-1}$. While the other light PAHs including Ace, Acy, Flu, Phen, Ant have concentrations between 45.62 and 2669.99 pg $mL^{-1}$. The less soluble PAHs including BaA, Chry, BbF, BkF, BaP, InP, DB(ah)A, and BGP were found at the concentration range of 4.49-26.58 pg $mL^{-1}$.

**Table 2.12.** Determination of PAHs in produced water by MMIP-DSPE[a].

| PAHs | Detected amount ± SD (pg $mL^{-1}$) | PAHs | Detected amount ± SD (pg $mL^{-1}$) |
|---|---|---|---|
| Naph | 360121.95 ± 19.00 | BaA | 5.37 ± 0.90 |
| Acy | 69.81 ± 4.28 | Chry | 5.44 ± 0.91 |
| Ace | 860.08 ± 51.12 | BbF | 4.49 ± 1.07 |
| Flu | 2669.99 ± 50.22 | Bkf | 5.62 ± 1.00 |
| Phen | 1189.32 ± 74.81 | BaP | 8.03 ± 1.36 |
| Ant | 45.62 ± 15.14 | InP | 14.38 ± 2.17 |
| Flut | <LOQ | DB(ah)A | 26.58 ± 6.14 |
| Pyr | <LOQ | BGP | 13.42 ± 2.07 |

[a] Naph spiked at 0, 100,000, 200,000, 500,000 and 1,000,000 pg $mL^{-1}$; Acy, Ace, Flu, Phe, Ant, Flut and Pyr spiked at 0, 400, 800, 2,000 and 4,000 pg $mL^{-1}$; BaA, Chry, BbF, BkF, BaP, InP, DB(ah)A and BGP spiked at 0, 50, 100 and 250 pg $mL^{-1}$.

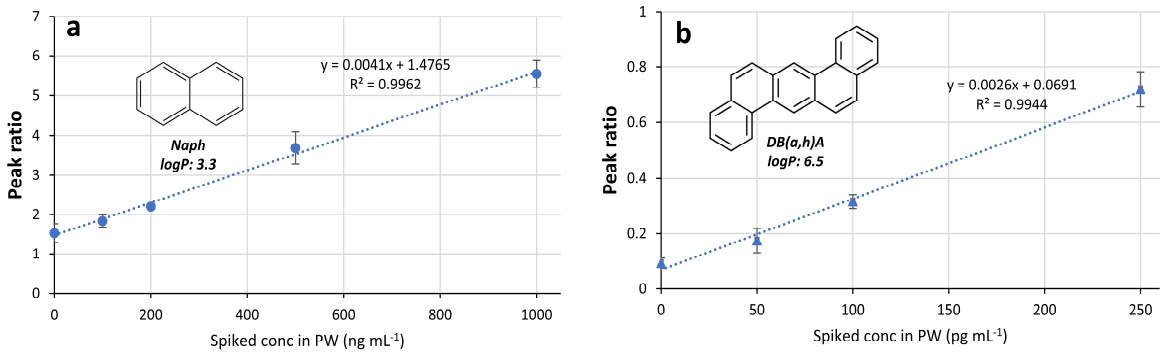


**Fig. 2.11.** Evaluation of the MMIP-DSPE-APCI-GC-MS/MS for determination of PAHs in the produced water a) Naph and b) DB(ah)A.

## 2.4. Conclusion

This work is the report of developing a MMIP-DSPE for simultaneous enrichment and quantitation of the US-EPA priority PAHs in environmental waters. The MMIP was prepared via RAFT polymerization as a controllable mechanism to create homogenous and well-distributed binding sites. After characterization by FT-IR, XRD, and SEM, the MMIP was implemented for extraction of PAHs from water samples. DSPE outweighs the disadvantages of conventional methods for analysis of PAHs, such as using toxic solvents in LLE or clogging SPE columns. Further, using the MMIPs improves the specificity and sensitivity of the analysis by employing a selective sorbent. The template–monomer interactions in the pre-polymerization complex are responsible for generating the selective recognition binding sites according to the size, shape and hydrophobicity of the analytes. The MMIPs are capable of superior adsorption compared to nanoparticles such as $Fe_3O_4$, and $Fe_3O_4$@$SiO_2$, as well as MNIP as a control sorbent. Because of diverse solubility and LogP values of PAHs, a single extraction method for quantitation of this group of analytes is appealing. Hence, during the development of MMIP-DSPE method, a comprehensive

study was conducted to recognize the factors with the greatest impact and optimize these factors. The number of experiments for optimization of extraction and desorption steps was notably shortened, whereas the extracted analytes and analytical response were maximized. An RSM was adopted for optimization of simultaneous extraction of PAHs using CCD and *DF* to observe the interactions between the variables and the response by altering the levels of factors. The feasibility of the optimized method demonstrates the potential advantages of MMIP-DSPE for precise and accurate extraction and analysis of PAHs from water samples. The MMIP-DSPE is a useful tool for analyzing complex environmental water samples over a broad concentration range of PAHs, yielding both the selectivity and sensitivity to be sufficient as a regulatory method.

## 2.5. References

[1] B.K. Behera, A. Das, D.J. Sarkar, P. Weerathunge, P.K. Parida, B.K. Das, P. Thavamani, R. Ramanathan, V. Bansal, Polycyclic Aromatic Hydrocarbons (PAHs) in inland aquatic ecosystems: Perils and remedies through biosensors and bioremediation, Environ. Pollut., 241 (2018) 212-233.

[2] H. Jiang, X. Hu, Y. Li, J. Qi, X. Sun, L. Wang, J. Li, Large-pore ordered mesoporous carbon as solid-phase microextraction coating for analysis of polycyclic aromatic hydrocarbons from aqueous media, Talanta, (2018).

[3] K.H. Kim, S.A. Jahan, E. Kabir, R.J. Brown, A review of airborne polycyclic aromatic hydrocarbons (PAHs) and their human health effects, Environ. Int., 60 (2013) 71-80.

[4] S.K. Bopp, T. Lettieri, Gene regulation in the marine diatom Thalassiosira pseudonana upon exposure to polycyclic aromatic hydrocarbons (PAHs), Gene, 396 (2007) 293-302.

[5] A. Fakhru'l-Razi, A. Pendashteh, L.C. Abdullah, D.R.A. Biak, S.S. Madaeni, Z.Z. Abidin, Review of technologies for oil and gas produced water treatment, J. Hazard. Mater., 170 (2009) 530-551.

[6] R. Yusta-García, M. Orta-Martínez, P. Mayor, C. González-Crespo, A. Rosell-Melé, Water contamination from oil extraction activities in Northern Peruvian Amazonian rivers, Environ. Pollut., 225 (2017) 370-380.

[7] C. Guigue, M. Tedetti, D.H. Dang, J.U. Mullot, C. Garnier, M. Goutx, Remobilization of polycyclic aromatic hydrocarbons and organic matter in seawater during sediment resuspension experiments from a polluted coastal environment: Insights from Toulon Bay (France), Environ. Pollut., 229 (2017) 627-638.

[8] E. Manoli, C. Samara, Polycyclic aromatic hydrocarbons in natural waters: sources, occurrence and analysis, TrAC, Trends Anal. Chem., 18 (1999) 417-428.

[9] V. Fernández-González, E. Concha-Graña, S. Muniategui-Lorenzo, P. López-Mahía, D. Prada-Rodríguez, Solid-phase microextraction–gas chromatographic–tandem mass spectrometric analysis of polycyclic aromatic hydrocarbons: towards the European Union water directive 2006/0129 EC, J. Chromatogr. A, 1176 (2007) 48-56.

[10] D.L. Poster, M.M. Schantz, L.C. Sander, S.A. Wise, Analysis of polycyclic aromatic hydrocarbons (PAHs) in environmental samples: a critical review of gas chromatographic (GC) methods, Anal. Bioanal. Chem., 386 (2006) 859-881.

[11] R. Ferrer, J.L. Beltran, J. Guiteras, Use of cloud point extraction methodology for the determination of PAHs priority pollutants in water samples by high-performance liquid chromatography with fluorescence detection and wavelength programming, Anal. Chim. Acta, 330 (1996) 199-206.

[12] E.P.A. TestMethod, Polynuclear Aromatic Hydrocarbons, Method 610, US Environmental Protection Agency, Environmental Monitoring and Support Laboratory: Cincinnati, OH, (1982).

[13] E. Carasek, L. Morés, J. Merib, Basic principles, recent trends and future directions of microextraction techniques for the analysis of aqueous environmental samples, Trends Environ. Anal, 19 (2018) e00060.

[14] G. Kiss, Z. Varga-Puchony, J. Hlavay, Determination of polycyclic aromatic hydrocarbons in precipitation using solid-phase extraction and column liquid chromatography, J. Chromatogr. A, 725 (1996) 261-272.

[15] R.-a. Doong, S.-m. Chang, Y.-c. Sun, Solid-phase microextraction for determining the distribution of sixteen US Environmental Protection Agency polycyclic aromatic hydrocarbons in water samples, J. Chromatogr. A, 879 (2000) 177-188.

[16] P. Popp, C. Bauer, L. Wennrich, Application of stir bar sorptive extraction in combination with column liquid chromatography for the determination of polycyclic aromatic hydrocarbons in water samples, Anal. Chim. Acta, 436 (2001) 1-9.

[17] M. Rezaee, Y. Assadi, M.-R.M. Hosseini, E. Aghaee, F. Ahmadi, S. Berijani, Determination of organic compounds in water using dispersive liquid–liquid microextraction, J. Chromatogr. A, 1116 (2006) 1-9.

[18] A. Speltini, A. Scalabrini, F. Maraschi, M. Sturini, A. Profumo, Newest applications of molecularly imprinted polymers for extraction of contaminants from environmental and food matrices: A review, Anal. Chim. Acta, 974 (2017) 1-26.

[19] M. Anastassiades, K. Maštovská, S.J. Lehotay, Evaluation of analyte protectants to improve gas chromatographic analysis of pesticides, J. Chromatogr. A, 1015 (2003) 163-184.

[20] V. Pichon, F. Chapuis-Hugon, Role of molecularly imprinted polymers for selective determination of environmental pollutants—a review, Anal. Chim. Acta, 622 (2008) 48-61.

[21] X. Song, S. Xu, L. Chen, Y. Wei, H. Xiong, Recent advances in molecularly imprinted polymers in food analysis, J. Appl. Polym. Sci., 131 (2014).

[22] D. Stevenson, H.F. El-Sharif, S.M. Reddy, Selective extraction of proteins and other macromolecules from biological samples using molecular imprinted polymers, Bioanalysis, 8 (2016) 2255-2263.

[23] J. Wackerlig, R. Schirhagl, Applications of molecularly imprinted polymer nanoparticles and their advances toward industrial use: a review, Anal. Chem., 88 (2015) 250-261.

[24] X.-Q. Mei, X.-P. He, J.-T. Wang, Molecularly imprinted polymer as efficient sorbent of solid-phase extraction for determination of gonyautoxin 1, 4 in seawater followed by high-performance liquid chromatography-fluorescence detection, Anal. Bioanal. Chem., 408 (2016) 5737-5743.

[25] C. Cai, P. Zhang, J. Deng, H. Zhou, J. Cheng, Ultrasensitive determination of highly polar trimethyl phosphate in environmental water by molecularly imprinted polymeric fiber headspace solid-phase microextraction, J. Sep. Sci., 41 (2018) 1104-1111.

[26] N. Sheng, F. Wei, W. Zhan, Z. Cai, S. Du, X. Zhou, F. Li, Q. Hu, Dummy molecularly imprinted polymers as the coating of stir bar for sorptive extraction of bisphenol A in tap water, J. Sep. Sci., 35 (2012) 707-712.

[27] L. Xie, R. Jiang, F. Zhu, H. Liu, G. Ouyang, Application of functionalized magnetic nanoparticles in sample preparation, Anal. Bioanal. Chem., 406 (2014) 377-399.

[28] M. Wierucka, M. Biziuk, Application of magnetic nanoparticles for magnetic solid-phase extraction in preparing biological, environmental and food samples, TrAC, Trends Anal. Chem., 59 (2014) 50-58.

[29] M. Niu, C. Pham-Huy, H. He, Core-shell nanoparticles coated with molecularly imprinted polymers: a review, Microchim. Acta, 183 (2016) 2677-2695.

[30] I. Vasconcelos, C. Fernandes, Magnetic solid phase extraction for determination of drugs in biological matrices, TrAC, Trends Anal. Chem., 89 (2017) 41-52.

[31] S. Boonpangrak, M.J. Whitcombe, V. Prachayasittikul, K. Mosbach, L. Ye, Preparation of molecularly imprinted polymers using nitroxide-mediated living radical polymerization, Biosens. Bioelectron., 22 (2006) 349-354.

[32] X. Hu, Y. Fan, Y. Zhang, G. Dai, Q. Cai, Y. Cao, C. Guo, Molecularly imprinted polymer coated solid-phase microextraction fiber prepared by surface reversible addition–

fragmentation chain transfer polymerization for monitoring of Sudan dyes in chilli tomato sauce and chilli pepper samples, Anal. Chim. Acta, 731 (2012) 40-48.

[33] Y. Fuchs, O. Soppera, K. Haupt, Photopolymerization and photostructuring of molecularly imprinted polymers for sensor applications—A review, Anal. Chim. Acta, 717 (2012) 7-20.

[34] X. Xie, X. Liu, X. Pan, L. Chen, S. Wang, Surface-imprinted magnetic particles for highly selective sulfonamides recognition prepared by reversible addition fragmentation chain transfer polymerization, Anal. Bioanal. Chem., 408 (2016) 963-970.

[35] C.-H. Lu, W.-H. Zhou, B. Han, H.-H. Yang, X. Chen, X.-R. Wang, Surface-imprinted core− shell nanoparticles for sorbent assays, Anal. Chem., 79 (2007) 5457-5461.

[36] H. Zhang, Controlled/“living” radical precipitation polymerization: a versatile polymerization technique for advanced functional polymers, Eur. Polym. J., 49 (2013) 579-600.

[37] E. Abdollahi, M. Abdouss, M. Salami-Kalajahi, A. Mohammadi, Molecular recognition ability of molecularly imprinted polymer nano-and micro-particles by reversible addition-fragmentation chain transfer polymerization, Polymer Reviews, 56 (2016) 557-583.

[38] L. Chang, Y. Li, J. Chu, J. Qi, X. Li, Preparation of core-shell molecularly imprinted polymer via the combination of reversible addition-fragmentation chain transfer polymerization and click reaction, Anal. Chim. Acta, 680 (2010) 65-71.

[39] X. Wu, X. Wang, W. Lu, X. Wang, J. Li, H. You, H. Xiong, L. Chen, Water-compatible temperature and magnetic dual-responsive molecularly imprinted polymers for recognition and extraction of bisphenol A, J. Chromatogr. A, 1435 (2016) 30-38.

[40] Y. Li, X. Li, J. Chu, C. Dong, J. Qi, Y. Yuan, Synthesis of core-shell magnetic molecular imprinted polymer by the surface RAFT polymerization for the fast and selective removal of endocrine disrupting chemicals from aqueous solutions, Environ. Pollut., 158 (2010) 2317-2323.

[41] F. Chen, J. Zhang, M. Wang, J. Kong, Magnetic molecularly imprinted polymers synthesized by surface-initiated reversible addition-fragmentation chain transfer polymerization for the enrichment and determination of synthetic estrogens in aqueous solution, J. Sep. Sci., 38 (2015) 2670-2676.

[42] J. Li, R. Dong, X. Wang, H. Xiong, S. Xu, D. Shen, X. Song, L. Chen, One-pot synthesis of magnetic molecularly imprinted microspheres by RAFT precipitation polymerization for the fast and selective removal of 17β-estradiol, RSC Adv., 5 (2015) 10611-10618.

[43] M. Yang, Y. Zhang, S. Lin, X. Yang, Z. Fan, L. Yang, X. Dong, Preparation of a bifunctional pyrazosulfuron-ethyl imprinted polymer with hydrophilic external layers by reversible addition–fragmentation chain transfer polymerization and its application in the sulfonylurea residue analysis, Talanta, 114 (2013) 143-151.

[44] M. Villar-Navarro, M.J. Martín-Valero, R.M. Fernández-Torres, M. Callejón-Mochón, M.Á. Bello-López, Easy, fast and environmental friendly method for the simultaneous extraction of the 16 EPA PAHs using magnetic molecular imprinted polymers (mag-MIPs), J. Chromatogr. B, 1044 (2017) 63-69.

[45] B. Benedetti, M. Di Carro, E. Magi, Multivariate optimization of an extraction procedure based on magnetic molecular imprinted polymer for the determination of polycyclic aromatic hydrocarbons in sea water, Microchem. J., 145 (2019) 1199-1206.

[46] R.J. Krupadam, B.A. Korde, M. Ashokkumar, S.D. Kolev, Novel molecularly imprinted polymeric microspheres for preconcentration and preservation of polycyclic aromatic hydrocarbons from environmental samples, Anal. Bioanal. Chem., 406 (2014) 5313-5321.

[47] S. Ncube, P. Kunene, N.T. Tavengwa, H. Tutu, H. Richards, E. Cukrowska, L. Chimuka, Synthesis and characterization of a molecularly imprinted polymer for the isolation of the 16 US-EPA priority polycyclic aromatic hydrocarbons (PAHs) in solution, J. Environ. Manage., 199 (2017) 192-200.

[48] X. Song, J. Li, S. Xu, R. Ying, J. Ma, C. Liao, D. Liu, J. Yu, L. Chen, Determination of 16 polycyclic aromatic hydrocarbons in seawater using molecularly imprinted solid-phase extraction coupled with gas chromatography-mass spectrometry, Talanta, 99 (2012) 75-82.

[49] S.N. Egli, E.D. Butler, C.S. Bottaro, Selective extraction of light polycyclic aromatic hydrocarbons in environmental water samples with pseudo-template thin-film molecularly imprinted polymers, Anal. Methods, 7 (2015) 2028-2035.

[50] P. Ruelle, M. Buchmann, H. Nam-Tran, U.W. Kesselring, Enhancement of the solubilities of polycyclic aromatic hydrocarbons by weak hydrogen bonds with water, J. Comput. Aided Mol. Des., 6 (1992) 431-448.

[51] L. Chen, B. Li, Application of magnetic molecularly imprinted polymers in analytical chemistry, Anal. Methods, 4 (2012) 2613-2621.

[52] H.K. Bojes, P.G. Pope, Characterization of EPA's 16 priority pollutant polycyclic aromatic hydrocarbons (PAHs) in tank bottom solids and associated contaminated soils at oil exploration and production sites in Texas, Regul. Toxicol. Pharm., 47 (2007) 288-295.

[53] C. Baggiani, L. Anfossi, P. Baravalle, C. Giovannoli, G. Giraudi, Molecular recognition of polycyclic aromatic hydrocarbons by pyrene-imprinted microspheres, Anal. Bioanal. Chem., 389 (2007) 413-422.

[54] A.B.G. Aghaie, M.R. Hadjmohammadi, Fe3O4@ p-Naphtholbenzein as a novel nano-sorbent for highly effective removal and recovery of Berberine: Response surface methodology for optimization of ultrasound assisted dispersive magnetic solid phase extraction, Talanta, 156 (2016) 18-28.

[55] G.E.P. Box, K.B. Wilson, On the Experimental Attainment of Optimum Conditions, J. R. Stat. Soc. B, 13 (1951) 1-45.

[56] R.H. Myers, D.C. Montgomery, C.M. Anderson-Cook, Response surface methodology: process and product optimization using designed experiments, John Wiley & Sons, 2009.

[57] S.H. Park, H.J. Kim, J.-I. Cho, Optimal central composite designs for fitting second order response surface linear regression models, in: Recent advances in linear models and related areas, Springer, 2008, pp. 323-339.

[58] S. Panchal, A. Asati, G.N.V. Satyanarayana, A. Raghav, J. Ahmad, D.K. Patel, Ionic liquid based microextraction of targeted lipids from serum using UPLC-MS/MS with a chemometric approach: a pilot study, RSC Adv., 6 (2016) 91629-91640.

[59] L.V. Candioti, M.M. De Zan, M.S. Camara, H.C. Goicoechea, Experimental design and multiple response optimization. Using the desirability function in analytical methods development, Talanta, 124 (2014) 123-138.

[60] G. Derringer, R. Suich, Simultaneous optimization of several response variables, J. Qual. Technol., 12 (1980) 214-219.

[61] T. Yang, S. Feng, Y. Lu, C. Yin, J. Wang, Dual-template magnetic molecularly imprinted particles with multi-hollow structure for the detection of dicofol and chlorpyrifos-methyl, J. Sep. Sci., 39 (2016) 2388-2395.

[62] X. Wang, P. Huang, X. Ma, H. Wang, X. Lu, X. Du, Preparation and evaluation of magnetic core-shell mesoporous molecularly imprinted polymers for selective adsorption of tetrabromobisphenol S, Talanta, 166 (2017) 300-305.

[63] Q.-Y. Zhao, H.-T. Zhao, X. Yang, H. Zhang, A.-J. Dong, J. Wang, B. Li, Selective recognition and fast enrichment of anthocyanins by dummy molecularly imprinted magnetic nanoparticles, J. Chromatogr. A, 1572 (2018) 9-19.

[64] D.-D. Wang, D. Gao, W.-J. Xu, F. Li, M.-N. Yin, Q.-F. Fu, Z.-N. Xia, Magnetic molecularly imprinted polymer for the selective extraction of hesperetin from the dried pericarp of Citrus reticulata Blanco, Talanta, 184 (2018) 307-315.

[65] E.D. Morgan, Chemometrics: experimental design, Wiley New York, 1995.

[66] A.M. Joglekar, A.T. May, Product excellence through design of experiments, Cereal Foods World, 32 (1987) 857-868.

[67] O. Water, Edition of the Drinking Water Standards and Health Advisories, EP Agency (ed.), (2012).

[68] C. Directive, 98/83/EC of 3 November 1998 on the quality of water intended for human consumption, ed, E. Union, (1998).

[69] E.U. Parliament, Directive 2008/105/EC of the European Parliament and of the Council of 16 December 2008 on environmental quality standards in the field of water policy, amending and subsequently repealing, Official Journal of the European Union, L, 348 (2008) 84-97.

# Chapter 3: High throughput direct analysis of water using thin film microextraction solvothermal headspace desorption (TFME-ST-HD)

A. Azizi, F. Shahhoseini, A. Modir-Rousta, C.S. Bottaro. “High throughput direct analysis of water using solvothermal headspace desorption with porous thin films.” Anal. Chim. Acta 1087 (2019) 51-61.

## 3.1. Introduction

Water contamination has become a serious concern during the last decades due to the constant release of the organic contaminants into the environment. Because of detrimental impacts of these pollutants, their presence in the water has been limited by regulatory agencies such as the United States Environmental Protection Agency (US-EPA) [1], European Union (EU) [2], and the Government of Canada [3]. Polycyclic aromatic hydrocarbons (PAHs) are considered persistent organic pollutants (POPs) due to their toxicity and low reactivity [4]. PAHs have carcinogenic, mutagenic, and teratogenic properties that threaten human health and the environment [5]. These organic contaminants can be released into the environment by natural sources such as oil seeps, forest fires, and volcanic eruptions or anthropogenic sources such as oil spills, leakage of petroleum products as well as incomplete combustion of fossil fuels [6]. Produced water, which is the main waste discharged during oil and gas extraction and contains a mixture of inorganic and organic compounds, is a source of entry for PAHs into water [7]. This wastewater includes natural water found in reservoirs, and the water injected into the reservoirs to enhance the oil and gas recovery [8]. Monitoring of this complex matrix is important to assess the level of PAHs, and as an indication of the amount of oil in water before discharging into the environment [9]. To measure and track these chemical pollutants in complex environmental samples, sample preparation methods to clean-up the samples and isolation and preconcentration of analytes are essential. Liquid-liquid extraction (LLE) [10] and solid phase extraction (SPE) [11] are well-validated techniques that are frequently employed before instrumental analysis. These sample preparation steps, which are time-

consuming and can be expensive, limit the throughput and increase analytical costs. Recent innovations in sample preparation have focused on microextraction techniques capable of replacing the traditional extraction methods [12-14].

Solid phase microextraction (SPME) as one of the first miniaturized and green sample preparation techniques has gained considerable interest due to its potential for automation and portability [15]. This technique has been employed for sampling and extraction of analytes with a wide range of physicochemical properties in food, biofluid and environmental samples [16]. Bruheim *et al.* [17] proposed thin film microextraction (TFME) by employing thin sheets of PDMS with a large surface area-to-volume ratio which improves the extraction rates of analytes. TFME enhances the adsorption efficiency and sensitivity of the analysis for short extraction intervals. PDMS sheets can also be impregnated with sorptive particles to improve the distribution coefficient of analytes between the sample and extraction phase [18]. This method has been applied for extraction of pesticides [19, 20] and volatile organic compounds [21] from water samples using small sample volumes and achieving the accuracy required by regulatory agencies [19]. This green alternative to conventional extraction methods is amenable to automation [22] and use for on-site sampling [23]. One drawback of PDMS films is bleeding of siloxanes in thermal desorption modes and instability of the films at high agitation rates or during direct exposure in harsh field conditions, which necessitates preparation of thin films on a stabilizing substrate [24]. Polyacrylonitrile (PAN) has been used as an alternative to PDMS as a polymeric binder to immobilize sorptive particles typically used in SPE, such as $C_{18}$ [25], divinylbenzene [22], and hydrophilic-lipophilic balance [26] particles. These PAN-based thin films are not compatible with thermal desorption and only suitable for solvent

desorption in liquid chromatography analyses [27]. Other innovative uses of natural materials for TFME include diatomaceous earth [28] and cork [29]. Despite considerable benefits of TFME for extraction of targeted compounds, preparation of the coatings is time-consuming and usually needs multiple preparation and curing steps.

For rapid analysis of organic pollutants, which are preconcentrated by TFME, thermal desorption is frequently employed to perform semi-automated and high throughput analysis by gas chromatography (GC) [30]. Thus, time-consuming solvent immersion and solvent evaporation steps can be eliminated; decreasing the sample manipulation steps and improving the repeatability. For accurate and precise analyte measurement when reusing SPME devices, exhaustive cleaning protocols that completely remove residual analytes are vital to avoid carry-over effects in successive extractions [31]. This makes development of single-use thin films with simple, fast, and cost-effective preparation and treatment steps attractive for high throughput analysis of pollutants.

In this work, single-use TFME devices are used to extract PAHs from water, followed by analysis using GC equipped with a flame ionization detector (FID). The films for TFME were prepared according to the procedure developed previously in our group for the fabrication of polymeric films [32] with UV curing on solid substrates [33]. These films, which are stable in organic solvents and saline matrices, are suitable for extraction with high agitation rates and direct analysis [34]. The desorption technique used in the literature for direct analysis of target analytes from thin films employs a thermal desorption unit which can contain these large-sized extraction devices [35-37]. However, this injection process needs continuous heating of the sample and a cryofocusing step to trap analytes before introduction into GC column [38]. A headspace (HS) interface with GC is a

convenient alternative system for thermal desorption. HS-GC is routinely used for environmental analysis of volatiles from water [39] and soil [40] and can be applied for desorption of molecules of interest from solid sorbents that have been used to extract targets directly from water samples [41, 42]. We have found that addition of a small volume of organic solvent assists with thermal desorption process, particularly for high boiling points PAHs. In solvothermal headspace desorption (ST-HD), the evaporated analytes in the gas phase are introduced into a GC column using solvent trapping instead of cryogenic trapping in the thermal desorption unit. The effects of operational factors influencing efficiency of desorption and the possible mechanism responsible for ST-HD are investigated. Additionally, the adsorption behavior of analytes to these porous films is assessed based on agitation rates, extraction time, and salt content. The prepared thin films show low bleed in ST-HS-GC-FID, which is a common and affordable detection system, and can provide sub-ppb detection limits for quantifying PAHs in complex samples. This is the first report of ST-HS-GC, with the additional benefit of employing single-use TFME devices requiring no preconditioning or time-consuming sample preparation steps.

## 3.2. Experimental

### 3.2.1. Reagents and Chemicals

All PAH standards: naphthalene (Naph, 99%); acenaphthylene (Acy, 99%); acenaphthene (Ace, 99%); fluorene (Flu, 98%); phenanthrene (Phe, ≥99.5 %); anthracene (Ant, ≥99.0% GC); fluoranthene (Flut, 98.7 % GC); and pyrene (Pyr, ≥99.0% GC); and deuterated PAHs: naphthalene-$d_8$ (Naph-d8, 99 atom % D); acenaphthene-$d_{10}$ (Ace-d10, 99

atom % D); and phenanthrene-$d_{10}$ (Phe-d10, 98% CP), were purchased from Sigma Aldrich (Oakville, ON, Canada). Chemical and physical properties of the PAHs are provided in detail in Table 3.1. Acetonitrile, hexane, and toluene (Optima grade) were obtained from Fisher Scientific (Whitby, ON, Canada) and cyclohexane (GC grade) was obtained from Sigma Aldrich (Oakville, ON, Canada). Reagents used for preparation of the films (the functional monomer 4-vinyl pyridine (4-VP, 95%), crosslinker ethylene glycol dimethacrylate (EGDMA, 98%), photoinitiator 2,2-dimethoxy-2-phenylacetophenone (DMPA, 99%), and porogen 1-octanol (>99%) were purchased from Sigma Aldrich (Oakville, ON, Canada). Sodium chloride was from ACP chemicals (Montreal, QC, Canada). To prepare PDMS films, Sylgard 184® including PDMS elastomer base and curing agent was purchased from Dow Corning (Midland, MI, USA). Frosted microscope slides (25 × 75 mm) for use as the film substrate were purchased from Fisher Scientific (Whitby, ON, Canada). Cover Glasses (18 $mm^2$) were obtained from VWR (Mississauga, ON, Canada). Ultrapure water (18.2 MΩ $cm^{-1}$) was produced by an SYBRON/Barnstead N water purification system (Boston, MA, USA). For method development and evaluation steps, individual stock solutions of PAHs were prepared in acetonitrile at 1000 mg $L^{-1}$. Working solutions of 8 PAHs were prepared in acetonitrile by appropriate dilution of the stock mixture of 8 PAHs at 100 mg $L^{-1}$; these were used for method development as well as validation studies. All the solutions were stored at 4 °C in a refrigerator until use. Aliquots of the mixtures described above were spiked into water samples to obtain required concentrations for each experiment.

**Table 3.1.** Physical and chemical properties of selected PAHs [43, 44].

| Compounds | Structure (# of rings) | MW (g $mol^{-1}$) | Solubility (ng $mL^{-1}$) | Vapor pressure (mm Hg) | LogP | Boiling point ($^0C$) |
|---|---|---|---|---|---|---|
| Naph | 2 | 128.17 | $3.1x10^4$ | $8.89x\ 10^{-2}$ | 3.30 | 218 |
| Acy | 3 | 152.20 | $1.61\ x10^4$ | $2.90\ x\ 10^{-2}$ | 3.94 | 280 |
| Ace | 3 | 154.21 | 3800 | $3.75\ x\ 10^{-3}$ | 3.92 | 279 |
| Flu | 3 | 166.22 | 1900 | $3.24\ x\ 10^{-3}$ | 4.18 | 294 |
| Phen | 3 | 178.23 | 1100 | $6.80\ x\ 10^{-4}$ | 4.46 | 338 |
| Ant | 3 | 178.23 | 45 | $2.55\ x\ 10^{-5}$ | 4.45 | 341 |
| Flut | 4 | 202.26 | 260 | $8.13\ x\ 10^{-6}$ | 5.16 | 384 |
| Pyr | 4 | 202.26 | 132 | $4.25\ x\ 10^{-6}$ | 4.88 | 394 |

### 3.2.2. Instrumentation

Analyses were conducted using an Agilent 7890B GC system equipped with an FID, and Agilent 7697A headspace sampler with 0.25 mL sample loop (Agilent Technologies, USA). Chromatographic separation was performed on an HP-5MS UI column (30 m×0.250 mm×0.25 μm) (Agilent Technologies, USA). The carrier gas used was ultra-high purity nitrogen (5.0 UHP) (Praxair, Canada) at a flow rate of 1.0 mL $min^{-1}$. The oven temperature programming was as follows: initial temperature 80 °C hold 2 mins; then ramp at 25 °C $min^{-1}$ to 220 °C; ramp to 240 °C at 10 °C $min^{-1}$; then to 250 °C by 3 °C $min^{-1}$. A post-run program at 300 °C held for 2 mins was applied to ensure that no residual of the injections remained on the column. The total run time for GC was 15 mins. The injector (equipped with a liner for headspace injection) was maintained at 280 °C in pulsed-splitless mode at 40 psi for 1.25 mins to ensure maximum transfer of analytes onto the GC

column. The FID temperature was maintained at 320 °C, with flow rates 400 mL $min^{-1}$ of Ultra Zero Air (Praxair, Canada), 25 mL $min^{-1}$ of 5.0 UHP nitrogen, and 30 mL $min^{-1}$ of hydrogen (5.0 UHP) (Praxair, Canada).

Instrumental method calibration curves were constructed from data using mixed standard solutions prepared from stock solutions of individual PAHs (1000 mg $L^{-1}$ in cyclohexane) and analyzed using the ST-HS-GC method as follows: a 60-µL aliquot of PAH standard solution (from 0.5 to 50 mg $L^{-1}$) in cyclohexane is dispensed onto an untreated single-use thin film inserted in a headspace vial and analyzed using the ST-HS-GC method. Each concentration was measured in triplicate, with new films used for each. This data was used to determine the extraction efficiency of PAHs from water samples.

The reusability and carry-over for the films were assessed using GC with mass spectrometry (GC-MS). For GC-MS analysis, an Agilent 7890B GC instrument (Agilent Technologies, CA, U.S.A.) coupled to Waters Xevo TQ-S equipped with an atmospheric pressure chemical ionization source (APCI) was utilized. Injections performed using a 7693A Automatic Liquid Sampler (Agilent Technologies, CA, U.S.A.). One-µL injections were made using pulsed splitless mode (25 psi, 1 min) with a liner temperature of 280 °C. A DB-5MS column (30 m × 0.250 mm, 0.25 µm film thickness) purchased from Agilent Technologies was used for the chromatographic separation. The GC separation using ultra-high purity helium (5.0 UHP) (Praxair, Canada) as carrier gas flowing at 1.2 mL $min^{-1}$ was conducted using the same temperature program as the GC-FID method. The temperature of the ion source was 150 °C with $N_2$ as auxiliary gas and cone gas, with flow rates of 200 and 190 L $hr^{-1}$, respectively. The corona pin was operated in constant current mode at 2 µA.

MRM transitions, cone voltages and collision energy used for all compounds are included in Table 3.2.

**Table 3.2.** Summary of tandem mass spectrometry parameters using APCI-GC-MS/MS.

| Compound | Precursor ion (m/z) | Product ion (m/z) | Cone (V) | Collision Energy (eV) |
|---|---|---|---|---|
| Naph | 128 | 102 | 55 | 20 |
| Acy | 152 | 151 | 65 | 28 |
| Ace-d10 | 164 | 162 | 40 | 20 |
| Ace | 154 | 153 | 40 | 20 |
| Flu | 166 | 165 | 35 | 20 |
| Phe-d10 | 188 | 186 | 65 | 25 |
| Phe | 178 | 177 | 65 | 25 |
| Ant | 178 | 177 | 65 | 25 |
| Flut | 202 | 201 | 70 | 35 |
| Pyr | 202 | 201 | 70 | 35 |

Morphologies of the films were investigated through micrographs of gold-sputtered thin films taken on a Quanta 650 FEG (field emission gun) SEM (Field Electron and Ion Company, OR, USA). The instrument was operated at a constant 5.0 kV and an Everhart-Thornley electron detector.

### 3.2.3. Preparation of porous thin films

Glass microscope slides with frosted (superficially roughened) end segments were used as substrates to prepare the porous film extraction devices. Physical stability of the sorbent is crucial for TFME devices to perform extractions in a highly turbulent sampling environment. For the preparation of thin film coating, glass was the best candidate as the

substrate, given that it is relatively inert, and it can easily withstand high agitation rates. The glass slides are cut to 11 mm (width) x 30 mm to allow for insertion into both standard sample vials and headspace vials. Cut slides were cleaned with detergent and water, then methanol, and dried in an oven at 50 °C for 30 mins. The prepolymer solution used to form the porous film coating was prepared with 21.25 µL of toluene, 58 µL 4-VP, 755 µL EDGMA, 16 mg DMPA, and 1000 µL 1-octanol thoroughly vortex mixed in a 4-mL vial and degassed in an ultrasonic bath for 5 minutes to remove dissolved oxygen that can interfere with radical polymerization. In a simple drop-casting method, an 8.0-µL portion of the prepolymer solution was pipetted onto the frosted glass surface and evenly spread by carefully applying the cover slide. The thin layer of solution, which is sandwiched between the two glass layers, was polymerized under UV light (254 nm) for 30 mins (Fig. 3.1). Following polymerization, the cover slides were removed using a sharp blade. The prepared thin films were then washed with methanol at 1000 rpm for 30 mins to remove unreacted components, then rinsed with methanol, dried and stored at room temperature until use. This simple approach to film fabrication has advantages over conventional methods to prepare TFME devices. Typical methods involve dispersion of sorptive particles in PDMS or PAN as binding agents in time-consuming preparation steps and thermal treatments, for example, heating the films for up to 200 °C for 16 h to remove interfering components [24].

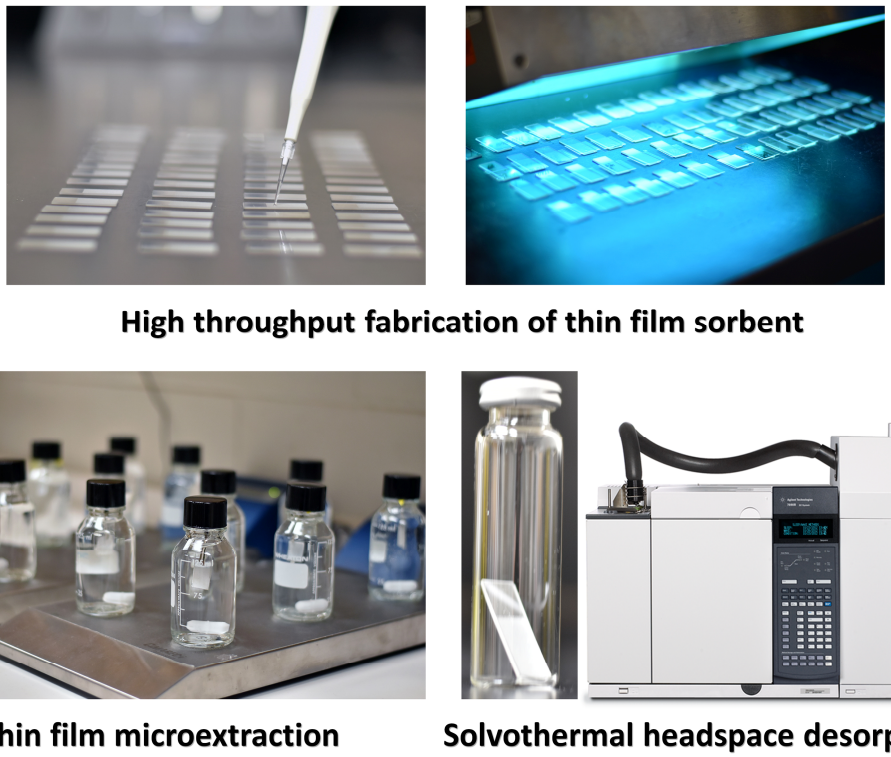


**Fig. 3.1.** Experimental set-up for high throughput fabrication, TFME, and ST-HS-GC-FID for the analysis of water samples.

### 3.2.4. High throughput TFME-ST-HD for PAHs analysis

For optimization of the ST-HD desorption process, studies of inter-device variability, reusability and durability, PAHs were loaded to the films from 20-mL of aqueous PAH solutions (18 samples simultaneously) agitated at 1400 rpm for 2 h (at room temperature) on a multi-position magnetic stirrer. For all other studies where higher sensitivity is required, PAH extraction studies were carried out using 140 mL of water agitated at 1100 rpm. The thin films were removed from the water and rinsed with 1-2 mL of ultrapure water to remove interfering substances, which is needed in the analysis of real

samples, and dried using a Kimwipe to remove residual water prior to transfer into 20 mL headspace vials.

The optimization of the ST-HD process and details regarding the proposed mechanisms of action are presented in detail in the Results and Discussion section. The final optimal method is as follows. Immediately prior to HS analysis, 60 µL of cyclohexane as the ST solvent was pipetted onto the surface of thin films and the vials were quickly sealed with crimp-caps lined with PTFE-silicone septum and transferred in the 96-position autosampler. For desorption, the headspace oven was maintained at 220 °C for 5 mins. After equilibrium, 1 mL of the headspace volume was flushed through the 0.250 mL sample loop and injected into the GC for analysis (Fig. 3.1). To avoid condensation of analytes during the ST-HD process, the temperature of the loop and transfer line were kept at 10 and 20 °C higher, respectively than the oven temperature.

### 3.2.5. Environmental samples

Seawater was collected from St. John's Harbor, NL, Canada. The sample was stored at 4 °C before extraction. PAHs were not detectable in the harbor sample, so this water was spiked to test the validity of using ultrapure water with salt for matrix-matching seawater. A produced water sample was received from an offshore site in sealed bottles and kept at 4 °C until use. The sealed sample was homogenized under low agitation at 25 °C for 12 hours before analysis. No other special sample handling or filtration was required prior to extraction of PAHs from the produced water and harbor water samples.

## 3.3. Results and discussion

### 3.3.1. ST-HD as a novel desorption technique for direct analysis

*3.3.1.1. Optimization of ST-HD Conditions*

Use of a headspace sampler as the desorption interface and sample introduction method can reduce sample handling steps in the lab and enhance method repeatability. In this sampler, a portion of sample (1 out of 80 in the current study) is injected into GC system. Although ST-HD compromises the sensitivity, this desorption technique improves the throughput and sample handling using a convenient inlet for GC. For quantitative transfer of adsorbed analytes from the thin films to the GC column, several key ST-HD parameters must be optimized, particularly type and volume of the desorption solvent, oven temperature, and equilibrium time.

Addition of solvent to the headspace vial can facilitate the desorption of analytes and increase sensitivity due to the increased diffusion rate of analytes from the film to the gas phase. The efficiency of this process is dependent on the nature of the solvent, its ratio to the solid phase and sample vial volume. As PAHs are mainly adsorbed through hydrophobic interactions, non-polar solvents including toluene, cyclohexane, and hexane were tested to aid in the desorption process. As shown in Fig. 3.2a, cyclohexane provided the highest signal intensity and repeatability. As well, chromatographic behavior was better, yielding more symmetric peaks. We also found that increasing the solvent volume enhances the desorption and sensitivity up to the point that the vapor pressure inside the vial exceeds the system limit, which can lead to venting and loss of sample. Thus, varied volumes of cyclohexane (20, 40, 60, 80, and 120 µL) were examined (shown in Fig. 3.2b).

Increasing the solvent volume from 20 to 60 µL, increased the signal intensity for PAHs. For volumes exceeding 60 µL, the response for the more volatile PAHs declined significantly. Therefore, 60 µL was selected as the optimum volume of cyclohexane for addition to the headspace vials.

It was also found that increasing the headspace oven temperature enhances the desorption of analytes from the thin films. Temperatures from 140 to 260 °C were tested to assess desorption efficiency and extent of background noise from the polymeric sorbent. There were dramatic improvements in signal intensity from 140 to 220 °C (Fig. 3.2c). However, there was undesirable background noise (data not shown) in chromatograms for 240 and 260°C related to the decomposition of the polymer.

The desorption process is time-dependent, thus optimal equilibration time in the headspace oven was assessed over a range of times (1, 2, 5, 10, 15 mins). The resultant peak intensities (Fig. 3.2d) demonstrated that lighter compounds such as Naph and Acy reached equilibrium within 2 minutes while high-boiling points PAHs such as Flut and Pyr reached equilibrium in 5 mins. Thus, 5 min equilibrium at 220 °C was used as an optimum headspace condition for further optimization and validation studies.

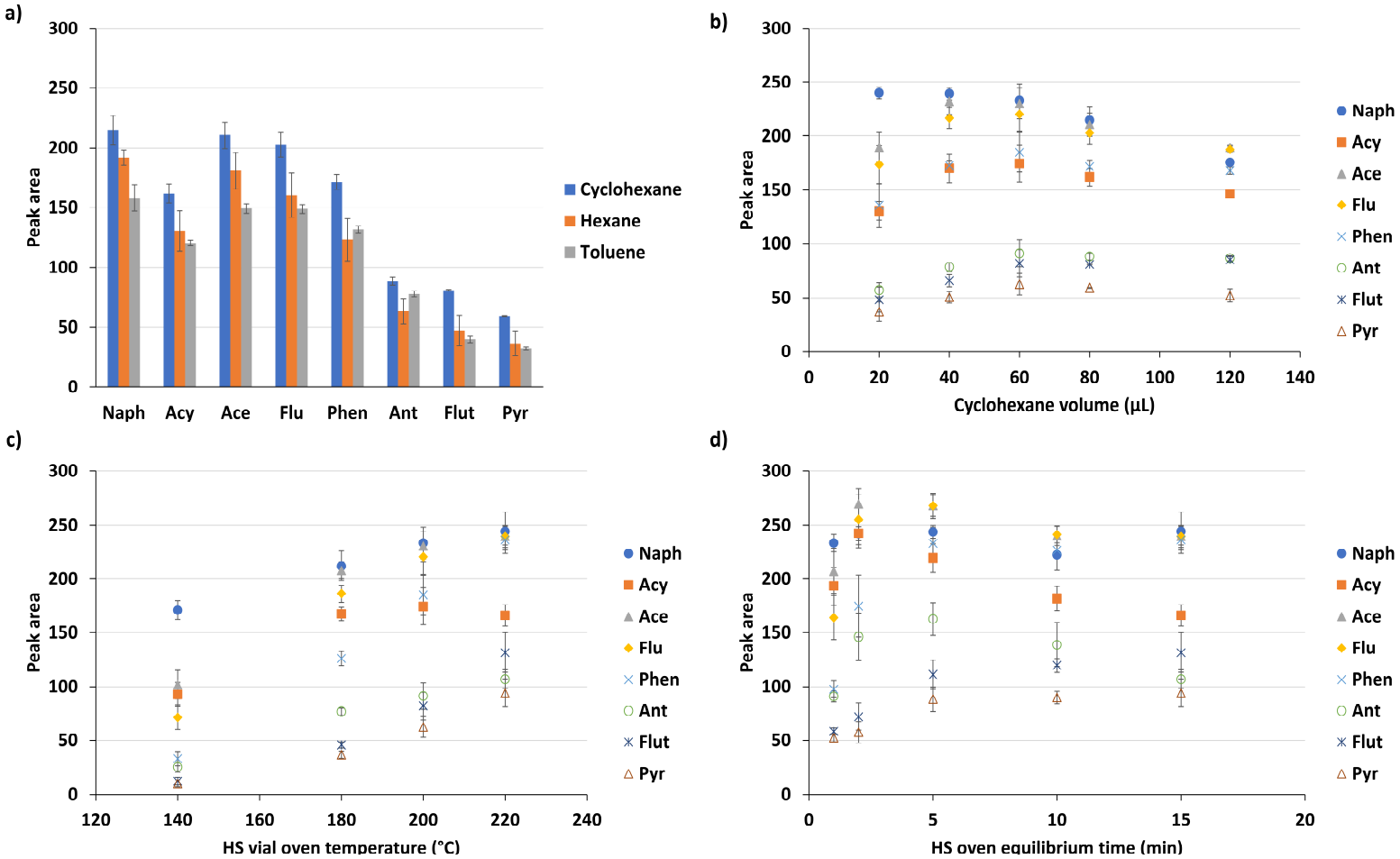


**Fig. 3.2.** Effect of parameters on ST-HD efficiency a) type of desorption solvent (80 µL) equilibrated at 200 °C for 15 min in headspace oven; b) volume of cyclohexane as desorption solvent equilibrated at 200 °C for 15 min in headspace oven; c) oven temperature using 60 µL cyclohexane equilibrated for 15 min in headspace oven; d) equilibrium time in the headspace oven using 60 µL cyclohexane at 220 °C; Sample: 20 mL sample solution of PAHs ( Naph, Acy, Ace, Flu, Phen, Ant, Flut, and Pyr) at 50 ng $mL^{-1}$; Extraction at 1400 rpm for 2 h.

*3.3.1.2. Mechanism of ST-HD*

A headspace sampler is typically used for the analysis of volatile compounds in solids and liquids [45]; this work extends the apparatus to desorption of analytes from thin films. The main advantage over traditional thermal desorption is that heating and desorption occurs in a closed system (i.e., sealed vial). Thus, equilibration with headspace occurs off-line prior to injection, which allows for adding reagents (e.g., solvents) to aid in the desorption process. Specifically, the use of solvent reduces the temperature needed for efficient desorption and, consequently, minimizes noise associated with polymer decomposition. However, the method relies on optimization of several parameters that should be guided by an understanding of the mechanism of action.

The effect of depositing the solvent directly to the polymer surface was compared to adding it to the bottom of the vial; with no difference in signal enhancement found. This might lead to a conclusion that the ST-HD mechanism is based on the presence of the solvent in the gas phase. However, we also observed that regardless of where the solvent was put, it would volatilize and condense on the polymer (the polymer turned from opaque to semi-transparent). We conclude that this wetting mechanism is driven by the relative hydrophobicity of the polymer surface, which favors the formation of a microlayer of solvent on the polymer surface over elevated gas-phase levels.

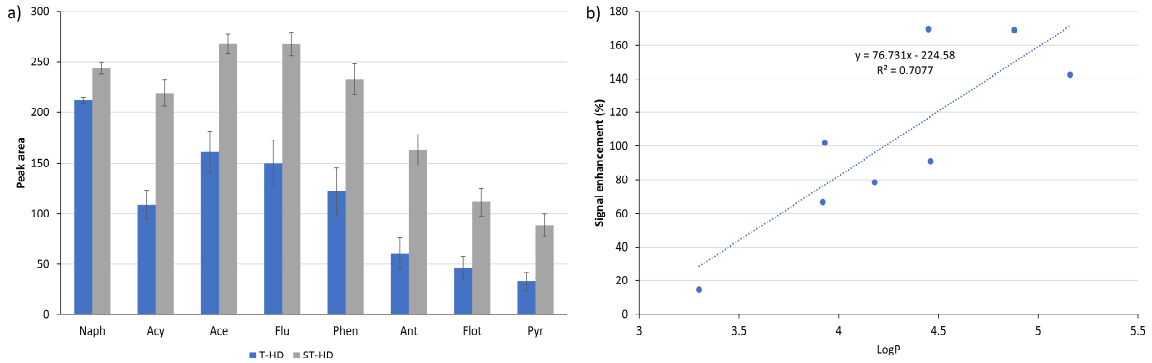


**Fig. 3.3.** Comparison of ST-HD and dry thermal desorption of PAHs, Sample: 20 mL sample solution of PAHs (Naph, Acy, Ace, Flu, Phen, Ant, Flut, and Pyr) at 50 ng $mL^{-1}$; Extraction at 1400 rpm for 2 h; Desorption: 60 µL cyclohexane, equilibrated at 220 °C for 5 min in the headspace oven.

In all cases, the addition of the solvent leads to improvements in sensitivity over simple thermal desorption (Fig. 3.3a). It is likely that this is, in part, a result of the extraction of the hydrophobic analytes into the layer of solvent on the polymer surface. Once extracted from the polymer surface, the PAHs can diffuse more easily into the gas phase (Fig 3.3a); this transfer into the gas phase is also aided by the evaporation of the solvent, which is promoted by heating. The data suggests that the energy required for the analytes to be first partition into solvent and then into the gas phase is lower than the energy required for desorption directly from the solid to the gas phase. A plot of the signal enhancement (ST-HD relative to dry-HD) versus LogP values (Fig 3.3b) shows that the improvement in desorption is correlated to hydrophobicity. This is better explained by the role of the solvent in overcoming the negative impact of increasing molecular weight with decreased vapor pressure. Fig. 3.4 shows the signals associated with headspace introduction of PAH standards in cyclohexane. Though the operational temperatures are much below the boiling points of most of the analytes (Table 3.1), the presence of the cyclohexane has a moderating

effect on the intermolecular forces that dictate the phase behavior in this mixed system, improving the volatilization of all PAHs heavier than naphthalene. When the same amount of standard solution is deposited on the film, the PAHs partition into the polymer and the gas phase composition reflects a reduced concentration of heavier PAHs in the solvent phase. This partitioning can be improved by addition of solvent to overcome the forces holding the PAHs.

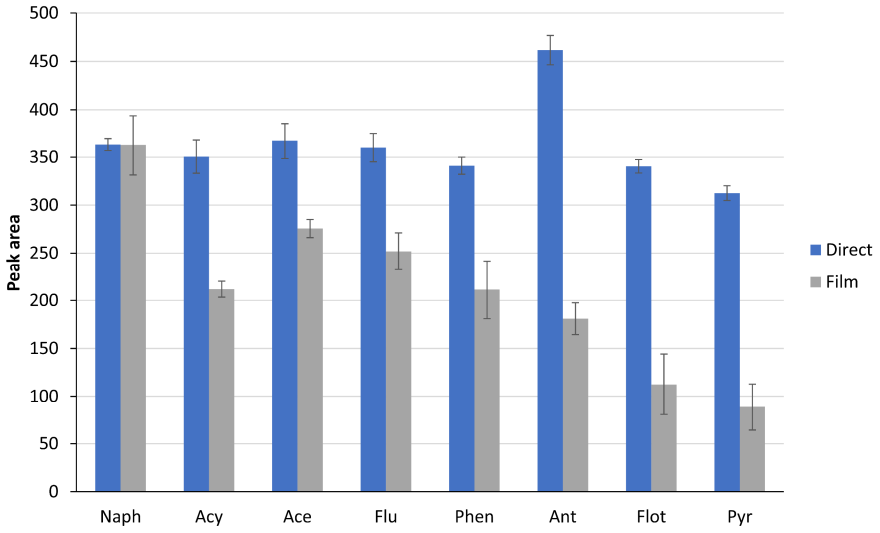


**Fig. 3.4.** Comparison of signal intensity of PAHs on headspace desorption with and without the presence of a thin film. (60 µL of PAHs standard solution in cyclohexane; 10 mg $L^{-1}$); Desorption: equilibrated at 220 °C for 5 min at headspace oven.

In headspace desorption, solvent addition has a greater signal enhancement effect for hydrophobic compounds. For these analytes, partitioning into the solvent is a key to improve their volatility. Increasing the volume of cyclohexane up to 60 µL improves the signal for all analytes (Fig. 3.2b), with more pronounced effects for more hydrophobic PAHs such as Pyr and Flut. This lends more support to the theory that the mechanism of ST-HD is based on the ability of the solvent to desorb the analytes from the sorbent. Therefore, increased solvent volume leads to a more favorable phase ratio for desorption

from the solid film into the solvent [46]. In addition to higher sensitivity, solvent addition also increases the repeatability of the analysis and improves the chromatographic attributes of analyte peaks.

*3.3.1.3. Calibration of ST-HD-GC-FID*

For all analytical techniques, the extent of the linear range and instrument sensitivity must be assessed prior to quantitative method development and validation. The use of a headspace sampler rather than direct injection to introduce extracted analytes into the GC adds a level of complexity to the sample introduction system, with only a portion of the headspace volume is delivered to the GC column. Solvent polarity and volatility, and desorption conditions, including residence time and equilibration temperature, contribute to the sensitivity and linearity of the instrumental method and can have a profound effect on analysis. Consequently, analyte calibration curves were obtained by depositing known quantities of PAH standards onto the films and performing headspace desorption as we have described, replicating the process for analyzing unknown masses of analytes adsorbed to the film through extraction using TFME. This allows us to more accurately calculate extracted mass and total recovery of analytes extracted from water samples. It is illustrated in Fig. 3.5 that the response of ST-HD-GC-FID has a good correlation with the concentration of PAHs (0.1-50 mg $L^{-1}$) with $R^2$ between 0.9985 and 0.9999.

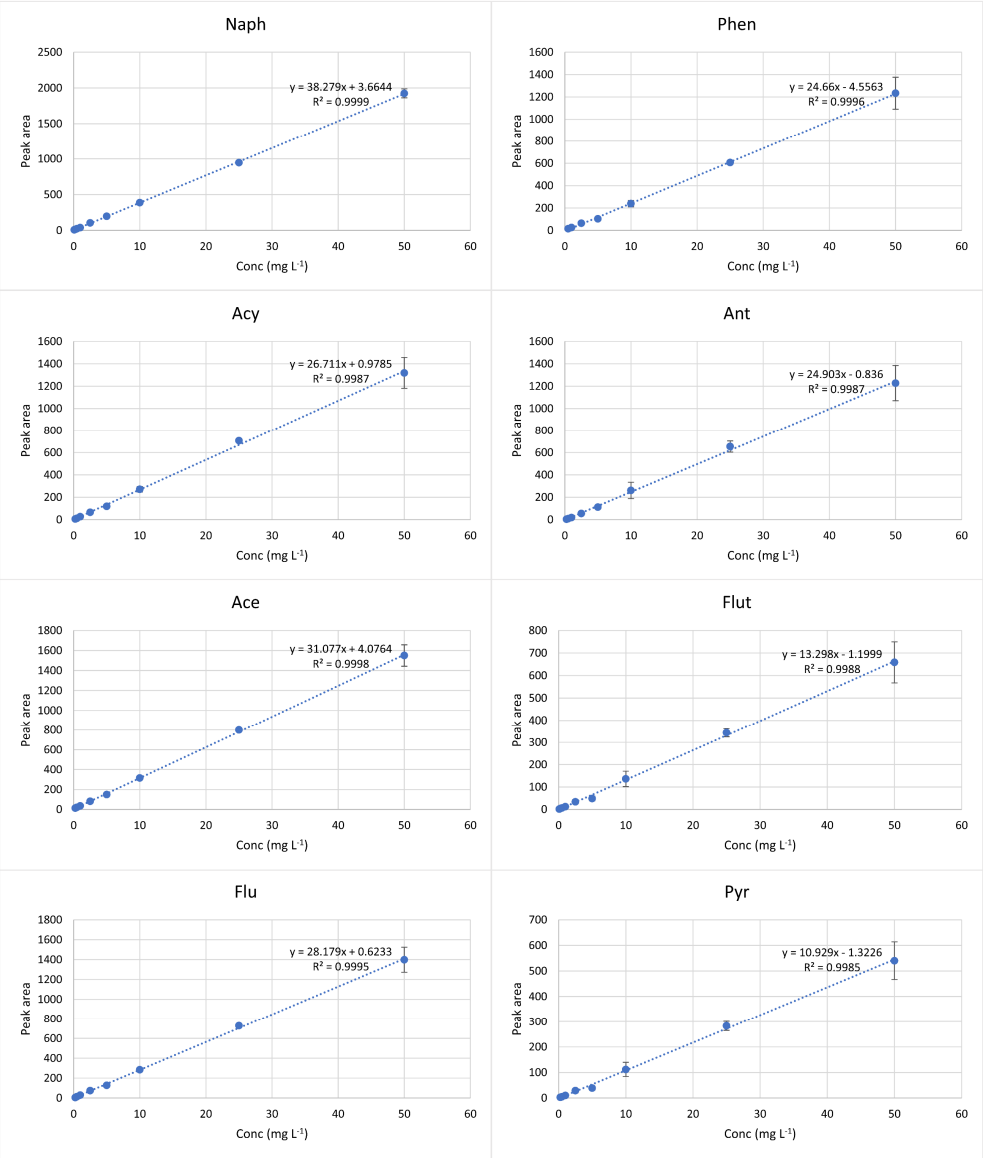


**Fig. 3.5.** Calibration curves for PAHs using ST-HD-GC-FID (60 µL of PAHs standard solution in cyclohexane deposited onto films in HS vials); Desorption: equilibrated at 220 °C for 5 min at headspace oven.

To assess the effect of the film on the headspace behavior, a comparative study was performed on standard solutions in headspace vials with no thin film. As can be seen in Fig. 3.4, the signal intensities of the standards decreased when the analytes were desorbed from the films. This decrease is most likely due to the affinity of the heavier PAHs for the

more hydrophobic film surface, where partitioning into the gas phase is dictated by both the volatility of analyte and the chemistry of the film. This observation also supports the proposed mechanism for partitioning of analytes between the sorbent and the gas phase, particularly since the desorption occurs well below the boiling point of the analytes.

### 3.3.2. Optimization of TFME

There are many factors that can be varied to improve the extraction efficiency of analytes from water into porous thin films. Here, agitation rate, extraction time and salinity are presented. Agitation rate and extraction time were chosen for optimization because they are frequently studied in SPME methods, they are easy to vary, and they usually have a significant impact on the experimental results. Salinity is also considered because of the salt effect and the potential range of salinities seen for environmental water samples.

#### *3.3.2.1. Agitation rate*

Agitation of the sample solution is crucial in TFME since higher agitation rates replenish analytes from the bulk solution to the film. As a result, rapid agitation shortens equilibrium time for analyte partitioning and increases the amount of analytes extracted under non-equilibrium conditions [47]. Agitation rates were controlled using a magnetic stir bar on a multi-position stirring plate. The agitation rates ranged from 200 to 1400 rpm for 20 mL and 600 to 1100 rpm for 140 mL. All extraction efficiencies were highest at the highest stirring speeds (Fig. 3.6 shows the effects on percent recovery for 20 mL and 140 mL samples).

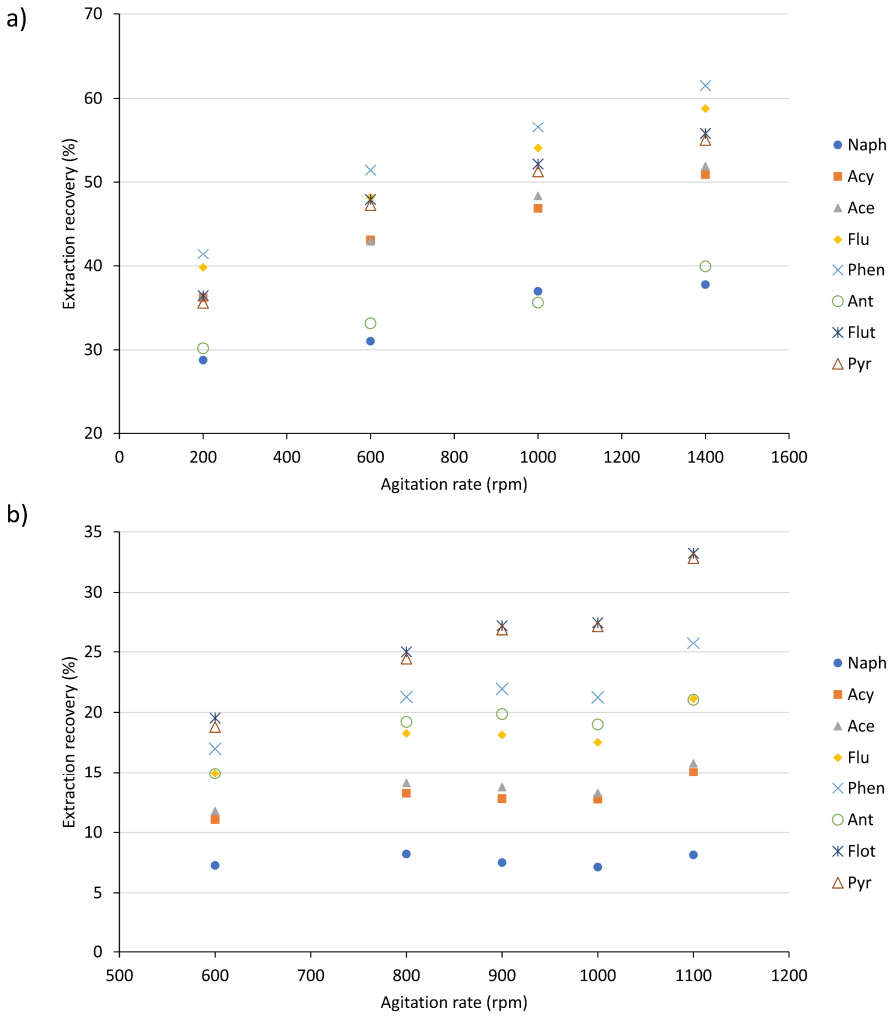


**Fig. 3.6.** Effect of the agitation rate of sample solution on extraction of PAHs using TFME; a) 20 mL sample solution of PAHs (Naph, Acy, Ace, Flu, Phen, Ant, Flut, and Pyr) at 50 ng $mL^{-1}$ agitated for 2 hours; b) 140 mL sample solution of PAHs (Naph, Acy, Ace, Flu, Phen, Ant, Flut, and Pyr) at 40 ng $mL^{-1}$ agitated for 2 hours; Desorption: 60 µL cyclohexane, equilibrated at 220 °C for 5 min in the headspace oven.

For example, a comparison between the lowest and highest agitation rates for Ant showed improvement from 30.2% to 39.9% for 20 mL samples, and from 14.9% to 21.0 % for 140 mL. Furthermore, the effect of stirring rates is more significant for higher molecular weight hydrophobic compounds (higher LogP). This can be explained in terms of the partition and

diffusion coefficients, where higher LogP value lead to greater mass loading on the polymer and rapid depletion at the boundary layer. However, replenishment of this layer is dependent on diffusion, which is slower for higher molecular weight compounds. This effect on the rate of mass loading can be minimized by reducing the thickness of the boundary layer using high agitation. Comparing Acy (LogP 3.94) and Flut (LogP 5.16), Acy showed an increase in the extraction efficiency from 11.1% at 600 rpm to 15.0 % at 1100 rpm for 140 mL, while Flut showed an improvement from 19.5 to 33.2 %. Therefore, the highest possible agitation rates for both sample volumes (1400 rpm for 20 mL and 1100 rpm for 140 mL) were selected for the remaining optimization steps and validation studies to obtain higher sensitivity and precision.

*3.3.2.2. Extraction time*

In TFME, the extraction mechanism is based on the equilibrium of compounds between the sample solution and extraction phase, which is small relative to sample volume compared to typical exhaustive extraction methods, i.e., LLE and SPE. The extracted mass of analytes increases with time of exposure until equilibrium is reached, and is proportional to the concentration of the analytes in the sample [48]. The time required to reach the equilibrium depends on several parameters such as the affinity of the analytes for the sorbent, diffusion coefficients of analytes, and the thicknesses of the film and the boundary layer [49]. The extraction time profiles for extraction of PAHs using porous films for 20 and 140 mL were obtained (Fig. 3.7).

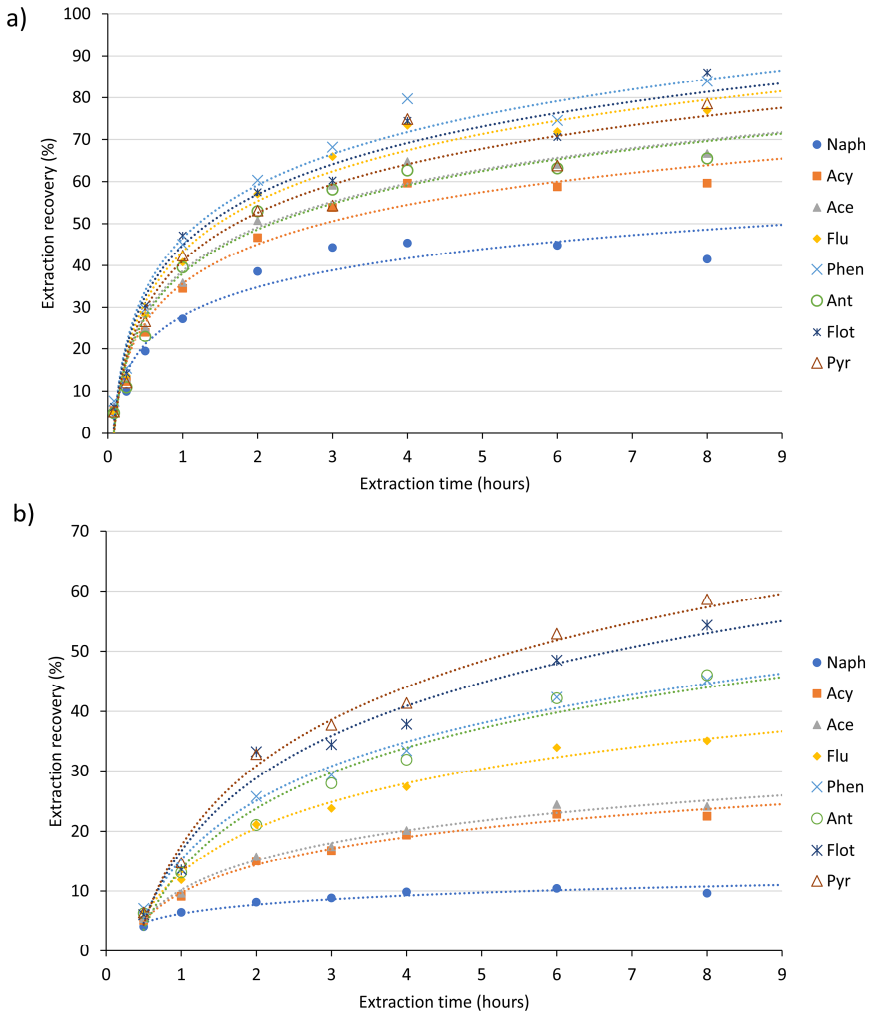


**Fig. 3.7.** Extraction time profile of PAHs, using a) 20 mL sample solution of PAHs (Naph, Acy, Ace, Flu, Phen, Ant, Flut, and Pyr) at 40 ng $mL^{-1}$ agitated at 1400 rpm, b) 140 mL sample solution of PAHs (Naph, Acy, Ace, Flu, Phen, Ant, Flut, and Pyr (40 ng $mL^{-1}$) agitated at 1100 rpm; Desorption: 60 µL Cyclohexane, equilibrated at 220 °C for 5 mins in the headspace oven.

For 20 mLs, Naph reached equilibrium within 3 h, while 4-h-extraction led to near-exhaustive or exhaustive uptake of other analytes, where sample depletion occurred which reduces the apparent partitioning and uptake of hydrophobic PAHs [50]. Therefore, no significant improvement can be observed for longer extraction intervals. Under these

conditions, exhaustive extraction (>70%) was achieved for four analytes: Flu, Phen, Flut, and Pyr at 20 mL.

The extraction time profile of PAHs using TFME in 140 mL (Fig. 3.7b) was also obtained through which different portioning behavior has been observed. Equilibrium for Naph was established within 4 h, while 6 h is required for equilibrium of Ace and Acy. Additionally, for the two most hydrophobic compounds including Flut and Pyr, the equilibrium was not reached even after a 12-hour extraction. The long equilibration time at 140 mL is due to the large volume of the sample and higher mass loading of analytes. For quantitative measurements, a 2-hour extraction time under non-equilibrium conditions was selected.

*3.3.2.3. Salinity (salt effect)*

Different amounts of salt were added to ultrapure water sample to evaluate the effect of salt on the extraction of PAHs and also to determine the need for matrix matching of environmental samples. As can be seen from Fig. 3.8, the addition of salt had no significant effect on extraction efficiency for PAHs with ppm-level solubility until 10 % (w/v). For example, the extraction efficiency of Phen has remained in the range of 23.6-25.8 %. Further addition of salt (10 to 20 % w/v) resulted in a significant reduction in the extraction efficiency for Phen, decreasing from 24.2 to 16.9 %. The negative effect of increasing salinity is more apparent for Ant, Flut, and Pyr, which are more hydrophobic and have lower solubility. The reduction is attributed to ionic strength and reduced solubility of PAHs in the saline solution, which is expected to lead to some deposition of PAHs on the apparatus surfaces [51]. Analytes that are adsorbed onto the surface of glass vials cannot

easily transfer to the surface of the film through the highly saline water. Since the aim is to reduce the number of steps for sample preparation, external calibration curves using analysis of films loaded with PAHs from standards made in ultrapure water with 3.5% NaCl were obtained; this salinity is typical of seawater. By obtaining a matrix-matched calibration in this solution, the minor effects of salinity on TFME performance can be minimized.

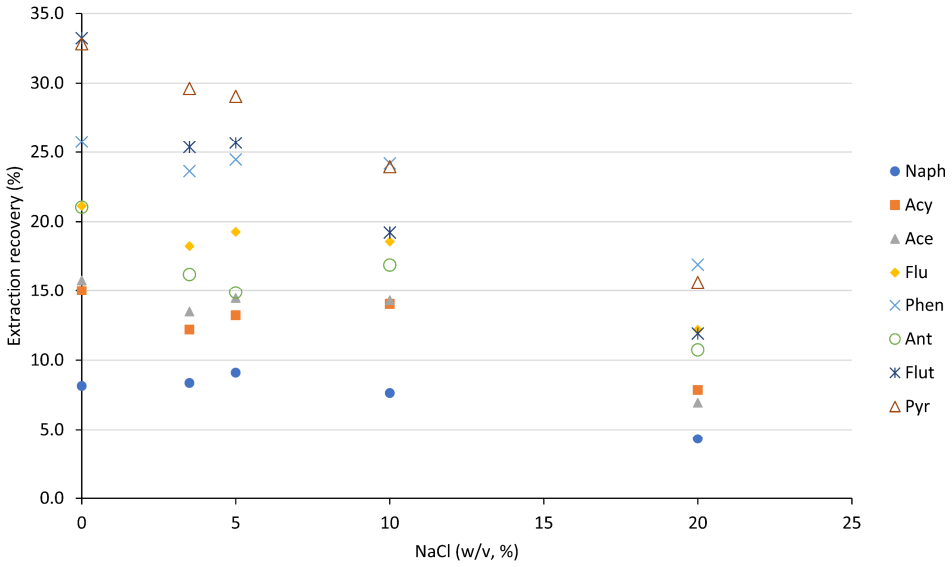


**Fig. 3.8.** Effect of salt addition on the extraction of PAHs using TFME, 140 mL sample solution of PAHs (Naph, Acy, Ace, Flu, Phen, Ant, Flut, and Pyr) at 40 ng $mL^{-1}$; Extraction: 1100 rpm for 2 hours; Desorption: 60 µL cyclohexane, equilibrated at 220 °C for 5 min in the headspace oven.

### 3.3.3. Evaluation of noise due to thermal decomposition of polymer films

Bleeding of siloxane groups from commercially available TFME devices during thermal desorption can lead to noisy background signals. This noise can reduce the accuracy of integration and separation quality by overlapping with analytes, which is a

greater problem with non-selective detection or if nontargeted analysis is the objective. These contaminants can also reduce the ionization efficiency in MS sources, contaminate the source, exclude analyte ions in trapping instruments, and reduce column life. One method proposed to reduce bleed from PDMS is to lower the mass of the PDMS phase using a carbon-based mesh to support PDMS membrane [24]. Another strategy is to use a polymer with less potential for thermal decomposition, such as the polymer films used here. A blank thin film was subjected for ST-HD-GC-FID and the background was compared with the background of a homemade PDMS membrane which has been reported in the literature for extraction of analytes. The resultant chromatograms, shown in Fig. 3.9, illustrate the lower level of background noise compared with PDMS. The lower background should improve detection limits.

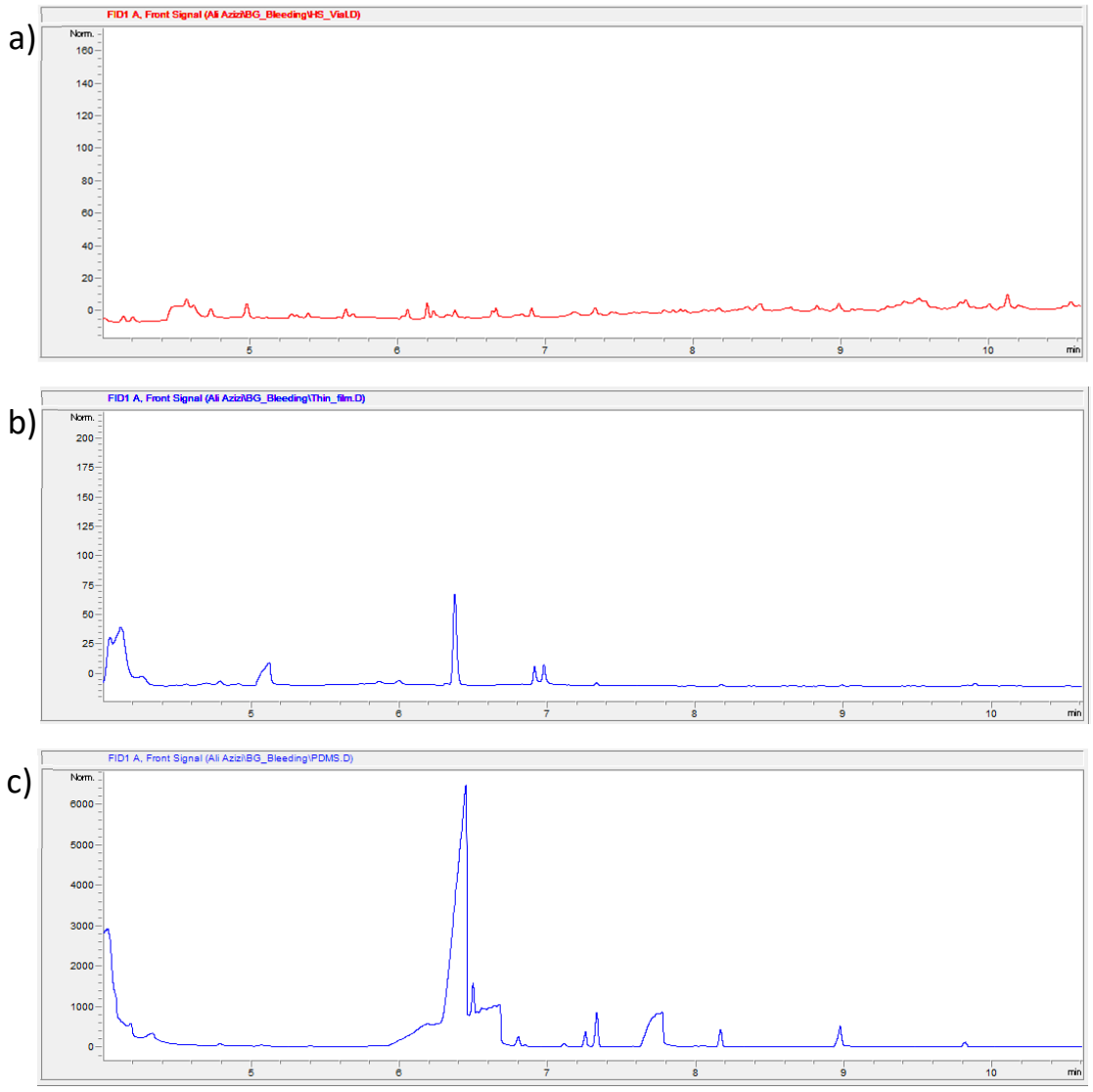


**Fig. 3.9.** Comparison of bleeding of background for a) headspace vial b) developed thin film c) PDMS, ST-HD performed by equilibration for 5 min at headspace oven at 220 °C.

### 3.3.4. Inter-device variability: Assessment of suitability for single-use applications

For high throughput analysis using TFME, developing single-use extraction devices with low inter-device variations is important. To investigate the reliability of the film preparation procedure, the relative standard deviation (RSD%) of the extracted mass of PAHs was assessed for 20 individual thin films. Extractions were performed using 20-mL

samples of 50 ng $mL^{-1}$ PAHs in ultrapure water. Analysis conducted by ST-HD-GC-FID as described in Section 3.2.4 gave inter-device repeatability (Fig. 3.10) ranging from 7.2 to 13.5% for manually prepared devices and without internal standard correction. These results show that TFME devices can be used for fast and efficient analysis specifically for field sampling without concern for gross inter-device variability. The high repeatability for these TFME devices demonstrates that they can be used effectively without internal standards, and in a single-use format the possibility of false-positives and loss of performance with reuse are eliminated, and it allows for high throughput.

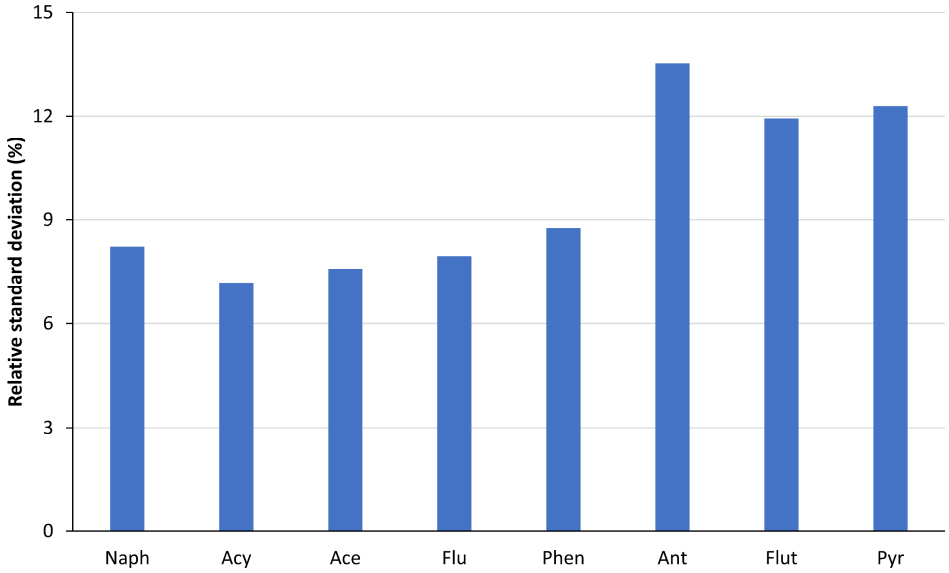


**Fig. 3.10.** Inter-thin film relative standard deviation (%) for extraction of PAHs; 20 mL sample solution of PAHs (Naph, Acy, Ace, Flu, Phen, Ant, Flut, and Pyr) at 50 ng $mL^{-1}$; Extraction: 1400 rpm for 2 hours; Desorption: 60 µL cyclohexene, equilibrated at 220 °C for 5 min at headspace oven (n=20).

### 3.3.5. Reusability and durability of thin films

The thin film devices are intended for single-use in environmental samples, however we investigated reuse to further reduce the cost of analysis [52]. Also, to demonstrate the applicability of these devices using more conventional protocols, a new method was employed based on solvent desorption and analysis by GC-MS. Three individual films were used for extraction of PAHs from 20 mL of sample (40 ng $mL^{-1}$ PAHs in ultrapure water). After extraction, the thin films were air-dried and immersed in toluene to desorb the PAHs. The resulting toluene solution from a single desorption step was analyzed using an APCI-GC-MS/MS method optimized and validated as part of other work in our lab. The immersion step was repeated for each film with two more aliquots of toluene, each of which was subjected to APCI-GC-MS/MS to assess carry-over. No carry-over was detected for any of the 8 PAHs (the instrument limits of detection (LOD) were 0.1-1.0 ng $mL^{-1}$), implying the porous structure of the coating allowed for efficient solvent desorption. Therefore, a simple treatment protocol consisting of a 30-minute wash with methanol was conducted to ensure removal of non-target trace residual contaminants from preceding extractions. As illustrated by Fig. 3.11a, each thin film was used for five extractions, and their performance showed no decrease in sensitivity or capacity. Additional studies were not performed to assess the reusability since it was beyond the scope of this work.

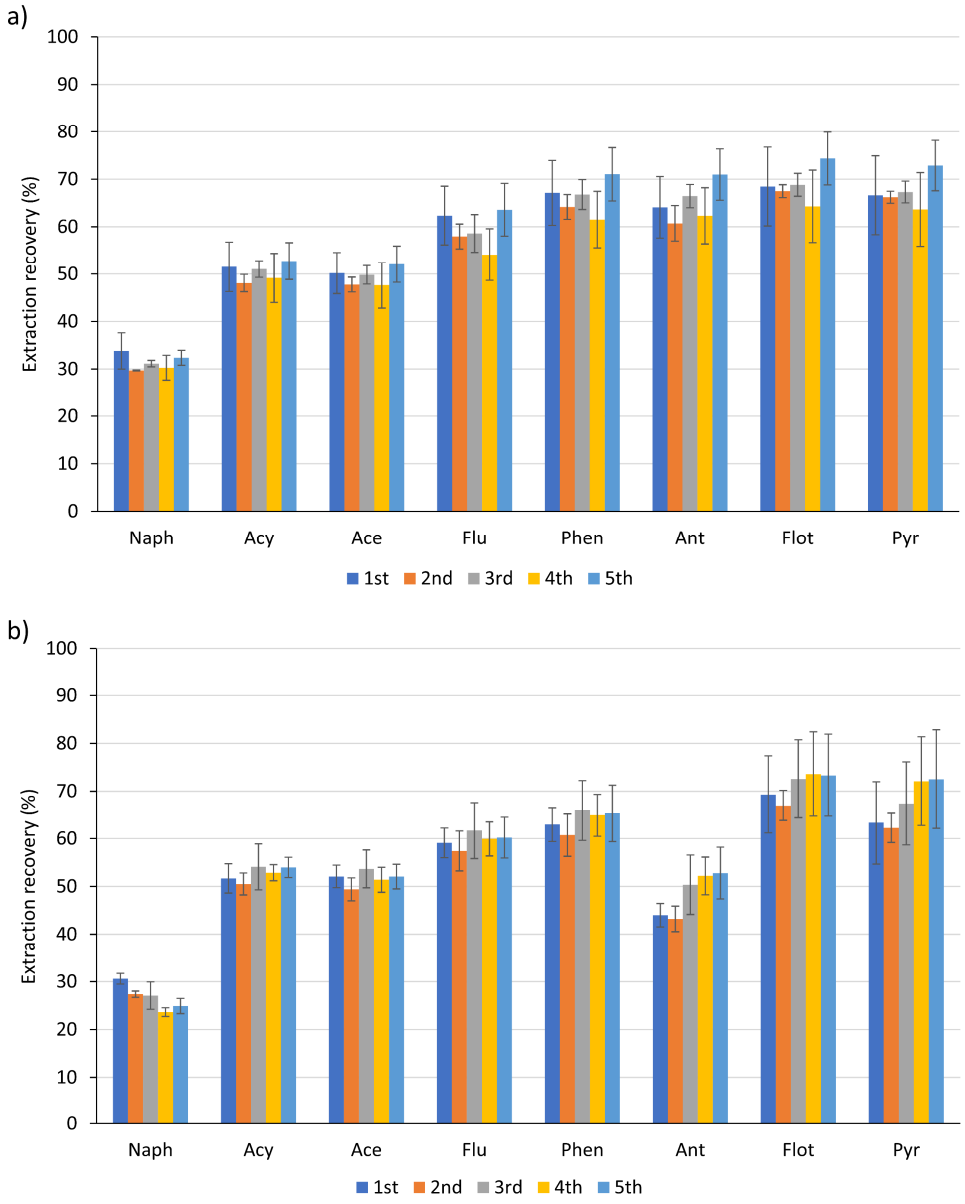


**Fig. 3.11.** Efficiency of thin film for 5 consecutive extraction a) using TFME-APCI-GC-MS/MS, b) TFME-ST-HS-GC-FID; 20 mL sample solution of PAHs (Naph, Acy, Ace, Flu, Phen, Ant, Flut, and Pyr) at 40 ng $mL^{-1}$; Extraction at 1400 rpm for 2 hours; Desorption: a) 4 mL of toluene spiked with Ace-d10 and Phen-d10 (5 ng $mL^{-1}$) as internal standard; b) 60 µL cyclohexane, equilibrated at 220 °C for 5 min in the headspace oven.

As thin film devices are subjected to high temperature (220 °C), it is essential to assess the performance of polymeric sorbents for several headspace desorption processes. For this purpose, three thin films were used for extraction PAHs mentioned in Section 2.4. After desorption and analysis, thin films were washed with methanol for 30 minutes before each set of preceding extractions. The thin films were then used for four more consecutive extraction and desorption processes. The results (Fig. 3.11b) obtained for the three thin films after five uses revealed that there was no substantial difference observed in the extraction efficiency after several cycles of the headspace oven. The obtained recovery values of analytes using ST-HD-GC-FID are in a good agreement with those of using solvent desorption-APCI-GC-MS/MS expect a slight difference in Ant % recovery. Regarding complete solvent desorption of Ant using toluene with no carryover effect, this difference is because of variations in portioning behavior of Ant. Subsequently, Ant adsorbed by films will be desorbed at lower efficiency than standard solution of Ant deposited on the films. Since the thin films experienced a slight color change from white to brown after five uses (ST-HD-GC-FID) (Fig. 3.12), they were inspected using SEM. These images which are shown in Fig. 3.13 show that exposing thin film into headspace oven has led to micro cracks on the surface of the thin films compared to original thin films. However, consistent performance with no measurable loss of extraction capability compared to the pristine coating, suggests that the thermal treatment and cracking this did not degrade adsorptive sites and the porous structure remains intact.

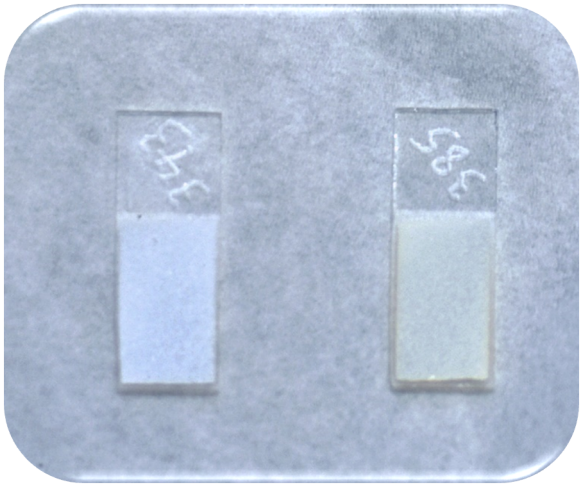

**Fig. 3.12.** Thin films before use (left) and after 5 headspace desorptions (right)

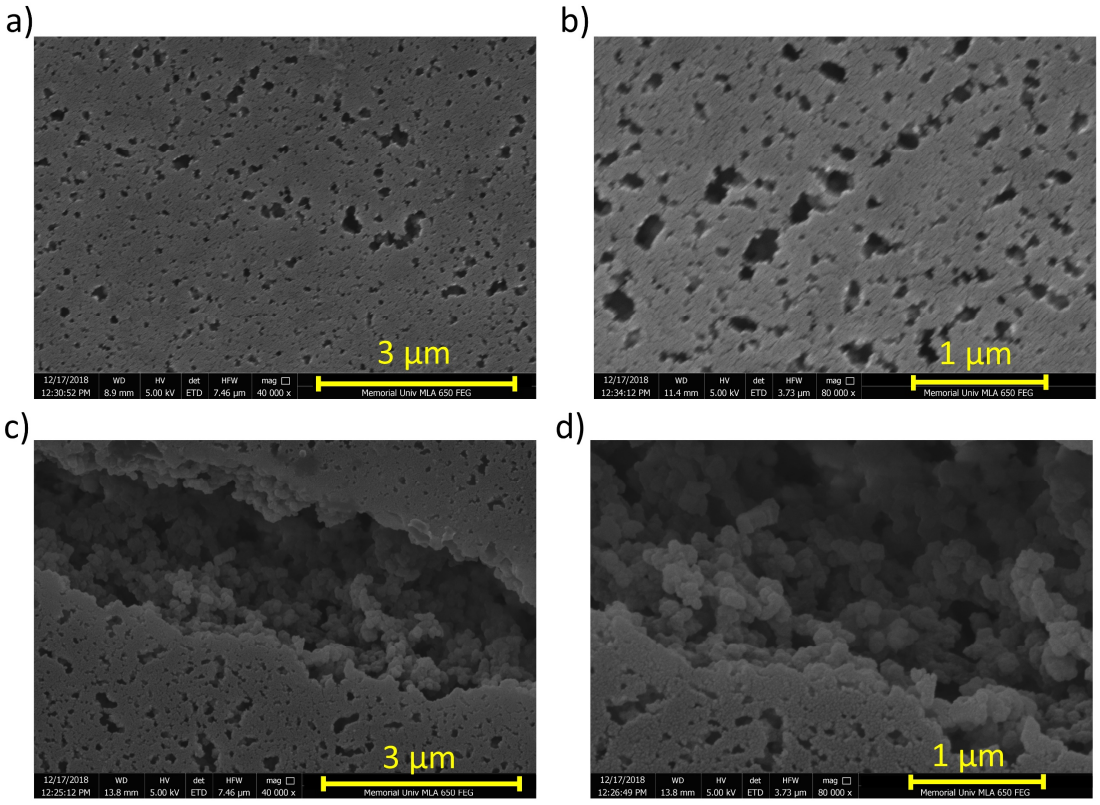


**Fig. 3.13.** Scanning electron micrographs of a) and b): unused porous thin films; c) and d) thin films that have been reused 5 times.

### 3.3.6. TFME-ST-HD-GC-FID for determination of PAHs in water samples

The performance of the optimized method was assessed by obtaining figures of merit such as LOD, limit of quantitation (LOQ), and linear range (LR). Experiments were carried using the optimized TFME and ST-HS conditions using 140 mL samples of ultrapure water with 3.5 % NaCl spiked with PAHs at concentrations of 0.1, 0.2, 0.4, 1.0, 2.0, 4.0, 10.0, 20.0, 40.0, 100.0, 200.0 and 500.0 ng $mL^{-1}$; the results are summarized in Table 3.3.

**Table 3.3.** Figures of merit for analysis of PAHs using TFME-ST-HD-GC-FID.

| PAHs | LOD (ng $mL^{-1}$) | LOQ (ng $mL^{-1}$) | LR (ng $mL^{-1}$) | Linear Calibration | $R^2$ | Extraction recovery%* | RSD%* | PF* |
|---|---|---|---|---|---|---|---|---|
| Naph | 0.2 | 0.4 | 0.4-500 | y=9.6648X+2.3329 | 0.9990 | 8.4 | 3.9 | 195 |
| Acy | 0.2 | 0.4 | 0.4-200 | y=7.7479x+7.3201 | 0.9985 | 12.2 | 5.7 | 285 |
| Ace | 0.4 | 1 | 1-200 | y=9.9113x+10.502 | 0.9985 | 13.5 | 5.5 | 315 |
| Flu | 0.4 | 1 | 1-200 | y=11.838x+6.5399 | 0.9990 | 18.2 | 5.1 | 426 |
| Phen | 0.4 | 1 | 1-200 | y=12.447x+15.227 | 0.9980 | 23.6 | 4.4 | 551 |
| Ant | 0.2 | 0.4 | 0.4-40 | y=11.828x-4.2725 | 0.9952 | 16.2 | 6.4 | 378 |
| Flut | 0.2 | 0.4 | 0.4-200 | y=8.08.6x-11.697 | 0.9991 | 25.4 | 4.2 | 592 |
| Pyr | 2 | 4 | 4-100 | y=7.2131x-10.751 | 0.9973 | 29.6 | 7.1 | 691 |

* spiked at 40 ng $mL^{-1}$

Based on the minimum acceptance criteria for the calibration curves, i.e., determination coefficients ($R^2$) higher than 0.99 and intercepts higher than LOD, the dynamic linear ranges were typically 0.4-200 ng $mL^{-1}$. Wide LR can be achieved using GC-FID for quantitation. However, the extraction of PAHs from ultrapure water with 3.5 % NaCl cannot be performed in concentrations higher than their maximum solubility. For example, the LR of Ant is between 0.4 and 40 ng $mL^{-1}$. Concentrations resulting in signal to noise ratios of 3 and 10 were calculated and reported as LOD (0.2-2 ng $mL^{-1}$) and LOQ

(0.4-4 ng $mL^{-1}$), respectively. The sub-ppb levels of LOD and LOQ values which were obtained using an FID demonstrate the sensitivity of analysis using the proposed method. A high preconcentration factor (PF) is one of the goals in sample preparation giving more sensitive methods. For PAHs loaded to the film from water, the amount of analyte desorbed from the film into the solvent in the headspace sampler was compared to the data using standards applied to the film to calculate the enrichment factor (Table 3.3). High PFs (195 to 691) result in low detection limits and demonstrate the potential of this method for environmental monitoring.

The method was validated for inter-day and intra-day accuracy and precision by extracting PAHs at low, mid, and high concentrations within the LR: 2.5, 25 and 125 ng $mL^{-1}$. The data is presented in Table 3.4. Although the data for Table 3.3 is based on normal linear regression, for the method validation weighted linear regression (1/x) was applied to obtain better fit and accuracy, especially for lower concentrations. Intra-day precision was evaluated using triplicate extraction and quantitation on the same day, while inter-day precision was assessed at each concentration on three different days. The precision for the single-use thin films without internal standard correction was very good, with intra-day %RSD of 1-4% for 125 ng $mL^{-1}$ and 5-21% for 2.5 ng $mL^{-1}$. The inter-day precision for the higher concentration was 9-19% and 3-22% for the low concentration. For accuracy, the data is within the acceptable range (77-128%). Note that for Ant, 125 ng $mL^{-1}$ exceeds its solubility limit.

Calibration curves in ultrapure water with 3.5 % NaCl were used for matrix-matched calibration to calculate the concentration of PAHs in seawater. Table 3.5 shows the results for harbor water spiked with 10, 20, 40 and 100 ng $mL^{-1}$ of PAHs. The accuracy

and precision show the suitability of the proposed method for analyzing real samples, such as seawater, without standard addition.

**Table 3.4.** Method validation data summary for analysis of PAHs using TFME-ST-HD-GC-FID.

| | Intra-day | | | | | | Inter-day | | | | | |
|---|---|---|---|---|---|---|---|---|---|---|---|---|
| | Accuracy (%) | | | Precision (%) | | | Accuracy (%) | | | Precision (%) | | |
| Spiked Conc (ng $mL^{-1}$) | 2.5 | 25 | 125 | 2.5 | 25 | 125 | 2.5 | 25 | 125 | 2.5 | 25 | 125 |
| Naph | 102 | 94.8 | 79.5 | 12 | 3.0 | 4.5 | 110 | 96.6 | 74.8 | 3.6 | 2.5 | 9.0 |
| Acy | 97.8 | 106 | 113 | 19 | 10 | 1.0 | 88.9 | 110 | 105 | 4.1 | 6.3 | 17 |
| Ace | 108 | 118 | 121 | 5.4 | 10 | 1.7 | 106 | 123 | 112 | 2.9 | 6.0 | 15 |
| Flu | 76.8 | 104 | 112 | 7.4 | 11 | 2.3 | 77.1 | 109 | 102 | 8.2 | 6.4 | 16 |
| Phen | 78.8 | 103 | 110 | 7.0 | 13 | 2.7 | 78.6 | 110 | 99.5 | 7.0 | 6.8 | 16 |
| Ant | 91.7 | 106 | - | 15 | 17 | - | 98.0 | 106 | - | 6.3 | 14 | - |
| Flut | 86.2 | 118 | 115 | 21 | 17 | 2.1 | 87.5 | 128 | 102 | 22 | 8.5 | 17 |
| Pyr | <LOQ | 87.0 | 96.0 | 0 | 20 | 3.8 | <LOQ | 95.5 | 84.0 | 0 | 12 | 19 |

**Table 3.5.** Performance of matrix matched calibration for analysis of spiked harbor seawater using TFME-ST-HD-GC-FID.

| PAHs | Fortified at 10 (ng $mL^{-1}$) | | Fortified at 20 (ng $mL^{-1}$) | | Fortified at 40 (ng $mL^{-1}$) | | Fortified at 100 (ng $mL^{-1}$) | |
|---|---|---|---|---|---|---|---|---|
| | Accuracy (%) | RSD (%) | Accuracy (%) | RSD (%) | Accuracy (%) | RSD (%) | Accuracy (%) | RSD (%) |
| Naph | 127 | 5.4 | 119 | 9.1 | 108 | 6.6 | 87.0 | 4.8 |
| Acy | 121 | 3.9 | 119 | 5.7 | 120 | 3.5 | 114 | 5.5 |
| Ace | 129 | 6.5 | 128 | 6.9 | 126 | 5.5 | 118 | 3.2 |
| Flu | 113 | 5.0 | 118 | 8.3 | 119 | 6.5 | 117 | 4.1 |
| Phen | 108 | 6.2 | 114 | 10 | 117 | 12 | 115 | 2.0 |
| Ant | 95.7 | 13 | 114 | 16 | 116 | 10 | - | - |
| Flut | 121 | 5.3 | 121 | 16 | 123 | 20 | 119 | 4.0 |
| Pyr | 66.9 | 7.8 | 85.3 | 19 | 96.0 | 24 | 99.1 | 6.7 |

### 3.3.7. TFME-ST-HD-GC-FID for complex matrices

The matrix-matched calibration was tested for analysis of a highly complex matrix, in this case, produced water, which contains dispersed droplets of oil as well as high concentrations of dissolved organics such as alkylphenols. Results revealed that matrix-matched calibration was not successful for such a complex matrix. Therefore, a standard addition method was applied to analyze the produced water. Table 3.6 summarizes the data for spiked produced water (140 mL sample volumes). The method provides a good correlation between the response and the spiked concentrations. The concentration of Naph in the produced water, which is expected to be high, was determined to be 744.4 ng $mL^{-1}$ based on the calibration (Fig. 3.14).

**Table 3.6.** Determination of PAH concentration in produced water using TFME-ST-HD-GC-FID.

| PAHs | Spiked conc range (ng $mL^{-1}$) | Slope | Intercept | $R^2$ | Detected conc (ng $mL^{-1}$) |
|---|---|---|---|---|---|
| Naph | 50-1000 | 3.0609 | +2278.6 | 0.9968 | 744.4 |
| Acy | 2-40 | 6.7971 | +76.054 | 0.9926 | 11.2 |
| Ace | 2-40 | 6.7143 | +37.523 | 0.9953 | 5.6 |
| Flu | 2-40 | 7.6811 | +96.951 | 0.9928 | 12.6 |
| Phen | 2-40 | 5.1859 | +90.873 | 0.9695 | 17.5 |
| Ant | 4-40 | 4.5711 | –5.7463 | 0.9968 | ND |
| Flut | 4-40 | 1.3815 | –0.0826 | 0.9993 | ND |
| Pyr | 4-40 | 1.2829 | –8.4953 | 1.000 | ND |

The concentrations of Acy, Ace, Flu, and Phen were 11.2, 5.6, 12.6, and 17.5 ng $mL^{-1}$, respectively. Ant, Flut, Pyr were not detected. These concentrations are in good

agreement with those reported previously in produced water [53]. Additionally, the wide linear range possible using this TFME method and relying FID is particularly advantageous for determination of PAHs in produced water. These samples show a high range of PAH concentrations with Naph frequently occurring at concentrations 2 orders of magnitude higher than other PAHs.

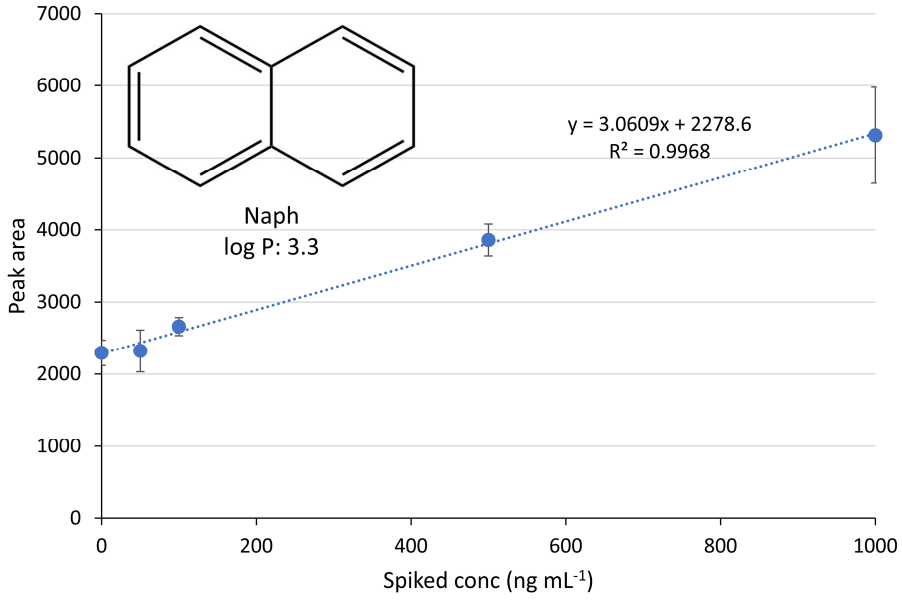


**Fig. 3.14.** Determination of Naph in produced water using TFME-ST-HD-GC-FID; 140 mL sample solution (Naph spiked in the range of 50-1000 ng $mL^{-1}$) agitated at 1100 rpm; Desorption: 60 µL Cyclohexane, equilibrated at 220 °C for 5 mins in the headspace oven.

## 3.4. Conclusion

A direct, high throughput and semi-automated method of analysis for organic pollutants was achieved in complex environmental samples using novel desorption technique (ST-HD) for introducing analytes enriched by TFME. TFME was performed using single-use thin films with no sample filtration and pretreatment. The suitability of

thin films for extraction of analytes without internal standards is supported by figures of merit, which show good repeatability and enrichment, linearity and sensitivity. The precision of method is attributable to the elimination of several sample handling and manipulation steps, such as solvent desorption from the film and evaporation. Moreover, simultaneous and high throughput sample analysis reduces the error by minimizing the effects of common variables such as changes in ambient room temperature and humidity. Such effects are illustrated in the inter- and intra-day variability. The introduction of the analytes onto the GC column through the headspace sampler was enhanced by employing a small volume of cyclohexane. The partition of analytes into a solvent microlayer is a key feature of as a mechanistic rationale for signal enhancement, especially for less volatile compounds. Under optimized conditions, ST-HD employs mild desorption conditions with less noise from polymer decomposition than with traditional thermal desorption allowing for sub-ppb detection limits using a conventional FID system. Moreover, successful application of matrix-matched calibration for seawater samples showed the enormous potential of high throughput TFME-ST-HD for environmental monitoring with no standard addition. The advantages of this method, such as throughput, simplicity, sensitivity, and repeatability, make it an attractive alternative to standard LLE and SPE methods for the analysis of environmental waters.

## 3.5. References

[1] W. United States. Environmental Protection Agency. Office of, 2018 Edition of the Drinking Water Standards and Health Advisories Tables, (2018).

[2] E.E. Commission, Directive 2013/39/EU of the European Parliament and of the Council of 12 August 2013 amending Directives 2000/60/EC and 2008/105/EC as regards priority substances in the field of water policy, Official Journal of the European Union, 226 (2013) 1-7.

[3] C.-C.E.P. Act, List of toxic substances managed under CEPA (Schedule 1), in, 1999.

[4] H. Jiang, X. Hu, Y. Li, J. Qi, X. Sun, L. Wang, J. Li, Large-pore ordered mesoporous carbon as solid-phase microextraction coating for analysis of polycyclic aromatic hydrocarbons from aqueous media, Talanta, 195 (2018) 647-654.

[5] K.H. Kim, S.A. Jahan, E. Kabir, R.J. Brown, A review of airborne polycyclic aromatic hydrocarbons (PAHs) and their human health effects, Environ. Int., 60 (2013) 71-80.

[6] Y. Zhang, S. Tao, Global atmospheric emission inventory of polycyclic aromatic hydrocarbons (PAHs) for 2004, Atmos. Environ., 43 (2009) 812-819.

[7] A. Fakhru'l-Razi, A. Pendashteh, L.C. Abdullah, D.R.A. Biak, S.S. Madaeni, Z.Z. Abidin, Review of technologies for oil and gas produced water treatment, J. Hazard. Mater., 170 (2009) 530-551.

[8] E.T. Igunnu, G.Z. Chen, Produced water treatment technologies, Int. J. Low-Carbon Tec., 9 (2012) 157-177.

[9] H.S. Dórea, J.R.L. Bispo, K.A.S. Aragão, B.B. Cunha, S. Navickiene, J.P.H. Alves, L.P.C. Romão, C.A.B. Garcia, Analysis of BTEX, PAHs and metals in the oilfield produced water in the State of Sergipe, Brazil, Microchem. J., 85 (2007) 234-238.

[10] E.P.A. TestMethod, Polynuclear Aromatic Hydrocarbons, Method 610, US Environmental Protection Agency, Environmental Monitoring and Support Laboratory: Cincinnati, OH, (1982).

[11] J.W. Eichelberger, T.D. Behymer, W.L. Budde, Determination of organic compounds in Drinking water by liquid-solid extraction and capillary column gas chromatography/mass spectrometry, US EPA Method, 525 (1988) 325-356.

[12] J.L. Benedé, J.L. Anderson, A. Chisvert, Trace determination of volatile polycyclic aromatic hydrocarbons in natural waters by magnetic ionic liquid-based stir bar dispersive liquid microextraction, Talanta, 176 (2018) 253-261.

[13] P. Nurerk, C.S.M. Liew, O. Bunkoed, P. Kanatharana, H.K. Lee, Environmentally friendly etching of stainless steel wire for plunger-in-needle liquid-phase microextraction of polycyclic aromatic hydrocarbons, Talanta, 197 (2019) 465-471.

[14] K.Z. Mousavi, Y. Yamini, B. Karimi, S. Seidi, M. Khorasani, M. Ghaemmaghami, H. Vali, Imidazolium-based mesoporous organosilicas with bridging organic groups for microextraction by packed sorbent of phenoxy acid herbicides, polycyclic aromatic hydrocarbons and chlorophenols, Microchim. Acta, 186 (2019) 239.

[15] É.A. Souza-Silva, R. Jiang, A. Rodríguez-Lafuente, E. Gionfriddo, J. Pawliszyn, A critical review of the state of the art of solid-phase microextraction of complex matrices I. Environmental analysis, TrAC, Trends Anal. Chem., 71 (2015) 224-235.

[16] N. Reyes-Garces, E. Gionfriddo, G.A. Gómez-Ríos, M.N. Alam, E. Boyacı, B. Bojko, V. Singh, J. Grandy, J. Pawliszyn, Advances in solid phase microextraction and perspective on future directions, Anal. Chem., 90 (2017) 302-360.

[17] I. Bruheim, X. Liu, J. Pawliszyn, Thin-film microextraction, Anal. Chem., 75 (2003) 1002-1010.

[18] E. Boyacı, K. Goryński, C.R. Viteri, J. Pawliszyn, A study of thin film solid phase microextraction methods for analysis of fluorinated benzoic acids in seawater, J. Chromatogr. A, 1436 (2016) 51-58.

[19] H. Piri-Moghadam, E. Gionfriddo, A. Rodriguez-Lafuente, J.J. Grandy, H.L. Lord, T. Obal, J. Pawliszyn, Inter-laboratory validation of a thin film microextraction technique for determination of pesticides in surface water samples, Anal. Chim. Acta, 964 (2017) 74-84.

[20] F. Wei, F.F. Zhang, H. Liao, X.Y. Dong, Y.H. Li, H. Chen, Preparation of novel polydimethylsiloxane solid-phase microextraction film and its application in liquid sample pretreatment, J. Sep. Sci., 34 (2011) 331-339.

[21] J.J. Grandy, V. Singh, M. Lashgari, M. Gauthier, J. Pawliszyn, Development of a hydrophilic lipophilic balanced thin film solid phase microextraction device for balanced determination of volatile organic compounds, Anal. Chem., 90 (2018) 14072-14080.

[22] M. Wohde, J.-O. Bartz, L. Böhm, C. Hartwig, B.M. Keil, K. Martin, R.-A. Düring, Automated thin-film microextraction coupled to a flow-through cell: somewhere in between passive and active sampling, Anal. Bioanal. Chem., 409 (2017) 1975-1984.

[23] H. Piri-Moghadam, E. Gionfriddo, J.J. Grandy, M.N. Alam, J. Pawliszyn, Development and validation of eco-friendly strategies based on thin film microextraction for water analysis, J. Chromatogr. A, 1579 (2018) 20-30.

[24] J.J. Grandy, E. Boyacı, J. Pawliszyn, Development of a carbon mesh supported thin film microextraction membrane as a means to lower the detection limits of benchtop and portable GC/MS instrumentation, Anal. Chem., 88 (2016) 1760-1767.

[25] P.-S. Cai, D. Li, J. Chen, C.-M. Xiong, J.-L. Ruan, Comparison of two thin-film microextractions for the analysis of estrogens in aqueous tea extract and environmental water samples by high performance liquid chromatography-ultraviolet detection, Food Chem., 173 (2015) 1158-1166.

[26] N. Reyes-Garcés, B. Bojko, J. Pawliszyn, High throughput quantification of prohibited substances in plasma using thin film solid phase microextraction, J. Chromatogr. A, 1374 (2014) 40-49.

[27] E. Gionfriddo, E. Boyacı, J. Pawliszyn, New generation of solid-phase microextraction coatings for complementary separation approaches: a step toward comprehensive metabolomics and multiresidue analyses in complex matrices, Anal. Chem., 89 (2017) 4046-4054.

[28] N. Kirschner, A.N. Dias, D. Budziak, C.B. da Silveira, J. Merib, E. Carasek, Novel approach to high-throughput determination of endocrine disruptors using recycled

diatomaceous earth as a green sorbent phase for thin-film solid-phase microextraction combined with 96-well plate system, Anal. Chim. Acta, 996 (2017) 29-37.

[29] L. Morés, A.N. Dias, E. Carasek, Development of a high-throughput method based on thin-film microextraction using a 96-well plate system with a cork coating for the extraction of emerging contaminants in river water samples, J. Sep. Sci., 41 (2018) 697-703.

[30] S. Li, D. Wu, X. Yan, Y. Guan, Acetone-activated polyimide electrospun nanofiber membrane for thin-film microextraction and thermal desorption-gas chromatography–mass spectrometric analysis of phenols in environmental water, J. Chromatogr. A, 1411 (2015) 1-8.

[31] S.-D. Huang, H.-I. Huang, Y.-H. Sung, Analysis of triazine in water samples by solid-phase microextraction coupled with high-performance liquid chromatography, Talanta, 64 (2004) 887-893.

[32] S.N. Egli, E.D. Butler, C.S. Bottaro, Selective extraction of light polycyclic aromatic hydrocarbons in environmental water samples with pseudo-template thin-film molecularly imprinted polymers, Anal. Methods, 7 (2015) 2028-2035.

[33] A.O. Gryshchenko, C.S. Bottaro, Development of molecularly imprinted polymer in porous film format for binding of phenol and alkylphenols from water, Int. J. Mol. Sci., 15 (2014) 1338-1357.

[34] G. Van Biesen, J.M. Wiseman, J. Li, C.S. Bottaro, Desorption electrospray ionization-mass spectrometry for the detection of analytes extracted by thin-film molecularly imprinted polymers, Analyst, 135 (2010) 2237-2240.

[35] S. Sisalli, A. Adao, M. Lebel, I. Le Fur, P. Sandra, Sorptive tape extraction—a novel sampling method for the in vivo study of skin, (2006).

[36] Z. Qin, S. Mok, G. Ouyang, D.G. Dixon, J. Pawliszyn, Partitioning and accumulation rates of polycyclic aromatic hydrocarbons into polydimethylsiloxane thin films and black worms from aqueous samples, Anal. Chim. Acta, 667 (2010) 71-76.

[37] Z. Qin, L. Bragg, G. Ouyang, J. Pawliszyn, Comparison of thin-film microextraction and stir bar sorptive extraction for the analysis of polycyclic aromatic hydrocarbons in aqueous samples with controlled agitation conditions, J. Chromatogr. A, 1196-1197 (2008) 89-95.

[38] R. Jiang, J. Pawliszyn, Thin-film microextraction offers another geometry for solid-phase microextraction, TrAC, Trends Anal. Chem., 39 (2012) 245-253.

[39] H. Hu, X. Sun, Z. Zhong, X. Chen, X. Zhang, Y. Guo, Determination of chlorobenzenes in pure, tap, and sea water by static headspace gas chromatography-electron capture detection, J. Sep. Sci., 35 (2012) 2922-2928.

[40] Q. Wan, L. Zhang, Determination of acrylonitrile in solid waste by automatic headspace gas chromatography, Procedia Environ. Sci., 31 (2016) 241-246.

[41] Y. Cai, Z. Yan, L. Wang, M. NguyenVan, Q. Cai, Magnetic solid phase extraction and static headspace gas chromatography–mass spectrometry method for the analysis of polycyclic aromatic hydrocarbons, J. Chromatogr. A, 1429 (2016) 97-106.

[42] H.Y. Hijazi, C.S. Bottaro, Selective determination of semi-volatile thiophene compounds in water by molecularly imprinted polymer thin films with direct headspace gas chromatography sulfur chemiluminescence detection, Analyst, 143 (2018) 1117-1123.

[43] H.K. Bojes, P.G. Pope, Characterization of EPA's 16 priority pollutant polycyclic aromatic hydrocarbons (PAHs) in tank bottom solids and associated contaminated soils at oil exploration and production sites in Texas, Regul. Toxicol. Pharm., 47 (2007) 288-295.

[44] C. Baggiani, L. Anfossi, P. Baravalle, C. Giovannoli, G. Giraudi, Molecular recognition of polycyclic aromatic hydrocarbons by pyrene-imprinted microspheres, Anal. Bioanal. Chem., 389 (2007) 413-422.

[45] N.K. Lima, A.R. Lopes, P.G. Guerrero Jr, C.I. Yamamoto, F.A. Hansel, Determination of volatile organic compounds in eucalyptus fast pyrolysis bio-oil by full evaporation headspace gas chromatography, Talanta, 176 (2018) 47-51.

[46] C.-Y. Zhang, M.-Q. Guo, Solvent-saturated solid matrix technique for increasing the efficiency of headspace extraction of volatiles, J. Chromatogr. A, 1511 (2017) 9-14.

[47] S. Risticevic, H. Lord, T. Górecki, C.L. Arthur, J. Pawliszyn, Protocol for solid-phase microextraction method development, Nat. Protoc., 5 (2010) 122.

[48] J. Ai, Solid phase microextraction for quantitative analysis in nonequilibrium situations, Anal. Chem., 69 (1997) 1230-1236.

[49] H. Piri-Moghadam, M.N. Alam, J. Pawliszyn, Review of geometries and coating materials in solid phase microextraction: opportunities, limitations, and future perspectives, Anal. Chim. Acta, 984 (2017) 42-65.

[50] T. Górecki, A. Khaled, J. Pawliszyn, The effect of sample volume on quantitative analysis by solid phase microextraction Part 2.† Experimental verification, Analyst, 123 (1998) 2819-2824.

[51] A.N. Dias, V. Simão, J. Merib, E. Carasek, Cork as a new (green) coating for solid-phase microextraction: Determination of polycyclic aromatic hydrocarbons in water samples by gas chromatography–mass spectrometry, Anal. Chim. Acta, 772 (2013) 33-39.

[52] T. Vasiljevic, G.A. Gómez-Ríos, J. Pawliszyn, Single-Use Poly (etheretherketone) Solid-Phase Microextraction–Transmission Mode Devices for Rapid Screening and Quantitation of Drugs of Abuse in Oral Fluid and Urine via Direct Analysis in Real-Time Tandem Mass Spectrometry, Anal. Chem., 90 (2017) 952-960.

[53] K.H. Chowdhury, T. Husain, B. Veitch, K. Hawboldt, Probabilistic risk assessment of polycyclic aromatic hydrocarbons (PAHs) in produced water, Hum. Ecol. Risk Assess., 15 (2009) 1049-1063.

# Chapter 4: Molecularly imprinted polymers for selective extraction of organophosphorus pesticides from water samples

## 4.1. Introduction

The widespread use of pesticides is one of the major causes of contamination of environmental water resources. Only 1% of the applied pesticides reach their target while the other 99% is released into soil, water and the atmosphere. Pesticides persist in those matrices according to their half-lives [1, 2]. Organophosphorus pesticides (OPPs) are a major class of pesticides having largely replaced organochlorine pesticides which are more toxic and have longer half-lives [3]. OPPs are neurotoxic compounds inhibiting acetylcholinesterase which functions to hydrolyse acetylcholine as a neurotransmitter. The accumulation of acetylcholine at synapses and myoneural junctions results in both acute and chronic toxicity [4].

The US-EPA has placed OPPs on the Contaminant Candidate Lists (CCLs) 1, 2 and 4 and applies to them the Unregulated Contaminant Monitoring Rules (UCMRs) 1, 2, and 4. Additionally, they are listed in the Drinking Water Standards and Health Advisories published in 2012 [5]. According to the council of the European Union, the maximum contaminant level (MCL) of each pesticide in water intended for human consumption is 0.1 $\mu g\ L^{-1}$ and the total concentration of the pesticides must not exceed 0.5 $\mu g\ L^{-1}$ [6]. Reliable analytical methods use gas chromatography (GC) [7-10] and liquid chromatography (LC) [11-13] techniques to trace these pesticides in real samples. However, low MCLs, complicated matrices, and incompatibility with chromatographic systems necessitate sample treatment steps including clean-up and extraction before instrumental analysis.

The most common preconcentration method, which has been widely used for environmental analysis, is liquid–liquid extraction (LLE). LLE is expensive, time-

consuming, labor-intensive and requires large volumes of both samples and toxic organic solvents. Solid phase extraction (SPE) is recommended by the EPA [14] and implemented for extraction of OPPs [15, 16]. SPE is a tedious technique and usually requires a large sample volume. Larger amounts of organic solvents used in elution step require further drying and evaporation steps which reduces the accuracy and precision of the analysis. The drying is also a key parameter to obtain desirable enrichment and needs to be optimized. Excessive drying of the sorbent could cause evaporation of the volatile compounds or oxidation of analytes exposed to the air [17]. Other drawbacks of SPE include analyte breakthrough during preconcentration from large volumes and the loss of analytes during filtration step required for real samples, particularly for hydrophobic analytes [18]. During the last two decades, several miniaturized techniques have been developed to reduce or eliminate the use of organic solvents, decrease sample size, increase throughput, and improve preconcentration factors. These methods are solid-phase microextraction (SPME) [19], stir bar sorptive extraction (SBSE) [20], dispersive liquid-liquid microextraction (DLLME) [21], and dispersive solid phase extraction (DSPE) [13]. These techniques use extraction phases (solid or liquid) that adsorb analytes with wide range of physical and chemical properties. Since the extraction phase is not a selective phase, these methods suffer co-extraction of interfering compounds and perform poorly in complex matrices [22].

MIPs have been extensively used for the selective extraction of OPPs [23]. Aside from their selectivity, MIP materials are also robust and easy to prepare, which can reduce the associated total cost of analysis [24]. MIPs reported in the literature, are mainly used as a packing material for SPE of OPPs [25-28]. Interfering compounds often can be easily

washed away when using MIP-SPE thereby enhancing analytical performance [28]. Nonetheless, MIP-SPE can become clogged from components of real samples, and the phase may also swell with use of organic solvents [29]. Furthermore, using MIP-SPE requires several steps that cannot easily be conducted during field sampling (i.e., the need for sample preparation such as filtration prior to extraction process, using of conditioning solvents and vacuum manifolds ). SPME is simultaneous clean-up and extraction method that can be utilized for on-site sampling. However, this technique uses non-selective commercial sorbents that adsorb compounds with wide ranges of physiochemical properties. To enhance the selectivity of SPME, a MIP coating can be used as an extraction phase. Wang et al. [30] developed a thermally-stable MIP-coated fiber for headspace-SPME of OPPs. Direct introduction of analytes was performed using thermal desorption that replaced solvent desorption and enhanced the sensitivity of analysis. The prepared MIP-fibers showed good affinity towards OPPs compared to non-imprinted polymers (NIPs) and commercially available SPME fibers. However, the synthesis procedure, which is a sol-gel method, requires several cycles of deposition and thermal curing to achieve a desirable thickness. MIP-coated stir bars can also be used for the extraction of OPPs. They can be prepared by polymerization of nylon-6 in presence of monocrotophos as a template [31]. Although the polymer showed good selectivity in organic solvents, the selectivity in water was negligible, which the authors attribute to the water interfering with hydrogen bonding between the nylon and target molecules. Thin film microextraction (TFME) is a new microextraction technique that is conducted using thin sheets of coating with or without a support. The extraction devices used feature a large surface area of the extraction which increases the speed and efficiency of the extraction. The unique tunable absorption

properties of MIPs (e.g. porosity and selectivity) make them a promising extraction phase for TFME.

In this work, thin film MIPs, which have been previously applied to extraction of polycyclic aromatic hydrocarbons [32], phenols [33], and thiophenes [34], are developed for the selective adsorption of OPPs. These MIPs are compatible for both solvent desorption [35] and thermal desorption [36] and can be used for direct analysis using ambient ionization techniques [37]. However, obtaining selective recognition of polar analytes in aqueous samples using thin film MIPs is challenging because of water can interfere with the some of the more desirable non-covalent binding regimes, including hydrogen bonding and electrostatic interactions. To achieve selectivity, several parameters must be considered in the design of the MIPs such as the type of template, monomer, crosslinker, porogenic solvent and their respective ratios. The prepolymer composition is optimized for both extraction capacity and selectivity. Each MIP composition was assessed for suitability for use in both thin film and mesh formats for extraction of OPPs from water samples. After extraction, the enriched analytes are rapidly desorbed using a small volume of organic solvent. This is the first report of a single use extraction MIP device with superior selectivity for pesticides analysis in water samples.

## 4.2. Experimental

### 4.2.1. Chemicals and reagents

OPPs standards malathion, parathion methyl, fenamiphos, diazinon, and chlorpyrifos were purchased from Sigma Aldrich (Oakville, ON, Canada). Standards

solutions of other OPPs used for validation studies (i.e., dichlorvos, mevinphos, dimethoate, demeton-S-methyl, ethoprophos, paraoxon methyl, parathion methyl, tolclofos methyl, methidathion, fenamiphos, diazinon, pirimiphos methyl, disulfoton sulfone, azinphos methyl, malathion, prothiofos, chlorpyrifos, tetrachlorvinphos, profenofos, pyrazophos, and ethion (shown in Table 4.1), Optima LC-MS grade acetonitrile (ACN), methanol (MeOH), and formic acid (FA) were obtained from Fisher Scientific (Whitby, ON, Canada). Sodium chloride (NaCl, 99%) and glacial acetic acid (>99.7%) were purchased from ACP chemicals (Montreal, QC, Canada). Ultrapure water (18.2 MΩ $cm^{-1}$) was produced by a Milli-Q purification system.

Individual stock solutions of OPPs were prepared in acetonitrile at 1000 mg $L^{-1}$. Working solutions of OPPs for development of MIPs were prepared in MeOH by appropriate dilution of the stock mixture of 5 OPPs at 10 mg $L^{-1}$. For MIP validation studies on coated mesh, a multi-component mixture of OPPs (4 – 40 mg $L^{-1}$) was prepared in MeOH. All the solutions were stored at 4 °C until use. Aliquots of the mixtures described above were spiked into water samples to obtain required concentrations for each experiment.

**Table 4.1.** Targeted OPPs with physical and chemical properties [38].

| Pesticide | Solubility in water ($mg \cdot L^{-1}$) | Log P * | Structure |
|---|---|---|---|
| Dichlorvos | 8000 | 1.43 | 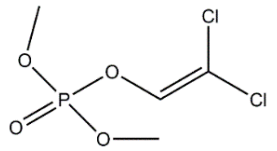 |
| Mevinphos | 600000 | 0.13 | 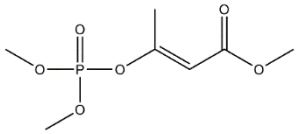 |
| Dimethoate | 5000 | 0.78 | 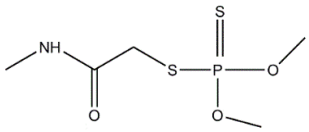 |
| Demeton-S-methyl | 3300 | 1.02 | 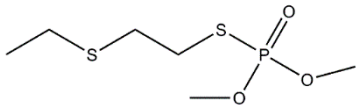 |
| Ethoprophos | 750 | 3.59 | 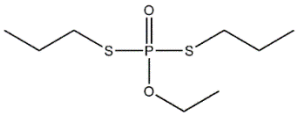 |
| Paraoxon methyl | 3640 | 1.33 | 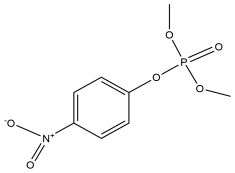 |
| Parathion methyl | 37.7 | 2.86 | 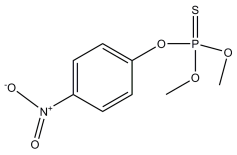 |
| Tolclofos-methyl | 0.4 | 4.56 | 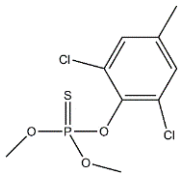 |

*(continued on next page)*

**Table 4.1.** (*continued*)

| Pesticide | Solubility in water ($mg.L^{-1}$) | Log P | Structure |
|---|---|---|---|
| Methidathion | 187 | 2.2 | 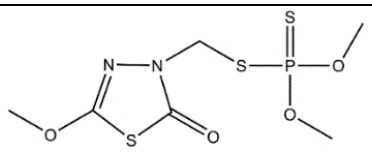 |
| Fenamiphos | 400 | 3.23 | 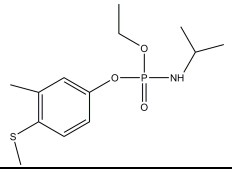 |
| Diazinon | 60 | 3.81 | 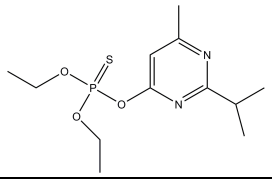 |
| Pirimiphos-methyl | 5 | 4.2 | 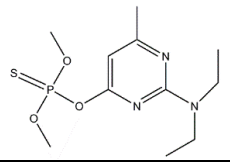 |
| Disulfoton sulfone | NA | 1.87 | 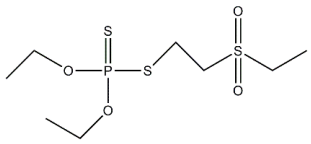 |
| Azinphos-methyl | 20.9 | 2.75 | 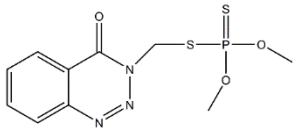 |
| Malathion | 145 | 2.36 | 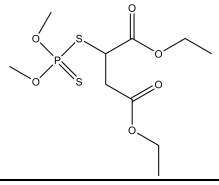 |
| Prothiofos | 0.07 | 5.67 | 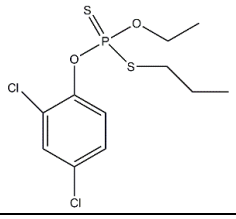 |

*(continued on next page)*

**Table 4.1.** (*continued*)

| Pesticide | Solubility in water ($mg.L^{-1}$) | Log P | Structure |
|---|---|---|---|
| Chlorpyrifos | 1.4 | 4.96 | 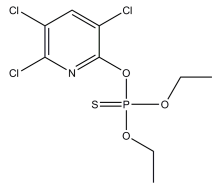 |
| Tetrachlorvinphos | 11 | 3.53 | 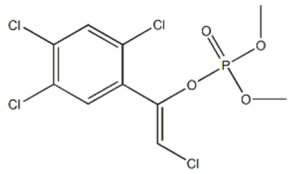 |
| Profenofos | 28 | 4.68 | 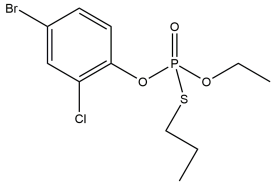 |
| Pyrazophos | 4.2 | 3.8 | 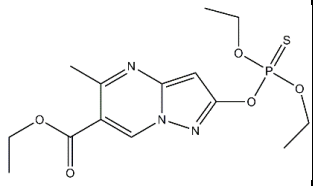 |
| Ethion | 2 | 5.07 | 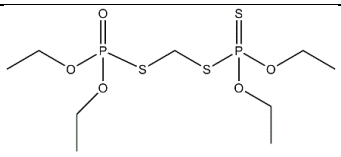 |

### 4.2.2. Instrumentation

The chromatographic separation and quantitative analyses were performed using a Waters Acquity ultra-performance liquid chromatography (UPLC) system (Waters, Milford, MA, USA) interfaced to a triple quadrupole mass spectrometer (Xevo TQ-S ,Waters, Milford, MA, USA) equipped with a Z-spray electrospray ionization (ESI) source. Chromatographic separation of 5 OPPs was performed using a PFP column 2.1 mm × 150

mm, 3 µm particle size (Canadian Life Science, Canada). The temperature of the column was maintained at 30 °C. The mobile phase consisted of an isocratic mixture of MeOH and water (90:10, v/v) containing 0.1% FA with a flow rate of 0.7 mL $min^{-1}$. Sample injections (1-µL) were made using a sample manager flow-through needle (SM-FTN), which maintained sample temperature at 4 °C.

For optimization and validation of MIP-coated mesh, 21 OPPs were extracted from water samples and separated using a Waters Acquity BEH $C_{18}$ column (2.1 × 50 mm, 1.7 µm) maintained at 30 °C. Gradient elution was employed as shown in Table 4.2. The injected volume was 5-µL, while samples were kept at 4 °C.

**Table 4.2.** LC gradient method for separation of selected OPPs.

| Time (min) | Flow rate (mL $min^{-1}$) | Water % | MeOH% | 10 % FA in water |
|---|---|---|---|---|
| Initial | 0.450 | 89 | 10 | 1 |
| 0.5 | 0.450 | 89 | 10 | 1 |
| 3 | 0.450 | 39 | 60 | 1 |
| 4.5 | 0.450 | 24 | 75 | 1 |
| 7.5 | 0.450 | 14 | 85 | 1 |
| 7.51 | 0.450 | 89 | 10 | 1 |
| 8.5 | 0.450 | 89 | 10 | 1 |

The MS/MS detection and quantitation were performed in positive mode under multiple reaction monitoring (MRM) conditions. MRM transitions, cone voltages and collision energy used for all compounds are included in Table 4.3. Nitrogen gas was supplied by a generator (Peak Scientific, Scotland, UK) and was used as both cone and desolvation gases, with flow rates of 150 and 1000 L $h^{-1}$, respectively. Other relevant mass spectrometer parameters were capillary voltages +3.5 kV; source temperature 150 °C and desolvation temperature 650 °C.

**Table 4.3.** Summary of tandem mass spectrometry parameters using LC-MS/MS

| Pesticide | Precursor ion (m/z) | Cone voltage (V) | Product ion 1 (m/z) | Collision energy (eV) | Product ion 2 (m/z) | Collision energy (eV) |
|---|---|---|---|---|---|---|
| Chlorpyrifos | 351.9 | 44 | 96.9 | 30 | 199.9 | 18 |
| Dichlorvos | 221 | 34 | 79 | 34 | 109 | 22 |
| Disulfoton sulfone | 307.1 | 24 | 97.1 | 28 | 153.1 | 12 |
| Paraoxon-methyl | 248 | 36 | 90 | 25 | 202 | 19 |
| Mevinphos | 225.1 | 24 | 127.1 | 15 | 193.1 | 8 |
| Tetrachlorvinphos | 364.8 | 32 | 127 | 16 | 238.9 | 20 |
| Dimethoate | 230.1 | 24 | 125 | 20 | 199 | 10 |
| Demeton-S-methyl | 231.1 | 16 | 61.2 | 30 | 89.1 | 10 |
| Ethoprophos | 243.2 | 32 | 97 | 31 | 131 | 20 |
| Parathion methyl | 263.9 | 38 | 79 | 36 | 109 | 22 |
| Tolclofos-methyl | 301 | 41 | 125 | 29 | 174.9 | 17 |
| Methidathion | 303 | 18 | 85.1 | 20 | 145 | 10 |
| Fenamiphos | 304.1 | 30 | 201.9 | 34 | 216.9 | 22 |
| Diazinon | 305.1 | 16 | 153.1 | 18 | 169.1 | 20 |
| Pirimiphos-methyl | 306.1 | 36 | 108.1 | 32 | 164.1 | 22 |
| Azinphos-methyl | 318 | 20 | 160 | 18 | 261 | 8 |
| Malathion | 331 | 18 | 99 | 20 | 127 | 10 |
| Prothiofos | 345.2 | 30 | 133 | 20 | 241 | 20 |
| Profenofos | 372.9 | 36 | 127.9 | 40 | 302.6 | 20 |
| Pyrazophos | 374 | 44 | 194 | 32 | 222.1 | 22 |
| Ethion | 385 | 25 | 171 | 20 | 199 | 10 |

### 4.2.3. Preparation of thin film MIPs and MIP-coated mesh

For optimization of the MIP composition, we prepared thin film MIPs according to our previous studies with some modifications [35, 36]. Pre-cut stainless steel metal blades (0.5 x 20 $mm^2$) with a triangular tip on one end were used as substrates to prepare thin film MIPs. This substrate is stable and can be used for extraction at high agitation rates. In addition, these metal substrates can be used for direct coupling of these devices to MS. The metal blades were cleaned with MeOH and dried using a gentle stream of nitrogen. The prepolymer solution with a proprietary composition was thoroughly vortex mixed and

degassed in an ultrasonic bath for 5 minutes. A 3.0-µL portion of the prepolymer solution was pipetted onto the metal blade and evenly spread by carefully applying a glass cover slide (25 $mm^2$). The thin layer of solution sandwiched between the two layers, was polymerized under UV light (254 nm) for 30 mins. Afterward polymerization, the cover slides were removed, and the resulting thin films (i.e. 30 thin film MIPs) (were washed with 100 mL MeOH: acetic acid (9:1, v/v) solution at 500 rpm for 2 h to remove the template molecules and unreacted components. The washing solution was changed every 30 min. After template removal, the thin films were rinsed with MeOH, dried and stored at room temperature until use.

To prepare MIP-coated mesh, fiber glass sheets were sprayed directly with pre-polymer solution with no pretreatment steps. After UV polymerization, a uniform layer of the polymer was formed on the glass fibers. The polymer-coated mesh was washed with MeOH for 2 h to remove residual unreacted components. Following that, the coated sheets were cut into 20 mm (width) x 80 mm strips. The cut strips were then rinsed MeOH (30 min at 500 rpm), conditioned in a vacuum oven (150 °C at 660 Torr vacuum for 12 h) and stored at room temperature until use.

### 4.2.4. Sample preparation procedure

For extraction of OPPs using thin film MIPs, mixed standard solutions (5.0 ng $mL^{-1}$ of each OPP) were prepared in 20 mL ultrapure water by spiking multi-component stock standards and used immediately to avoid adsorption of analytes to the glass vial. The organic solvent content must lower than 1% of the sample volume to avoid any effect of solvent during extraction. The thin films were directly exposed to the aqueous solutions

with no preconditioning step. The extraction of analytes into the films was performed by agitating at 1000 rpm using a multi-position stirrer (Fisher Scientific, Canada) . The optimal extraction time was 60 min at room temperature. After that, the thin films were washed with 1-2 mL of ultrapure water and allowed to dry. Analytes desorption from the film was performed in 700 µL MeOH by agitating at 1500 rpm for 10 min using a vortex mixer (Fisher Scientific, Canada). For analysis, samples were filtered using 0.22 µm PTFE filters and 1 µL of the extract was injected into the LC/MS-MS system. The apparatus used are illustrated in Fig. 4.1.

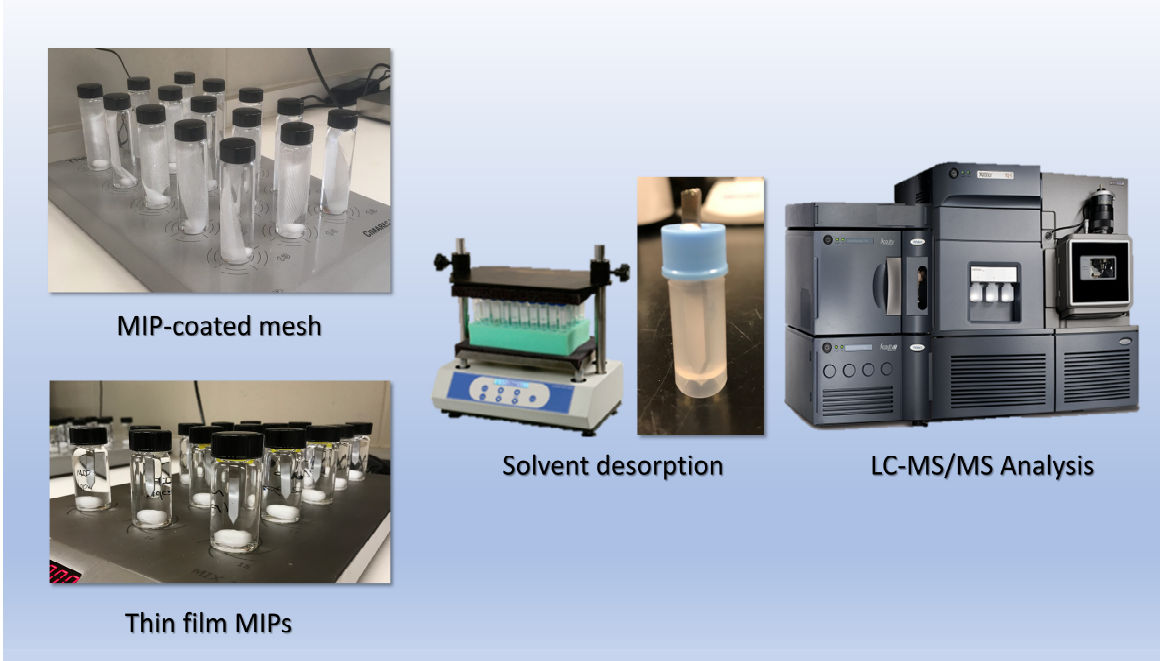


**Fig. 4.1.** Experimental set-up for extraction and determination of OPPs using thin film MIPs and MIP-coated mesh.

MIP-coated mesh extraction devices were immersed in 40 mL of the OPPs mixed standard solution with concentration ranges of 10-100 ng $mL^{-1}$ for 30 min agitated at 1000 rpm. The MIP mesh were then removed from vials and allowed to air dry. For desorption of OPPs, the mesh was folded and placed in a 5.0-mL screw cap PP centrifuge

tube (Eppendorf) with 2 mL MeOH agitated at 1500 rpm for 30 min. The extraction and desorption processes were carried out in a high throughput manner utilizing multi-position stirrer and vortex mixing devices, respectively. Following desorption, the MeOH containing the desorbed analytes was filtered using a 0.22 µm filter and injected to the LC/MS-MS system.

## 4.3. Results and discussions

### 4.3.1. Optimization of MIP composition

Performance and selectivity of MIPs for recognition of target compounds can be influenced by MIP composition including factors such as the type and amount of template, monomer and crosslinker [39]. The template must possess functionality and shape close to the target molecules [40]. Other criteria for an appropriate template are its stability in prepolymer mixture and the robustness of resulting MIP coatings. We fabricated MIPs using 6 different template molecules which were synthesized in house. The structure of the templates is proprietary and will not described further. The results of extractions using these MIPs are presented in Fig. 4.2. MIP(T5) prepared using Template 5 yielded an unstable coating and could not be tested for sorption behavior. The other templates demonstrated very similar extraction efficiencies and very good selectivity relative to the NIP, which can be attributed to formation of a stable complex between the template molecules and monomers prior to and after polymerization, which leads to successful imprinting. MIP(T2) was selected for further studies due to its stability in the prepolymer solution and in the prepared films.

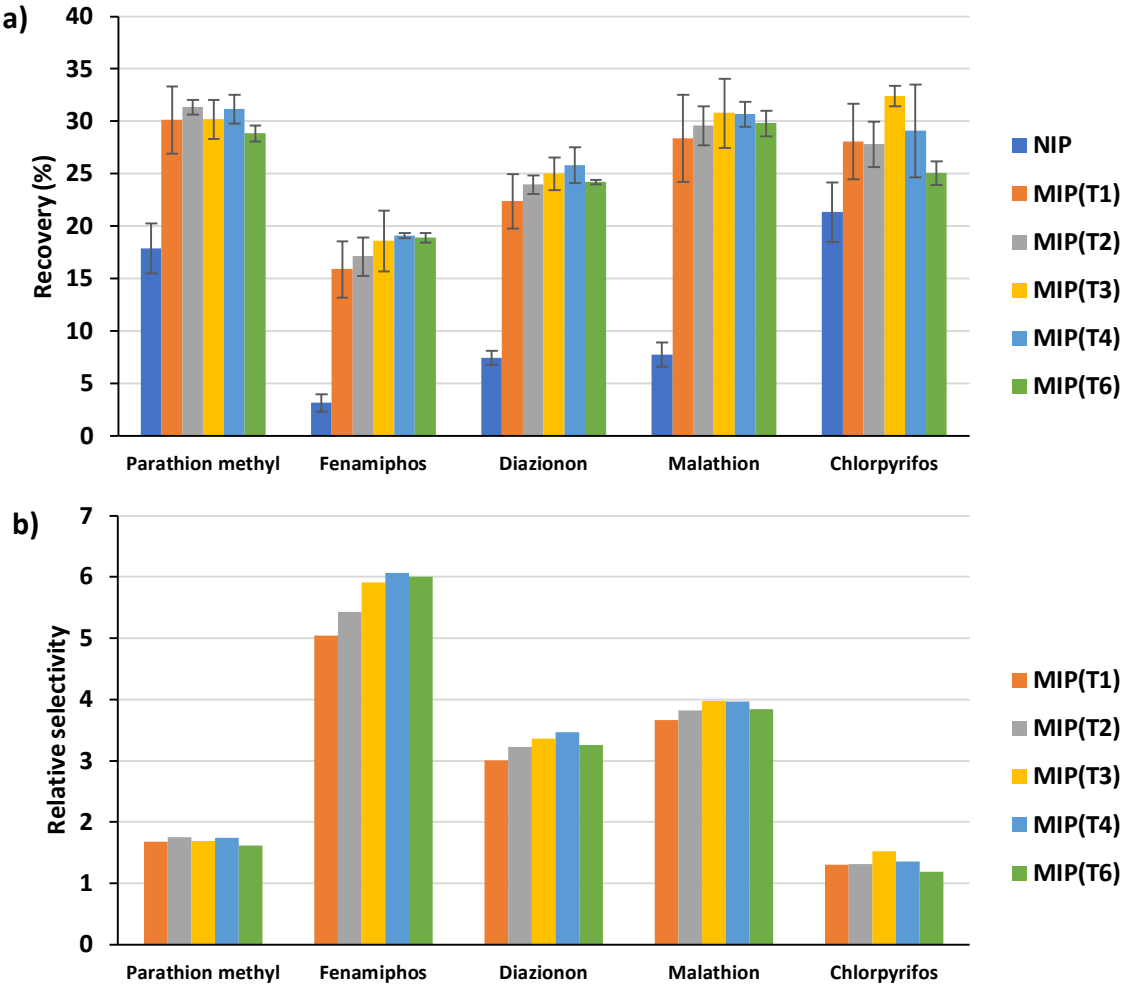


**Fig. 4.2.** Effect of different templates on the a) extraction efficiency and b) relative selectivity of thin film MIPs compared to thin film NIPs, Sample: 20 mL sample solution of OPPs (parathion methyl, fenamiphos, diazinon, malathion, and chlorpyrifos) at 50 ng $mL^{-1}$; Extraction at 1000 rpm for 1 h; Desorption: 700 µL MeOH agitated at 1500 rpm for 30 min.

The ratio between the monomer and crosslinker determines the stability of the polymer as well as binding sites [41]. Therefore, thin films using different ratios (i.e. 1:6, 1:4, and 1:2 of monomer to crosslinker) were prepared and used for extraction of OPPs. In these prepared formulations, we used a fixed amount of crosslinker to obtain stable thin films. As illustrated in Fig. 4.3a, increasing amount of functional monomer (from 1:6 to

1:2 of monomer to crosslinker) enhances the extraction recovery of OPPs using MIPs while the efficiency of the NIPs remains constant regardless of the amount of monomer. This is evidence that the template-monomer complex is important in producing appropriate binding sites.

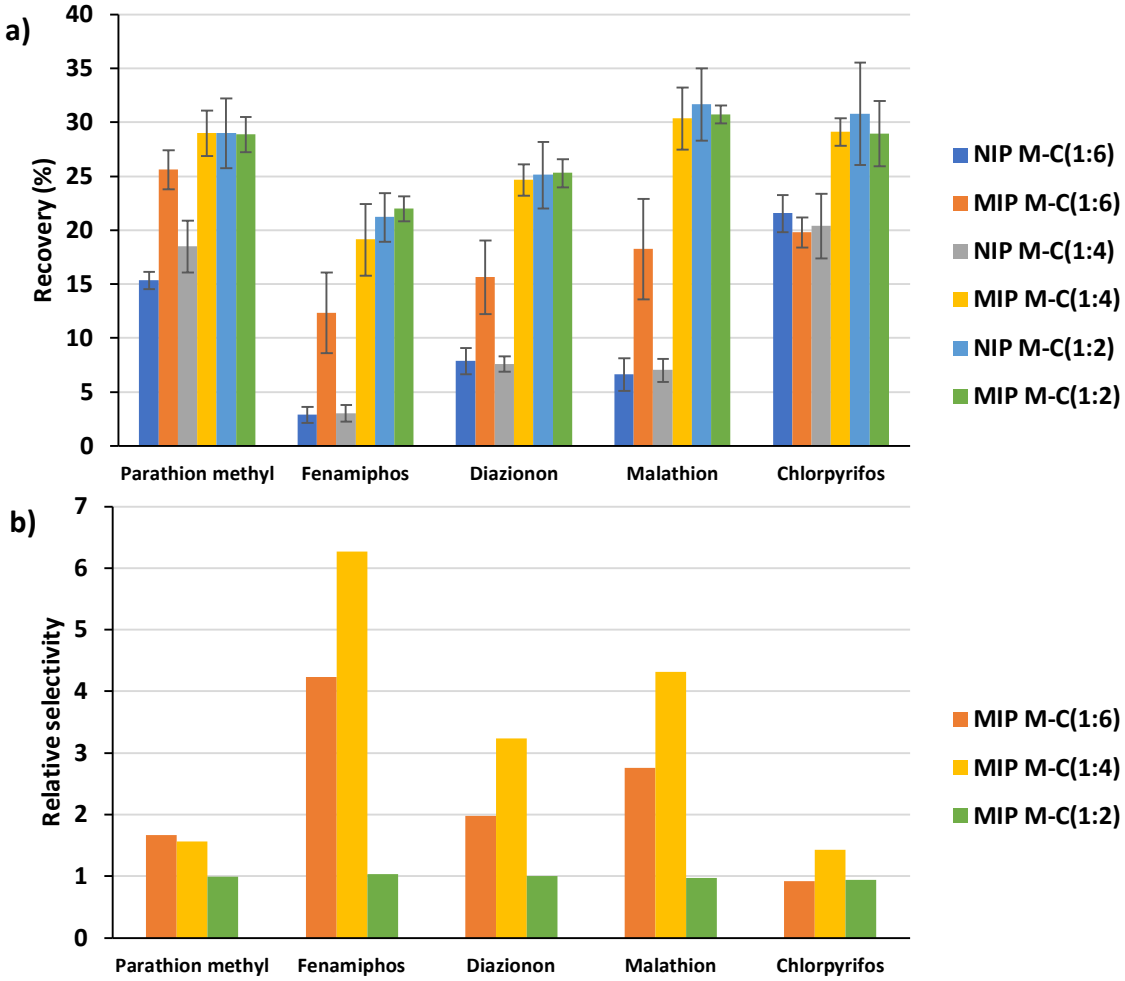


**Fig. 4.3.** Effect of monomer to crosslinker ratio on the a) extraction efficiency and b) relative selectivity of thin film MIPs compared to thin film NIPs, Sample: 20 mL sample solution of OPPs (parathion methyl, fenamiphos, diazinon, malathion, and chlorpyrifos) at 50 ng $mL^{-1}$; Extraction at 1000 rpm for 1 h; Desorption: 700 µL MeOH agitated at 1500 rpm for 30 min.

This is rationalized through the theoretical number of template-monomer complexes in each film, which increases with a decrease relative loading of cross-linker. However, increase from M-C (1:4) to (M-C (1:2)) had no effect on performance of MIPs, but led to a dramatic increase in the extraction efficiency using NIPs. This is explained by an increase in sorption sites in the NIP, which is likely to be manifested as more non-selective sorption sites in the analogous MIPs, which is commonly estimated as relative selectivity, which is obtained by dividing the extraction efficiency of MIPs over NIPs. Based on extraction efficiency and selectivity, the ratio of 1:4 of monomer to crosslinker was chosen as the optimal value.

In non-covalent imprinting strategies, the monomer is usually used in excess to ensure equilibrium favors the establishment of pre-polymerization complexes necessary for selective adsorption using MIPs [42]. The amount of template must be enough to provide maximum number interactions with functional groups in the monomer and therefore selective binding sites [43], however large amounts of template could be problematic due to low solubility in pre-polymer mixture or instability of the coating. We assessed the template–monomer ratio by increasing the molar ratio of template to monomer from no template added (NIP) to 1:2 ratio of template to monomer.

The results shown in Fig. 4.4 reveal that adding template molecule, even small amount (1:16), enhances the extraction capacity of the polymeric sorbent. Increasing the amount of template from 1:16 to 1:8 results in an improvement in extraction efficiency and selectivity of MIPs. Further increase has slight effect on the efficiency of the extraction, though MIPs prepared with a 1:2 ratio of template to monomer was not stable and yielded

irreproducible results. The T-M ratio of 1:4 was selected as the optimum and was used in fabrication of the MIPs in both formats.

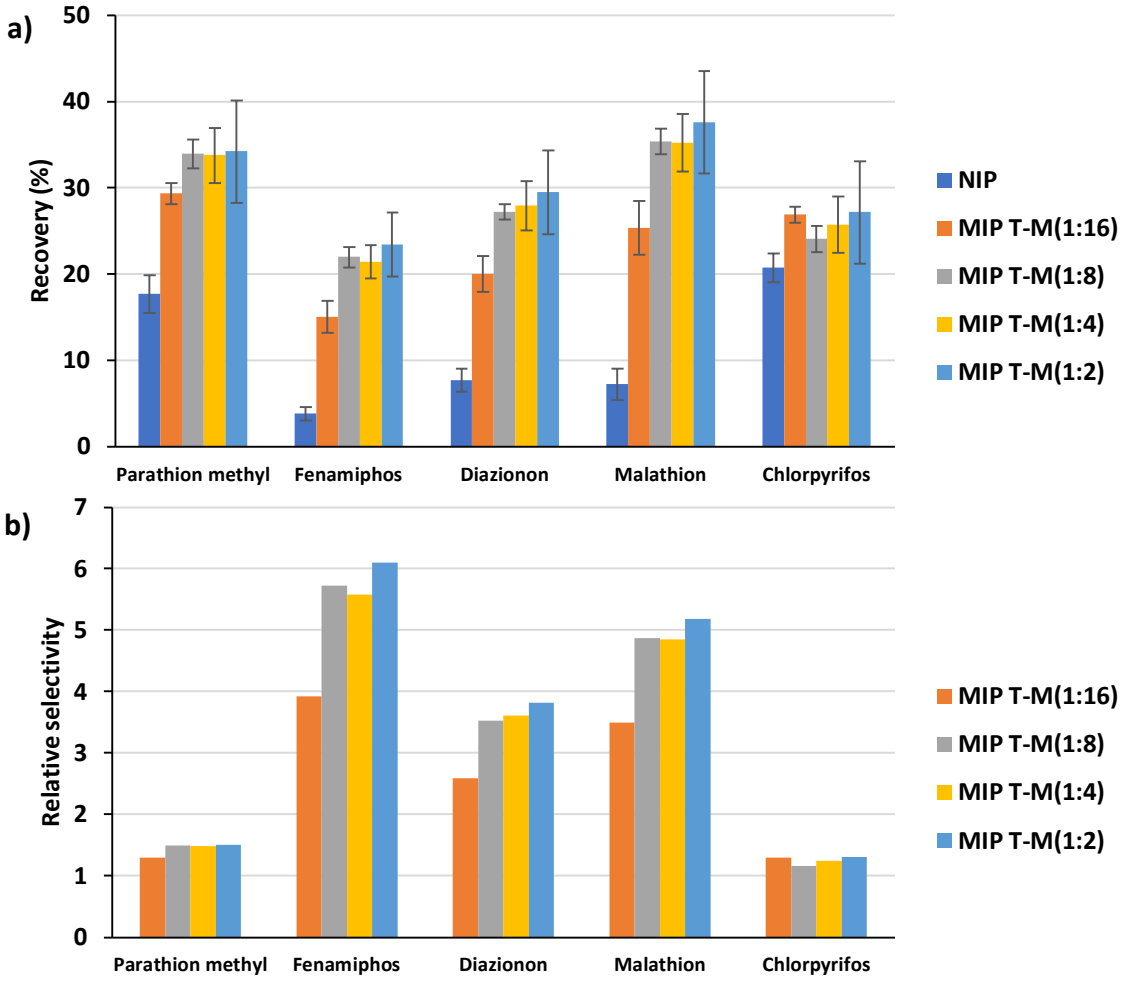


**Fig. 4.4.** Effect of template to monomer ratio on the a) extraction efficiency and b) relative selectivity of thin film MIPs compared to thin film NIPs, Sample: 20 mL sample solution of OPPs (parathion methyl, fenamiphos, diazinon, malathion, and chlorpyrifos) at 50 ng $mL^{-1}$; Extraction at 1000 rpm for 1 h; Desorption: 700 µL MeOH agitated at 1500 rpm for 30 min.

### 4.3.2. Optimization of extraction using MIPs

To optimize the analytical method, experimental parameters for sample preparation were investigated. First the desorption process was optimized by studying the three

effective parameters including type of the organic solvent, agitation speed and desorption time. The desorption solvent should have the ability to desorb the analytes and must be compatible with the sorbent and the detection instrument. These criteria will result in reproducible and reliable analytical data. High chemical resistance of our proposed sorbent makes it compatible with most of the commonly available organic solvents such as ACN, MeOH, DCM, hexane, and toluene as described in our previous work [35].

For thin film MIPs, ACN and MeOH, which are compatible with liquid chromatography, were tested and the recovery values determined (Fig. 4.5 a). Both solvents were able to quantitatively desorb OPPs from thin film extraction devices. However, MeOH gave more reproducible results and better chromatographic behaviour. For mesh MIPs, three different solvents including MeOH, ACN and mixture MeOH/water (85/15, v/v), the composition of mobile phase with highest organic content, were evaluated for OPP desorption (Fig. 4.5 b).

As can be seen, higher recoveries of OPPs using the MIP mesh were obtained when MeOH was used as the desorption solvent. This is mainly due to the ability of MeOH to disrupt hydrogen bonding responsible for adsorption of OPPs using MIPs. A mixture of MeOH and water is also efficient at disrupting hydrogen bonding, which resulting in good recovery for most of analytes except the more hydrophobic compounds, such as ethion and chlorpyrifos. Therefore, MeOH alone was used for desorption using both extraction thin film MIPs and MIP-coated mesh.

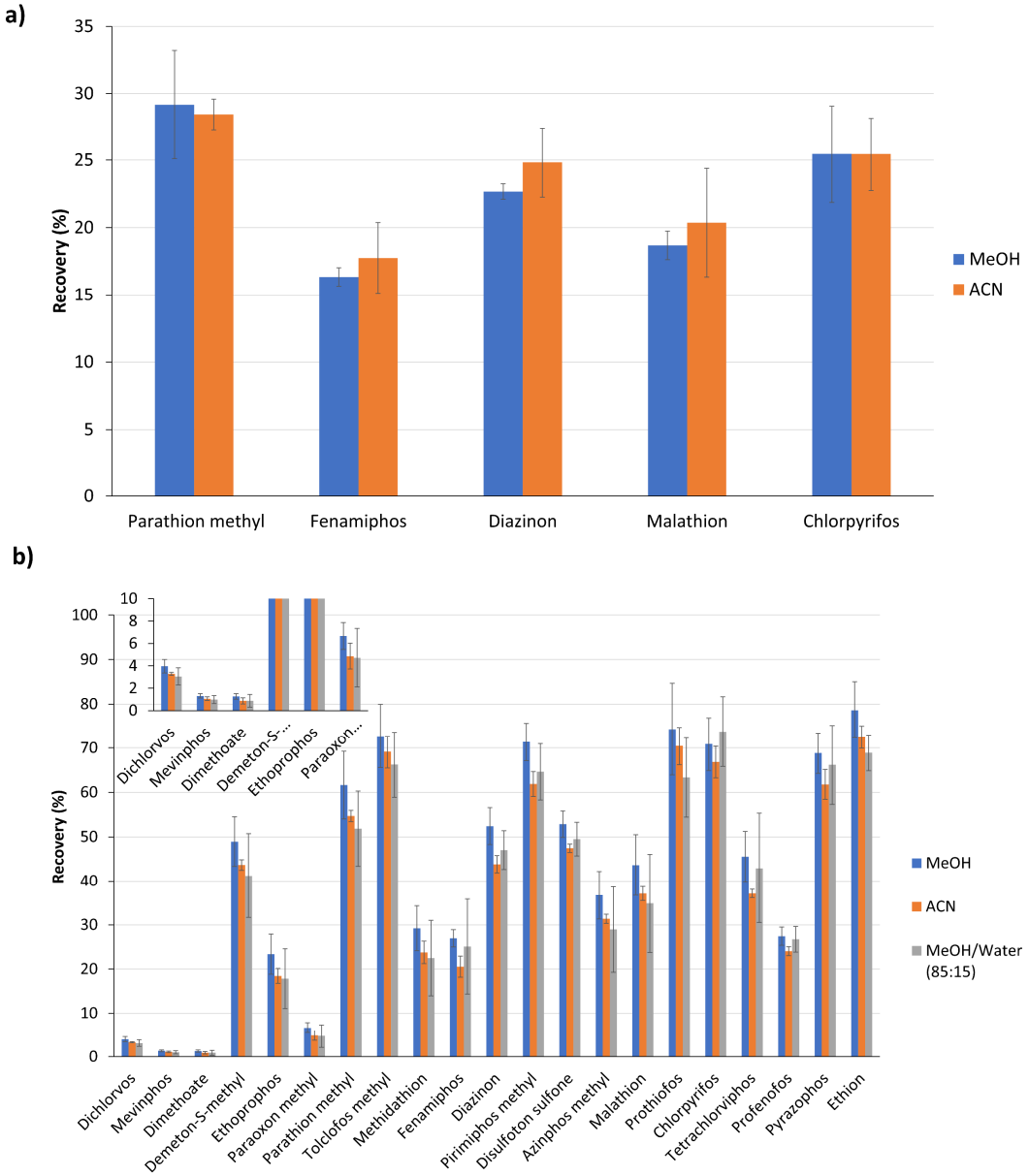


**Fig. 4.5.** Effect of type of solvent on the desorption of OPPs using a) thin film MIPs and b) MIP-coated mesh.

A multi-position vortex mixer was selected to desorb OPPs from the MIP devices. The efficiency of absorption was investigated using 3 different speeds (500, 1000, 1500 rpm) and the results are showed in Fig. 4.6. Increases in the agitation speed did not significantly affect recoveries but did seem to improve the reproducibility of the desorption

process. Fast desorption even at the slower agitation speeds is attributed to the efficiency of agitation using vortex mixer, as well as the porous MIP structure of MIPs. Since the coating was stable at all speeds, 1500 rpm was selected to ensure maximum efficiency and repeatability of the desorption.

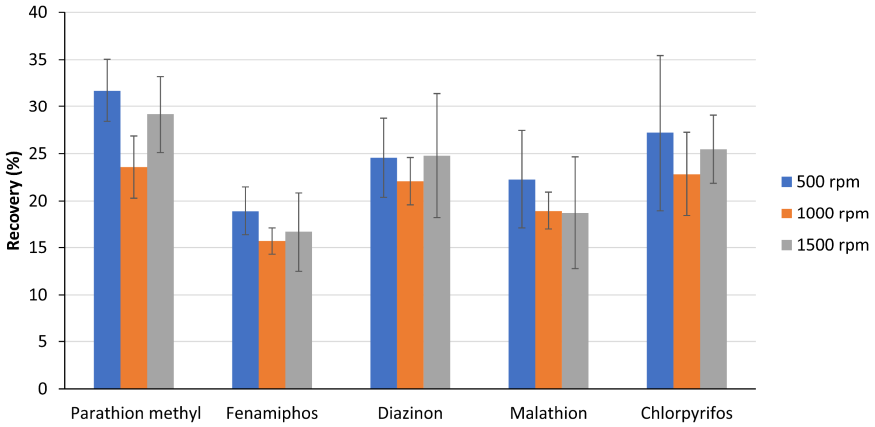


**Fig. 4.6.** Effect of agitation rate using multi-position vortex mixer on desorption of OPPs.

Desorption time is also a significant factor in the process and should only be long enough to provide complete desorption of analytes. Spending a more time than needed makes the analytical method more costly because of lower throughput. In this study, agitation times from 2 to 30 min were evaluated (Fig. 4.7). For the thin film MIP devices, with no significant increase beyond 10 min. Based on the results for MIP-coated mesh in Fig. 4.7 b), no significant difference between desorption intervals was observed. This can be attributed to the porous structure of prepared MIP sorbent. To ensure maximum desorption of OPPs from MIP coated mesh, 30 min was selected as the optimal desorption time.

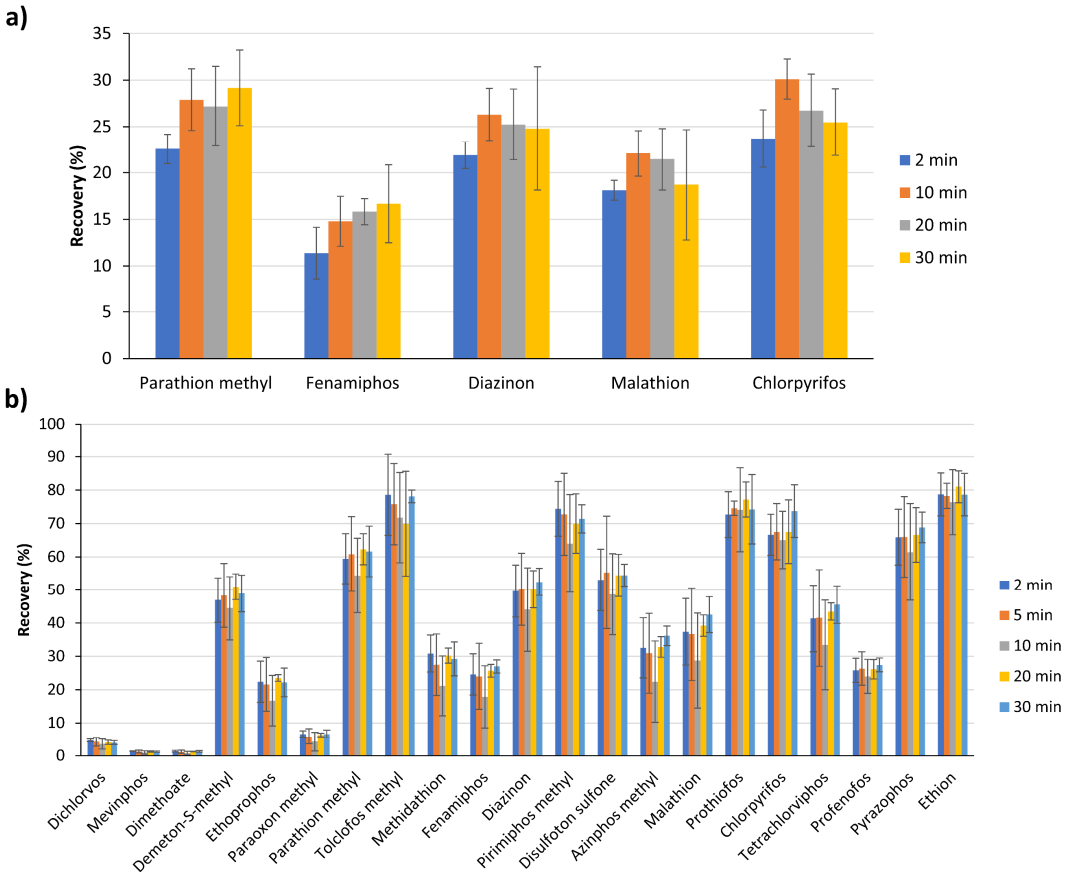


**Fig. 4.7.** Effect of agitation time on the desorption of OPPs using a) thin film MIPs and b) MIP-coated mesh.

As we demonstrated with the thin film MIPs previously [36], the extent of agitation of sample solution is critical for efficient extraction of analytes. The importance of the agitation in the maximizing the extraction rate into MIP-coated mesh is demonstrated in Fig. 4.8. Even incremental increases in mixing over static conditions resulted in large increases in extraction recovery. The higher agitation speeds are necessary to increase mass transfer of the analytes from the bulk solution to the boundary layer near the film surface, where they are rapidly adsorbed [44].

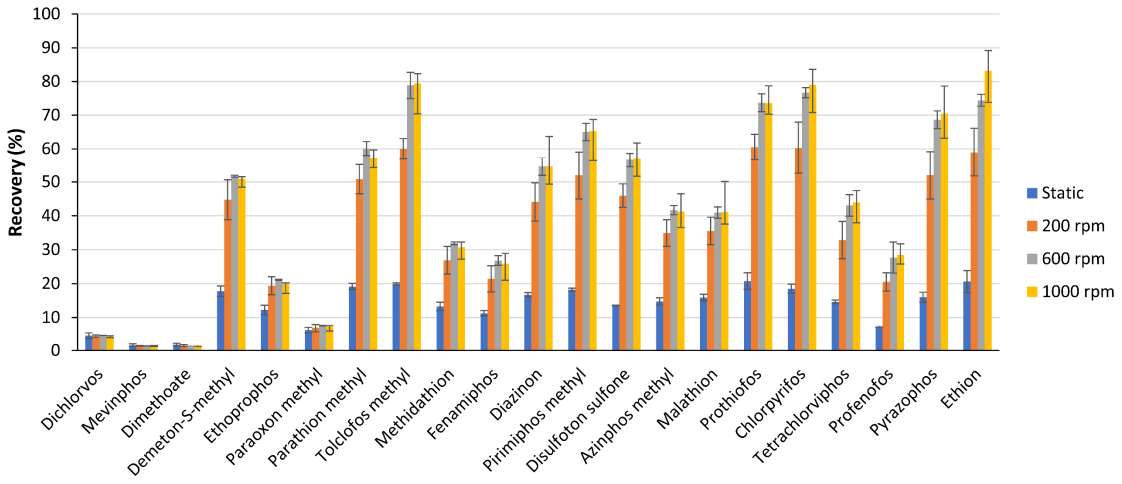


**Fig. 4.8.** Effect of the agitation rate of sample solution on extraction of OPPs using MIP-coated mesh.

It is worth mentioning that the adsorption under static conditions is enough to meet sensitivity requirements for determination of OPPs in water, which qualifies it for use in on-site sampling. This is mainly due to the large surface area provided by the mesh. For some of the pesticides such as dichlorvos, mevinphos, dimethoate and paraoxon methyl, agitation had very minimal effects on the extraction efficiency. This is likely because they have a low partition coefficient and only minimal improvements can be made to their poor extraction recoveries [36]. In accordance with the results, 1000 rpm was selected as the optimum stirring rate for further studies.

### 4.3.3. Extraction time profile using MIPs

A kinetic adsorption study can reveal information about the extraction mechanism. As it is shown in the extraction time profile for OPPs uptake using the MIP-coated mesh (Fig. 4.9), the mechanism is similar to those reported for SPME [45] and thin film-SPME devices [36]. The extent of extraction increases linearly with exposure time for

approximately 30 min until equilibrium is approached. Equilibration is achieved within 90 min for most of OPP. A similar increasing trend can be seen by comparing this graph with extraction time profile using thin film MIPs presented in Fig. 4.10. However, enrichment of these pesticides reached equilibrium far faster with MIP-coated mesh devices rather than MIP thin films. This behaviour can be explained by higher surface area associated with the mesh supported MIP which typically increases the rate of the extraction [46]. According to the formula (Eq. 4.1) developed for SPME devices, the extraction rate is proportional to the surface area of the sorbent ($A$), the analyte diffusion coefficient ($D_s$) and the analyte concentration in the sample ($C_s$), and inversely proportional to the thickness of the boundary layer ($\delta_s$). Thus, mesh format with higher surface area provides an increased extraction efficiency in a shorter exposure time. It should be noted that the mass of the MIP on mesh device is also higher, and thus exhaustive extraction is obtained.

$$\frac{dn}{dt} = \left(\frac{D_S A}{\delta_s}\right) C_S \qquad (4.1)$$

High surface area, ease of use and rapid extraction make the coated-mesh sorptive phases an ideal device for fast analysis of water samples. Since extraction increases with extraction time, extraction efficiency and sensitivity are best with longer extractions, increases sample preparation time. As a compromise, the shortest time to obtain the required sensitivity to meet regulatory limits was chosen for each type of device, was 30 min for the mesh and 1 h for the thin film.

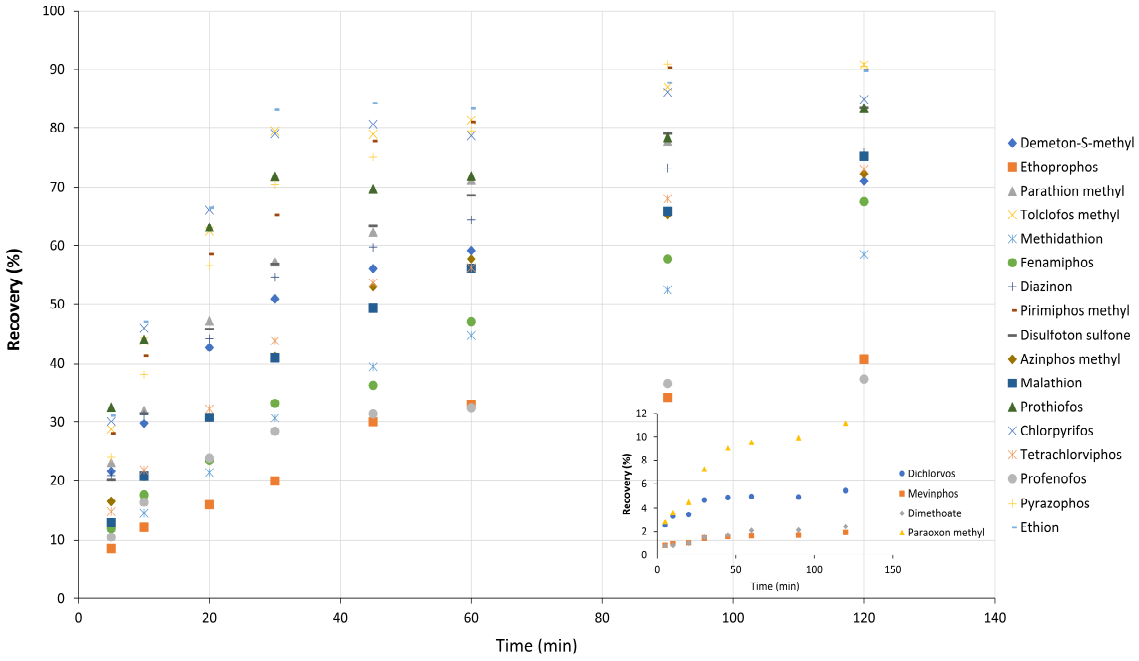


**Fig. 4.9.** Extraction time profile using MIP-coated mesh.

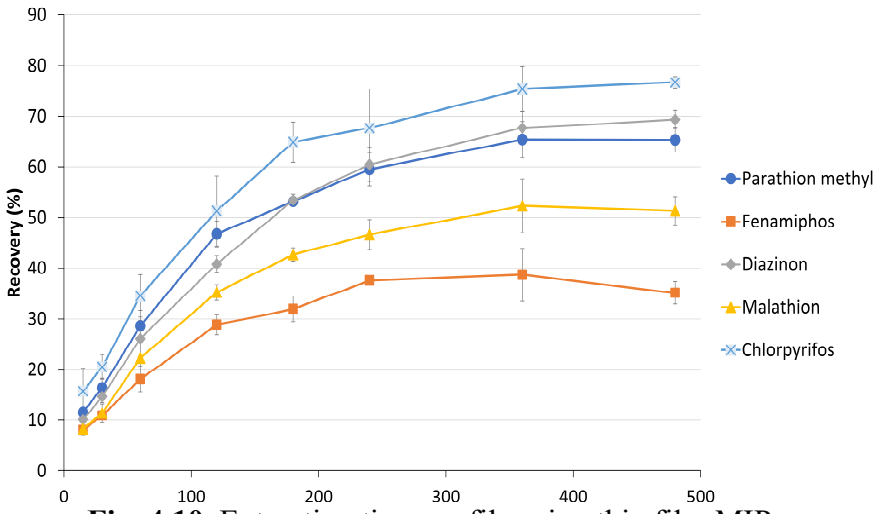


**Fig. 4.10.** Extraction time profile using thin film MIPs.

### 4.3.4. Inter device variability

One of the problems associated with laboratory-made extraction devices is poor inter-device repeatability. These variations necessitate device reuse for calibration and sample analysis to obtain acceptable analytical data. We use a reproducible spraying technique to prepare MIP-coated mesh which reduces inter-device variability. To assess

inter–device variability and demonstrate the potential of these devices for single use applications, 15 individual mesh devices were used to extract OPPs. Fig. 4.11 illustrates the RSD% values of these 15 experiments. The average of RSD values was less than 10% with no internal standard added, demonstrating excellent reproducibility.

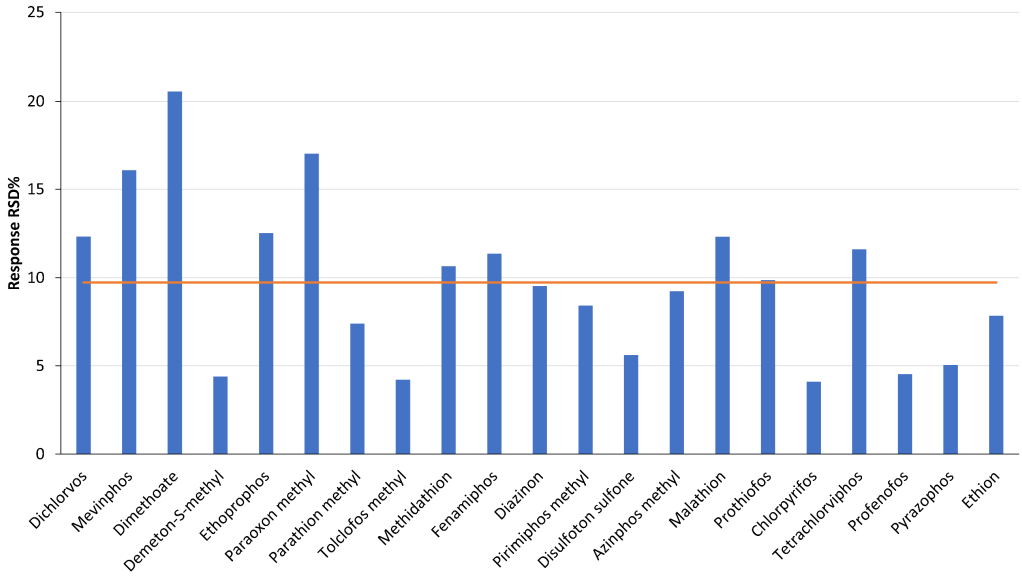


**Fig. 4.11.** Inter-mesh variability for extraction of OPPs (n=15).

### 4.3.5. Selectivity evaluation

To evaluate the selectivity of MIPs (thin film and mesh) kinetic studies of MIPs were compared were compared with their corresponding NIPs. Thin film MIPs and NIPs were utilized for extraction of 5 OPPs from water, with extraction time ranged from 10 to 480 min (Fig. 4.12). Higher extraction efficiencies were obtained using MIPs due to the selective interactions for adsorption of OPPs particularly fenamiphos, diazinon, and malathion. Similarly, the selectivity of the MIP-coated mesh for adsorption of 21 selected OPPs was compared to mesh coated with NIPs coated mesh with extraction time between 5 and 120 min (Fig. 4.13). Equilibrium conditions were attained quickly for the more polar

analytes such as dichlorvos, mevinphos, and dimethoate, due to low LogP which results in low portioning into the sorbent. As is well illustrated by their extraction time profiles, using a selective MIP coating for these analytes is advantageous as the MIP has the benefit of templated sites with higher affinities for these analytes. Some researchers believe that NIPs possess only non-specific binding sites with lower affinity for analytes, therefore equilibrium extraction is longer for NIPs [47]. It is thought that the MIPs have a more selective binding sites that are also readily accessible to the analytes, which shortens the time to equilibrium [48].

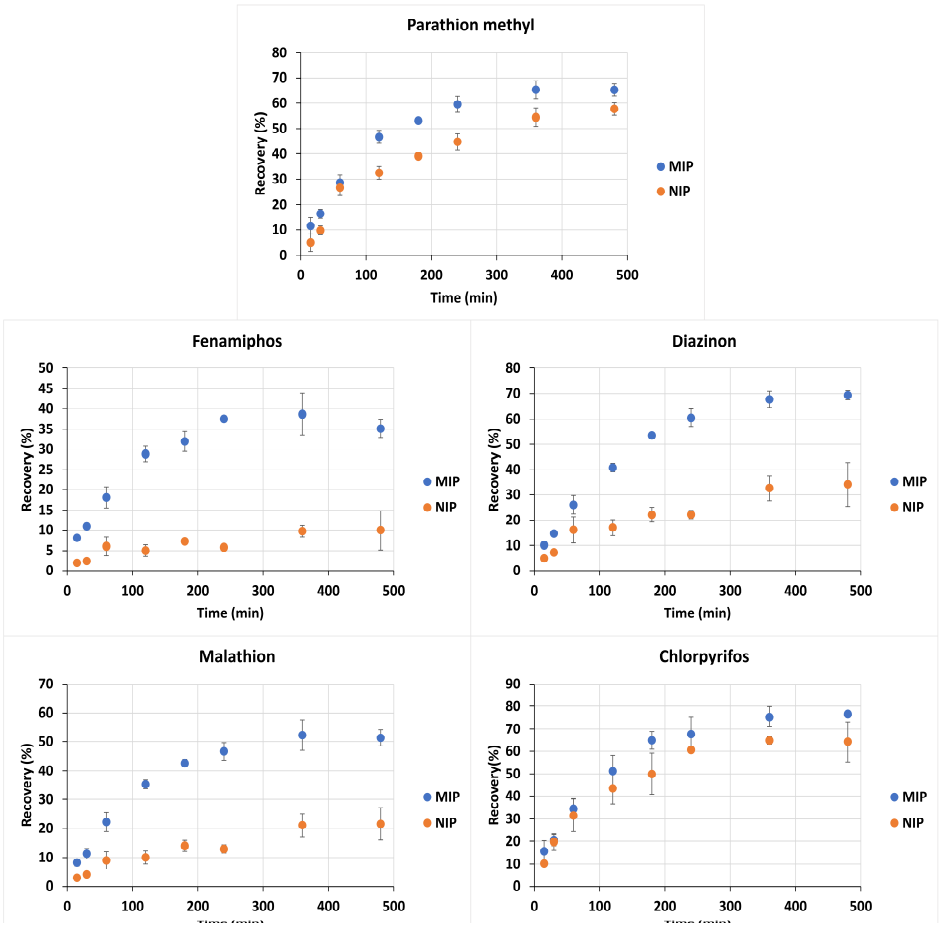


**Fig. 4.12.** Effect of extraction time on the efficiency of adsorption of OPPs using thin films.

Further evidence for the extraction mechanism can be elucidated from the extraction time profiles of the analytes with the higher selectivity values, specifically fenamiphos and ethoprophos (Fig. 4.13). Each of these analytes reached equilibrium conditions within 45 min for the NIPs, while the extraction using MIP coating continued to increase even after 120 min. This long equilibrium for MIPs can be attributed to a larger number of available binding sites, but perhaps sites that are less accessible. Although the NIP materials have large adsorption capacity demonstrated through exhaustive or near exhaustive extraction of analytes such as prothiofos, ethion, and chlorpyrifos, the evidence supports conclusions that the MIPs have a larger adsorption capacity, higher affinity binding sites and perhaps higher surface area related to the porosity of the MIP material. The favourable binding site energy and porosity in the MIPs allow for faster equilibration for analytes with low relative selectivity such as chlorpyrifos and ethion (Fig. 4.13). This demonstrates the availability or affinity of selective binding sites for adsorption of those analytes. Therefore, an extraction mechanism using MIP based extraction devices involves both the nature of analytes and properties of the binding sites in addition to porosity and capacity. Since the only difference is the presence of template molecules, selective binding sites are created and promote the interaction particularly for analytes with lower extraction efficiency.

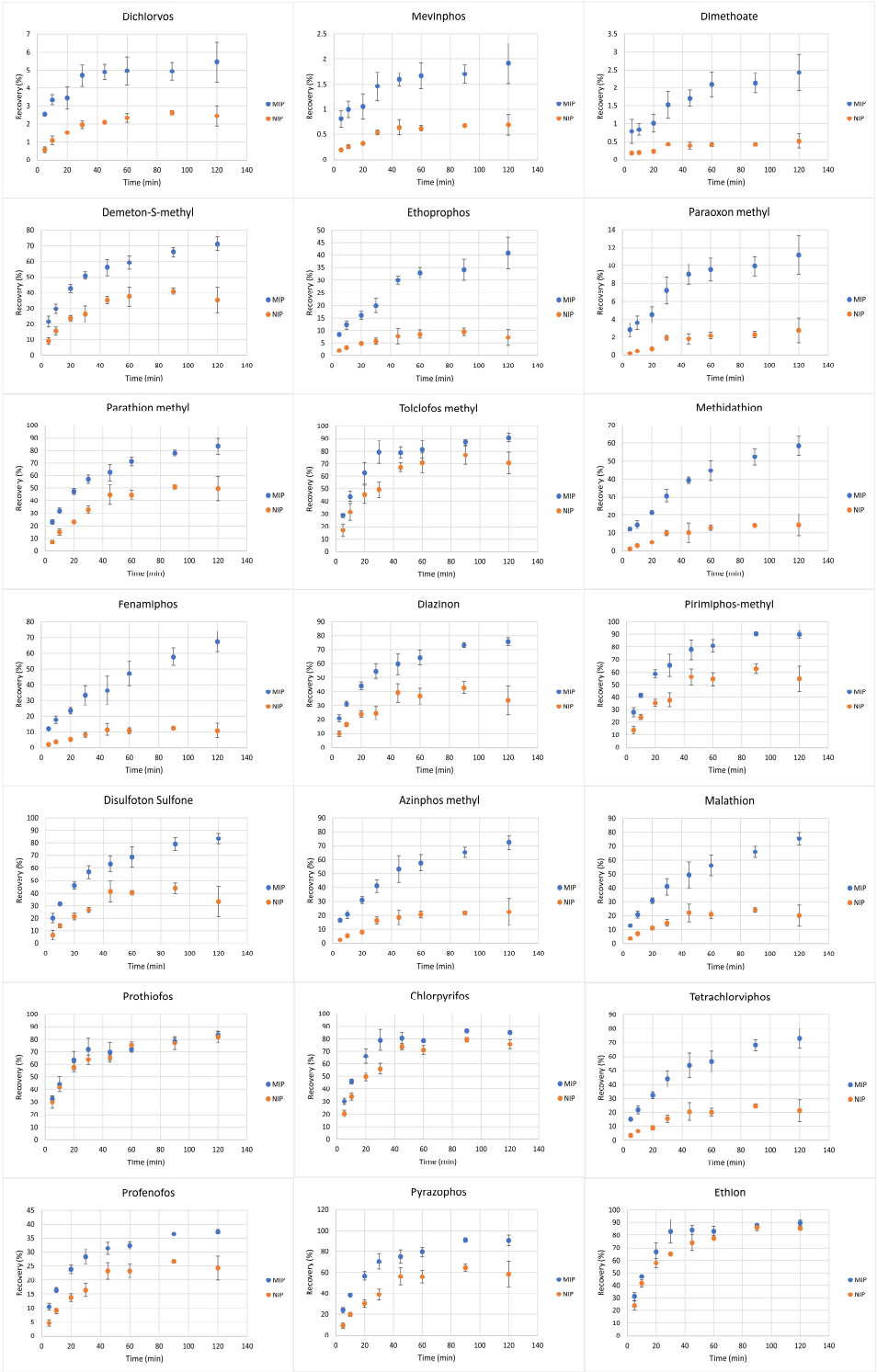


**Fig. 4.13.** Effect of extraction time on the efficiency of adsorption of OPPs using MIP- and NIP-coated meshes.

Cross-selectivity of MIPs for extraction of other analytes that could be present in the sample matrix was also evaluated. The MIPs and NIPs were used to extract OPPs from solutions that also contained acidic herbicides and tricyclic antidepressants (Fig. 4.14). As can be seen MIPs yielded in high extraction efficiency of OPPs compared NIPs. Although the pharmaceuticals and acidic herbicides were extracted using MIPs, the standard deviations are high, and efficiencies were low relative to those for the OPPs. These findings reveal selective recognition properties of MIPs for OPPs and non-selective recognition mechanism responsible for adsorption of matrix components. This non-selective adsorption can be reduced by performing a proper washing step. However, thin film NIPs can adsorb matrix components with better precision in comparison with MIPs. The repeatable extraction of pharmaceuticals and acidic herbicides using NIPs indicates the different interactions that are responsible for adsorption of matrix components than MIPs. Thus, thin film NIPs are sorbents with high affinity for a wide range of compounds, and co-extraction of matrix components can be reduced with application of MIPs.

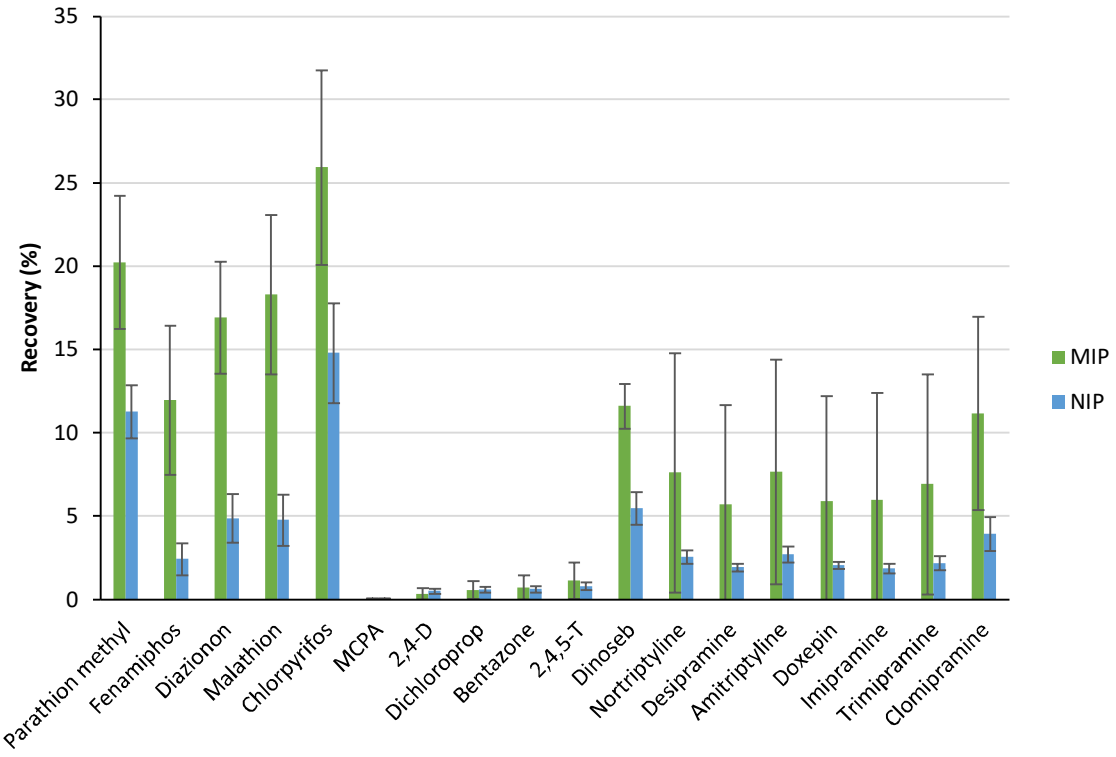


**Fig. 4.14.** Extraction efficiency of different classes of compounds using thin film MIPs and NIPs. Sample: 20 mL sample solution of OPPs (parathion methyl, fenamiphos, diazinon, malathion, and chlorpyrifos) at 50 ng $mL^{-1}$, tricyclic antidepressants (25 ng $mL^{-1}$), and acidic herbicides (250 ng $mL^{-1}$); Extraction at 1000 rpm for 1 h; Desorption: 700 µL MeOH agitated at 1500 rpm for 30 min.

### 4.3.6. Method validation

Analytical methods are validated by obtaining figures of merit such as limit of detection (LOD), limit of quantitation (LOQ), and linear range (LR) under optimized conditions. The results are summarized in Tables 4.4 and 4.5. LOD and LOQ are defined as signal-to-noise (S/N) ratio of 3 and 10, respectively, obtained by analyzing blank ultrapure water samples. LODs and LOQs using thin films were obtained in the ranges of

0.002-0.02 ng $mL^{-1}$ and 0.005-0.05 ng $mL^{-1}$, respectively. This method provided good linearity ($R^2$>0.99) with high sensitivity.

**Table 4.4.** Figures of merit for analysis of OPPs using thin film MIPs-LC-MS/MS.

| OPPs | LOD (ng $mL^{-1}$) | LOQ (ng $mL^{-1}$) | LR (ng $mL^{-1}$) | Function | $R^2$ |
|---|---|---|---|---|---|
| Parathion methyl | 0.02 | 0.05 | 0.05-50 | y = 5336.1x + 1746.4 | 0.9986 |
| Fenamiphos | 0.002 | 0.005 | 0.005-20 | y = 150314x - 1336.1 | 0.9999 |
| Diazinon | 0.002 | 0.005 | 0.005-20 | y = 903075x + 20914 | 0.9998 |
| Malathion | 0.005 | 0.02 | 0.02-50 | y = 106020x + 39351 | 0.9981 |
| Chlorpyrifos | 0.005 | 0.02 | 0.02-50 | y = 70660x + 22105 | 0.9983 |

Introduction of MIP-coated mesh devices into the method greatly enhances the sensitivity. As can be seen in Table 4.5, The LOD and LOQ were 0.00025–1.0 ng $mL^{-1}$ and 0.0005–2.0 ng $mL^{-1}$ respectively with good linearity of $R^2$>0.99. Higher sensitivity of mesh devices can be attributed to higher preconcentration factor of this mode of extraction with greater efficiency even with shorter extraction intervals. The data reported in Table 4.5 was obtained by 30 min extraction, therefore, longer extraction times can lower the detection limits further, particularly if the greater sensitivity is required.

Precision was characterized in terms of %RSD by analyzing triplicate spiked water samples in different concentrations (within low and high concentration ranges) in the same day (intra-day precision) and on three different days (inter-day precision). Accuracy was assessed based on the percentage error between the measured and spiked concentration. For better fitting and more accuracy of quantitation, weighted calibration curves using 1/x as the weighting factor were used, particularly for lower concentrations. Tables 4.6 and 4.7

summarize the intra-day and inter-day accuracy and precision. The results represent a validated analytical method with acceptable accuracy and precision of ± 20% for most of the analytes.

**Table 4.5.** Figures of merit for analysis of OPPs using MIP-coated mesh-LC-MS/MS.

| OPPs | LOD | LOQ | LR ($ng\ mL^{-1}$) | Function | $R^2$ |
|---|---|---|---|---|---|
| Dichlorvos | 0.05 | 0.1 | 0.1-100 | y = 13470x + 14371 | 0.9985 |
| Mevinphos | 0.125 | 0.25 | 0.25-50 | y = 1138.6x + 1193.3 | 0.9969 |
| Dimethoate | 1.0 | 2.0 | 2-20 ppb | y = 1922.2x + 1140.3 | 0.9969 |
| Demeton-S-methyl | 0.2 | 0.5 | 0.5-10 | y = 4943.2x + 930.18 | 0.9933 |
| Ethoprophos | 0.025 | 0.05 | 0.05-50 | y = 61284x + 51364 | 0.9929 |
| Paraoxon methyl | 0.0125 | 0.025 | 0.025-5 | y = 23676x + 919.91 | 0.9970 |
| Parathion methyl | 0.025 | 0.05 | 0.05-5 | y = 19032x + 445.76 | 0.9999 |
| Tolclofos methyl | 0.005 | 0.01 | 0.01-10 | y = 45548x + 4305.3 | 0.9984 |
| Methidathion | 0.01 | 0.02 | 0.02-1 | y = 7450.9x + 74.596 | 0.9987 |
| Fenamiphos | 0.00125 | 0.0025 | 0.0025-50 | y = 200122x + 66756 | 0.9986 |
| Diazinon | 0.0005 | 0.00125 | 0.00125-25 | y = 3384426x + 451017 | 0.9987 |
| Pirimiphos methyl | 0.00025 | 0.0005 | 0.0005-10 | y = 2388360x + 33527 | 0.9993 |
| Disulfoton sulfone | 0.005 | 0.0125 | 0.0125-50 | y = 46721x + 7363.6 | 0.9972 |
| Azinphos methyl | 0.02 | 0.04 | 0.04-20 | y = 1762.5x + 477.39 | 0.9975 |
| Malathion | 0.005 | 0.01 | 0.01-10 | y = 57315x + 5111 | 0.9982 |
| Prothiofos | 0.001 | 0.002 | 0.002-20 | y = 96397x - 2518.2 | 0.9993 |
| Chlorpyrifos | 0.015 | 0.03 | 0.03-60 | y = 99403x + 11317 | 0.999 |
| Tetrachlorvinphos | 0.005 | 0.0125 | 0.0125-50 | y = 92430x + 13379 | 0.9986 |
| Profenofos | 0.001 | 0.002 | 0.002-20 | y = 84051x + 5188.8 | 0.9997 |
| Pyrazophos | 0.00125 | 0.0025 | 0.0025-50 | y = 506429x + 29895 | 0.9972 |
| Ethion | 0.005 | 0.01 | 0.01-20 | y = 102884x + 1708.6 | 0.9997 |

**Table 4.6.** Intra-day method validation summary for analysis of OPPs using MIP-coated mesh (n=3).

| | Accuracy (%) | | | | | %RSD | | | | |
|---|---|---|---|---|---|---|---|---|---|---|
| **Added Conc (ng mL$^{-1}$)** | **0.003125** | **0.03125** | **0.3125** | **1.875** | **18.75** | **0.003125** | **0.03125** | **0.3125** | **1.875** | **18.75** |
| Disulfoton-sulfone | NQ | 109.7 | 113.2 | 109.5 | 89.2 | – | 7.7 | 2.9 | 13.9 | 12.7 |
| Mevinphos | NQ | NQ | 79.0 | 92.2 | 76.9 | – | – | 5.9 | 7.3 | 47.5 |
| Ethoprophos | NQ | NQ | 115.4 | 123.5 | 101.8 | – | – | 7.8 | 10.0 | 3.8 |
| Paraoxon-methyl | NQ | NQ | 94.5 | 95.2 | 94.3 | – | – | 7.4 | 17.9 | 17.9 |
| Parathion methyl | NQ | NQ | 106.1 | 114.1 | 98.6 | – | – | 5.2 | 9.2 | 1.9 |
| Fenamiphos | 96.5 | 139.7 | 109.1 | 109.5 | 108.6 | 14.2 | 3.0 | 16.6 | 22.2 | 12.0 |
| Diazinon | 94.8 | 122.1 | 109.8 | 118.0 | 91.1 | 20.3 | 3.3 | 8.4 | 8.8 | 12.3 |
| Tetrachlorvinphos | NQ | 115.8 | 108.0 | 111.0 | 88.6 | – | 9.8 | 12.7 | 17.4 | 31.9 |
| Pyrazophos | NQ | 108.1 | 98.2 | 95.6 | 97.8 | – | 2.0 | 6.5 | 13.5 | 11.1 |
| **Added Conc (ng mL$^{-1}$)** | **0.000625** | **0.00625** | **0.0625** | **0.375** | **3.750** | **0.000625** | **0.00625** | **0.0625** | **0.375** | **3.750** |
| Pirimiphos-methyl | 103.3 | 110.8 | 107.6 | 108.0 | 91.3 | 11.5 | 2.3 | 5.4 | 11.2 | 4.7 |
| **Added Conc (ng mL$^{-1}$)** | – | **0.0125** | **0.125** | **0.75** | **7.5** | – | **0.0125** | **0.125** | **0.75** | **7.5** |
| Dimethoate | – | NQ | NQ | NQ | 100.6 | – | – | – | – | 25.4 |
| Demeton-S-methyl | – | NQ | NQ | 109.8 | 111.1 | – | – | – | 30.5 | 8.4 |
| Malathion | – | 99.0 | 115.7 | 119.4 | 97.6 | – | 3.0 | 12.2 | 13.6 | 4.8 |
| Prothiofos | – | 93.8 | 87.2 | 92.0 | 91.2 | – | 9.0 | 19.9 | 11.8 | 5.4 |
| Methidathion | – | NQ | 110.8 | 115.4 | 93.8 | – | – | 10.9 | 14.8 | 7.5 |
| Profenofos | – | 112.6 | 109.7 | 107.9 | 98.1 | – | 4.2 | 11.1 | 14.2 | 7.9 |
| Ethion | – | 96.1 | 90.2 | 86.3 | 121.2 | – | 18.6 | 14.2 | 19.9 | 11.9 |
| **Added Conc (ng mL$^{-1}$)** | **0.0625** | **0.375** | **3.75** | **37.5** | – | **0.0625** | **0.375** | **3.75** | **37.5** | – |
| Dichlorvos | – | 96.2 | 100.5 | 99.5 | – | – | 13.1 | 5.1 | 2.7 | – |
| Tolclofos-methyl | 106.8 | 114.3 | 100.1 | – | – | 3.8 | 12.6 | 4.5 | – | – |
| **Added Conc (ng mL$^{-1}$)** | – | **0.0375** | **0.375** | **2.25** | **22.5** | – | **0.0375** | **0.375** | **2.25** | **22.5** |
| Chlorpyrifos | – | 87.0 | 99.7 | 102.3 | 101.6 | – | 6.7 | 5.4 | 11.5 | 4.5 |
| **Added Conc (ng mL$^{-1}$)** | – | **0.25** | **1.5** | **15** | – | – | – | **0.25** | **1.5** | **15** |
| Azinphos-methyl | – | 106.6 | 110.4 | 85.9 | – | – | – | 17.2 | 16.9 | 6.0 |

**Table 4.7.** Inter-day method validation summary for analysis of OPPs using MIP-coated mesh (n=3).

| | Accuracy (%) | | | | | %RSD | | | | |
|---|---|---|---|---|---|---|---|---|---|---|
| **Added Conc (ng mL$^{-1}$)** | **0.003125** | **0.03125** | **0.3125** | **1.875** | **18.75** | **0.003125** | **0.03125** | **0.3125** | **1.875** | **18.75** |
| Disulfoton-sulfone | NQ | 95.6 | 113.4 | 102.0 | 96.7 | – | 18.6 | 11.8 | 14.8 | 0.8 |
| Mevinphos | NQ | NQ | 98.3 | 103.0 | 94.9 | – | – | 36.2 | 38.6 | 12.4 |
| Ethoprophos | NQ | NQ | 120.3 | 119.6 | 99.9 | – | – | 31.1 | 33.6 | 11.2 |
| Paraoxon-methyl | NQ | NQ | 109.5 | 107.0 | 94.5 | – | – | 28.0 | 35.6 | 18.2 |
| Parathion methyl | NQ | NQ | 100.2 | 111.3 | 98.8 | – | – | 12.9 | 16.6 | 0.7 |
| Fenamiphos | 110.9 | 127.5 | 117.0 | 111.7 | 113.9 | 3.0 | 13.9 | 20.5 | 29.1 | 16.9 |
| Diazinon | 110.9 | 104.5 | 106.3 | 110.4 | 95.7 | 15.9 | 19.4 | 17.6 | 24.6 | 2.7 |
| Tetrachlorvinphos | NQ | 99.5 | 101.7 | 106.3 | 102.3 | – | 4.6 | 16.2 | 23.0 | 10.3 |
| Pyrazophos | NQ | 97.0 | 90.3 | 92.5 | 101.3 | – | 9.8 | 21.8 | 13.6 | 3.4 |
| **Added Conc (ng mL$^{-1}$)** | **0.000625** | **0.00625** | **0.0625** | **0.375** | **3.750** | **0.000625** | **0.00625** | **0.0625** | **0.375** | **3.750** |
| Pirimiphos-methyl | 123.5 | 108.9 | 106.3 | 106.1 | 100.2 | 6.6 | 10.5 | 15.1 | 8.4 | 5.1 |
| **Added Conc (ng mL$^{-1}$)** | **–** | **0.0125** | **0.125** | **0.75** | **7.5** | **–** | **0.0125** | **0.125** | **0.75** | **7.5** |
| Dimethoate | – | NQ | NQ | NQ | 118.8 | – | – | – | – | 22.3 |
| Demeton-S-methyl | – | NQ | NQ | 102.2 | 110.2 | – | – | – | 30.7 | 2.1 |
| Malathion | – | 88.3 | 110.1 | 110.8 | 96.4 | – | 17.9 | 16.2 | 25.9 | 6.8 |
| Prothiofos | – | 79.3 | 96.5 | 84.9 | 98.6 | – | 6.9 | 24.3 | 18.6 | 9.1 |
| Methidathion | – | NQ | 102.9 | 116.8 | 96.4 | – | – | 9.4 | 19.6 | 10.9 |
| Profenofos | – | 98.6 | 104.7 | 103.2 | 103.9 | – | 12.0 | 17.6 | 14.5 | 3.6 |
| Ethion | – | 93.8 | 102.0 | 84.3 | 110.3 | – | 36.4 | 22.6 | 17.0 | 22.7 |
| **Added Conc (ng mL$^{-1}$)** | **0.0625** | **0.375** | **3.75** | **37.5** | – | **0.0625** | **0.375** | **3.75** | **37.5** | – |
| Dichlorvos | - | 131.6 | 102.9 | 90.6 | – | – | 13.9 | 28.8 | 9.7 | – |
| Tolclofos-methyl | 99.0 | 107.8 | 96.9 | – | – | 18.2 | 9.7 | 4.4 | – | – |
| **Added Conc (ng mL$^{-1}$)** | – | **0.0375** | **0.375** | **2.25** | **22.5** | – | **0.0375** | **0.375** | **2.25** | **22.5** |
| Chlorpyrifos | – | 71.3 | 86.3 | 95.3 | 100.4 | – | 12.2 | 28.9 | 13.0 | 2.7 |
| **Added Conc (ng mL$^{-1}$)** | – | – | **0.25** | **1.5** | **15** | – | – | **0.25** | **1.5** | **15** |
| Azinphos-methyl | – | – | 97.8 | 105.6 | 94.9 | – | – | 12.5 | 26.0 | 8.7 |

## 4.4. Conclusion

A protocol to fabricate a MIP using custom templates for selective and efficient extraction of OPPs has be described. After optimization of the MIP components, thin film MIPs on steel and mesh were used for TFME of OPPs. Thin film MIPs and MIP-coated mesh for OPPs can improve the workflow for analysis of water samples. Due to the porous MIP surface, the extraction is performed quickly with no preconditioning of the MIP coating required. The porous structure of the coating also facilitates the fast and complete desorption to avoid long elution times. Single use application of the prepared extraction devices avoids carry-over effects. Superior selectivity of MIPs explored via extraction time and cross-selectivity studies demonstrate the strengths of MIP technology to introduce selective interactions for adsorption of a specific class of compounds. Given the simple fabrication procedure, MIPs can replace the traditional sample preparation techniques for pesticide analysis such as LLE and SPE. Furthermore, the flexibility of the MIP composition, provides the opportunity to prepare mesh with MIP coating. The formats presented can be used for extraction of organic contaminants on-site due to their robustness and efficient targeted extraction abilities. MIP-coated mesh with a larger surface area accelerates and enhances the extraction of analytes. Consequently, incredibly sensitive methods can be developed due to the high extraction efficiency using MIP-coated mesh. The validity of proposed extraction devices coated with MIP sorbents demonstrates the benefits of MIP technology for the reliable measurement of OPPs.

## 4.5. References

[1] P. Kumar, K.-H. Kim, A. Deep, Recent advancements in sensing techniques based on functional materials for organophosphate pesticides, Biosens. Bioelectron., 70 (2015) 469-481.

[2] S.O. Obare, C. De, W. Guo, T.L. Haywood, T.A. Samuels, C.P. Adams, N.O. Masika, D.H. Murray, G.A. Anderson, K. Campbell, Fluorescent chemosensors for toxic organophosphorus pesticides: a review, Sensors, 10 (2010) 7018-7043.

[3] K.V. Ragnarsdottir, Environmental fate and toxicology of organophosphate pesticides, J. Geol. Soc. London, 157 (2000) 859-876.

[4] T.C. Kwong, Organophosphate pesticides: biochemistry and clinical toxicology, Ther. Drug Monit., 24 (2002) 144-149.

[5] O. Water, Edition of the Drinking Water Standards and Health Advisories, EP Agency (ed.), (2012).

[6] C. Directive, 98/83/EC of 3 November 1998 on the quality of water intended for human consumption, ed, E. Union, (1998).

[7] M. Shamsipur, N. Yazdanfar, M. Ghambarian, Combination of solid-phase extraction with dispersive liquid–liquid microextraction followed by GC–MS for determination of pesticide residues from water, milk, honey and fruit juice, Food Chem., 204 (2016) 289-297.

[8] L. Villarosa, M.J. McCormick, P.D. Carpenter, P.J. Marriott, Determination of Trace Levels of Diazinon and Propetamphos in Water and Sewage by Solid Phase Extraction, Int. J. Environ. Anal. Chem., 54 (1994) 93-103.

[9] S. Samadi, H. Sereshti, Y. Assadi, Ultra-preconcentration and determination of thirteen organophosphorus pesticides in water samples using solid-phase extraction followed by dispersive liquid-liquid microextraction and gas chromatography with flame photometric detection, J. Chromatogr. A, 1219 (2012) 61-65.

[10] M. Saraji, M.T. Jafari, M. Mossaddegh, Carbon nanotubes@silicon dioxide nanohybrids coating for solid-phase microextraction of organophosphorus pesticides followed by gas chromatography-corona discharge ion mobility spectrometric detection, J. Chromatogr. A, 1429 (2016) 30-39.

[11] F.F. Donato, N.M.G. Bandeira, C. Gabriel, O.D. Prestes, M.B. Adaime, R. Zanella, Evaluation of the rotating disk sorptive extraction (RDSE) technique with polymeric sorbent for multiresidue determination of pesticides in water by ultra-high-performance liquid chromatography-tandem mass spectrometry, J. Chromatogr. A, 1516 (2017) 54-63.

[12] Z. Soutoudehnia Korrani, W.A. Wan Ibrahim, H. Rashidi Nodeh, H.Y. Aboul-Enein, M.M. Sanagi, Simultaneous preconcentration of polar and non-polar organophosphorus pesticides from water samples by using a new sorbent based on mesoporous silica, J. Sep. Sci., 39 (2016) 1144-1151.

[13] S. Meseguer-Lloret, S. Torres-Cartas, M. Catala-Icardo, E.F. Simo-Alfonso, J.M. Herrero-Martinez, Extraction and preconcentration of organophosphorus pesticides in water by using a polymethacrylate-based sorbent modified with magnetic nanoparticles, Anal. Bioanal. Chem., 409 (2017) 3561-3571.

[14] P.E. Grimmett, J.W. Munch, Development of EPA Method 525.3 for the analysis of semivolatiles in drinking water, Anal. Methods, 5 (2013) 151-163.

[15] E. Ballesteros, M.J. Parrado, Continuous solid-phase extraction and gas chromatographic determination of organophosphorus pesticides in natural and drinking waters, J. Chromatogr. A, 1029 (2004) 267-273.

[16] H.K. Rotich, Z. Zhang, J. Li, Optimization of high-performance liquid chromatography and solid-phase extraction for determination of organophosphorus pesticide residues in environmental samples, Int. J. Environ. Anal. Chem., 83 (2003) 851-860.

[17] M.M. Domino, Method 525.3 determination of semivolatile organic chemicals in drinking water by solid phase extraction and capillary column gas chromatography/mass spectrometry (GC/MS), (2012).

[18] H. Piri-Moghadam, F. Ahmadi, J. Pawliszyn, A critical review of solid phase microextraction for analysis of water samples, TrAC, Trends Anal. Chem., 85 (2016) 133-143.

[19] D.A. Lambropoulou, T.A. Albanis, Optimization of headspace solid-phase microextraction conditions for the determination of organophosphorus insecticides in natural waters, J. Chromatogr. A, 922 (2001) 243-255.

[20] C. Hu, M. He, B. Chen, B. Hu, A sol-gel polydimethylsiloxane/polythiophene coated stir bar sorptive extraction combined with gas chromatography-flame photometric detection for the determination of organophosphorus pesticides in environmental water samples, J. Chromatogr. A, 1275 (2013) 25-31.

[21] S. Berijani, Y. Assadi, M. Anbia, M.R. Milani Hosseini, E. Aghaee, Dispersive liquid-liquid microextraction combined with gas chromatography-flame photometric detection. Very simple, rapid and sensitive method for the determination of organophosphorus pesticides in water, J. Chromatogr. A, 1123 (2006) 1-9.

[22] P. Lucci, O. Núñez, M.T. Galceran, Solid-phase extraction using molecularly imprinted polymer for selective extraction of natural and synthetic estrogens from aqueous samples, J. Chromatogr. A, 1218 (2011) 4828-4833.

[23] S. Boulanouar, S. Mezzache, A. Combès, V. Pichon, Molecularly imprinted polymers for the determination of organophosphorus pesticides in complex samples, Talanta, 176 (2018) 465-478.

[24] F.G. Tamayo, E. Turiel, A. Martín-Esteban, Molecularly imprinted polymers for solid-phase extraction and solid-phase microextraction: recent developments and future trends, J. Chromatogr. A, 1152 (2007) 32-40.

[25] Z.L. Shen, D. Yuan, Q.D. Su, H. Zhang, J. Wang, J.H. Zhu, Y.M. Liu, Selective solid-phase extraction using molecularly imprinted polymer for analysis of methamidophos in water and soil samples, Biosci. Biotechnol. Biochem., 75 (2011) 473-479.

[26] H.G. Zuo, J.X. Zhu, C.R. Zhan, L. Shi, M. Xing, P. Guo, Y. Ding, H. Yang, Preparation of malathion MIP-SPE and its application in environmental analysis, Environ. Monit. Assess., 187 (2015) 394.

[27] Z. Xu, G. Fang, S. Wang, Molecularly imprinted solid phase extraction coupled to high-performance liquid chromatography for determination of trace dichlorvos residues in vegetables, Food Chem., 119 (2010) 845-850.

[28] X. Zhu, J. Yang, Q. Su, J. Cai, Y. Gao, Selective solid-phase extraction using molecularly imprinted polymer for the analysis of polar organophosphorus pesticides in water and soil samples, J. Chromatogr. A, 1092 (2005) 161-169.

[29] J. Zhan, G. Fang, Z. Yan, M. Pan, C. Liu, S. Wang, Preparation of a semicovalent, molecularly surface imprinted polymer for the rapid determination of trace acid orange II in food and environmental samples, Anal. Bioanal. Chem., 405 (2013) 6353-6363.

[30] Y.L. Wang, Y.L. Gao, P.P. Wang, H. Shang, S.Y. Pan, X.J. Li, Sol-gel molecularly imprinted polymer for selective solid phase microextraction of organophosphorous pesticides, Talanta, 115 (2013) 920-927.

[31] X. Zhu, J. Cai, J. Yang, Q. Su, Y. Gao, Films coated with molecular imprinted polymers for the selective stir bar sorption extraction of monocrotophos, J. Chromatogr. A, 1131 (2006) 37-44.

[32] S.N. Egli, E.D. Butler, C.S. Bottaro, Selective extraction of light polycyclic aromatic hydrocarbons in environmental water samples with pseudo-template thin-film molecularly imprinted polymers, Anal. Methods, 7 (2015) 2028-2035.

[33] A. Gryshchenko, C. Bottaro, Development of molecularly imprinted polymer in porous film format for binding of phenol and alkylphenols from water, Int. J. Mol. Sci., 15 (2014) 1338-1357.

[34] H.Y. Hijazi, C.S. Bottaro, Analysis of thiophenes in seawater: Molecularly imprinted polymer thin-film extraction with desorption electrospray ionization mass spectrometry, Int. J. Mass spectrom., 443 (2019) 9-15.

[35] F. Shahhoseini, A. Azizi, S.N. Egli, C.S. Bottaro, Single-use porous thin film extraction with gas chromatography atmospheric pressure chemical ionization tandem mass spectrometry for high-throughput analysis of 16 PAHs, Talanta, 207 (2020) 120320.

[36] A. Azizi, F. Shahhoseini, A. Modir-Rousta, C.S. Bottaro, High throughput direct analysis of water using solvothermal headspace desorption with porous thin films, Anal. Chim. Acta, 1087 (2019) 51-61.

[37] G. Van Biesen, J.M. Wiseman, J. Li, C.S. Bottaro, Desorption electrospray ionization-mass spectrometry for the detection of analytes extracted by thin-film molecularly imprinted polymers, Analyst, 135 (2010) 2237-2240.

[38] https://pubchem.ncbi.nlm.nih.gov/, in, 2020, Jan 15.

[39] L. Chen, S. Xu, J. Li, Recent advances in molecular imprinting technology: current status, challenges and highlighted applications, Chem. Soc. Rev., 40 (2011) 2922-2942.

[40] V. Pichon, F. Chapuis-Hugon, Role of molecularly imprinted polymers for selective determination of environmental pollutants—a review, Anal. Chim. Acta, 622 (2008) 48-61.

[41] G. Vasapollo, R.D. Sole, L. Mergola, M.R. Lazzoi, A. Scardino, S. Scorrano, G. Mele, Molecularly imprinted polymers: present and future prospective, Int. J. Mol. Sci., 12 (2011) 5908-5945.

[42] A. Martín-Esteban, Recent molecularly imprinted polymer-based sample preparation techniques in environmental analysis, Trends Environ. Anal, 9 (2016) 8-14.

[43] D.A. Spivak, Optimization, evaluation, and characterization of molecularly imprinted polymers, Adv. Drug Del. Rev., 57 (2005) 1779-1794.

[44] S. Risticevic, H. Lord, T. Gorecki, C.L. Arthur, J. Pawliszyn, Protocol for solid-phase microextraction method development, Nat. Protoc., 5 (2010) 122.

[45] É.A. Souza-Silva, R. Jiang, A. Rodríguez-Lafuente, E. Gionfriddo, J. Pawliszyn, A critical review of the state of the art of solid-phase microextraction of complex matrices I. Environmental analysis, TrAC, Trends Anal. Chem., 71 (2015) 224-235.

[46] H. Piri-Moghadam, M.N. Alam, J. Pawliszyn, Review of geometries and coating materials in solid phase microextraction: opportunities, limitations, and future perspectives, Anal. Chim. Acta, 984 (2017) 42-65.

[47] H.R. Geng, S.S. Miao, S.F. Jin, H. Yang, A newly developed molecularly imprinted polymer on the surface of TiO2 for selective extraction of triazine herbicides residues in maize, water, and soil, Anal. Bioanal. Chem., 407 (2015) 8803-8812.

[48] L. Chen, X. Huang, Preparation and application of a poly (ionic liquid)-based molecularly imprinted polymer for multiple monolithic fiber solid-phase microextraction of phenolic acids in fruit juice and beer samples, Analyst, 142 (2017) 4039-4047.

# Chapter 5: Conclusions and future work

Selective sample preparation using MIPs has drawn significant attention in the field of water analysis. The selectivity afforded by MIPs increases the sensitivity and repeatability of water analysis in analytical methods for targeted molecules. These features of MIPs have triggered innovations in sample preparation primarily in the form of MIP-based sorbents, which has been the impetus for the research presented in this thesis.

In the last decade, several reviews have been published on MIP technology for the analysis of environmental and biological samples [1-5]. These reviews have focused on innovative applications of MIPs, such as novel synthetic procedures and operational formats. However, none of these critically assess MIP technology, especially the performance and selectivity in water samples. Chapter 1 is the culmination of a thorough investigation of the literature on the selectivity and efficiency MIP-based extraction phases for the enrichment of organic contaminants in the water. The synthetic and fabrication strategies used in MIP technologies were reviewed and examined considering the selectivity and performance for sample preparation. To evaluate the applicability such sorptive phases, different application formats, namely MIP-SPE, MIP-DSPE, MIP-SPME, MIP-SBSE, and membrane-based MIPs, were discussed. Even though MIPs can provide selectivity for target analytes, their applicability can be restricted by factors such as the nature of analytes, as well as hydrophobicity and heterogeneity of the MIP sorbents. MIPs sorbent can be fabricated into various formats, which allows for novel applications of MIPs for direct and online analysis with minimal sample manipulation.

The advent of microextraction techniques has led to a considerable expansion in the sample preparation field. These techniques are miniaturized, fast, simple, green, cheaper than LLE and SPE, and suitable for automation [6]. Among these techniques, DSPE has

gained much attention due to the rapid growth of applications of nanoparticles with superior efficiency [7]. In Chapter 2, a MMIP was developed for selective enrichment 16 PAHs listed by US-EPA. The sorptive MMIP particles were synthesized using a controlled polymerization technique reversible addition fragmentation chain transfer (RAFT) to obtain homogenous MIPs. MMIPs were used for extraction of PAHs via dispersion in the sample solution. The MMIPs improved the selective recognition of PAHs due to the imprinting effect resulting from the template-monomer complex in the prepolymer solution.

An experimental design approach consisting of a screening step and central composite design was employed to optimize the MMIP-DSPE method. In this optimization, the 16 analytes were categorized into 3 groups based on their physical and chemical properties to investigate the effective parameters on their extraction. Optimization of MMIP-DSPE using experimental design is crucial to achieve the goal of using MIP sorbents for selective extraction. This optimization not only maximizes the response for each analyte but also identifies the behavior of developed MMIPs for adsorption. For example, high extraction efficiency can be obtained for both MIPs and NIPs if using a small sample volume and a large amount of MMIPs sorbent, thus, selectivity cannot be assessed under these conditions. Since the experimental design employs data from a range of sorbent loadings, it allows the selectivity to be assessed. Experimental design also helped us to avoid one-at-a-time optimization, which requires analysis of a greater number of samples does not allow for identification of synergistic effects of co-varying key parameters, such as polymer mass and sample volume. The other feature of our optimization methodology is that these analytes with different characteristics such as solubility and hydrophobicity

responded differently to each variable. Therefore, simultaneous optimization using desirability function (*DF*) is necessary. This approach is recommended for use with other classes of compounds.

The sample treatment technique was used to analyze PAHs in simple and complex (produced water) water samples and showed excellent sensitivity, accuracy, and precision. In comparison to previously reported methods, our RAFT-MMIPs have the main advantages of providing fast adsorption/desorption due to the thin-coating provided by RAFT polymerization, is selective for extraction from water samples, and requires low amounts of sorbent and organic solvent. These materials can also be dispersed in other film-based systems to impart selectivity. Li et al. [8] prepared particle loaded sorbent by incorporation of $Fe_3O_4$@$SiO_2$ in polyacrylonitrile (PAN)-octadecylsilane(ODS) thin films (Fig. 5.1). The ODS particles are crucial to improve the extraction efficiency of the thin film. In addition, the magnetic properties of the particles are retained by the thin film, which can be used to aid TFME process, for example as a means to hold or retrieve films from samples. Use of MMIPs to amend less selective thin films lends the desirable selectivity and surface area features of MIP to the thin film devices.

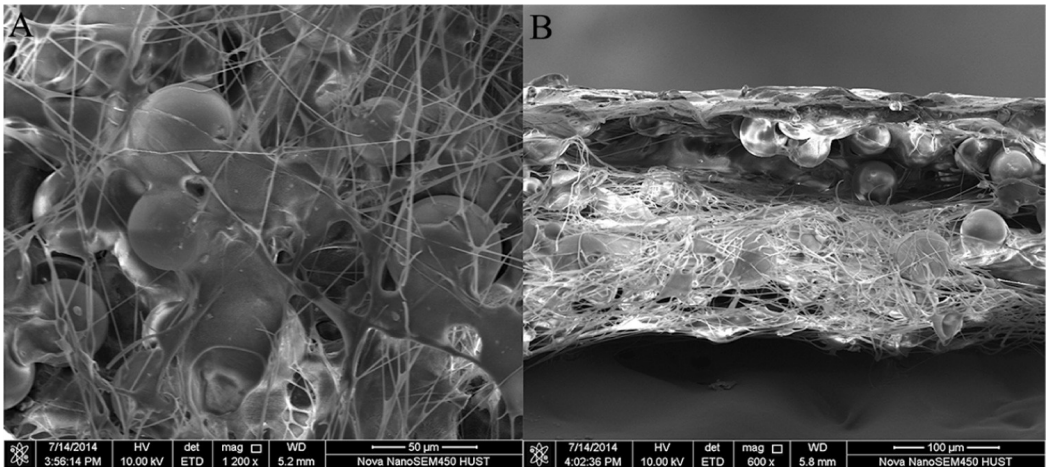


**Fig. 5.1.** SEM images of the surface (A) and section (B) for magnetic ODS-PAN thin-films. Reprinted from [8] with permission from Elsevier.

MMIPs can also be employed for direct coupling with mass spectrometry, most easily with ambient ionization techniques. These soft ionization techniques have revolutionized chemical analysis by introducing high throughput and direct analysis of samples [9]. However, direct analysis of complex matrices can lead to contamination of the detection system or matrix components can reduce sensitivity. An excellent example of direct coupling magnetic sorptive particles has been shown by Chen et al. [10] They coupled magnetic core particles coated with polypyrrole with desorption corona beam ionization-mass spectrometry. After extraction, the sorbent was collected using a lab-made magnetic glass capillary and transferred to the ionization source for quantitation. Using direct introduction eliminated the solvent desorption and chromatographic separation steps and yielded in a 3-min total analysis time including sample preparation and measurement.

MIP sorbents were broadly reported as microextraction devices. These devices, which follow SPME theory, offer additional benefits such as simultaneous sample clean-up and extraction. Thin film MIPs, which were introduced in our group for extraction of

pollutants such as PAHs [11], is another geometry that could enhance the extraction rate of analytes due to larger surface area. However, most of the reported methods rely on time-consuming solvent immersion for desorption of analytes and solvent evaporation for further preconcentration. Chapter 3 presents the first report of solvothermal-headspace desorption (ST-HS) of analytes adsorbed by thin film extraction devices. Single-use thin film devices were fabricated in-house using sorptive phase developed previously in our group [12] with some modification to perform in-vial extraction and desorption. Using simple techniques and equipment, it was possible to overcome the current limitations of thin film devices, such as need for preconditioning, availability of a range of sorbent chemistries, and device cost, while avoiding carry-over effects by eliminating the need to reuse devices. The effectiveness of our approach was demonstrated in the analysis of PAHs as exemplar priority pollutants in aquatic environments. The direct and high-throughput method for analysis of adsorbed PAHs was performed using headspace desorption to introduce analytes into GC system. Thermal desorption into the headspace can be assisted through the addition of a small volume of solvent, which extracts the analytes from the solid surface of the film into a thin layer of solvent that forms on the polymer surface. This process lowers the temperature required for desorption reducing polymer decomposition and background noise, which is a common issue associated with thermal desorption from TFME devices [13].

This novel desorption technique was assessed in terms of effective parameters and a mechanism is proposed to understand the effect of solvent addition on desorption process. Thin films that presented inter-device variabilities from 7.2 to 13.5% were validated for determination of PAHs in the water samples. The method provided exceptional detection

limits in μg $L^{-1}$ range using GC-FID, as a conventional detection system. This is mainly due to the high extraction efficiency, and introduction of a large proportion of extracted analytes into the GC-FID system. The resulting technique allows for rapid generation of data in environmental analysis using high throughput direct analysis of analytes with minimal sample handling.

Using the ST-HD technique as a gentle desorption technique enhances the applicability of thin film devices by reducing the background noise. To further understand the desorption mechanism, there is a need to assess the feasibility of this technique for the desorption of other classes of compounds with various functionalities. One approach to understanding the controlling mechanisms, is to use solvents with lower volatility than the cyclohexane used in this research [14]. This will help to decouple the role of the solvent in desorption of the analytes into the gas phase. Therefore, the partitioning mechanism as the main driving force proposed in this research can be evaluated.

One of the main advantages of thin film devices is the possibility of performing on-site sampling. Our thin films can tolerate high agitation rates and are suitable to be used as a sorbent in on-site sampling. Thus, all the steps required for sample collection, transfer, extraction in the lab can be eliminated, and sample contamination, analyte loss can be avoided, leading to rapid, precise, and accurate analytical methods [15].

In Chapter 4, a MIP coating was developed for OPPs, which are a leading group of pesticides. The risks associated with the presence of this group in water resources has led regulatory agencies to set limits at sub-ppb MCL values. Therefore, the development of extraction techniques with high efficiency and selectivity is crucial. We used stainless steel as an inert substrate to prepare the coating. The protocol for preparation of MIP coating

was optimized with respect to the essential components such as template, monomer, and crosslinker in the polymerization mixture. Following the development of the coating materials, which offer an excellent selectivity towards these analytes, the composition was used to prepare mesh extraction devices coated with OPPs-MIPs. For both extraction devices (i.e., mesh and thin film), full analytical protocols consisting of solvent desorption and extraction were developed and evaluated. The provided LODs for OPPs using these two methods in the range of 0.025-0.05 ng $mL^{-1}$ and 0.00025–1.0 ng $mL^{-1}$ for MIP-coated mesh and thin film MIPs, respectively.

Thin film MIPs are user-friendly extraction devices which can boost the prospects for application of MIPs. After the successful development of thin film MIPs for POPs and pesticides, the necessary knowledge and experience to prepare these devices were obtained which can be used for developing thin film MIPs for the determination of emerging pollutants in environmental water samples (i.e., plastizers, hormones, and pharmaceutical compounds). These thin films can be superior to other extraction techniques that use MIPs as adsorbents. For example, MIP-SPE consists of time-consuming operation steps, or MIP-SPME employs extraction devices with long fabrication methods and limited inter-device repeatability. Thus thin film can improve environmental analysis due to the easy preparation and easy operation. Another feature of thin film MIPs, which is still unexplored, is the possibility to perform headspace extraction. These sorbents have a highly porous structure and can be used for the extraction of volatile organic compounds (VOCs) from water samples. It is expected that the extraction efficiency of these componds in direct immersion of thin film MIPs in the sample solution is low due to their volatility. This deficiency, which was also observed during extraction of light PAHs such as Naph, can be

overcome using exposure of thin films to the headspace of sample solution. the extraction of analytes can be enhanced by adding salt and heating the sample solution. In headspace mode, non-volatile and high molecular weight compounds can not interfere with analytes of interest [16].

Besides, thin film MIPs have the advantageous clean-up effect in real samples. Therefore, deployment of these devices for analysis of more complicated samples such as biofluids, including urine, plasma, and whole blood, can improve the analysis in healthcare in which reliable and sensitive protocols are required.

The prepared thin film MIPs can be used to perform the direct introduction of analytes using electrospray desorption. This technique, introduced by Gomez-Rios and Pawliszyn [17], employs a metal substrate coated with a sorbent. After placing the extraction device using a blade holder in front of the mass spectrometer, the desorption of analytes is performed by deposition of a desorption solvent and application of a high voltage. The advantages of this technique are high sensitivity due to introduction of the whole extracted mass, simple workflow, and short analysis time by elimination of chromatographic separation step [9]. The selectivity with thin film MIP sprayer could boost the prospects for using electrospray ionization for the analysis of complex matrices (Fig. 5.2).

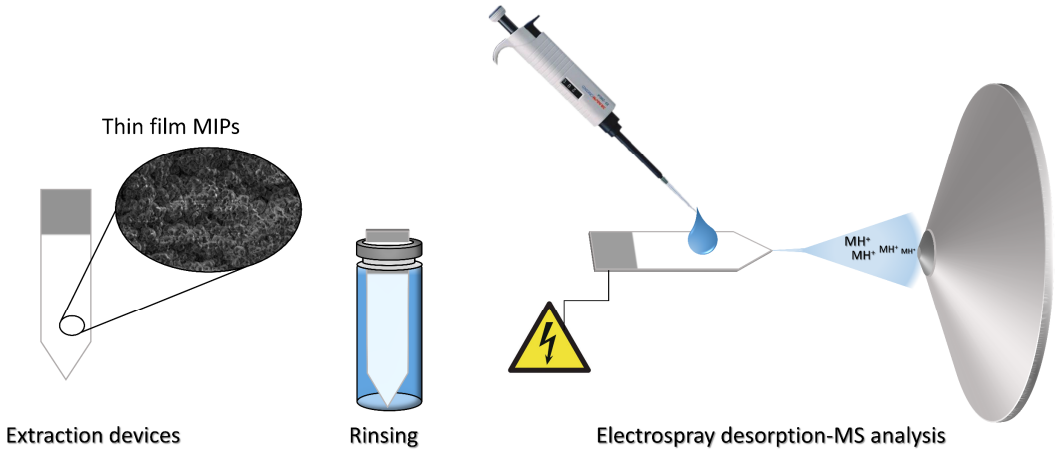


**Fig. 5.2.** Workflow for MIP sprayer in direct MS analysis.

Portable instruments, especially mass spectrometers, are of utmost importance in conducting in-situ analysis. The introduction of the sample in these instrumentations is a critical step. M908 which is the first commercially available handheld mass spectrometer, can analyze gaseous samples or solid samples using inert Teflon swabs as the sampling interface. In Chapter 4, we prepared MIP-coated mesh for the adsorption of OPPs. These extraction devices, which can be used to detect organophosphates as chemical warfare agents, were validated by extraction of OPPs from water followed by LC-MS/MS analysis. MIP-coated mesh as a new format of MIPs was interfaced with an MX908 mass spectrometer (the MX relies on a corona discharge for chemical ionization). We were able to obtain preliminary results using such a configuration; however, the working concentration range was high, and the data are not presented in this thesis. Nevertheless, the results were promising enough to demonstrate that using the right sorbent in an appropriate format will allow such an instrument to analyze liquid samples such as bio-fluids. Further research will need optimization of the MIP-coated mesh format and

instrumental parameters, and as well as software modification to achieve the necessary detection limits and linearity for routine analysis.

## 5.1. References


[1] C. He, Y. Long, J. Pan, K. Li, F. Liu, Application of molecularly imprinted polymers to solid-phase extraction of analytes from real samples, J. Biochem. Bioph. Methods, 70 (2007) 133-150.

[2] G. Vasapollo, R.D. Sole, L. Mergola, M.R. Lazzoi, A. Scardino, S. Scorrano, G. Mele, Molecularly imprinted polymers: present and future prospective, Int. J. Mol. Sci., 12 (2011) 5908-5945.

[3] F.G. Tamayo, E. Turiel, A. Martín-Esteban, Molecularly imprinted polymers for solid-phase extraction and solid-phase microextraction: recent developments and future trends, J. Chromatogr. A, 1152 (2007) 32-40.

[4] L. Chen, X. Wang, W. Lu, X. Wu, J. Li, Molecular imprinting: perspectives and applications, Chem. Soc. Rev., 45 (2016) 2137-2211.

[5] A. Speltini, A. Scalabrini, F. Maraschi, M. Sturini, A. Profumo, Newest applications of molecularly imprinted polymers for extraction of contaminants from environmental and food matrices: A review, Anal. Chim. Acta, 974 (2017) 1-26.

[6] M. Mei, X. Huang, L. Chen, Recent development and applications of poly (ionic liquid)s in microextraction techniques, TrAC, Trends Anal. Chem., 112 (2019) 123-134.

[7] E. Turiel, A. Martín-Esteban, Molecularly imprinted polymers-based microextraction techniques, TrAC, Trends Anal. Chem., 118 (2019) 574-586.

[8] D. Li, J. Zou, P.-S. Cai, C.-M. Xiong, J.-L. Ruan, Preparation of magnetic ODS-PAN thin-films for microextraction of quetiapine and clozapine in plasma and urine samples followed by HPLC-UV detection, J. Pharm. Biomed. Anal., 125 (2016) 319-328.

[9] L. Fang, J. Deng, Y. Yang, X. Wang, B. Chen, H. Liu, H. Zhou, G. Ouyang, T. Luan, Coupling solid-phase microextraction with ambient mass spectrometry: Strategies and applications, TrAC, Trends Anal. Chem., 85 (2016) 61-72.

[10] D. Chen, H.-B. Zheng, Y.-Q. Huang, Y.-N. Hu, Q.-W. Yu, B.-F. Yuan, Y.-Q. Feng, Magnetic solid phase extraction coupled with desorption corona beam ionization-mass spectrometry for rapid analysis of antidepressants in human body fluids, Analyst, 140 (2015) 5662-5670.

[11] F. Shahhoseini, A. Azizi, S.N. Egli, C.S. Bottaro, Single-use porous thin film extraction with gas chromatography atmospheric pressure chemical ionization tandem mass spectrometry for high-throughput analysis of 16 PAHs, Talanta, 207 (2020) 120320.

[12] S.N. Egli, E.D. Butler, C.S. Bottaro, Selective extraction of light polycyclic aromatic hydrocarbons in environmental water samples with pseudo-template thin-film molecularly imprinted polymers, Anal. Methods, 7 (2015) 2028-2035.

[13] J.J. Grandy, E. Boyacı, J. Pawliszyn, Development of a carbon mesh supported thin film microextraction membrane as a means to lower the detection limits of benchtop and portable GC/MS instrumentation, Anal. Chem., 88 (2016) 1760-1767.

[14] C.-Y. Zhang, M.-Q. Guo, Solvent-saturated solid matrix technique for increasing the efficiency of headspace extraction of volatiles, J. Chromatogr. A, 1511 (2017) 9-14.

[15] Q. Hu, S. Liu, Y. Liu, X.a. Fang, J. Xu, X. Chen, F. Zhu, G. Ouyang, Development of an on–site detection approach for rapid and highly sensitive determination of persistent organic pollutants in real aquatic environment, Anal. Chim. Acta, 1050 (2019) 88-94.

[16] J. Pawliszyn, Theory of Solid-Phase Microextraction, J. Chromatogr. Sci., 38 (2000) 270-278.

[17] G.A. Gómez-Ríos, J. Pawliszyn, Development of coated blade spray ionization mass spectrometry for the quantitation of target analytes present in complex matrices, Angew. Chem. Int. Ed., 53 (2014) 14503-14507.